THE UNIVERSITY OF CHICAGO

MICROSCOPIC DEFINITIONS OF TOPOLOGICAL DATA

A DISSERTATION SUBMITTED TO
THE FACULTY OF THE DIVISION OF THE PHYSICAL SCIENCES
IN CANDIDACY FOR THE DEGREE OF
DOCTOR OF PHILOSOPHY

DEPARTMENT OF PHYSICS

BY
KYLE KAWAGOE

CHICAGO, ILLINOIS
AUGUST 2022

For my family, which has sacrificed for the past century

to build the future in which I now live.

"This is a story of how a Baggins had an adventure, and found himself doing and saying things altogether unexpected. He may have lost the neighbours' respect, but he gained–well, you will see whether he gained anything in the end." — J.R.R. Tolkien in "The Hobbit"

TABLE OF CONTENTS

LIST OF FIGURES

ACKNOWLEDGMENTS

It is wholly insufficient to thank so many for so much in a space that can fit neither the names nor actions of those who are due gratitude. So, in my own imperfect way, I will give thanks.

First, thank you to my advisor, Michael Levin. Throughout my PhD, he has given me steady and sound guidance. Though he is a master at spotting errors, I never once felt that these corrections were a reflection of myself or my abilities. Rather, he patiently worked with me to help me to become a better physicist. Although it is difficult to sum up six years of mentorship, I would like to describe one lesson he taught me. A research project is not done when the problem has been solved, nor is it even done when the results have been written up! It is done when the story of the work has been written elegantly and in a way that others can understand. I am fortunate to have been taught this skill from a true master.

I would also like to thank other University of Chicago professors, including the other members of my thesis committee, Dam T. Son, Arvind Murugan, and Jonathan Simon for helping me to understand how to motivate and communicate my work. Additionally, thank you to Arvind Murugan, Vincenzo Vitelli, and Peter Littlewood for nourishing my desire to solve fun math and physics problems outside of my main field.

Although I had many great mentors as an undergraduate at the University of California, Santa Barbara, I want to highlight two in particular. Sathya Guruswamy taught me how to think like a physicist. I am incredibly lucky to have had her as my academic advisor at the College of Creative Studies at UCSB. Greg Huber was my first research advisor in theoretical physics. He never missed an opportunity to teach me about the wider world of physics and he never failed to introduce that wider world to me when a member of it visited. For the past decade, Greg has been my advisor, my collaborator, and my friend.

I had a multitude of excellent teachers before entering college as well. Thank you to Mr. Deibert, Mr. Friesen, Ms. Adams, Mrs. Hardcastle, Ms. Ruth, Mr. Rodriguez, and

Mrs. Mello for encouraging my curiosity and my love of math. Without the confidence you instilled in me, this thesis would not have been completed. To Mrs. Hutchinson, better known as Frau, thank you for two generations of academic service to my family and to Reedley. You are so missed.

To my friends in Chicago, whom I have come to love, thank you Matt, Brendan, Mark, Jody, Chih-Kai, and Melody. From Dungeons and Dragons to cooking adventures, thank you for being with me through some of the most fun and meaningful years of my life. Thank you, also, to Mark Rychnovsky who has been my friend since we were undergraduates, and has become a wonderful collaborator. Finally, thank you to Andy and Peter for reminding me that I will always have friends back home.

Thank you to a man named Eli Macha, for whom obsessive problem solving is not just a skill, it is a way of life. Thank you for teaching me how to obsess until the problem is done. It gave us many hours of play as children and it is now the backbone of my PhD.

Thank you, Grammy, for the many conversations we have had throughout graduate school. Thank you for believing that I'm the one who can find the solutions, even when I don't believe that myself. Thank you, Papa, for teaching me how to strategize and for playing countless board games with me. Thank you, Obaachan, for being one of the first scientists in our family and for building our family to be centered around love and connection. Thank you, as well, for teaching me how to cook and, perhaps even more importantly, how to eat well.

Thank you, Uncle Joe, for giving up your education after World War II so that Obaachan and the rest of your siblings would be able to go to school. To my great-grandparents who stood tall and proud in the face of oppression and incarceration, I am proud to be your great-grandson.

On a lighter note, I would like to thank the cast and crew of the Bob and Tom Show. From listening to you in my dad's truck on the way to elementary school to preparing to

defend my PhD thesis, you have always been there to make me laugh. Thank you for putting a smile on my face every morning. You guys rock.

To Shannon Jacoby, I am so grateful that we re-met each other. From being friends for over a decade to the love that we now share, thank you from the bottom of my heart. You help me do what I am not strong or wise enough to do myself and you give me the courage to be me. I can't wait to finally be with you in Columbus!

Finally, I say thank you to my parents and siblings. I am at a total and complete loss for words to describe our family and what you have done for me. I don't know if there is really a word to describe the ephemeral quality of our family or the emotions which it evokes. The more I reach for words, the further I get from whatever it is that makes our family so special, and to say that I am grateful feels like a hallow expression for the emotion I am feeling, fully recognizing that gratitude is not even slightly hallow. So maybe it is best to use the one phrase that always seems to fall short of describing the emotion that it conveys. I love you. This thesis is dedicated to you.

ABSTRACT

Condensed matter physics rests its foundation on the notion of universal phases of matter. As it is not possible to understand the detailed motions of large collections of particles by tracking them individually, we must rely on the fact that, much of the time, these details are irrelevant to a comprehensive understanding of a macroscopic system. Rather, we must understand the collective behavior of materials via a small set of quantities which summarize this information. For topological phases of matter, we can understand their most basic properties from information called "topological data." This topological data describes the phase of matter of these systems and carries with it a broad array of information about their behavior. Previously, the nature of this data was broadly understood, but in most cases was lacking a concrete interpretation in terms of the microscopic details of these systems.

The goal of this thesis is to resolve this issue by giving concrete definitions of the topological data in terms of a small number of microscopic properties of these systems. These definitions serve not only as a tool to analyze these theories, but also bridge a conceptual gap between the abstract mathematical understanding of these phases of matter with the concrete physical models that physicists study. This thesis achieves this goal for two types of (2+1)D topological phases of matter: intrinsic topological phases and symmetry protected topological phases (SPTs).

Intrinsically topologically ordered phases, exemplified by the fractional quantum Hall states, are characterized by long range entanglement. These systems have particle-like excitations known as anyons and their properties are summed up by information called the anyon data. The anyon data is the topological data associated with these theories, with the two most subtle pieces of data being called the F and R-symbols. In the first part of the thesis, I present microscopic definitions of all of the anyon data and then proceed to calculate the F and R-symbols in a variety of exactly solvable models. Furthermore, I show that these definitions are consistent with the known mathematical structure of the anyon data.

Symmetry protected topological phases, exemplified by topological insulators, do not have long range entanglement, but are non-trivial because of their symmetries. These phases are characterized by robust modes which propagate along their boundary. The fact that the bulk ensures this non-trivial property of the boundary is a consequence of the bulk-boundary correspondence. In the second part of this thesis, I show how to make this correspondence precise by defining the bulk topological data using microscopic boundary theories. I do this for both bosonic and fermionic SPTs in 2+1 dimensions. I show how to implement these definitions in a variety of examples and, in particular, show that these definitions reproduce the known data for the (2+1)D topological insulator.

CHAPTER 1

INTRODUCTION

1.1 What is this?

"What is this?" This question has been one of the guiding motivations of science since its foundation.

Implicitly, this question has two parts. There is the question itself and another question which precedes it invisibly: "What is the framework in which an answer can be given?" For example, it would not make much sense to tell an ancient Greek philosopher that the recently hypothesized atom was made of quantum fields since they didn't have a framework for quantum field theory. In order to describe the evolutionary tree of a frog, we would need to first have a notion of evolution. Once we have a framework for the study of a thing, we may ask our original question, "What is this?" and have a hope of the answer being satisfactory.

One of the primary achievements of the last century and a half of physics has been to answer this question with increasing detail for the materials we see around us in terms of atoms and their interactions. For example, although we tend to take it for granted, everything[1] we interact with on a day-to-day basis is made of a large collection of atoms. Technologically, it has been extremely important to understand the collective behavior of these atoms, especially as it relates to the motion of their electrons. Understanding materials at the quantum level has been the basis of the field of hard condensed matter physics.

One class of exotic materials are the so-called "topological phases" of matter. Condensed matter physicists and mathematicians have created an extensive framework to classify these phases over the past few decades and to understand their properties. So we are now aptly able to answer the "What is this?" question when given a physical system in a topological

1. By "everything" I mean all of the matter. I am excluding photons.

phase of matter. The answer to this question is the subject of this thesis.

However, before we discuss topological phases of matter, we need to understand some of the background of condensed matter physics. When we look out at the world, we see a lot of stuff. It is then natural to ask the titular question "What is this?" when we see all this stuff around us. One of the major scientific philosophies that we use to answer this question is reductionism. This mode of thinking helps us to break things apart to understand what constitutes all this "stuff." This led to the discoveries of elements, the atom, subatomic particles, and much more. Condensed matter physics answers this question another way and takes the philosophy of emergence. Given the properties of many small objects which constitute some "stuff" (or simply given that the stuff is made up of many small objects), can we understand what this stuff is and how it behaves?

Condensed matter physics is primarily concerned with understanding physical systems which are composed of many particles, such as a material. One of the crowning achievements of condensed matter physics is the understanding of different phases of matter like solids, liquids, and gases and understanding the phase transitions between them.

In condensed matter physics, we understand a phase more generally as a collection of systems which exhibit similar behaviors. For example, even though there are differences between oil and water, they are both liquids. On the other hand, when one changes the conditions under which a substance exists, such as by increasing the temperature, its behavior can change wildly. This substance is now described by a different phase of matter and has undergone a phase transition.

1.2 The Landau Paradigm

The Landau paradigm of phases and phase transitions is based on symmetry. As an example, we will consider the ferromagnetic phase transition. To do so, we will consider a toy model of a ferromagnet. We can imagine a ferromagnet as being made up of many smaller magnets

called domains.[2] Since magnets like to align with one another, the entire system will have a tendency to have all of the domains align in the same direction. However, if we heat up the system enough, the domains will orient themselves randomly because the system will become highly entropic.

To describe the ferromagnetic phase transition, let's consider what happens when we cool down the system. To begin with, the domains have orientations in random directions. However, as we cool, the domains will start to align in larger and larger patches. At this point, there will still be many patches pointed in random directions, with no preferred direction on average. Once the system is cool enough, it undergoes the ferromagnetic phase transition and almost all of the domains will be aligned in the same direction.

At this point, we must recognize an oddity. Originally, the heated system had no preferred orientation. This system has "full rotational symmetry." However, by the end of the cooling process, the system picked a particular direction as special. Even though the rules of the universe did not ordain a particular direction and the rules are still fully rotationally symmetric, the state of the system still picks one direction. This is what is called "spontaneous symmetry breaking."

Spontaneous symmetry breaking is the corner stone of the Landau paradigm of phase transitions. That is, we start with a system with some symmetry where the state of the system obeys that symmetry. We then change the parameters of the system, often temperature, so that while keeping the same symmetric constituent rules of the system, the state itself breaks the symmetry. This story dominated the field of condensed matter physics for decades. It was hugely successful and gave us a seemingly complete description of phase transitions. However, systems eventually arose which could not be explained by Landau's paradigm.

2. It is important to note that these "smaller" magnets are not the spins of the particles in the system. Magnetism is induced by the motion of electrons caused by the exchange interactions between the electrons which are a consequence of the Pauli exclusion principle.

1.3 Beyond Landau's Paradigm

The discovery of fractional quantum hall states marked a dramatic change in the way we think about phases of matter. In 1982, Tsui, Störmer, and Gossard published a letter reporting their recent experiments on 2D sheets of $GaAs - Ga_xAl_{1-x}$ heterojunctions in low temperatures in the presence of high magnetic fields [136]. This experiment marked the beginning of the study of the Fractional Quantum Hall Effect.

In this experiment, there was a strong magnetic field oriented in the direction perpendicular to the sample. A voltage difference was then applied to two ends of this sheet. The (non-quantum) Hall Effect was a known, century old phenomenon at the time which says that, in such a system, there will be a current due to the magnetic field which flows in a direction perpendicular to the voltage difference in addition to the normal current which flows in the direction of the voltage difference. This perpendicular, or transverse, current is proportional to the difference in the voltage across the sample with the Hall resistivity ρ_{xy} being the ratio between these quantities. The standard Hall Effect prediction is that ρ_{xy} is proportional to the magnetic field. However, Tsui, Störmer, and Gossard found that their results were in stark contrast with this prediction once the magnetic field was strong enough such that there were three quantized magnetic fluxes per electron. It was found that the plot of Hall resistivity ρ_{xy} vs. the magnetic field B leveled out at this point, which is referred to as the $\nu = 1/3$ filling fraction. This value of ρ_{xy} seemed to be robust to small changes in the magnetic field strength. This is the kind of robustness that was normally associated with a phase of matter. However, there was no apparent symmetry being broken when perturbing away from this plateau, and thus, Landau's paradigm of phase transitions didn't seem to play a role.

Two years later, in 1983, an explanation was offered by Robert Laughlin in another letter for the so-called "1/3" effect [82]. Laughlin wrote down his famous wavefunction which described the state of the electrons in that mysterious experiment. This state represented

a totally new phase of matter. In fact, if instead of having a filling fraction of $\nu = 1/3$, we had $\nu = 1/m$ for any odd integer m, we would have yet a different phase of matter. The transitions between these phases of matter did not seem to have anything to do with symmetry. Rather, the phases were distinguished by the Hall conductance ($\sigma_{xy} = 1/\rho_{xy}$) which was quantized and took on the specific value $\frac{1}{m}e^2/h$, where e is the charge of an electron and h is Plank's constant. Unlike the Landau paradigm where the phases were marked by order parameters, these phases were now marked by some special discrete number $1/m$.

In addition to explaining this phenomenon, this paper also showed that this system could have emergent localized excitations with a fractional charge of $1/m$. Although it was not realized at the time, these quasiparticles also had fractional statistics making these particles a generalization of the classification of all particles into bosons and fermions. Eventally, these quasiparticles would be called anyons [158] which had actually been previously imagined by Jon Magne Leinaas and Jan Myrheim in 1977 as a purely theoretical exercise [83].

The standard description of states with multiple identical particles, which persists to the present day, relies on labeling the various particles in the system with indices and insisting that the observable characteristics of the wavefunction are invariant to the permutation of the particle indices. However, interchanging these particle labels has no physical meaning and so this invariance "at most reflects the redundancy in the notation" [83]. Disturbed by this, Leinaas and Myrheim set out to put the foundations of several-body quantum mechanics on a more firm foundation. At the heart of their solution was the realization that a system of two identical particles in n dimensional Euclidean space could be described by the "relative space" $r(n, 2)$ whose coordinates were the center of mass and displacement vector $\boldsymbol{x}$ between the two particles. They then considered swapping the two particles via a process of parallel transport. From this, they were able to recover the classic result that in three spatial dimensions and greater, the result of swapping two particles results in the wave function picking up a phase of ± 1, corresponding to two identical bosons or fermions,

respectively. However, in one and two spatial dimensions, they found that more possibilities were allowed because the space $r(n,2)$ minus the point $\boldsymbol{x} = 0$, where the particles' positions are coincident, is no longer simply connected. In these cases, swapping the particles could result in the wavefunction changing by some other complex phase $e^{i\phi}$ which gives these particle a character that interpolates between bosons and fermions. In 1982, Frank Wilczek would dub these particles "anyons" due to the fact that their exchange statistics could be of any phase $e^{i\phi}$ [158][3]. Although the Leinaas-Myrheim view that the statistics of these anyons could be seen via parallel transport was revolutionary, it wouldn't be until 2003 that there was a precise, microscopic definition of these statistics in physical systems [86]. Furthermore, the statistics from braiding two distinct anyons around one another was not precisely defined in general condensed matter systems until 2020 in the paper corresponding to Chapter 3 of this thesis. In this chapter, we discuss the precise definitions of all of the data which describe systems with anyons.

Although Laughlin did not cite Leinaas and Myrheim or Wilczek, Laughlin's quasiparticles that he found in describing the wavefunction of the Tsui, Störmer, and Gossard observation were actually an example of the anyons that Leinaas and Myrheim had imagined. Additionally, Wilczek's idea that these anyons could be constructed as "flux-tube-particle composites" would later turn out to be the phenomenon that gives rise to anyons in the $\nu = 1/3$ FQH system [159, 158, 4].

1.4 Topological Quantum Field Theory

With the discovery of the Fractional Quantum Hall states in the early 80's, the field was in need of a framework with which to understand these results. In 1989 and 1990, there

3. Wilczek intended for this to be a joke since, technically, every particle is an anyon. Some anyons just happen to be bosons or fermions. We will see that there is actually a meaningful distinction between "trivial" bosons and fermions and those that are topologically interesting and are usually labeled as (non-trivial) anyons.

was a series of influential theoretical works which helped find that framework. In September of 1989, Edward Witten published his famous paper on the relationship between the Jones polynomials of knot theory and quantum field theory [161]. One of the implications of this paper for physics was the invention of Topological Quantum Field Theories (TQFTs). These theories enjoyed general covariance, but unlike other theories with this property, these theories did not depend on the metric. Therefore, the partition function of these theories depended on topology rather than geometry. These topological field theories would later be connected with the theory of the Fractional Quantum Hall Effect.

One short month after the publication of Edward Witten's paper on Jones polynomials, in October 1989, Xiao-Gang Wen submitted his paper, which would be published in 1990 [148], and helped to establish the foundations of the modern notion of intrinsically topologically ordered phases [15, 23]. In this paper, Xiao-Gang Wen considered the role of topology in what he called "rigid states." Rigid states have no gapless excitations. One of the characteristics of these theories is that their ground state denereracy on various closed manifolds helps us to probe the theory. In particular, the ground state degeneracy of these theories seemed to be highly robust to perturbations and could be used to distinguish between different phases of matter which he called "topological orders." However, Wen realized that this was only the beginning of the story. He considered the space of theories of rigid states where one varies the parameters of these theories. This is an example of a moduli space. Wen's insight was that studying the non-abelian gauge structure on these moduli spaces revealed a significant amount of information about these rigid states. This included the braiding statistics of the quasiparticles found in the Laughlin state. Wen would later consider other pieces of topological data found on the edge states of these systems arising from the "collective dancing" of the two dimensional interior of a material [150]. Furthermore, it was seen that these theories could be generated on the lattice from the topological data [88]. In this thesis I will reverse this task and show how to define this topological data in terms of

microscopic models.

The topological data that describes intrinsic topological phases is usually called an "anyon theory" which is a type of mathematical object from category theory (see Sec. 2.2 for a brief review). I will not describe this object in full, but I will take the time here to review some of references that introduced this category theoretic language into topological physics. In 1988 and 1989, Gregory Moore and Nathan Seiberg published a pair of papers which introduced some of the categorical structures we see in anyon theories [103, 104]. In Appendix E of his 2006 paper [74], Alexei Kitaev gave an exposition of the mathematical structure of anyon theories in terms of category theory and cited a variety of more mathematical resources which helped develop the formalism of anyon theories [116, 41, 141, 138]. Chapter 9 of John Preskill's lecture notes are a resource for the structure of anyon theories in a more physical language [112]. Xiao-Gang Wen's review in Ref. [157] gives an overview of the terminology used to label various phases and helps to disambiguate the terms used in the literature.

1.5 Symmetry after Landau

Although I have just presented a story about how phases of matter can be described without invoking symmetry, there is a parallel story to be told about how symmetry takes on a new character in light of topology. Rather than invoking symmetry for the purposes of symmetry breaking, we may invoke it in the context of topological phases of matter by asking, "What phases exist if we have symmetry, but insist on not breaking it?" This is the fundamental question to which symmetry protected topological phases are the modern answer. The history of these phases of matter starts in roughly the same period as the intrinsic topological phases of matter. However, unlike topological order, the history of symmetry protected topological phases starts with theoretical discoveries, namely, topological insulators [66, 43] and the AKLT [2, 3] analysis of the Haldane phase [50, 51].

Although there were many other theoretical developments along the way [114, 53], we

will now turn our attention to the work of Chales Kane and Eugene Mele from 2005 [66] and Liang Fu, Chales Kane, and Eugene Mele from 2007 [43] where they constructed the first topological insulators and the invariants which could distinguish topological insulators from trivial (atomic) insulators. Importantly, these theories are time reversal invariant which distinguished them from the previously known Chern insulators. Fu, Kane, and Mele came up with invariants that could distinguish between the two possible phases with this symmetry in both (2+1)D and (3+1)D[4]. In the (2+1)D case, they studied graphene and defined a quantity akin to the Chern number which is an integer used to classify Chern insulators via band theory. Due to the time reversal symmetry which is inherent to topological insulators, however, this integer only had meaning modulo 2 in this context. This allowed them to distinguish the trivial insulator from the topological insulator. This work helped us to understand the classification of non-interacting theories where band theory approaches were applicable. The interacting generalization of this story would be discovered years later.

An example of an SPT which predates the topological insulator is the AKLT (Affleck-Lieb-Kennedy-Tasaki) chain which was inspired by work from F. Duncan Haldane from 1982. In this work, Haldane realized that the continuum limit of an antiferromagnetic 1D chain of integer (as opposed to half-integer) spins could be mapped to a non-linear sigma model with $O(3)$ symmetry [51]. This, he argued, showed that there was a finite energy gap between the ground state and the elementary excitations of the theory. Additionally, this implies that correlations in the ground state decayed exponentially. This was highly surprising since Hans Bethe had famously shown that in the spin-1/2 case [11], there was no gap and there was power-law decay of correlations in the ground state. At first glance, one might guess that a state with these properties is just an atomic insulator, which was well-understood at that point. However, it would later be realized that this is the first example of a symmetry protected topological state.

4. In the (3+1)D case, Ref. [43] discusses four phases. However, as they mention, there are only two phases of "strong" topological insulators which don't require translation symmetry.

After this work by Haldane, Ian Affleck, Elliott H. Lieb, Tom Kennedy, and Hal Tasaki (AKLT) published an exactly solvable model which offered an explanation for Haldane's observation [2, 3]. Although they analyzed 1D spin chains of arbitrary spin s, their insight into Haldane's result can be summarized in terms of their analysis of their model of the spin 1 chain which would later be called the AKLT model. They were able to rigorously prove that this system was gapped and that the correlation between spins decayed exponentially with distance.

AKLT conjectured that the ground state of their model served as a good variational ground state for the spin 1 antiferromagnetic 1D chain which was studied by Haldane. Furthermore, they generalized the model into a 1 parameter famly of models and constructed a phase diagram which exhibited a phase transition without symmetry breaking. These models all had $SO(3)$ symmetry and it was suggested that almost all of these models were gapped. However, AKLT knew that there was a gapless model in this phase diagram which had been solved using the Bethe Ansatz. This singular point represented the gapless critical point separating two gapped phases with the AKLT side of this transition representing the topologically non-trivial phase. This would later be recognized as an example of a bosonic SPT.

In 2010, multiple concurrent papers generalized the AKLT phase diagram and the classification of topological insulators by inventing, at least in (1+1)D, the notation of SPTs, which often stands for Symmetry Protected Topological phases [23, 40, 110]. However, in many of Xiao-Gang Wen's papers, he refers to these as Symmetry Protected *Trivial* phases and the reason for this is very informative. If we think back to the analysis by Haldane and AKLT, the correlations in the system decayed exponentially. This is also the case in the topological insulator. So, in the sense of intrinsic topological order, these phases are trivial. That is, these states can be adiabatically deformed into the product (atomic insulator) state without closing the energy gap. However, these systems were non-trivial in that they could

not be connected in this way to the product state without breaking the symmetry or closing the gap. For instance, in the AKLT phase diagram, the two gapped phases were separated by a gapless model. The invention of SPT order now had generalized the idea that there were phase transitions with symmetry which did not require symmetry breaking. Rather, between two distinct phases, the closing of the energy gap while preserving the symmetry represented the critical point. In Refs. [26, 120, 28], it was proposed that these phases, at least in the case of bosonic phases of matter, such as the AKLT model, could be classified in any dimension by a mathematical formalism called group cohomology. In particular, each phase in d+1 dimensions with a symmetry group G is identified with a function $\omega : G^{d+1} \to U(1)$, up to some equivalence relations and with some restrictions, called a cocycle. They showed that a lattice model could be constructed from each distinct cocycle. In their 2011 paper, it was shown how to extract the cocycle from the microscopic models they generated in (2+1)D. Additonally, in 2014, Dominic Else and Chetan Nayak showed how to calculate the cocycle in (2+1)D in a large class of models and in higher dimensions for a more limited class of models [39]. In Chapter 4, we show how to calculate this cocycle from the boundary theory of (2+1)D bosonic SPTs in any phase. We also generalize this story to fermionic SPTs in (2+1)D in Chapter 5.

1.6 Purpose of this thesis

The developments over the past four decades have left us with a very good understanding of the classification of topological phases of matter in (2+1)D. For each type of topological phase (anyon theories, symmetry protected topological phases, and symmetry enriched topological phases), we have a complete (or nearly complete) set of topological invariants which distinguish the various associated phases of matter. However, while many of these invariants are associated with physical processes, such as the braiding of anyons, there had been relatively little work on the precise definitions of these data in physical systems. In

particular, there was no set definition of the anyon data in which could be applied to a given microscopic model, say on the lattice. The goal of this thesis is the following: When given a microscopic model of a topological phase of matter how can we answer the question "What is this?" We answer this question for two types of (2+1)D topological phases: (i) intrinsic topological phases with anyon excitations and (ii) symmetry protected topological phases.

Intrinsic topological phases in (2+1)D are characterized by:

1. Anyon Types $\mathcal{M} = \{a, b, c, ...\}$
2. Fusion Rules $a \times b = \sum_{c \in \mathcal{M}} N_c^{ab}$
3. R-Symbol
4. F-Symbol

The anyon types are the various equivalence classes of excitations which cannot be related to one another by using local operators. When two anyons are near each other, we can ask what anyon type is represented by the sum total of the pair of anyons. We can think of this as two anyons being fused together and the result is described by the fusion rules. The R-symbol describes the non-trivial statistics associated with braiding anyons around one another. Finally, the F-symbol describes how to relate the various states with three anyons, say with types a, b, c, to one another. In Chapter 3, we will show how to identify these four pieces of data in any given microscopic model. A definition of the R and F-symbols are the main focus of this chapter. The text in this chapter is taken directly from Ref. [69]

The next chapter is focused on (2+1)D bosonic SPT phases. This chapter is taken from the paper Ref. [70]. Bosonic SPT phases are classified by group cohomology. I review this classification in Sec. 2.3.1. To summarize, if the symmetry group of the theory is G, then there is a function called a cocycle $\omega : G \times G \times G \to U(1)$ that characterizes each phase of matter [28]. In Ref. [26], the authors showed how to extract this datum in the context of tensor network theories. Later, Ref. [39] showed how to extract this data on the boundary of

certain SPTs by considering the action of the symmetry on the boundary. However, neither of these works defined this cocycle in the case of general anti-unitary symmetries. In Chapter 4, we show how to use the F-symbol formalism from Chapter 3 to define the cocycle ω. In particular, we consider the G-valued domain walls on the boundary which fuse according to the group law and compute their F-symbol. This method works not just in the case of unitary symmetries, but also for anti-unitary symmetries. Additionally, we show that any time the procedure in Ref. [39] can be used, our method can also compute ω and our result matches with theirs.

In the final substantive chapter, Chapter 5, we show how to define the data in (2+1)D fermionic SPT phases[5]. This chapter is from a portion of my upcoming work with Michael Levin Ref. [71]. The data that describes fermionic SPT phases is reviewed in Sec. 2.3.2.

By providing a precise and careful definition of the topological data in microscopic models, we have established a program of research which seeks to bring the physical and mathematical views of topological phases of matter into closer connection. This is the aim of this thesis.

5. We exclude the case where there are Majorana degrees of freedom on the boundary in this thesis. We will explore this case in our upcoming work [71].

CHAPTER 2

REVIEW OF TOPOLOGICAL PHASES OF MATTER

2.1 Entanglement

Entanglement is a way of describing shared information between different parts of a quantum system. The most basic example of entanglement is a pair of spin-1/2 particles in a state called an Einstein-Podolsky-Rosen (EPR) pair. This state is of the form

$$|\text{EPR}\rangle = \frac{1}{\sqrt{2}} \left(|\uparrow\rangle |\downarrow\rangle - |\downarrow\rangle |\uparrow\rangle \right). \tag{2.1}$$

In this state, if we measure the first spin to be up, then the second spin will be down. Likewise, if we measure the first spin to be down, the second will be up. These two possibilities occur with probability $\frac{1}{2}$, but the probability of the spins being in opposite spin states is 1. So, even with the randomness inherent in quantum systems, there can be extremely strong correlations in entangled systems.

Topological systems use entanglement to create large scale effects by imposing local rules via a local Hamiltonian. In particular, topological systems have a variety of interesting phenomena such as robust edge modes, fractionalized charge, and bulk excitations which cannot be destroyed locally.

2.2 Intrinsic Topological Order

We say that a system is intrinsically topologically ordered if it is (i) gapped and (ii) long range entangled. I will now describe these two conditions. Gapped systems are quantum systems in which there are a finite number of ground states and there is a "gap" in the spectrum between the ground state energy and the energy of the first excited state. Importantly, we require that both of these statements are true even in the limit as the system size grows to

infinity.

Secondly, long range entangled systems are systems whose ground state is entangled and there is no way to continuously deform the Hamiltonian such that the ground state becomes a product state without closing the gap.

Formally, we define the long range entangled property of a topological system by first defining what we mean by *short* range entanglement (SRE). Let H be a local gapped Hamiltonian on the Hilbert space $\mathcal{H}$. We can extend this system by adding ancillary qubits. This gives us a Hilbert space $\mathcal{H}_{tot} = \mathcal{H} \otimes \mathcal{H}_{anc}$ where we impose that the qubits which make up $\mathcal{H}_{anc}$ are associated with positions in space for the purpose of locality. We also have a Hamiltonian $H_{tot} = H \otimes I_{anc}$ where I_{anc} is the identity operator on on the ancillary Hilbert space. Define an interpolating Hamiltonian

$$G : [0, 1] \to Ham \tag{2.2}$$

where Ham is the space[1] of all gapped Hamiltonians on $\mathcal{H}_{tot}$ and G is continuous. We say that the original system with Hamiltonian H is short range entangled if we can define an ancillary Hilbert space $\mathcal{H}_{anc}$ and interpolating Hamiltonian G such that that $G(0) = H_{tot}$ and $G(1) = H_{prod}$ where H_{prod} is a Hamiltonian whose ground state is a product state[2]. Thus, a long range entangled system is one for which such an interpolation to a product state doesn't exist. We call these systems intrinsically topologically ordered.

1. By calling Ham a space and invoking a notation of continuity, I am implying that it has a topology. In lattice models with a finite dimensional Hilbert space on each site, I am taking it to be a topology such that, when projected onto the operator space on any finite region of the lattice, it reproduces the standard topology. Any further discussion of functional analysis would take us beyond the scope of this thesis.

2. The usual notion of product states for bosonic systems can be suitably generalized for fermionic systems.

2.2.1 Abelian Anyon Theories

The definition of long range entanglement naturally lends itself to a definition of equivalence classes of distinct topological phases. In particular, we say that two gapped systems are in the same topological phase if we can interpolate between the two systems without closing the gap using ancillary qubits and an interpolating Hamiltonian. It has been one of the major achievements of condensed matter theory to create a classification for a large class of the intrinsic topological phases in (2+1)D. This classification is achieved by distinguishing theories by the properties of their anyons. The collection of these properties is called an anyon theory [74, 112].

Anyons are excitations in intrinsically topologically ordered systems. They can be thought of as a generalization of the notion of bosons and fermions. For instance, if we consider two identical bosonic excitations, we can swap them by moving them in space such that their locations are exchanged. The defining property of bosons is that the wave function should remain invariant under this change. On the other hand, if we swap two fermions, the wave function should change by $\psi \to -\psi$. Swapping anyons, in general, can result in any phase change $\psi \to e^{i\theta}\psi$. This phase is called the "self-statistics" and are a characteristic property of each type of anyon. We will see that anyons actually have many interesting properties that distinguish them from bosons and fermions. In fact, in perhaps the most famous example of a solvable topological model, the toric code, the anyons actually have self-statistics that look like bosons and fermions. However, if we treated the particles that look like bosons in this point of view as bosons, then we would find that two of these "bosons" could fuse together to look like a fermion. This is a tell-tale sign that anyons are far more exotic than bosons and fermions, even when their statistics match those of bosons and fermions.

The classification of anyon theories says that for any two theories in the same intrinsic topological phase, these theories have anyons which are equivalent. The converse is still a conjecture, although it is widely believed to be true.

At this point, I will introduce the rough notion of an "abelian anyon theory." Anyon theories are comprised of four pieces of data which I will explain shortly:

1. Anyon Types $\mathcal{M} = \{a, b, c, ...\}$
2. Fusion Rules $a \times b = c$
3. R-Symbol $R : \mathcal{M} \times \mathcal{M} \to U(1)$
4. F-Symbol $F : \mathcal{M} \times \mathcal{M} \times \mathcal{M} \to U(1)$

The anyon types are the excitations of the system which cannot be destroyed by a local operator. Additionally, an anyon of type "a" cannot be transmuted into another anyon type "b" by any local operator. For example, in a $\nu = 1/3$ Fractional Quantum Hall (FQH) system, there are two non-trivial anyons [82]. The first non-trivial anyon of type t has a charge of $1/3$. Since the total charge of the system is an integer, there is no way to annihilate one third of a charge or turn it into a $2/3$ charge which we will call t^2; we can only move it around. There is also an anyon with a charge of $2/3$ which can be thought of as two of the first type of anyon. There is also the trivial anyon which is included in M, but can be thought of as the absence of an anyon. Its meaning will become more clear in the following paragraph where I describe the fusion rules.

The fusion rules tell us how to combine two nearby anyons into one anyon. That is, if we consider a state with two nearby anyons, we can use local operators to bring these two anyons together and we can assign an anyon type to the resulting composite excitation. We denote the fusion of anyons of type a and b into an anyon of type c by $a \times b = c$. In the $\nu = 1/3$ Fractional Quantum Hall example, we have the fusion rule $t \times t = t^2$. This corresponds to fusion two anyons of charge $1/3$ into one of charge $2/3$. The fusion rules also give meaning to the "trivial" anyon in $\mathcal{M}$. The trivial anyon, which we will call 1, has the fusion rules $1 \times a = a \times 1 = a$ for any anyon a.

The R-symbol describes the most well-known property of anyons. This property is that exchanging two identical anyons can result in a change to the wave function which is not just a multiplication by ± 1. Instead, the process of exchanging two a anyons results in a complex phase of $R(a,a)$ being applied to the original wave function. However, we will see that this interpretation of the R-symbol is actually too naive to be used as is. For instance, the t anyon in the $\nu = 1/3$ FQH state, is expected to have $R(t,t) = e^{i2\pi/3}$. However, in the presence of an additional magnetic field, we would also accrue an Aharanov-Bohm phase related to the flux enclosed by the area encircled by the two t anyons. This is an indication that we must be more careful with the definition of the R-symbol. We will present the solution to this problem in Chapter 3, which was first discovered in Ref. [86]. So far, we have only described $R(a,a)$ which describes the exchange statistics of a. However, there is an interpretation of $R(a,b)$ as a half braid where as $R(a,b)R(b,a)$ can be seen as the phase accumulated by braiding b completely around a. To be more specific, consider one process where we take an anyon of type ab and split (the opposite of fusion) it into anyons of type a and b at positions x and y, respectively. We can compare that to a state where we split ab into b and a at x and y and then exchange the two anyon positions so that we again have a and b at x and y, respectively. $R(a,b)$ is the phase difference between these two states. Again, we will examine the details of this problem in Chapter 3. Unlike the self-statistics, however, the microscopic definition of this datum was previously unknown.

Lastly, we have the F-symbol, the most subtle piece of anyon data. Like the R-symbol, it is a complex phase represented by a physical process. The fusion of anyons is associative. This means that $(a \times b) \times c = a \times (b \times c)$. If we consider fusion as a physical process, we can fuse a and b using a local operator, and then fuse the resulting anyon with c using another local operator. We can also consider a state where we fuse b and c and then fuse the result with a. Comparing these states, we find that they are the same, up to a complex phase. This phase is called the F-symbol. However, just like the R-symbol, we must take care to

define the F-symbol in a way that is not ambiguous. This is described in Chapter 3.

These four pieces of data describe an abelian anyon theory. As I mentioned previously, if we consider two physical systems with different anyon data, then we know that they must be in different topological phases of matter. The main theme of Chapter 3 will be to show how to extract this data from a given physical model in a well-defined way.

2.2.2 Non-Abelian Anyon Theories

In the previous subsection, I described the data in abelian anyon theories. These are called abelian theories because they often arise from abelian gauge theories. However, there are also non-ablian anyon theories which often come from non-abelian gauge theories. I will now describe the four pieces of data for non-abelian anyon theories. There is no change to the notion of anyon types, so we will proceed right to the description of the fusion rules.

In non-abelian anyon theories, the fusion of anyons a and b no longer has a unique outcome. To describe this precisely, let's compare two states in a given theory, each with an anyon a at the point x and an anyon b at the point y which is many correlation lengths away from x. We will enforce that the local density matrices of these two states are identical in any simply connected region containing at most one of these two anyons. Naively, we would expect that these two states are the same. However, in non-abelian anyon theories, it is possible for these two states to be different. It is possible that in these two seemingly identical states, the fusion of the two anyons yield different results. We can measure this by braiding another anyon around these two anyons in each state and comparing the braiding statistics (which are still well-defined in non-abelian anyon theories, as we will see).

In addition to the fusion of anyons not having a unique outcome, there is additional non-local data being stored in states with two anyons. Consider the same set up as before, where we have two states which are locally distinguishable, each with anyons a and b which are well-separated at positions x and y, respectively. This time, however, we will impose

that in both states, these anyons fuse into some anyon c. Even in this case, our two states might not be identical. There is additional non-local information being stored between our two anyons. In particular, there is a subspace spanned by all such states with dimension N_c^{ab}. Let's call this space V_c^{ab}. We then denote the fusion rules by

$$a \times b = \sum_{c \in \mathcal{M}} N_c^{ab} c \tag{2.3}$$

where $N_c^{ab} = 0$ if a and b cannot fuse into an anyon of type c. Although these anyons are called "non-abelian," we still have

$$\begin{aligned} a \times b &= b \times a \\ N_c^{ab} &= N_c^{ba} \end{aligned} \tag{2.4}$$

In the following paragraphs, we will see how $N_c^{ab} > 1$ changes the R and F-symbols.

In the case where $a \times b = c$, the R-symbol $R(a, b)$ has the same definition as the abelian case. However, it may be that there are multiple possible results for the fusion of a and b or it may be that $N_c^{ab} > 1$ for some c. In this case, we will label the R-symbol as R_c^{ab}. However, now, R_c^{ab} is not just a complex phase; it will be a unitary matrix of dimension N_c^{ab}. Let's consider the following scenario to motivate why this might be. If we have a state with anyons of type a and b, then even when a and b fuse to a particular anyon c, there are still N_c^{ab} different states distinguished by non-local information. If we braid the b anyon around the a anyon, it is possible that we end up in a different state in V_c^{ab} than we started in. Ensuring that this transformation preserves the magnitude of the state, this process must be described by an $N_c^{ab} \times N_c^{ab}$ unitary matrix. This is the matrix $R_c^{ba} R_c^{ab}$. This is not a proof, but it does lend credence to the idea that R_c^{ab} should be a unitary matrix of dimension N_c^{ab}. Now, let's consider two processes where we split an anyon of type c into anyons of type a and b: (i) split c into a and b at positions x and y, respectively; (ii) split c into a and b at

positions y and x, respectively, and then swap their locations so that a is at x and b is at y, just as in (i). In the first process, we are considering a state in the subspace V_c^{ab}. Let's take this to be the νth basis state of this space. The second process starts by splitting c into the anyons b and a so that we are in the subspace V_c^{ba}. Let's take this state to be in the μth basis state of this space. The anyons b and a are then exchanged so that a and b are in the same position as in the first process. The inner product between these two states gives the complex number $\left(R_c^{ab}\right)_\nu^\mu$.

Similarly to the R-symbol, the F-symbol will also be promoted to a matrix. In particular, we will consider the following two processes where we start with anyon an anyon of type f and split it into anyons of type a, b, c: (i) split anyon f into d and c and anyon d into anyons a and b; (ii) split anyon f into a and e and anyon e into anyons b and c. We will use these two processes to define the F-symbol F_{def}^{abc}. As a matter of accounting, we now need to consider the number of states with anyons a, b, c at fixed points in space. By considering all ways to perform the two processes described, consistency requires that

$$\sum_{d\in\mathcal{M}} N_d^{ab} N_f^{dc} = \sum_{e\in\mathcal{M}} N_e^{bc} N_f^{ae} \tag{2.5}$$

Physically, when we split f into a, b, c, in the first process, we have to choose an intermediate state in V_f^{dc} and then a final state which puts the a and b anyons in V_d^{ab}. We will choose the νth basis state of V_f^{dc} and the μth basis state of V_d^{ab}. In the second process, we must choose an intermediate state in V_f^{ae} and then a final state which puts the b and c anyons in V_e^{bc}. We will choose the λth basis state of V_{ae} and the κth basis state of V_e^{bc}. The inner product of the final state in these two processes is the complex number $\left(F_{def}^{abc}\right)_{\mu\nu}^{\kappa\lambda}$.

In Chapter 3, Section 3.6, we will show that a microscopic definition of this non-abelian anyon data is actually just as simple as defining the anyon data microscopically in the abelian case.

2.3 Symmetry Protected Topological Phases

Symmetry protected topological phases of matter are gapped theories which are trivial in the sense of intrinsic topological order, but are symmetry protected. In this chapter, I will describe what I mean by this statement as well as provide some basic background for these theories and their status as non-trivial topological phases.

In the definition of intrinsic topological phases, we defined long range entangled systems as those which cannot be continuously connected to the trivial system without closing the gap. Short range entangled systems are those which are not long range entangled. Symmetry protected topological phases are a case of short range entangled systems which are interesting. In particular, we define a symmetry protected topological phase as one that is short range entangled, but cannot be continuously connected trivial state without breaking the symmetry. Hence, these systems are "symmetry protected" from being totally trivial.

One famous example of a symmetry protected phase is the topological insulator. This is a short range entangled system which is protected by time reversal and charge conservation symmetries. In (2+1)D, we can detect the non-trivial nature of this system by counting the number of edge modes in this system. It turns out that trivial insulators with these symmetries have 0 mod 4 edge modes, but topological insulators have 2 mod 4 edge modes. This is a band theory approach to detecting and classifying non-trivial SPTs, which means that such types of analysis can only work in non-interacting fermion theories. I will now introduce the classification of these theories in the case of interacting bosonic and fermionic SPTs.

2.3.1 Classification of Bosonic SPTs

In a bosonic SPT, we constrain our local degrees of freedom to be bosonic. As a consequence of this notion of locality, the operators which we define to be local are fermion parity even. In the case of fermionic SPTs, this constraint will be lifted and will give rise to a different

and rich classification of SPTs. For now though, we will stick with the bosonic case.

Although there is a rich literature of all kinds of bosonic SPTs for many types of symmetries [28, 128, 97, 134], we will be primarily concerned with "on-site" symmetries. These are symmetries which act in the bulk of an SPT as the product of operators in the neighborhood of each bulk lattice site. The spin flip symmetry of the paramagnet is an example of an on-site symmetry. I am explicitly barring symmetries such as translation symmetry and point group symmetries as these cannot be written as a product of local operators.

It is known that bosonic SPTs with on-site symmetries are classified by a mathematical structure called group cohomology [28].

I will present an introduction to a particular form of group cohomology here. Let's work with discrete symmetry groups G for now. First, recall that an abelian group M is a $G-$module if it has a linear group action under the elements of G. That is, $g(a+b) = (ga) + (gb)$ for elements $g \in G$ and $a, b \in M$. We will define group cohomology for the G-module M. In the case of bosonic SPTs, we will always take M to be $U(1)$, but we keep the discussion general here as it will be useful in the fermionic case. We will work with additive notation for now, although we will switch to multiplicative notation when applying this to bosonic SPTs since the elements of $U(1)$ will be represented by complex phases.

Given a discrete group G and a $G-$module M, we will call functions

$$f : G^n \to M \tag{2.6}$$

cochains. The collection of all such cochains is $C^n(G, M)$. There is an operation on cochains called the coboundary

$$d^{n+1} : C^n(G, M) \to C^{n+1}(G, M) \tag{2.7}$$

It has the action

$$(d^{n+1}f)(g_1,...,g_{n+1}) = g_1 f(g_2,...,g_{n+1} + \sum_{k=1}^{n}(-1)^k f(g_1,...,g_{k-1},g_k g_{k+1},g_{k+2},...,g_{n+1}) + (-1)^{n+1} f(g_1,...,g_n) \tag{2.8}$$

where we are using + to denote the group multiplication of M.

n-Cocycles are n-cochains f for which $d^{n+1}f(g_1,...,g_{n+1}) = 0$ where 0 is the identity element of M. We label the group of cocycles as

$$Z^n(G,M) = ker(d^{n+1}) \tag{2.9}$$

n-Coboundaries are n-cochains f such that there exists an $n-1$-cochain g with $d^n g = f$. We label the group of coboundaries as

$$B^n(G,M) = Im(d^n) \tag{2.10}$$

The group cohomology of the group G is a collection of groups $H^d(G,M)$ where

$$H^d(G,M) \equiv \frac{Z^d(G,M)}{B^d(G,M)} \tag{2.11}$$

That is, elements of $H^d(G,M)$ are equivalence classes of cocycles where the equivalence class equates two cocycles if they differ by a coboundary.

Bosonic symmetry protected topological phases with symmetry group G in d spatial dimensions with on-site symmetry are classified by $H^{d+1}(G,U(1))$. In particular, each distinct symmetry protected topological phase of matter of this type can be identified by a cocycle in $H^{d+1}(G,U(1))$. In Chapter 4, I will show how this cocycle can be computed from the boundary theory of such a bosonic SPT in $2+1$D. This shows that the bulk phase of an SPT

can be computed from its microscopic boundary theory. Moreover, to compute this cocycle in practice, we will only need to know how the symmetry acts on a small number of local operators on the boundary.

To be more precise, in the context of bosonic SPTs, we are choosing $U(1)$ to be the trivial G-module (the group elements act as the identity function) if the symmetry group is unitary. If there are anti-unitary symmetry group elements, such as time reversal, then these anti-unitary symmetry group elements act as complex conjugation on elements of $U(1)$ interpreted as complex units. Additionally, although the above discussion was for discrete symmetry groups, this formalism can be generalized to continuous groups by requiring that every cochain is Borel measurable.

2.3.2 Classification of Fermionic SPTs

I will now review the classification of fermionic SPTs in (2+1)D [47, 68, 35, 146, 147]. These theories have local fermionic degrees of freedom. Additionally, fermion parity symmetry is a normal subgroup of the full symmetry group G. This is represented by a $\mathbb{Z}_2$ extension

$$\mathbb{Z}_2 \to G \to G_0 = G/\mathbb{Z}_2^F \tag{2.12}$$

generated by the cocycle $\lambda \in H^2(G_0, \mathbb{Z}_2)$. In particular, the elements of G can be represented by a pair (g, s) where $g \in G_0$ and $s \in \mathbb{Z}_2^F = \{0, 1\}$ with the group multiplication law

$$[g, s] \cdot [h, t] = [gh, s + t + \lambda(g, h)] \tag{2.13}$$

With this structure in mind, I will now describe the supercohomological classification of fermionic SPTs [47]. I will follow up this discussion with a beyond supercohomology generalization. Within supercohomology, the fermionic SPTs are labeled by a pair of data

(ρ, ν) where $\rho \in Z^2(G_0, \mathbb{Z}_2)$ and $\nu \in C^3(G_0, U_T(1))$. ν is subject to the constraint

$$d\nu(g,h,k,l) = e^{(\rho(g,h)+\lambda(g,h))\rho(k,l)} \tag{2.14}$$

Furthermore, (ρ, ν) is equivalent to (ρ', ν') if

$$\rho(g,h) - \rho'(g,h) = \mu(g) + \mu(h) + \mu(gh) + s\lambda(g,h) \tag{2.15}$$

and

$$\begin{aligned}\frac{\nu(g,h,k)}{\nu'(g,h,k)} =& \frac{e^{i\alpha(g,h)}e^{i\alpha(gh,k)}}{(ge^{i\alpha(h,k)})e^{i\alpha(g,hk)}} \\ & \cdot (-1)^{(\rho(g,h)+\lambda(g,h))\mu(k)+\mu(g)(\rho(h,k)+(d\mu)(h,k))} \\ & \cdot (-1)^{s(\rho(gh,k)\lambda(g,h)+\rho(g,hk)\lambda(h,k))}\end{aligned} \tag{2.16}$$

for some cochain $\mu : G_0 \to \mathbb{Z}_2 = \{0, 1\}$, for some cochain $\alpha : G_0 \times G_0 \to U(1)$, for some number $s \in \{0, 1\}$, and where g acts as complex conjugation if $(g, 0) \in G$ is anti-unitary. Each equivalence class of these pairs of data specifies a different fermionic SPT.

There is also a classification of fermionic SPTs that goes beyond supercohomology. In this case the data is now represented by a triple (η, ρ, ν). Although I will not analyze this case in the thesis, it will be addresseed in an upcoming work with Michael Levin [71]. The only beyond supercohomology case we will consider in that work is the one where G is unitary and is of the form $G_0 \times \mathbb{Z}_2^F$. In this case, ρ and ν are are constrained exactly as before and $\eta : G_0 \to \mathbb{Z}_2$ is a homomorphism. In this case, we say that (η, ρ, ν) is equivalent to (η', ρ', ν') if

$$\eta(g) = \eta'(g) \tag{2.17}$$

and

$$(\rho, \nu) \sim (\rho', \nu') \tag{2.18}$$

in the sense of supercohomology. This completes our review of the topological phases of matter discussed in this thesis.

CHAPTER 3

MICROSCOPIC DEFINITIONS OF ANYON DATA

This chapter is reprinted with permission from:

Kyle Kawagoe and Michael Levin. Microscopic definitions of anyon data. Phys. Rev. B, 101:115113, Mar 2020.

Abstract

We present microscopic definitions of both the F-symbol and R-symbol – two pieces of algebraic data that characterize anyon excitations in (2+1)-dimensional systems. An important feature of our definitions is that they are operational; that is, they provide concrete procedures for computing these quantities from microscopic models. In fact, our definitions, together with known results, provide a way to extract a *complete* set of anyon data from a microscopic model, at least in principle. We illustrate our definitions by computing the F-symbol and R-symbol in several exactly solvable lattice models and edge theories. We also show that our definitions of the F-symbol and R-symbol satisfy the pentagon and hexagon equations, thereby providing a microscopic derivation of these fundamental constraints.

3.1 Introduction

It is generally believed that every (2+1)-dimensional many-body system with local interactions and an energy gap can be associated with a corresponding anyon theory (also known as a unitary braided fusion category). This anyon theory consists of a collection of algebraic data characterizing the anyon excitations of the many-body system. More specifically, an anyon theory consists of three pieces of data: (i) a set of anyon types $\{a, b, c, ...\}$; (ii) a collection of "fusion rules" describing the outcomes of fusing pairs of anyons a, b; and (iii) an

"F-symbol" and an "R-symbol", which can be thought of as collections of complex numbers that describe fusion and braiding properties of anyons [74, 112, 42, 5].

The mapping between gapped many-body systems and anyon theories has proven to be a powerful tool in the theory of topological phases of matter and it has been applied successfully in many different contexts [4, 151, 73, 102, 61]. Nevertheless, this mapping is still missing an important ingredient, namely a systematic procedure for extracting anyon data from a microscopic model. Another way to say this is that we are lacking *microscopic* definitions of the anyon data, i.e. definitions that express each piece of data in terms of the underlying quantum many-body system. The goal of this paper is to find such definitions.

Our main results are microscopic definitions of both the F-symbol and the R-symbol. These definitions, together with the known definitions of anyon types and fusion rules[1], provide a way to extract a *complete* anyon theory from a microscopic model, at least in principle. To illustrate our definitions, we compute the F-symbol and R-symbol for several exactly solvable lattice models and edge theories. We also show that our definitions of the F-symbol and R-symbol have all the expected properties. In particular, we show that these quantities obey the pentagon and hexagon equations – algebraic relations that hold in any consistent anyon theory.

To get a sense of the problem that we address, consider one of the simplest pieces of anyon data: the exchange statistics of an Abelian anyon, a. Naively, one might try to define the exchange statistics, which we denote by $R(a,a)$, by considering an adiabatic process in which two identical a particles are exchanged with one another in the counterclockwise direction. One could then define $R(a,a)$ as the Berry phase accumulated during this exchange process. The problem with this definition is that the Berry phase for such a process will generally include a *geometric* phase, which depends on the details of the paths that the particles traverse, in addition to the statistical phase of interest. For example, if the anyon

1. See Secs. 3.2 and 3.6.1.

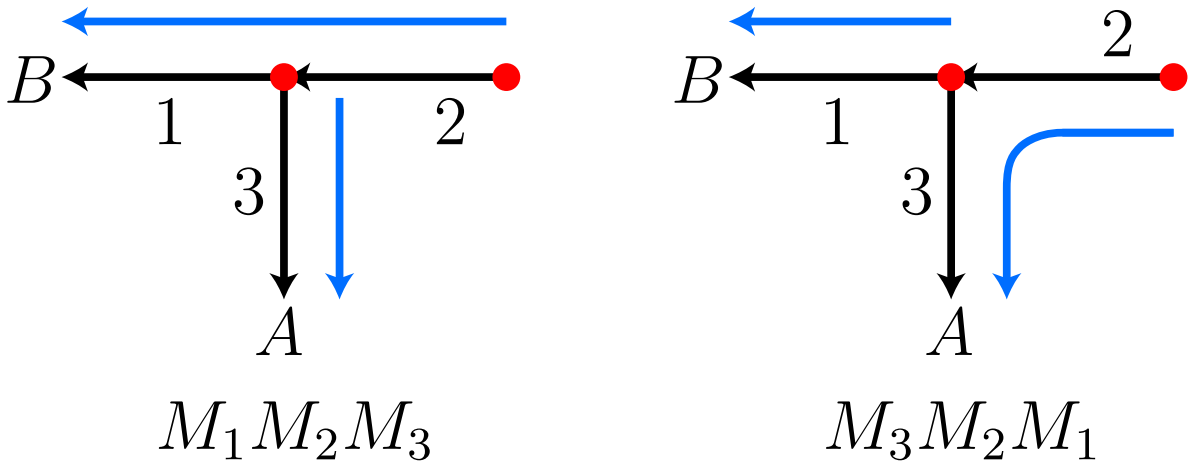

Figure 3.1: Two processes involving two identical Abelian anyons moving along three paths $1, 2, 3$. In the first process ($M_1M_2M_3$), the anyon on the left travels to point A and the anyon on the right travels to point B, and vice-versa in the second process ($M_3M_2M_1$). The final states of the two processes differ by $R(a, a)$, the exchange statistics of the anyons.

a is charged and there is an external magnetic field, then the Berry phase will contain a contribution coming from the Aharonov-Bohm effect.

To deal with this problem, Ref. [86] proposed a more careful definition which ensures that all geometric phases cancel. The idea is to start with an initial state, $|i\rangle$, with two identical a particles, and then apply three "movement operators" M_1, M_2, M_3 that move the anyons along the three paths, labeled $1, 2, 3$ in Fig. 3.1. By applying these operators to $|i\rangle$ in two different orders, namely $M_1M_2M_3$ vs. $M_3M_2M_1$, one obtains two final states that differ from one another by an exchange. The relative phase between $M_1M_2M_3|i\rangle$ and $M_3M_2M_1|i\rangle$ defines the exchange statistics $R(a, a)$:

$$M_1M_2M_3|i\rangle = R(a, a) \cdot M_3M_2M_1|i\rangle \tag{3.1}$$

Note that this definition is manifestly independent of the phases of the three movement operators since each operator appears on both the left and right hand side of (3.1). Thus, this definition succeeds in isolating the exchange statistics, $R(a, a)$, from extraneous geometric

phases. In this paper, we present microscopic definitions of F and R that are similar in spirit to the above example.

Previous work on the problem of defining anyon data can be divided into two categories depending on whether the authors considered Abelian or non-Abelian anyons. In the Abelian case, most work has focused on computing the exchange statistics and mutual statistics of anyon excitations – i.e., the statistical phases associated with exchanging two identical anyons or braiding one anyon around another. This line of work has been very successful: exchange statistics and mutual statistics have been computed for many microscopic models (see e.g. Refs. [4, 73]), and a general procedure for computing/defining these quantities was presented in Ref. [86]. Moreover, all other anyon data is determined by the exchange and mutual statistics (Proposition 2.5.1 of Ref. [115]) so one could argue that the problem of computing Abelian anyon data has already been solved. This case is further supported by Refs. [107, 19], which showed how to *rigorously* define and compute a complete set of Abelian anyon data.

The situation for non-Abelian anyons is different, however. In the non-Abelian case, most work has focused on the "topological S-matrix" and the "topological T-matrix"[74] – two pieces of data that reduce to the mutual statistics and exchange statistics in the Abelian case. Several methods have been proposed that allow one to extract S or T directly from ground state wave functions [148, 169, 170, 106, 167, 137, 49]. The problem is that S and T carry some, but not all, of the physical information in the F and R symbols. Therefore, these methods do not provide a way to compute the complete set of anyon data. This paper fills in this gap in the literature by showing how to compute the F and R symbols (and hence all other data) in the general, non-Abelian case.

Although the generality of our approach is one of its most important features, we will first present our definition of F and R in the context of Abelian anyons and only later discuss non-Abelian anyons. The reason that we organize the paper in this way is that the main

subtlety in defining F and R has to do with the $U(1)$ *phases* of these quantities, and this subtlety is the same in the Abelian and non-Abelian cases. Indeed, we will see that the generalization from the Abelian to the non-Abelian case is straightforward.

This paper is organized as follows. In Sec. 3.2, we review the basic data in Abelian anyon theories. Section 5.3 presents our microscopic definition of the F-symbol in the case of Abelian anyons. In Sec. 3.4, we illustrate our definition by computing the F-symbol in several lattice models and edge theories. This leads into Sec. 3.5, where we present our microscopic definition of the R-symbol in the case of Abelian anyons. We extend both definitions to the non-Abelian case in Sec. 3.6. We present our conclusions in Sec. 3.7. Technical details are contained in the appendices.

3.2 Review: Abelian anyon data

We begin by reviewing some basic aspects of Abelian anyon theories [74, 112]. These theories consist of four pieces of data:

1. **Set of anyon types**: a finite set of anyon types,
   $\mathcal{A} = \{a, b, c, ...\}$.

2. **Fusion product**: an associative and commutative multiplication law on $\mathcal{A}$, denoted $a \times b$ or ab.

3. F**-symbol**: a function $F : \mathcal{A} \times \mathcal{A} \times \mathcal{A} \to U(1)$, denoted $F(a, b, c)$.

4. R**-symbol**: a function $R : \mathcal{A} \times \mathcal{A} \to U(1)$, denoted $R(a, b)$.

We now explain the physical meaning of this data in the context of two-dimensional many-body systems with local interactions and an energy gap.

We begin with the idea of "anyon types." At an intuitive level, the set of anyon types $\mathcal{A}$ is simply the set of topologically distinct particle-like excitations of the many-body system.

More precisely, to define the anyon types associated with some many-body Hamiltonian H, consider all Hamiltonians of the form $H+V$ that have a unique gapped ground state, where H is defined on an infinite plane geometry and V is supported on a finite region of the plane. (We can think of V as a trapping potential for particle-like excitations.) Denote the set of all ground states generated in this way as $\{|\Psi\rangle\}$. We define an equivalence relation on the set $\{|\Psi\rangle\}$ as follows: $|\Psi'\rangle \sim |\Psi\rangle$ if there exists a unitary operator, U, supported in a finite region of the plane with $|\Psi'\rangle = U|\Psi\rangle$. Under this equivalence relation, the collection of states $\{|\Psi\rangle\}$ breaks up into equivalence classes. These equivalence classes define the set of anyon types $\mathcal{A} = \{a, b, c, ...\}$. The infinitely many states contained within each equivalence class describe the infinitely many ways to realize an anyon excitation of type a, type b, type c, etc.

This discussion leads naturally to the idea of the "fusion product." Let a, b be any pair of (Abelian) anyons. We say that $a \times b = c$ if a pair of anyons a, b can be converted into c and vice-versa, by applying a unitary operator supported in a finite region around a, b. It is clear from this definition that the fusion product is both associative and commutative, as mentioned above. (For an alternative definition of anyon types and fusion rules, see Refs. [126, 125].)

To complete the picture, we need to explain the physical meaning of the F and R symbols. This is the main subject of this paper, so we will say much more about this below. For now, we only mention that the F-symbol describes $U(1)$ phases associated with fusing three anyons in different orders, while the R-symbol describes $U(1)$ phases associated with braiding or exchanging two anyons. In particular, the quantity $R(a, a)$ can be interpreted as the exchange statistics of anyon a, while $R(a, b)R(b, a)$ is the mutual statistics of a and b – that is, the phase associated with braiding anyon a around anyon b.

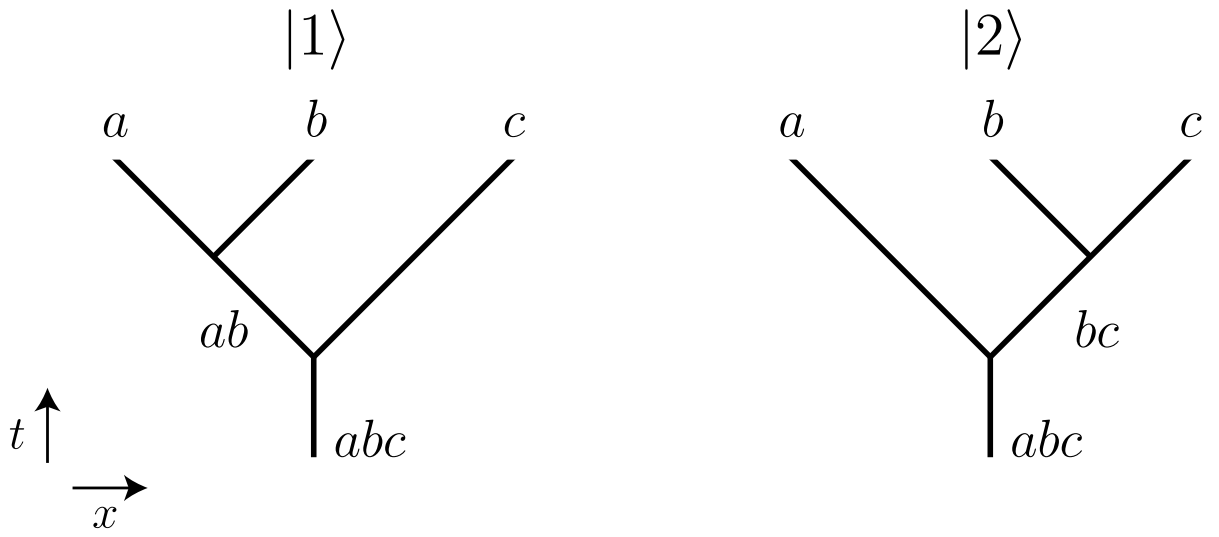

Figure 3.2: Spacetime diagrams for two processes in which an anyon abc splits into anyons a, b, c. The horizontal and vertical axes denote the space and time directions while the lines denote anyon worldlines. The final states produced by these processes, $|1\rangle, |2\rangle$, are equal up to the $U(1)$ phase $F(a, b, c)$.

3.3 Defining F for Abelian anyons

3.3.1 Abstract definition of F

Before explaining our microscopic definition of the F-symbol, we first review the *abstract* definition [74, 112]. We say that this definition is "abstract" because it captures the mathematical properties of the F-symbol but it is not obvious, a priori, how to make sense of it in a microscopic lattice model.

The basic idea is to consider two different physical processes in which an anyon of type abc splits into three anyons of types a, b, c (Fig. 3.2). In one process, abc splits into ab and c, and then ab splits into a and b; in the other process, abc splits into a and bc and then bc splits into b and c. By construction, the final states $|1\rangle, |2\rangle$ produced by these processes contain the same anyons a, b, c, at the same three positions. Therefore, the two final states $|1\rangle, |2\rangle$ must be the same up to a phase. The F-symbol $F(a, b, c)$ is defined to be the phase

difference between the two states:

$$|1\rangle = F(a,b,c)|2\rangle. \tag{3.2}$$

The abstract definition of the F-symbol has two important implications. First, the F-symbol has an inherent ambiguity: it is only well-defined up to transformations of the form

$$F(a,b,c) \to F(a,b,c)\frac{e^{i\nu(ab,c)}e^{i\nu(a,b)}}{e^{i\nu(a,bc)}e^{i\nu(b,c)}} \tag{3.3}$$

where $\nu(a,b) \in \mathbb{R}$. To understand where this ambiguity comes from, it is helpful to think about the physical processes in Fig. 3.2 as being implemented by a sequence of two "splitting operators" applied to an initial state, $|abc\rangle$. The key point is that the phases of these splitting operators are arbitrary. If we multiply each of the four splitting operators by a corresponding phase, namely, $e^{i\nu(ab,c)}, e^{i\nu(a,b)}$ for the two splitting operators in the first process and $e^{i\nu(a,bc)}, e^{i\nu(b,c)}$ in the second, F changes by exactly the above transformation (5.20). We will call the transformations in (5.20) "gauge transformations."

The second implication of the above definition is that F must satisfy a non-trivial constraint known as the "pentagon identity":

$$F(a,b,c)F(a,bc,d)F(b,c,d) = F(ab,c,d)F(a,b,cd) \tag{3.4}$$

To derive this identity, consider the 5 processes shown in Fig. 3.3. The first step is to note that the final states produced by these processes, namely $\{|1\rangle, ..., |5\rangle\}$, are all the same up to a phase. Next, we compute the phase difference between states $|1\rangle$ and $|5\rangle$ in two different ways. In the first way, we compute the relative phases between $(|1\rangle, |2\rangle)$, $(|2\rangle, |3\rangle)$, and $(|3\rangle, |5\rangle)$ using (5.15); in the second way, we compute the relative phases between $(|1\rangle, |4\rangle)$ and $(|4\rangle, |5\rangle)$. Demanding consistency between the two calculations gives the pentagon identity

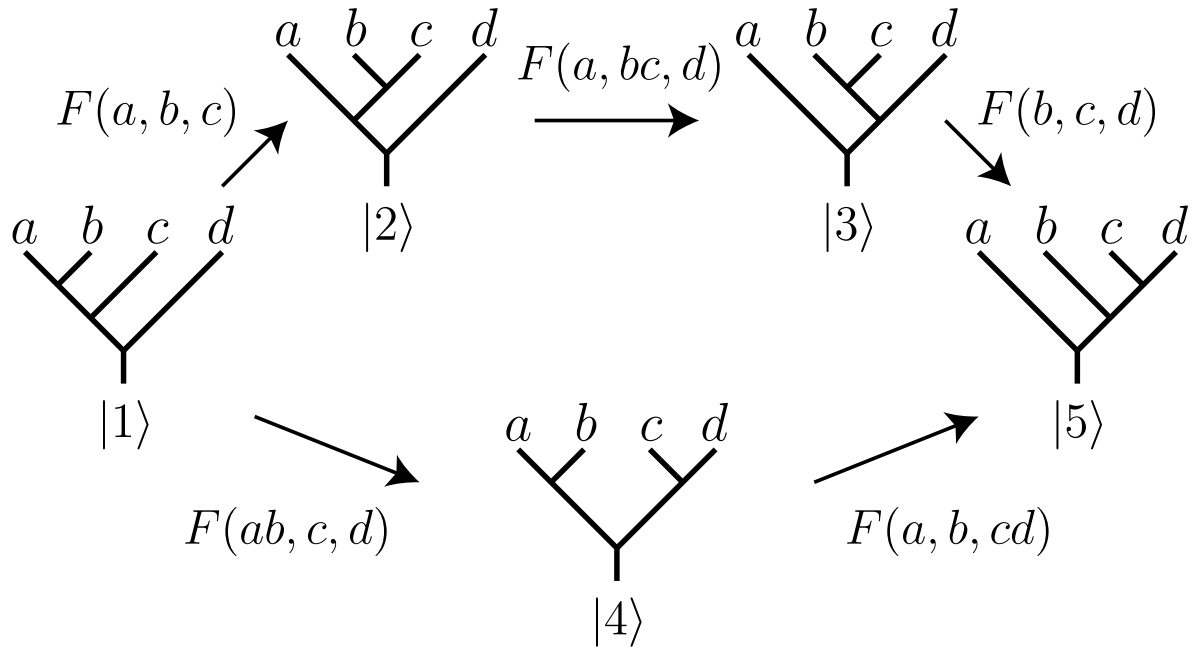

Figure 3.3: The pentagon identity: consistency requires that the product of the three F-symbols on the upper path is equal to the product of the two F-symbols on the lower path.

(5.17). Below, we will show that our microscopic definition of F also obeys the pentagon equation.

3.3.2 Microscopic definition of F

The main problem with applying the above definition to a microscopic lattice model is that some of the anyon splittings in Fig. 3.2 occur at different points in space. This means that the corresponding splitting operators are distinct operators which can be multiplied by *independent* phases. For example, the two splitting operators in the first process in Fig. 3.2 can be multiplied by two independent phases $e^{i\nu_1(ab,c)}, e^{i\nu_2(a,b)}$. This leads to a larger ambiguity in $F(a,b,c)$ than (5.20). To solve this problem, we need to perform all anyon splittings using the same set of splitting operators, defined at the same location in space. However, this introduces another problem: to do this, we need to *move* anyons in addition to splitting them. The operators that move anyons have arbitrary phases, just like

the splitting operators; so, unless we are careful, the arbitrary choice of these phases will introduce additional ambiguities into F, beyond the ones in Eq. (5.20). In this section, we overcome this problem by constructing two microscopic processes in which these extraneous phases cancel out.

To begin, we introduce some notation for labeling anyon states. The first step is to fix a line in the 2D plane, say the x-axis. We will only consider states with anyons living along this line. Next, for each anyon type a and for each point x on the line, we let $|a_x\rangle$ denote a state containing a single[2] anyon a located at point x.[3] Similarly, we let

$$|a_{x_1}, b_{x_2}, c_{x_3}, ...\rangle$$

be the (normalized) multi-anyon state with the anyon a at point x_1, the anyon b at point x_2, and so on. Here we assume that the points are ordered left to right as $x_1 < x_2 < \cdots$. We also assume that $x_1, x_2, ...$ are *well-separated*: every pair of neighboring anyons is separated by a distance that is much larger than the correlation length ξ of the ground state. Given this assumption, we will neglect finite size corrections that are exponentially small in the distance between the anyons.

For reasons that will become clear below, it is useful to have a precise definition of multi-anyon states in terms of the single anyon states. To this end, we define $|a_{x_1}, b_{x_2}, c_{x_3}, ...\rangle$ to be the unique[4] state that has the same expectation values as the ground state for local operators supported away from all the anyons, the same expectation values as $|a_{x_1}\rangle$ for operators supported near x_1, the same expectation values as $|b_{x_2}\rangle$ for operators supported

2. Although anyons can only be created in pairs, it is possible to have a state containing a *single* anyon where the partner is located far away (i.e. "at infinity"); this is the setup envisioned here.

3. This step involves an arbitrary choice since there are infinitely many states that contain an anyon a at point x, differing in their microscopic details; we will check that our definition of F does not depend on these choices.

4. In this discussion, multi-anyon states are *unique* because the anyons are assumed to be Abelian. In the non-Abelian case, multi-anyon states come in multiplets, as discussed in Sec. 3.6.

near x_2, and so on. In other words, multi-anyon states are characterized by the fact that

$$\langle ..., a_x, ...|O|..., a_x, ...\rangle = \langle a_x|O|a_x\rangle \tag{3.5}$$

for every operator O supported in the neighborhood of a single anyon a_x.

Having fixed our definitions of anyon states, the next step is to define *movement* operators. For any anyon, a, and any pair of points, x, x', we say that $M^a_{x'x}$ is a movement operator if it satisfies two conditions: (i) $M^a_{x'x}$ obeys

$$M^a_{x'x}|a_x\rangle \propto |a_{x'}\rangle \tag{3.6}$$

where the proportionality constant is a $U(1)$ phase; (ii) $M^a_{x'x}$ is *local* in the sense that it is supported in the neighborhood of the interval containing x, x'.

The locality condition on $M^a_{x'x}$ is important because it guarantees that $M^a_{x'x}$ acts the same way on any multi-anyon state of the form $|..., a_x, ...\rangle$: that is,

$$M^a_{x'x}|..., a_x, ...\rangle \propto |..., a_{x'}, ...\rangle \tag{3.7}$$

as long as the other anyons in $|..., a_x, ...\rangle$ are well-separated from the interval containing x and x'.

Indeed, to derive Eq. 5.38 from Eq. 5.35, consider the expectation value of any operator, O, supported in the neighborhood of $a_{x'}$, in the two states $|..., a_{x'}, ...\rangle$ and $M^a_{x'x}|..., a_x, ...\rangle$. Using (3.5) and (5.35), we can see that O has the same expectation value in the two states:

$$\begin{aligned}\langle ..., a_{x'}, ...|O|..., a_{x'}, ...\rangle &= \langle a_{x'}|O|a_{x'}\rangle \\ &= \langle a_x|(M^a_{x'x})^\dagger O M^a_{x'x}|a_x\rangle \\ &= \langle ..., a_x, ...|(M^a_{x'x})^\dagger O M^a_{x'x}|..., a_x, ...\rangle \end{aligned} \tag{3.8}$$

This is also true for operators supported near any other anyon, since $M^a_{x'x}$ is supported away from those anyons. It follows that these two states must be the same, up to a phase.

In addition to the movement operators, we also define *splitting* operators for our anyons. Fix two well-separated points on the line, which we will call '1' and '2'. For any pair of anyons a, b, we say that $S(a, b)$ is a splitting operator if it satisfies two conditions: (i) $S(a, b)$ satisfies

$$S(a, b)|ab_1\rangle \propto |a_1, b_2\rangle \tag{3.9}$$

where the proportionality constant is a $U(1)$ phase; (ii) $S(a, b)$ is supported in the neighborhood of the interval $[1, 2]$. Again, the second condition guarantees that the splitting operators can be applied to any multi-anyon state of the form $|..., ab_1, ...\rangle$ provided that the other anyons are located far from the interval $[1, 2]$:

$$S(a, b)|..., ab_1, ...\rangle \propto |..., a_1, b_2, ...\rangle \tag{3.10}$$

where the proportionality constant is a $U(1)$ phase. Note that, unlike the movement operators, we only define splitting operators that act at a *single* location '1' on the x-axis.

With this setup, we are now ready to define the F-symbol. The first step is to fix some choice of anyon states $|a_x\rangle$ and some choice of movement and splitting operators $M^a_{x'x}, S(a, b)$. Next, consider the initial state $|abc_1\rangle$, i.e. the state with a single anyon abc at position 1. We then apply two different sequences of movement and splitting operators to $|abc_1\rangle$, denoting the final states by $|1\rangle$ and $|2\rangle$:

$$\begin{aligned} |1\rangle &= M^b_{12} M^a_{01} S(a, b) M^c_{32} S(ab, c)|abc_1\rangle \\ |2\rangle &= M^c_{32} S(b, c) M^{bc}_{12} M^a_{01} S(a, bc)|abc_1\rangle \end{aligned} \tag{3.11}$$

These two processes are shown in Figure 3.4. By construction, the final states $|1\rangle, |2\rangle$ pro-

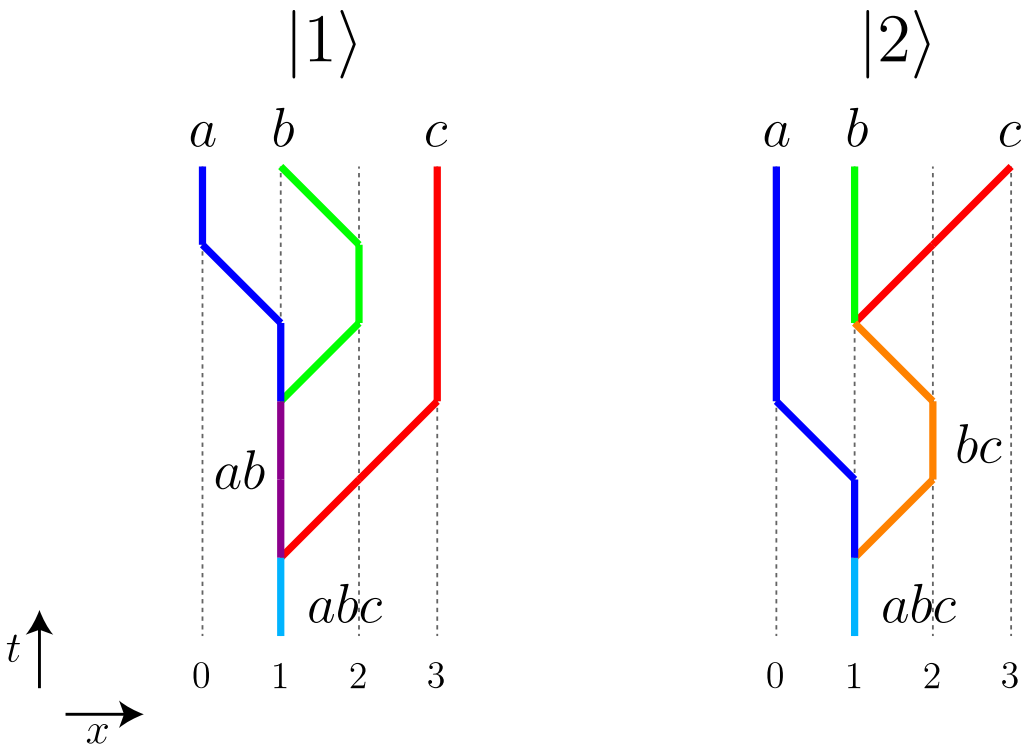

Figure 3.4: The two processes that are compared in the microscopic definition of the F-symbol.

duced by these processes both contain anyons a, b, c at positions $0, 1, 3$, respectively. In particular, this means that $|1\rangle, |2\rangle$ are the same up to a phase. We define the F-symbol $F(a, b, c)$ to be this phase difference:

$$F(a, b, c) = \langle 2|1\rangle \tag{3.12}$$

3.3.3 Checking the microscopic definition

To show that our microscopic definition is sensible, we need to establish two properties of F: (i) F is well-defined in the sense that different choices of anyon states and movement and splitting operators give the same F up to a gauge transformation (5.20); and (ii) F obeys the pentagon identity (5.17). We prove property (ii) in Appendix 7.1; the goal of this section is to prove property (i).

As a warm-up, let us see how F transforms if we change the *phase* of the movement and splitting operators. That is, suppose we replace

$$M^a_{x'x} \to e^{i\theta_{x'x}(a)} M^a_{x'x}, \quad S(a,b) \to e^{i\phi(a,b)} S(a,b) \tag{3.13}$$

for some real-valued θ, ϕ. Substituting these transformations into (3.11-3.12) gives

$$F(a,b,c) \to F(a,b,c) \frac{e^{i\phi(ab,c)} e^{i\phi(a,b)} e^{i\theta_{12}(b)}}{e^{i\phi(a,bc)} e^{i\phi(b,c)} e^{i\theta_{12}(bc)}} \tag{3.14}$$

Crucially, this transformation is identical to a gauge transformation (5.20) with

$$\nu(a,b) = \phi(a,b) + \theta_{12}(b) \tag{3.15}$$

This is exactly what we want: different phase choices lead to the same F, up to a gauge transformation. Although the above calculation is very simple, we would like to emphasize that this is actually a non-trivial test of our definition of F. In fact, the two processes in (3.11) were designed specifically to pass this test.

With this warm-up, we are now ready to consider the general case where we change the movement and splitting operators in an arbitrary way (for a fixed choice of anyon states $|a_x\rangle$). Denoting the new movement and splitting operators by

$$M^a_{x'x} \to \tilde{M}^a_{x'x}, \qquad S(a,b) \to \tilde{S}(a,b), \tag{3.16}$$

it follows from properties (5.38), (5.41) that

$$\tilde{M}^a_{x'x} |..., a_x, ...\rangle = \omega_1 \cdot M^a_{x'x} |..., a_x, ...\rangle \tag{3.17}$$

$$\tilde{S}(a,b) |..., ab_1, ...\rangle = \omega_2 \cdot S(a,b) |..., ab_1, ...\rangle \tag{3.18}$$

where ω_1, ω_2 are $U(1)$ phases. These $U(1)$ phases are highly constrained: taking the inner product of the two sides of (5.70) with $M^a_{x'x}|..., a_x, ...\rangle$ and using property (3.5), we can see that ω_1 can only depend on a, x, x'. By the same reasoning, ω_2 can only depend on a, b. Hence, we must have

$$\begin{aligned} \tilde{M}^a_{x'x}|..., a_x, ...\rangle &= e^{i\theta_{x'x}(a)} M^a_{x'x}|..., a_x, ...\rangle \\ \tilde{S}(a,b)|..., ab_1, ...\rangle &= e^{i\phi(a,b)} S(a,b)|..., ab_1, ...\rangle \end{aligned} \tag{3.19}$$

for some real-valued θ, ϕ. Substituting these relations into (3.11), we again see that F changes by a gauge transformation with ν given by (5.66).

At this point, we have shown that different choices of movement and splitting operators lead to the same F, up to a gauge transformation. To complete the proof of property (i), we need to check that different choices of representative anyon states $|a_x\rangle$ also lead to the same F, up to a gauge transformation. In order to investigate this issue, we make a physical assumption which is inspired by the definition of anyon types given in Sec. 3.2: we assume that different choices of anyon states are related to one another by a local unitary transformation, U. (By a 'local unitary transformation', we mean a unitary operator generated by the finite time evolution of a local Hamiltonian that is supported near the x-axis [23]). Given this assumption, our task is to understand how F changes if we replace

$$|a_{x_1}, b_{x_2}, c_{x_3}, ...\rangle \to |a_{x_1}, b_{x_2}, c_{x_3}, ...\rangle' \tag{3.20}$$

where

$$|a_{x_1}, b_{x_2}, c_{x_3}, ...\rangle' = U|a_{x_1}, b_{x_2}, c_{x_3}, ...\rangle \tag{3.21}$$

for some local unitary transformation U. To understand the effect on F, observe that we

can choose movement and splitting operators for the states $\{|a_{x_1}, b_{x_2}, c_{x_3}, ...\rangle'\}$ however we like, changing F by at most a gauge transformation. The simplest choice is

$$(M^a_{x'x})' = U M^a_{x'x} U^\dagger, \qquad S'(a,b) = U S(a,b) U^\dagger \tag{3.22}$$

where $M^a_{x'x}$ and $S(a,b)$ are movement and splitting operators for $\{|a_{x_1}, b_{x_2}, c_{x_3}, ...\rangle\}$. With this choice, it is clear that $|1'\rangle = U|1\rangle$, and $|2'\rangle = U|2\rangle$. It follows that $F' = \langle 2'|1'\rangle = \langle 2|1\rangle = F$. Thus, we conclude that F is invariant under a replacement of the anyon states, $|a_{x_1}, b_{x_2}, c_{x_3}, ...\rangle \to |a_{x_1}, b_{x_2}, c_{x_3}, ...\rangle'$. This completes the proof of property (i) above.

3.4 Examples of F-symbol calculations

In this section, we illustrate our definition by computing the F-symbol for several lattice models and edge theories.

3.4.1 Toric code model

Hamiltonian

The toric code model is an exactly solvable spin-1/2 model where the spins live on the links of the square lattice [73]. The Hamiltonian is

$$H = -\sum_v A_v - \sum_p B_p \tag{3.23}$$

where the two sums run over the vertices, v, and plaquettes, p, of the square lattice. The two operators A_v, B_p are defined by

$$A_v = \prod_{\ell \in v} \sigma^x_\ell, \qquad B_p = \prod_{\ell \in \partial p} \sigma^z_\ell \tag{3.24}$$

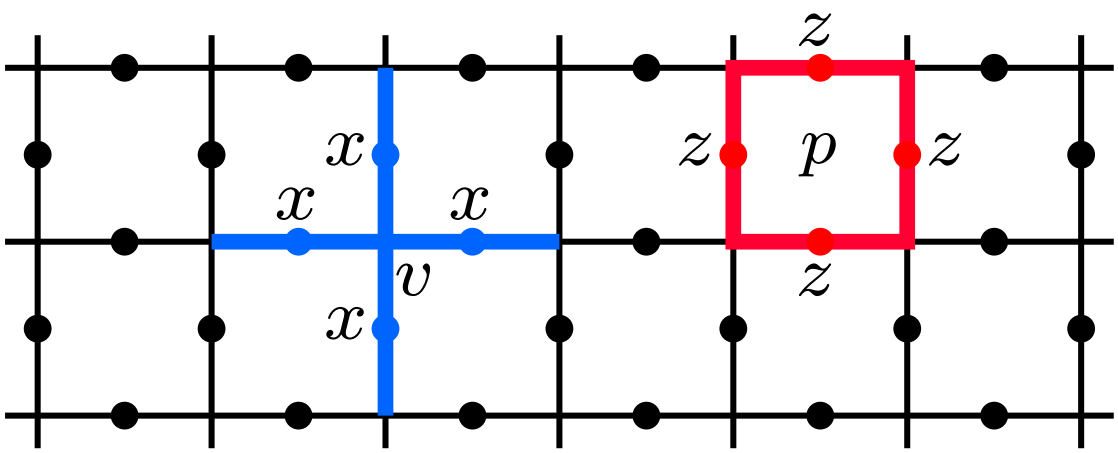

Figure 3.5: The two operators A_v and B_p in the toric code Hamiltonian.

where the first product runs over the four links, ℓ, that are adjacent to the vertex v, and the second product runs over the four links, ℓ, that belong to the boundary of the plaquette p (Fig. 3.5).

To find the ground state of this model in an infinite plane geometry, notice that the A_v, B_p operators commute with one another and have eigenvalues ± 1. From this, one can deduce that the state $|A_v = B_p = 1\rangle$ is the ground state since this state minimizes the energies of all the terms in the Hamiltonian.

As for excitations, the toric code model supports four different (anyon) types, which we denote by $\{1, e, m, em\}$. All four anyon types have simple realizations on the lattice: the 'e' anyon corresponds to an excitation where $A_v = -1$ for a single vertex v; the 'm' anyon corresponds to an excitation where $B_p = -1$ for a single plaquette p; the 'em' anyon corresponds to an excitation where $A_v = -1$ and $B_p = -1$ for both a vertex v and nearby plaquette p; finally the '1' anyon (also known as the "trivial" anyon) corresponds to having no excitation at all. The fusion rules for these anyons are

$$e \times e = m \times m = 1, \qquad e \times m = em \tag{3.25}$$

F-symbol calculation

We now illustrate our definition of F by computing $F(e,e,e)$. First, we define some notation for labeling anyon states. Following the procedure outlined in Sec. 3.3.2, we focus on anyon states where the anyons live along a line, specifically the x-axis. We then label the vertices along the x-axis by integers, $n = 0, \pm 1, \pm 2, ...$ (Fig. 3.6), and we define $|e_n\rangle$ to be the state with $A_{v=n} = -1$, and all other A_v's and B_p's equal to $+1$.

Next, we need to construct movement and splitting operators for the e anyons. We define the movement operator between neighboring vertices n and $n+1$ by

$$M^e_{(n+1)n} = \sigma^z_{n,n+1} \tag{3.26}$$

Here $\sigma^z_{n,n+1}$ denotes the σ^z operator on the link $\ell = \langle n(n+1)\rangle$ (Fig. 3.6). It is easy to check that this movement operator obeys the required property, $M^e_{(n+1)n}|e_n\rangle \propto |e_{n+1}\rangle$ using the fact that $\sigma^z_{n,n+1}$ anticommutes with the A_v operators on vertex n and vertex $n+1$.

We define the reverse movement operator in the same way:

$$M^e_{n(n+1)} = \sigma^z_{n,n+1} \tag{3.27}$$

Also, we define the splitting operator for the e anyon to be (Fig. 3.6)

$$S(e,e) = \sigma^z_{1,2} \tag{3.28}$$

Again, one can check that $S(e,e)$ has the required property, $S(e,e)|1_1\rangle \propto |e_1, e_2\rangle$, using the fact that $\sigma^z_{1,2}$ anticommutes with A_v on vertex 1 and vertex 2.

We will also need the splitting operator $S(1,e)$, which we define as

$$S(1,e) = \sigma^z_{1,2} \tag{3.29}$$

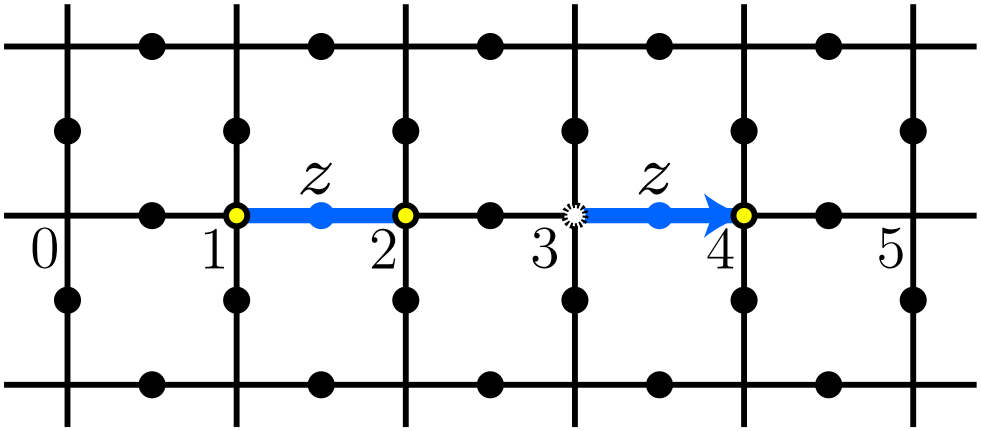

Figure 3.6: Movement and splitting operators for e anyons. The splitting operator for e is $S(e,e) = \sigma^z_{1,2}$. The movement operator that moves e from vertex 3 to 4 is $M^e_{4,3} = \sigma^z_{3,4}$.

Finally, we will need the movement operator $M^1_{n'n}$ and the splitting operator $S(e,1)$, which we take to be the identity operator:

$$M^1_{n'n} = S(e,1) = 1 \tag{3.30}$$

(The reason why we can take $S(e,1) = 1$ is that $S(e,1)$ is defined by the condition $S(e,1)|e_1\rangle \propto |e_1, 1_2\rangle$, which is satisfied by the identity operator $S(e,1) = 1$.)

With these definitions, we are now equipped to calculate $F(e,e,e)$. Following Eq. (3.11), we have

$$\begin{aligned} |1\rangle &= M^e_{12} M^e_{01} S(e,e) M^e_{32} S(1,e)|e_1\rangle \\ &= \sigma^z_{1,2}\sigma^z_{0,1}\sigma^z_{1,2}\sigma^z_{2,3}\sigma^z_{1,2}|e_1\rangle \end{aligned} \tag{3.31}$$

Similarly,

$$\begin{aligned} |2\rangle &= M^e_{32} S(e,e) M^1_{12} M^e_{01} S(e,1)|e_1\rangle \\ &= \sigma^z_{2,3}\sigma^z_{1,2}\sigma^z_{0,1}|e_1\rangle \end{aligned} \tag{3.32}$$

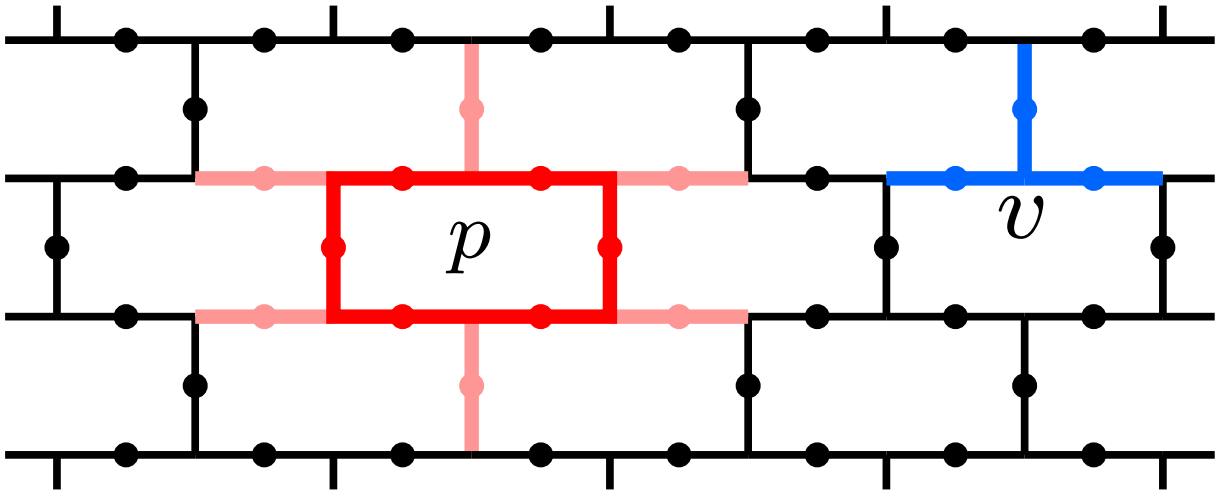

Figure 3.7: The two operators Q_v and B_p in the doubled semion Hamiltonian: Q_v is a product of σ^x operators acting on the three blue links adjacent to the vertex v, while B_p involves a product of σ^z operators on the six red links adjacent to the plaquette p and a product of $i^{(1-\sigma^x)/2}$ on the six pink "legs" of the plaquette p.

Comparing the two expressions, we see that $|1\rangle = |2\rangle$, so that

$$F(e,e,e) = \langle 2|1\rangle = 1 \tag{3.33}$$

More generally, one can check that all the F-symbols are 1 for this model, i.e.

$$F(a,b,c) = 1 \tag{3.34}$$

for all $a, b, c \in \{1, e, m, em\}$ for an appropriate choice of movement and splitting operators.

3.4.2 Doubled semion model

Hamiltonian

The doubled semion model is an exactly solvable spin-1/2 model where the spins live on the links of the honeycomb lattice [88]. The Hamiltonian is

$$H = -\sum_{v} Q_v - \sum_{p} B_p \tag{3.35}$$

where the two sums run over the vertices, v, and plaquettes, p, of the honeycomb lattice. The operator Q_v is defined by

$$Q_v = \frac{1}{2}\left(1 + \prod_{\ell \in v} \sigma_\ell^x\right) \tag{3.36}$$

Likewise, B_p is defined by

$$B_p = \frac{1}{2}\left(1 - \prod_{\ell \in \partial p} \sigma_\ell^z \prod_{\ell \in \text{legs of } p} i^{\frac{1-\sigma_\ell^x}{2}}\right) P_p \tag{3.37}$$

where the second product runs over the six links, ℓ, that form the "legs" of the plaquette p (Fig. 3.7) and P_p is the projector

$$P_p = \prod_{v \in \partial p} Q_v \tag{3.38}$$

Like the toric code model, the Q_v, B_p operators commute with one another. Also, one can check that Q_v and B_p have eigenvalues 0 and 1 so that the ground state in an infinite plane geometry is the state $|Q_v = B_p = 1\rangle$.

As for excitations, it is known that the doubled semion model supports four types of

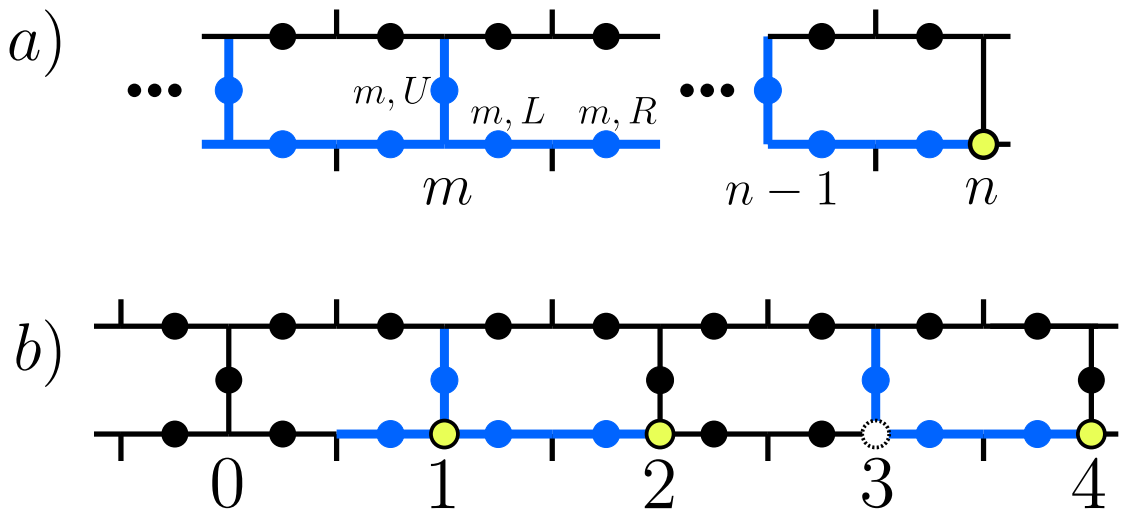

Figure 3.8: (a) Definition of semion creation operator $a_n^\dagger$: the operator $a_n^\dagger$ acts on all (m, U), (m, L) and (m, R) links with $m < n$. (b) Movement and splitting operators for semions: the splitting operator $S(s, s)$ acts on the blue links near 1 and 2 according to Eq. 3.44, while the movement operator M_{43}^s acts on the blue links near 3 and 4 according to Eq. 3.42.

anyons, which we denote by $\{1, s, \bar{s}, s\bar{s}\}$. The fusion rules for these anyons are

$$s \times s = \bar{s} \times \bar{s} = 1, \qquad s \times \bar{s} = s\bar{s} \tag{3.39}$$

Similarly to the toric code model, these anyon excitations correspond to defects where $Q_v = 0$ or $B_p = 0$ for some collection of vertices and plaquettes. However, unlike the toric code model, the excitations are not completely characterized by their Q_v and B_p eigenvalues due to degeneracies in the simultaneous eigenspaces of $\{Q_v, B_p\}$. Therefore, we cannot define these excitations unambiguously in terms of their Q_v and B_p eigenvalues; instead, we will define/construct them by writing down explicit (string-like) creation operators.

F-symbol calculation

To illustrate our definition, we now compute the F-symbol $F(s, s, s)$. As before, we focus on anyon states where the s anyons live along the x-axis. More specifically, we focus on states where the s anyons live at vertices of type '$\perp$' along the x-axis (Fig. 3.8b). We label these

vertices by integers $n = 0, \pm 1, \pm 2, \cdots$. We then define $|s_n\rangle$ to be a particular state with an s anyon at vertex n. More specifically, we define

$$|s_n\rangle = a_n^\dagger |0\rangle \tag{3.40}$$

where $|0\rangle \equiv |Q_v = B_p = 1\rangle$ denotes the ground state, and where $a_n^\dagger$ is the following string-like creation operator for s anyons:

$$\begin{aligned} a_n^\dagger = \prod_{m<n} \sigma_{m,L}^z \sigma_{m,R}^z \cdot \prod_{m<n} (-1)^{\frac{1}{4}(1+\sigma_{m,L}^x)(1-\sigma_{m,R}^x)} \\ \cdot \prod_{m<n} i^{\frac{1-\sigma_{m,U}^x}{2}} \end{aligned} \tag{3.41}$$

Here, we have introduced some notation: we denote the three links near vertex m by the labels (m, U), (m, L), (m, R) (see Fig. 3.8a). The justification for this string operator comes from Ref. [88], where it was argued that string operators of the form (3.41) create semion excitations at their endpoints.

Next we need to construct movement and splitting operators for s. We define the movement operator between vertices n and $n+1$ as (see Fig. 3.8b):

$$M_{(n+1)n}^s = \sigma_{n,L}^z \sigma_{n,R}^z (-1)^{\frac{1}{4}(1+\sigma_{n,L}^x)(1-\sigma_{n,R}^x)} i^{\frac{1-\sigma_{n,U}^x}{2}} \tag{3.42}$$

It is clear that $M_{(n+1)n}^s$ obeys the required property $M_{(n+1)n}^s |s_n\rangle \propto |s_{n+1}\rangle$ since $M_{(n+1)n}^s a_n^\dagger \propto a_{n+1}^\dagger$. Likewise, we define the reverse movement operator by

$$M_{n(n+1)}^s = (M_{(n+1)n}^s)^{-1} \tag{3.43}$$

As for the splitting operator, we define

$$S(s,s) = \sigma^x_{0,R}\sigma^z_{1,L}\sigma^z_{1,R}(-1)^{\frac{1}{4}(1+\sigma^x_{1,L})(1-\sigma^x_{1,R})}i^{\frac{1-\sigma^x_{1,U}}{2}} \tag{3.44}$$

(see Fig. 3.8b). Notice that

$$S(s,s) = M^s_{21}\sigma^x_{0,R} \tag{3.45}$$

The extra factor of $\sigma^x_{0,R}$ is necessary to make sure that the two excitations created by S are the same as those created by $a^\dagger_n$, i.e.

$$S(s,s)|0\rangle \propto a^\dagger_1 a^\dagger_2|0\rangle \tag{3.46}$$

(see Appendix 7.3 for a derivation). Equation (3.46) guarantees that $S(s,s)$ has the required property for a splitting operator: $S(s,s)|1_1\rangle \propto |s_1, s_2\rangle$.

We will also need the splitting operator $S(1,s)$, which we define as

$$S(1,s) = M^s_{21} \tag{3.47}$$

Finally, we will need the movement operator $M^1_{n'n}$ and the splitting operator $S(s,1)$, which we define as

$$M^1_{n'n} = S(s,1) = 1 \tag{3.48}$$

We are now ready to compute the F-symbol $F(s,s,s)$. Using Eq. (3.11), we have:

$$\begin{aligned} |1\rangle &= M^s_{12}M^s_{01}S(s,s)M^s_{32}M^s_{21}|s_1\rangle \\ |2\rangle &= M^s_{32}S(s,s)M^s_{01}|s_1\rangle \end{aligned} \tag{3.49}$$

To proceed further, we note that all movement operators commute with one another since they act on non-overlapping spins. We also note that the splitting operator $S(s,s)$ *anticommutes* with M^s_{01} and M^s_{10} but commutes with every other movement operator, as one can see from (3.45). Using these facts, we can simplify $|1\rangle$ to

$$|1\rangle = -M^s_{32}S(s,s)M^s_{01}|s_1\rangle \tag{3.50}$$

Hence, $|1\rangle = -|2\rangle$ so

$$F(s,s,s) = \langle 2|1\rangle = -1 \tag{3.51}$$

In fact, using the same movement and splitting operators, one can show that all the other F-symbols involving 1 and s are trivial:

$$F(1,1,1) = F(1,1,s) = F(1,s,1) = F(1,s,s) = 1$$
$$F(s,1,1) = F(s,1,s) = F(s,s,1) = 1$$

In particular, this means that

$$F(s,s,s)F(s,1,s) = -1 \tag{3.52}$$

The latter result is significant because one can check that $F(s,s,s)F(s,1,s)$ is *invariant* under the gauge transformation (5.20). Therefore we have shown that the F-symbol for the doubled semion model is not gauge equivalent to $F(a,b,c) = 1$. A corollary of this result is that the toric code model and the doubled semion model must belong to different phases since they have different F-symbols.

3.4.3 Semion edge theory

We now show how to compute the F-symbol using an *edge* theory of a topological phase. Specifically, we consider the simplest non-trivial topological phase, namely the Laughlin $\nu = 1/2$ bosonic fractional quantum Hall state. This topological phase supports two types of anyon excitations, which we denote by $\{1, s\}$. Here, s can be thought of as the charge $1/2$ quasihole (which happens to be a semion), while 1 denotes the trivial anyon. The anyons obey the following fusion rule: $s \times s = 1$.

Our goal is to compute the F-symbol for this topological phase using its edge theory. The edge theory consists of a single chiral boson field ϕ obeying commutation relations [151]

$$[\phi(x), \partial_y \phi(y)] = \pi i \delta(x - y) \tag{3.53}$$

The Hamiltonian for the edge theory is

$$H = \int dx \frac{v}{4\pi} (\partial_x \phi)^2 \tag{3.54}$$

where v describes the velocity of the chiral boson edge mode.

To fully define the edge theory, it is important to specify the set of local operators. For the above edge theory, the fundamental local operators are $e^{\pm i 2\phi}$, which can be thought of as the creation/annihilation operators for the (charge 1) boson on the edge, respectively. All other local operators can be constructed by taking derivatives and products of $e^{\pm i 2\phi}$.

We now compute the F-symbol $F(s, s, s)$. The first step is to define the anyon states that we will manipulate. Following the standard edge theory formalism [151], we define the anyon state $|s_x\rangle$ by

$$|s_x\rangle = a_x^\dagger |0\rangle \tag{3.55}$$

where $|0\rangle$ denotes the ground state of the edge theory, and $a_x^\dagger$ is defined by

$$a_x^\dagger = e^{i\int_{-\infty}^{x}\partial_y\phi(y)dy} \tag{3.56}$$

Here, a_x can be thought of as a (string-like) creation operator for s at position x along the edge.

Next we define movement and splitting operators for s. We define the movement operator by

$$M^s_{x'x} = e^{i\int_{x}^{x'}\partial_y\phi(y)dy} \tag{3.57}$$

Notice that $M^s_{x'x}a_x^\dagger \propto a_{x'}^\dagger$ which guarantees that $M^s_{x'x}$ obeys the required property $M^s_{x'x}|s_x\rangle \propto |s_{x'}\rangle$.

Likewise, we define the splitting operator for s by

$$\begin{aligned} S(s,s) &= M^s_{21}e^{i2\phi(1)} \\ &= e^{i\int_1^2\partial_x\phi(x)dx}e^{i2\phi(1)} \end{aligned} \tag{3.58}$$

Here the extra factor of $e^{2i\phi(1)}$ is necessary to ensure that

$$S(s,s)|0\rangle \propto a_1^\dagger a_2^\dagger|0\rangle \tag{3.59}$$

The other splitting and movement operators that we need are $S(1,s)$, which we define by

$$S(1,s) = M^s_{21} \tag{3.60}$$

and $M^1_{x'x}$ and $S(s,1)$ which we define as

$$M^1_{x'x} = S(s,1) = 1 \tag{3.61}$$

We are now ready to compute the F-symbol $F(s,s,s)$. Following the definition (3.11), we have

$$\begin{aligned} |1\rangle &= M^s_{12} M^s_{01} M^s_{21} e^{i2\phi(1)} M^s_{32} M^s_{21} |s_1\rangle \\ |2\rangle &= M^s_{32} M^s_{21} e^{i2\phi(1)} M^s_{01} |s_1\rangle \end{aligned} \tag{3.62}$$

To compare these two expressions we need to rearrange the order of these operators. We can do this with the help of the following relations, which can be derived from the Baker-Campbell-Hausdorff formula:

$$\begin{aligned} M^s_{x''x'} M^s_{x'x} &= e^{i\pi/2} M^s_{x'x} M^s_{x''x'}, \quad x < x' < x'' \\ e^{i2\phi(1)} M^s_{1x} &= -M^s_{1x} e^{i2\phi(1)}, \quad x \neq 1 \end{aligned} \tag{3.63}$$

With these formulas and the identity $M^s_{xx'} = (M^s_{x'x})^{-1}$, we can rewrite $|1\rangle$ as:

$$|1\rangle = -M^s_{32} M^s_{21} e^{i2\phi(1)} M^s_{01} |s_1\rangle \tag{3.64}$$

Hence,

$$F(s,s,s) = \langle 2|1\rangle = -1 \tag{3.65}$$

In exactly the same way, one can show that $F(a,b,c) = 1$ for every other choice of $a,b,c \in \{1,s\}$.

Before concluding, we need to address a question that may worry some readers: our

microscopic definition of the F-symbol assumes a finite correlation length ξ, so what is the justification for applying it to a gapless edge theory? Our answer is that, in some edge theories, the anyon states in the bulk can be transformed into anyon states at the edge by a local unitary transformation. If this is the case, an edge calculation is guaranteed to give the same answer as a bulk calculation where our definition is on firmer ground. We believe that the edge theory analyzed above (and in the next section) has this property.

3.4.4 General chiral boson edge theory

We now extend the calculation of the previous section to a general bosonic Abelian topological phase. According to the K-matrix formalism, every bosonic Abelian topological phase can be described by a multi-component $U(1)$ Chern-Simons theory of the form [151]

$$L = \sum_{ij\mu\nu} \frac{K_{ij}}{4\pi} \epsilon^{\lambda\mu\nu} a_{\lambda i} \partial_\mu a_{\nu j} \tag{3.66}$$

where K_{ij} is a non-degenerate $N \times N$ integer symmetric matrix with even elements on the diagonal. Our goal will be to compute the F-symbol corresponding to any given K_{ij}. (The example in the previous section corresponds to the case $K = 2$).

A word about notation: in the standard K-matrix formalism, anyon excitations are parameterized by equivalence classes of N-component integer vectors, where the equivalence relation is defined by $l \sim m$ if $l - m = K\Lambda$ for some integer vector Λ. Here, we use a slightly different notation: instead of working with equivalence classes of integer vectors, we choose a single *representative* from each equivalence class, and we label each anyon by the corresponding representative l. In this notation, the set of anyons is given by a finite collection of integer vectors $\{l, m, n, ...\}$. The fusion rules are given by

$$l \times m = [l + m] \tag{3.67}$$

where $[l+m]$ denotes the unique representative that belongs to the same equivalence class as $l+m$.

As in the previous section, we will compute the F-symbol using an edge theory. In particular, we will use the standard chiral boson edge theory consisting of N chiral boson fields, $\Phi_1, ..., \Phi_N$, obeying the commutation relations [151]

$$[\Phi_i(x), \Phi_j(y)] = \pi i K^{-1}_{ij} \text{sgn}(y-x) + \pi i (K^{-1} X K^{-1})_{ij} \tag{3.68}$$

with an edge Hamiltonian of the form

$$H = \int dx \sum_{ij} \frac{V_{ij}}{4\pi} \partial_x \Phi_i \partial_x \Phi_j$$

In the above commutation relation, X is (any) skew-symmetric integer matrix with $X \equiv K \pmod 2$. The $K^{-1}XK^{-1}$ term in (3.68) is not included in standard treatments of chiral boson edge theories [151] but it plays the same role as the more well-known Klein factors[130]: it guarantees that non-overlapping local operators commute with one another (see Eq. 3.69 below).

To complete the edge theory, we need to specify the set of local operators. In this case, the fundamental local operators are those of the form

$$\exp(i\Lambda^T K \Phi) \equiv \exp\left(i \sum_{ij} \Lambda_i K_{ij} \Phi_j \right) \tag{3.69}$$

where Λ is an N component integer column vector. All other local operators can be constructed by taking derivatives and products of $e^{i\Lambda^T K \Phi}$. Physically, $\exp(i\Lambda^T K\Phi)$ can be thought of as a product of boson creation/annihilation operators acting on the different edge modes.

We now compute the F-symbol $F(l,m,n)$. The first step is to define the anyon states

that we will manipulate. For each anyon type, l, we define a state with anyon l at position x, by

$$|l_x\rangle = (a_x^l)^\dagger |0\rangle \tag{3.70}$$

where $|0\rangle$ denotes the ground state of the edge theory and

$$(a_x^l)^\dagger = e^{il^T \int_{-\infty}^{x} \partial_y \Phi(y) dy} \tag{3.71}$$

As in the previous example, $(a_x^l)^\dagger$ can be thought of as the string-like creation operator for anyon l at position x.

Next we define movement and splitting operators. We define the movement operator for l by

$$M_{x'x}^l = e^{il^T \int_{x}^{x'} \partial_y \Phi(y) dy} \tag{3.72}$$

Likewise, we define the splitting operator by

$$S(l,m) = M_{21}^m \cdot C(l,m) \tag{3.73}$$

where $C(l,m)$ denotes the operator $C(l,m) = e^{i(l+m-[l+m])^T \Phi(1)}$. As in the previous example, the extra factor of $e^{i(l+m-[l+m])^T \Phi(1)}$ is necessary to ensure that

$$S(l,m)|[l+m]_1\rangle \propto (a_1^l)^\dagger (a_2^m)^\dagger |GS\rangle \tag{3.74}$$

We are now ready to compute the F-symbol $F(l,m,n)$. From the definition (3.11) we

have:

$$\begin{aligned}
|1\rangle &= M_{12}^{m} M_{01}^{l} M_{21}^{m} C(l,m) M_{32}^{n} M_{21}^{n} \\
&\quad \cdot C([l+m],n) |[l+m+n]_1\rangle \\
|2\rangle &= M_{32}^{n} M_{21}^{n} C(m,n) M_{12}^{[m+n]} M_{01}^{l} M_{21}^{[m+n]} \\
&\quad \cdot C(l,[m+n]) |[l+m+n]_1\rangle
\end{aligned} \tag{3.75}$$

To simplify these expressions we use the following commutation relations:

$$\begin{aligned}
M_{x''x'}^{l} M_{x'x}^{m} &= e^{i\alpha(l,m)} \cdot M_{x'x}^{m} M_{x''x'}^{l}, \quad x < x' < x'' \\
M_{x1}^{l} e^{i\Lambda^T K \Phi(1)} &= e^{i\alpha(l,K\Lambda)} \cdot e^{i\Lambda^T K \Phi(1)} M_{x1}^{l} \quad x \neq 1
\end{aligned} \tag{3.76}$$

where

$$\alpha(l,m) = \pi l^T K^{-1} m. \tag{3.77}$$

We also use the relation

$$e^{i\Lambda^T K \Phi(1)} e^{i\Xi^T K \Phi(1)} = e^{-i\beta(K\Lambda, K\Xi)} \cdot e^{i(\Lambda+\Xi)^T K \Phi(1)} \tag{3.78}$$

where

$$\beta(\Lambda,\Xi) = \frac{\pi}{2} \Lambda^T (K^{-1} X K^{-1}) \Xi. \tag{3.79}$$

All of these relations follow from Eq. 3.68, together with the Baker-Campbell-Hausdorff formula.

Using the above relations, together with the identity $M_{xx'}^{l} = (M_{x'x}^{l})^{-1}$, we simplify

$|1\rangle, |2\rangle$ to:

$$\begin{aligned}
|1\rangle &= e^{i\alpha_1} M_{01}^l M_{32}^n M_{21}^n e^{i(l+m+n-[l+m+n])^T \Phi(1)} \\
&\quad \cdot |[l+m+n]_1\rangle \\
|2\rangle &= e^{i\alpha_2} M_{01}^l M_{32}^n M_{21}^n e^{i(l+m+n-[l+m+n])^T \Phi(1)} \\
&\quad \cdot |[l+m+n]_1\rangle
\end{aligned} \tag{3.80}$$

where

$$\begin{aligned}
\alpha_1 &= \alpha(l,m) + \alpha(n, l+m-[l+m]) \\
&\quad - \beta(l+m-[l+m], [l+m]+n-[l+m+n]) \\
\alpha_2 &= \alpha(l,m) \\
&\quad - \beta(m+n-[m+n], l+[m+n]-[l+m+n])
\end{aligned} \tag{3.81}$$

We conclude that

$$F(l,m,n) = \langle 2|1\rangle = \exp[i(\alpha_1 - \alpha_2)] \tag{3.82}$$

To complete the calculation, we simplify the expression for F by making a gauge transformation (5.20) with

$$\nu(l,m) = \beta(l+m-[l+m],[l+m]) + \beta(m,l) + \alpha(m,l) \tag{3.83}$$

After this gauge transformation, we obtain

$$F(l,m,n) = \exp[i\pi l^T K^{-1}(K-X)K^{-1}(m+n-[m+n])] \tag{3.84}$$

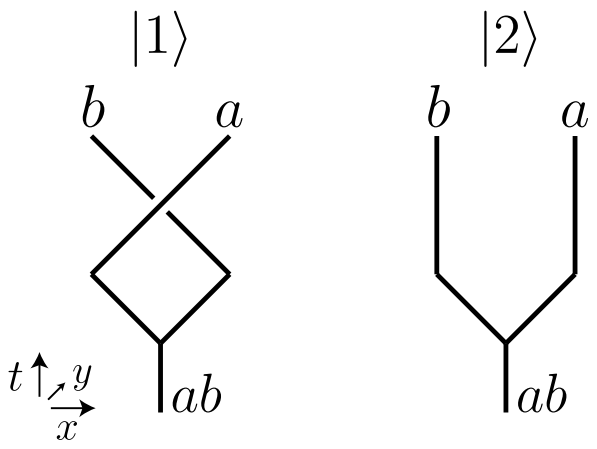

Figure 3.9: Spacetime diagrams for two processes in which an anyon ab splits into anyons a, b. The final states $|1\rangle, |2\rangle$ are equal up to a $U(1)$ phase, $R(a, b)$.

3.5 Defining the R-Symbol for Abelian anyons

3.5.1 Abstract definition of R

We begin by reviewing the *abstract* definition of the R-symbol in the case of Abelian anyons [74, 112]. According to this definition, R is defined by comparing two different physical processes (Fig. 3.9). In one process, an anyon of type ab splits into two anyons of type a, b, with a on the left and b on the right, and then a, b are exchanged in the counterclockwise direction; the other process, ab splits into a, b with b on the left and a on the right, without any subsequent exchange. By construction, the final states $|1\rangle, |2\rangle$ produced by these processes contain the same anyons a, b in the same positions. Therefore, $|1\rangle, |2\rangle$ are the same up to a phase. The R-symbol $R(a, b)$ is defined to be the phase difference between the two states:

$$|1\rangle = R(a, b)|2\rangle \tag{3.85}$$

Two properties of the R-symbol follow from this definition. First, R has an inherent

ambiguity: it is only well-defined up to gauge transformations of the form

$$R(a,b) \to R(a,b)\frac{e^{i\nu(a,b)}}{e^{i\nu(b,a)}} \tag{3.86}$$

where $\nu(a,b) \in \mathbb{R}$. As with F, this ambiguity comes about because the phases of splitting operators can be varied arbitrarily. In particular, if we multiply the two splitting operators in Fig. 3.9 by two phases, $e^{i\nu(a,b)}, e^{i\nu(b,a)}$, this changes R by exactly the above transformation (3.86). An important point is that the $\nu(a,b)$ in (3.86) is the same as the $\nu(a,b)$ that appears in the gauge transformation (5.20): that is, R and F transform under the same gauge transformation ν.

The second property of the R-symbol is that it obeys two constraints, known as the hexagon equations:

$$\begin{aligned} R(a,b)F(b,a,c)R(a,c) &= F(a,b,c)R(a,bc)F(b,c,a) \\ R(b,a)^{-1}F(b,a,c)R(c,a)^{-1} &= F(a,b,c)R(bc,a)^{-1} \\ &\quad \cdot F(b,c,a) \end{aligned} \tag{3.87}$$

To derive the second equation, consider the 6 processes shown in Fig. 3.10. Denote the final states produced by these processes by $\{|1\rangle, ..., |6\rangle\}$. We can compute the phase difference between states $|1\rangle$ and $|6\rangle$ using either the upper or lower path of Fig. 3.10. Demanding consistency between the two calculations gives the second hexagon equation. The first hexagon equation follows in the same way by considering the 6 processes shown in Fig. 7.8. In Appendix 7.2, we will show that our microscopic definitions of F and R also obey the hexagon equations.

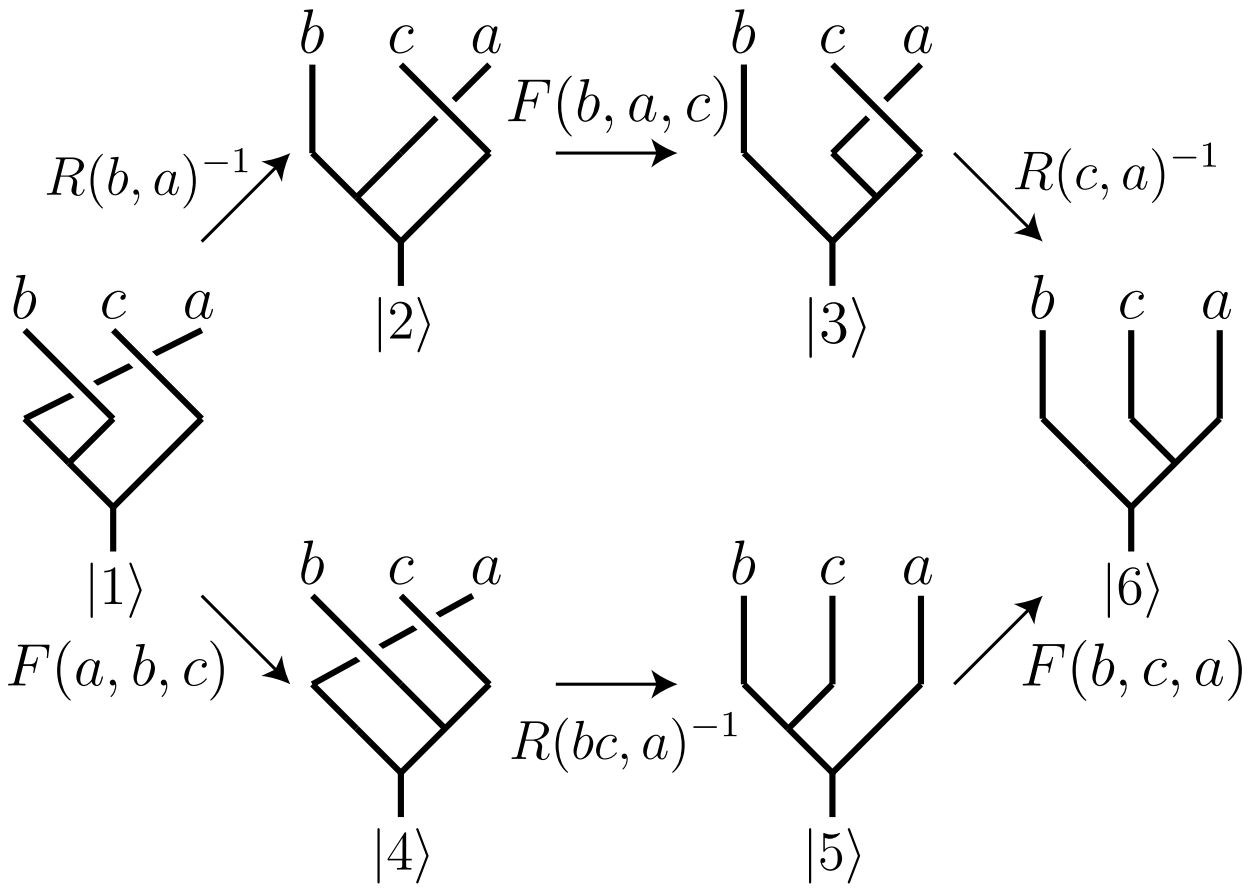

Figure 3.10: The second hexagon equation (3.87). Consistency requires that the product of the $U(1)$ phases along the upper path is equal to the product along the lower path.

3.5.2 Microscopic definition of R

As with the F-symbol, the first step in the microscopic definition of the R-symbol is to choose a representative anyon state, $|a_x\rangle$, for each anyon type a and each point x. The only new element here is that we need to consider a larger set of positions for x: specifically, in addition to the anyon states $\{|a_x\rangle\}$, where the position x is located on the x-axis, we also include the anyon states $|a_Y\rangle$ for some point, labeled Y, that is *not* on the x-axis. For concreteness, we will use a convention where the y-coordinate of Y is *negative* and larger in magnitude than the correlation length of the ground state, ξ, while the x-coordinate of Y lies between the two points '1' and '2' where our splitting operators are defined (Fig. 3.11a).

Moving on to *multi*-anyon states, we use the same notation as in our definition of F: we label these states as $|a_{x_1}, b_{x_2}, c_{x_3}, ...\rangle$, where $a, b, c, ...$ are the different anyons in the state and $x_1, x_2, x_3...$ are their positions. Like before, we assume that $x_1, x_2, x_3, ...$ are ordered according to their x-coordinate and that every pair of x_i's is separated by a distance of at least ξ.

Likewise, we use the same movement and splitting operators as before, but with one addition: we include two additional movement operators M^a_{Y1} and M^a_{1Y} which move an anyon, a, from point 1 to point Y and vice-versa. Formally, these operators are defined by the condition

$$M^a_{Y1}|a_1\rangle \propto |a_Y\rangle, \qquad M^a_{1Y}|a_Y\rangle \propto |a_1\rangle \tag{3.88}$$

where both proportionality constants are $U(1)$ phases. Note that we do *not* include any movement operators between Y and any other point on the x-axis: all anyon movements occur within the T-junction geometry shown in Fig. 3.11a.

With this setup we are now ready to give our definition of R. Consider the initial state $|ab_1\rangle$, i.e. the state with a single anyon of type ab at position 1. Starting with this state, we apply two different sequences of movement and splitting operators, denoting the final states by $|1\rangle$ and $|2\rangle$:

$$\begin{aligned} |1\rangle &= M^b_{01} M^b_{12} M^a_{Y1} S(a,b)|ab_1\rangle \\ |2\rangle &= M^a_{Y1} M^a_{12} M^b_{01} S(b,a)|ab_1\rangle \end{aligned} \tag{3.89}$$

These two processes are shown in Figure 3.11b. By construction, the final states $|1\rangle, |2\rangle$ produced by these processes both contain anyons a, b at positions $Y, 0$, respectively. In particular, this means that $|1\rangle, |2\rangle$ are the same up to a phase. We define $R(a,b)$ to be this

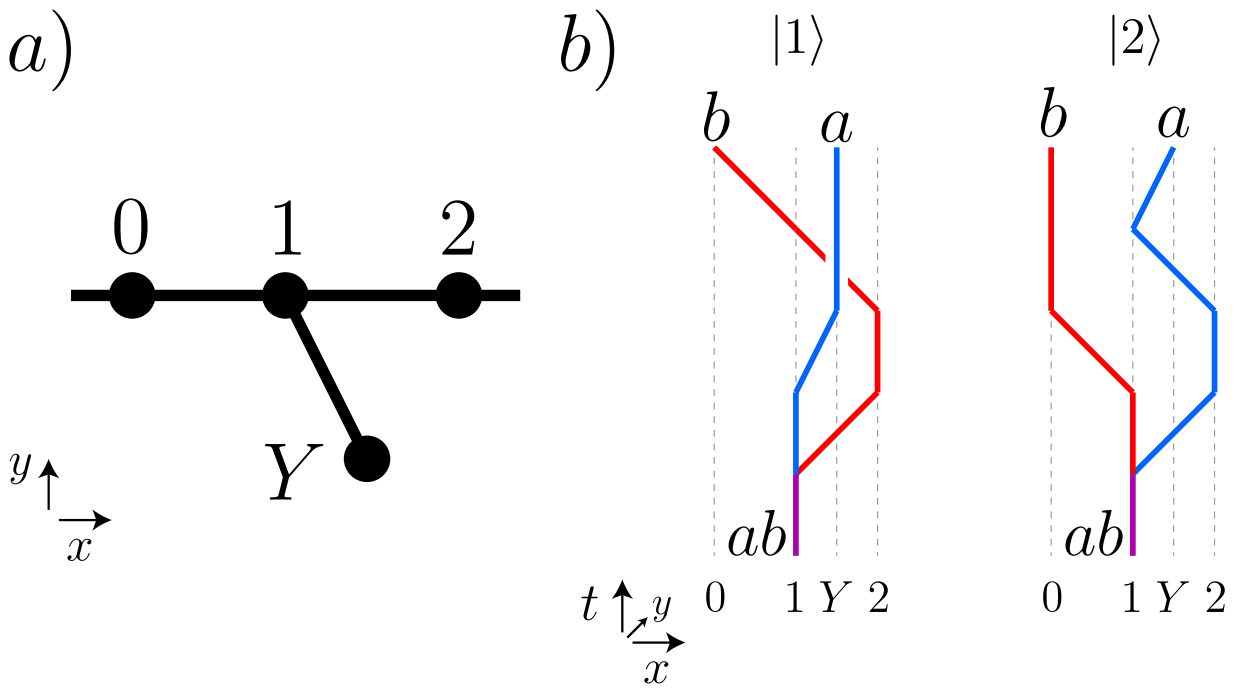

Figure 3.11: (a) To define R, we include an additional set of anyon states $\{|a_Y\rangle\}$ located at a point Y that is not on x-axis. We assume that Y has a negative y-coordinate and an x-coordinate between 1 and 2. (b) The two processes that are compared in the microscopic definition of the R-symbol.

phase difference:

$$R(a,b) = \langle 2|1\rangle \tag{3.90}$$

At this point, one can check that our definition of $R(a,a)$ matches the definition from Ref. [86] reviewed in the introduction.

3.5.3 Checking the microscopic definition

To show that the microscopic definition is sensible, we need to establish two properties of R: (i) R is well-defined in the sense that different choices of anyon states and movement and splitting operators give the same R up to a gauge transformation; and (ii) R obeys the hexagon equations (3.87). We prove property (ii) in Appendix 7.2; the goal of this section is to prove property (i).

To start, we analyze how R transforms if we change the phase of the movement and splitting operators:

$$M^a_{x'x} \to e^{i\theta_{x'x}(a)} M^a_{x'x}, \quad S(a,b) \to e^{i\phi(a,b)} S(a,b) \tag{3.91}$$

Substituting these transformations into (3.89-3.90) gives

$$R(a,b) \to R(a,b) \frac{e^{i\phi(a,b)} e^{i\theta_{12}(b)}}{e^{i\phi(b,a)} e^{i\theta_{12}(a)}} \tag{3.92}$$

We conclude that R changes by a gauge transformation (3.86) with

$$\nu(a,b) = \phi(a,b) + \theta_{12}(b) \tag{3.93}$$

Notice that the above expression for ν is the same as in Eq. (5.66). In other words, when we change the phases of the movement and splitting operators, the F and R-symbols undergo gauge transformations generated by the *same* $\nu(a,b)$. This is exactly what we want from our microscopic definition, as explained in Sec. 3.5.1.

Next, consider the more general situation where the movement and splitting operators are changed in an arbitrary way (for fixed choice of anyon states $|a_x\rangle$). Denoting the new movement and splitting operators by

$$M^a_{x'x} \to \tilde{M}^a_{x'x}, \qquad S(a,b) \to \tilde{S}(a,b), \tag{3.94}$$

it follows from the same arguments as in Sec. 5.3.5, that

$$\begin{aligned} \tilde{M}^a_{x'x} |..., a_x, ...\rangle &= e^{i\theta_{x'x}(a)} M^a_{x'x} |..., a_x, ...\rangle \\ \tilde{S}(a,b) |..., ab_1, ...\rangle &= e^{i\phi(a,b)} S(a,b) |..., ab_1, ...\rangle \end{aligned} \tag{3.95}$$

for some real-valued θ, ϕ. Substituting these relations into (3.89-3.90), we again see that $R(a,b)$ changes by a gauge transformation (3.86) with ν given by (3.93).

To complete the proof of property (i), we need to check how R transforms if we choose different representative anyon states $|a_x\rangle$. As in Sec. 5.3.5, we will assume that different choices of anyon states are related to one another by a local unitary transformation, U. Given this assumption, our task is to understand how R changes if we replace

$$|a_{x_1}, b_{x_2}, c_{x_3}, ...\rangle \to |a_{x_1}, b_{x_2}, c_{x_3}, ...\rangle' \tag{3.96}$$

where

$$|a_{x_1}, b_{x_2}, c_{x_3}, ...\rangle' = U|a_{x_1}, b_{x_2}, c_{x_3}, ...\rangle \tag{3.97}$$

for some local unitary transformation U. To answer this question, notice that we can choose movement and splitting operators for the states $|a_{x_1}, b_{x_2}, c_{x_3}, ...\rangle'$ however we like since we have already checked that this choice does not affect R, except by a gauge transformation. The simplest choice is

$$(M^a_{x'x})' = UM^a_{x'x}U^\dagger, \qquad S'(a,b) = US(a,b)U^\dagger \tag{3.98}$$

where $M^a_{x'x}$ and $S(a,b)$ are movement and splitting operators for the states $|a_{x_1}, b_{x_2}, c_{x_3}, ...\rangle$. With this choice, it is clear that $|1'\rangle = U|1\rangle$, and $|2'\rangle = U|2\rangle$. It follows that $R' = \langle 2'|1'\rangle = \langle 2|1\rangle = R$. Thus, we conclude that R is invariant under a replacement of the anyon states, $|a_{x_1}, b_{x_2}, c_{x_3}, ...\rangle \to |a_{x_1}, b_{x_2}, c_{x_3}, ...\rangle'$.

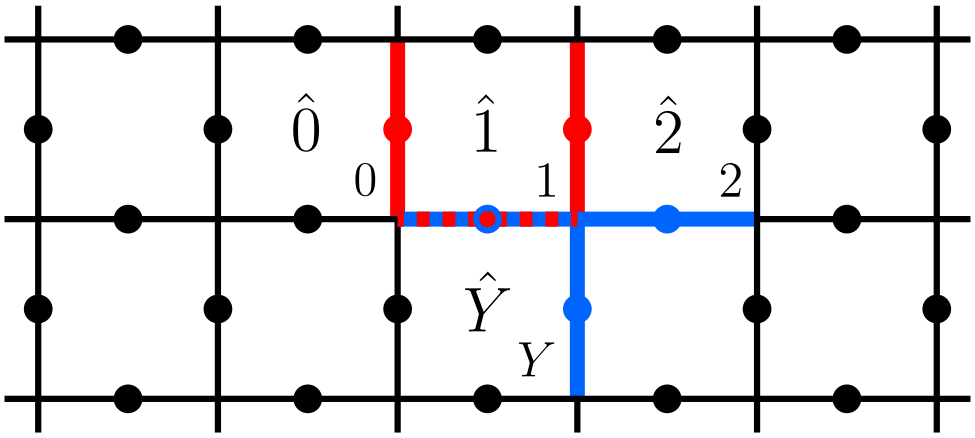

Figure 3.12: R-symbol calculation for the toric code model. Vertices and plaquettes are labeled by n and $\hat{n}$ respectively. The σ^z operators applied for M^e or $S(e,m)$ are colored in red. The σ^z operators applied for $M^m, S(m,e)$ are colored in blue.

3.5.4 Examples

We now illustrate our microscopic definition by computing the R-symbol of several different systems.

Toric code

We begin by computing the R-symbol $R(m,e)$ for the toric code. The first step is to label the anyon states that we will manipulate. For our calculation, we need the states corresponding to the e, m, and em anyons. In the case of the e anyons, we use the same notation as in Sec. 3.4.1: we label the vertices along the x-axis by integers $n = 0, \pm 1, \pm 2, ...$ and we define $|e_n\rangle$ to be the state with $A_{v=n} = -1$. Similarly, for the m anyons, we label the plaquettes that lie just above the x-axis by $\hat{n} = \hat{0}, \pm\hat{1}, \pm\hat{2}, ...$ and we define $|m_{\hat{n}}\rangle$ to be the state with $B_{p=\hat{n}} = -1$ (Fig. 3.12). Likewise, for the em anyons, we define $|em_n\rangle$ to be the state with $A_{v=n} = B_{p=\hat{n}} = -1$. Lastly, we will need two more anyon states, which we denote by $|e_Y\rangle$ and $|m_{\hat{Y}}\rangle$. Here, Y denotes a vertex, and $\hat{Y}$ denotes an adjacent plaquette, both of which are just below the x-axis (Fig. 3.12).

Next, we need to choose the movement operators for the two types of anyons. For the e

anyons, we use the same movement operators as in Sec. 3.4.1: we define $M^e_{n'n} = M^e_{nn'} = \sigma^z_{n,n'}$ where $\sigma^z_{n,n'}$ denotes the σ^z operator on the link between adjacent vertices n and n'. Likewise, for the m anyons, we define

$$M^m_{\hat{n}\hat{n}'} = M^m_{\hat{n}'\hat{n}} = \sigma^x_{\hat{n},\hat{n}'} \tag{3.99}$$

where $\sigma^x_{\hat{n},\hat{n}'}$ denotes the σ^x operator on the link between adjacent plaquettes $\hat{n}$ and $\hat{n}'$.

Finally we need the splitting operators $S(e,m)$ and $S(m,e)$, which we define by

$$\begin{aligned} S(e,m) &= \sigma^x_{\hat{1},\hat{2}} \\ S(m,e) &= \sigma^z_{1,2} \end{aligned} \tag{3.100}$$

With this setup, we are now ready to compute $R(m,e)$. Using the definition (3.89), we have

$$\begin{aligned} |1\rangle &= M^e_{01} M^e_{12} M^m_{Y1} S(m,e) |em_1\rangle \\ &= \sigma^z_{0,1} \sigma^z_{1,2} \sigma^x_{\hat{1},\hat{Y}} \sigma^z_{1,2} |em_1\rangle \\ &= \sigma^z_{0,1} \sigma^x_{\hat{1},\hat{Y}} |em_1\rangle \end{aligned} \tag{3.101}$$

and

$$\begin{aligned} |2\rangle &= M^m_{Y1} M^m_{12} M^e_{01} S(e,m) |em_1\rangle \\ &= \sigma^x_{\hat{1},\hat{Y}} \sigma^x_{\hat{1},\hat{2}} \sigma^z_{0,1} \sigma^x_{\hat{1},\hat{2}} |em_1\rangle \\ &= \sigma^x_{\hat{1},\hat{Y}} \sigma^z_{0,1} |em_1\rangle \end{aligned} \tag{3.102}$$

To compare the two states, we note that the operators $\sigma^z_{0,1}$ and $\sigma^x_{\hat{1},\hat{Y}}$ act on the same link

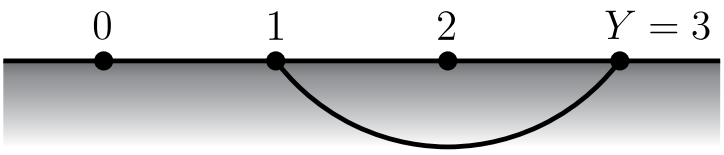

Figure 3.13: To compute R from a chiral boson edge theory, we choose Y to be the point 3 located on the edge of the topological phase. This choice is acceptable because we can think of the movement operator M_{Y1} as being supported along an arc which only touches the edge at points 1 and 3.

and therefore anticommute with one another. We conclude that $|1\rangle = -|2\rangle$; so

$$R(m, e) = -1 \tag{3.103}$$

Repeating the calculation for $R(e, m)$, one finds that $R(e, m) = +1$ due to the absence of anticommuting operators. More generally, with a suitable choice of conventions, it is easy to check that $R(a, b) = 1$ for all $a, b \in \{1, e, m, em\}$ except for

$$R(m, e) = R(em, e) = R(m, em) = R(em, em) = -1$$

Chiral boson edge theory

Next, we compute the R-symbol for a general bosonic Abelian topological phase described by an $N \times N$ K-matrix, K_{ij}. As in Sec. 3.4.4, our calculation is based on the chiral boson edge theory (3.68).

The first step is to specify our conventions for anyon states and movement and splitting operators. For this step, we use exactly the same definitions as in Sec. 3.4.4. The only new element of this calculation is that we need to define an additional set of anyon states in which the anyons are located at the special point Y shown in Fig. 3.11a. There is some subtlety in choosing the point Y: it is tempting to choose Y to be in the *bulk*, as suggested by the geometry in Fig. 3.11a, but such a choice is not convenient since our calculation is based on

an edge theory. Instead, we take Y to be the point 3 on the edge[5] shown in Fig. 3.13. With this choice the movement operator M^l_{Y1} is simply the operator M^l_{31} defined in Eq. 3.72. This movement operator can be thought of as being supported along an arc in the bulk which meets the edge only at points 1 and 3 (Fig. 3.13).

Having fixed our conventions, we are now ready to compute $R(l,m)$. Using the definition (3.89) together with the expression for the splitting operator (3.73), we obtain:

$$\begin{aligned} |1\rangle &= M^m_{01} M^m_{12} M^l_{31} M^m_{21} C(l,m) |[l+m]_1\rangle \\ |2\rangle &= M^l_{31} M^l_{12} M^m_{01} M^l_{21} C(m,l) |[l+m]_1\rangle \end{aligned} \tag{3.104}$$

To find the phase difference between these two states, we first rearrange the order of the movement operators using the commutation relations (3.76) and $M^l_{31} M^m_{21} = e^{i\alpha(l,m)} \cdot M^m_{21} M^l_{31}$:

$$\begin{aligned} |1\rangle &= M^l_{31} M^m_{01} C(l,m) |[l+m]_1\rangle e^{2i\alpha(l,m)} \\ |2\rangle &= M^l_{31} M^m_{01} C(m,l) |[l+m]_1\rangle e^{i\alpha(l,m)} \end{aligned} \tag{3.105}$$

where $\alpha(l,m)$ is given by definition (3.77). Then using the fact that $C(l,m) = C(m,l)$ we obtain $|1\rangle = e^{i\alpha(l,m)} |2\rangle$ so that

$$R(l,m) = e^{i\alpha(l,m)} \tag{3.106}$$

Making the gauge transformation (3.86) with ν given as in equation (3.83), we obtain

$$R(l,m) = \exp[i\pi l^T K^{-1}(K-X)K^{-1} m] \tag{3.107}$$

5. The point $Y = 3$ should not be confused with the point '3' that appears in the definition of the F-symbol: in that context it should be thought of as the point '1000' – i.e. far from the region where anyons are manipulated.

Together with the F-symbol in Eq. (3.84), this gives the complete anyon data for the bosonic Abelian topological phase with K-matrix K_{ij}.

We can check these results in two ways. First, it is easy to verify that F and R obey the pentagon identity (5.17) and hexagon equations (3.87). Second, we can compute the two gauge invariant quantities

$$\begin{aligned} R(l,l) &= \exp[i\pi l^T K^{-1} l] \\ R(l,m)R(m,l) &= \exp[2\pi i l^T K^{-1} m] \end{aligned} \tag{3.108}$$

which describe the exchange statistics and mutual statistics of the anyons. These expressions agree with standard K-matrix theory [151].

3.6 Non-Abelian anyons

In this section, we explain how our microscopic definitions of F and R generalize to non-Abelian anyons.

3.6.1 Review: non-Abelian anyon data

We begin by reviewing some basic aspects of non-Abelian anyon theories [74, 112]. These theories consist of four pieces of data:

1. **Set of anyon types**: a finite set of anyon types,

   $\mathcal{A} = \{a, b, c, ...\}$.

2. **Fusion product**: an associative and commutative multiplication law on $\mathcal{A}$ of the form

$$a \times b = \sum_c N_c^{ab} c \tag{3.109}$$

   where N_c^{ab} are non-negative integers called "fusion multiplicities."

3. F**-symbol**: a complex tensor, $(F^{abc}_{def})^{\kappa\lambda}_{\mu\nu}$, where $a, b, .., f \in \mathcal{A}$, while μ runs over the set $\{1, ..., N^{ab}_e\}$ with κ, λ, ν indexed similarly (see Fig. 3.14).

4. R**-symbol**: a complex tensor, $(R^{ab}_c)^{\mu}_{\nu}$, where $a, b, c \in \mathcal{A}$, while μ, ν run over the set $\{1, ..., N^{ab}_c\}$ (see Fig. 3.16).

The definition of "anyon types" is the same as in the Abelian case, so we begin by explaining the non-Abelian fusion product. Given any pair of anyons a, b, we say that an anyon of type c is a "fusion product" of a and b if c can be converted into a pair of anyons a, b by applying a unitary operator supported in a finite region around c. We then define the "fusion multiplicity" of c, denoted N^{ab}_c, as follows: $N^{ab}_c = 0$ if c is not a fusion product of a and b. Otherwise, $N^{ab}_c = m$ where m is the largest integer such that there exist m orthonormal states, $|a, b; c; 1\rangle, ..., |a, b; c; m\rangle$, consisting of two anyons a, b, and satisfying the following properties. First, each state $|a, b; c; \mu\rangle$ can be obtained from a single anyon of type c by applying a unitary operator supported in a finite region around c. Second, the $|a, b; c; \mu\rangle$ states are "locally indistinguishable": that is, they obey

$$\langle a, b; c; \mu'|O|a, b; c; \mu\rangle = (\text{const.}) \cdot \delta_{\mu\mu'} \tag{3.110}$$

for any local operator, O. Having defined N^{ab}_c, we define the fusion product of a and b by $a \times b = \sum_c N^{ab}_c c$. (For an alternative definition of non-Abelian fusion rules, see Refs. [126, 125].)

All that remains is to explain the meaning of the F and R symbols. We will discuss this in detail below, but the rough picture is as follows: the F-symbol can be interpreted as a collection of (unitary) change of basis matrices relating multi-anyon states obtained by splitting anyons in different orders. Likewise, the R-symbol is a collection of (unitary) matrices that describe the non-Abelian Berry phases associated with braiding or exchanging anyons. For example, $(R^{aa}_c)^{\mu}_{\nu}$ can be interpreted as the unitary matrix associated with exchanging two a particles in the fusion channel c.

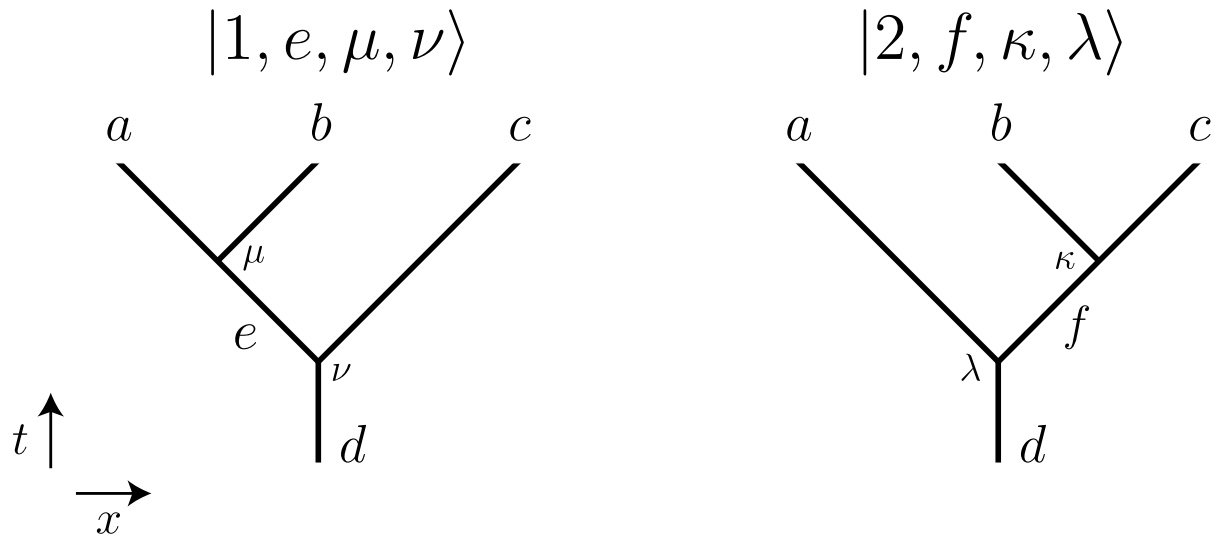

Figure 3.14: Two processes in which an anyon d splits into anyons a, b, c. The inner product of the final states $|1, e, \mu, \nu\rangle, |2, f, \kappa, \lambda\rangle$ defines the non-Abelian F-symbol.

3.6.2 Abstract definition of F

We now review the abstract definition of the F-symbol in the non-Abelian case [74, 112]. The basic idea is to consider two different physical processes in which an anyon, d, splits into three anyons, a, b, c (Fig. 3.14). In one process, d splits into anyons e and c and then e splits into a and b; in the other process, d splits into a and f and then f splits into b and c. In general, there will be more than one way to split the anyons if the fusion multiplicities are larger than 1. That is, there are multiple "locally indistinguishable" final states which can be obtained by each splitting. Therefore, we label the four splittings by additional indices $\mu, \nu, \kappa, \lambda$ where $\mu = 1, ..., N_e^{ab}$ and the others are indexed similarly. We then denote the final states of these processes by $|1, e, \mu, \nu\rangle$ and $|2, f, \kappa, \lambda\rangle$. By construction, the set of states $\{|1, e, \mu, \nu\rangle\}$ and $\{|2, f, \kappa, \lambda\rangle\}$ are both orthonormal bases for the same subspace — namely the subspace of states consisting of three anyons a, b, c fusing to d. It follows that these states must be related by a unitary matrix. The F-symbol $(F^{abc}_{def})^{\kappa\lambda}_{\mu\nu}$ is defined to be this

unitary matrix:

$$|1, e, \mu, \nu\rangle = \sum_{f,\kappa,\lambda} (F^{abc}_{def})^{\kappa\lambda}_{\mu\nu} \cdot |2, f, \kappa, \lambda\rangle \tag{3.111}$$

As in the Abelian case, the above definition implies two properties of the F-symbol. The first property is that the F-symbol is only well-defined up to gauge transformations. These transformations take the form

$$\begin{aligned}(F^{abc}_{def})^{\kappa\lambda}_{\mu\nu} \to \sum_{\kappa'\lambda'\mu'\nu'} & (F^{abc}_{def})^{\kappa'\lambda'}_{\mu'\nu'} \\ & \cdot (\alpha^{ec}_{d})^{\nu'}_{\nu} (\alpha^{ab}_{e})^{\mu'}_{\mu} (\alpha^{d}_{af})^{\lambda}_{\lambda'} (\alpha^{f}_{bc})^{\kappa}_{\kappa'}\end{aligned} \tag{3.112}$$

where $(\alpha^{ab}_{c})^{\mu'}_{\mu}$ is a family of unitary matrices of dimension $N^{ab}_{c} \times N^{ab}_{c}$, parameterized by triplets of anyons, a, b, c, and $\alpha^{c}_{ab} \equiv (\alpha^{ab}_{c})^{-1}$ is the inverse matrix. To understand where these gauge transformations come from, it is useful to think of each splitting, $c \to a, b$, as being implemented by a collection of splitting operators, $S^{ab}_{c,\mu}$, where $\mu = 1, ..., N^{ab}_{c}$. We are free to mix different splitting operators with one another by multiplying by a unitary matrix, $(\alpha^{ab}_{c})^{\mu'}_{\mu}$:

$$S^{ab}_{c,\mu} \to \sum_{\mu'} (\alpha^{ab}_{c})^{\mu'}_{\mu} S^{ab}_{c,\mu'} \tag{3.113}$$

If we make this replacement for each of the four splittings, then F changes by exactly the above gauge transformation (3.112).

The second property of the F-symbol is that it obeys the pentagon identity. In the

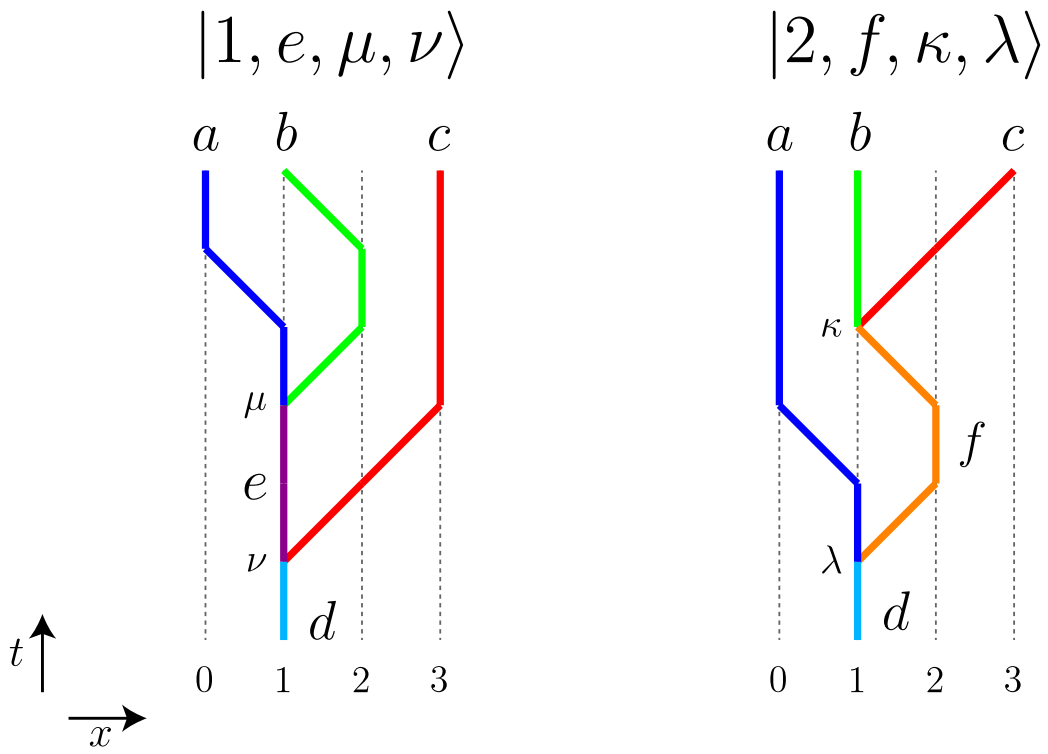

Figure 3.15: The two microscopic processes that define the non-Abelian F-symbol.

non-Abelian case, this identity takes the form

$$\sum_{h\lambda'\mu'\rho} (F^{abc}_{gfh})^{\lambda'\mu'}_{\lambda\mu} (F^{ahd}_{egk})^{\rho\sigma}_{\mu'\nu} (F^{bcd}_{khl})^{\tau\rho'}_{\lambda'\rho} = \sum_{\kappa} (F^{fcd}_{egl})^{\tau\kappa}_{\mu\nu} (F^{abl}_{efk})^{\rho'\sigma}_{\lambda\kappa} \tag{3.114}$$

This identity follows from the same reasoning as in the Abelian case.

3.6.3 Microscopic definition of F

The microscopic definition of F follows the same basic steps as is in the Abelian case. As before, we fix a line in the 2D plane and we only consider states with anyons living along this line. For each anyon a and each position x, we let $|a_x\rangle$ denote a state that contains a single anyon a located at point x. Likewise, for any finite set of well-separated points

$x_1 < x_2 < x_3 < ...$ we let

$$|a_{x_1}, b_{x_2}, c_{x_3}, ...; t; \mu\rangle, \quad \mu = 1, ..., N_t^{abc...} \tag{3.115}$$

denote an orthonormal basis of "locally indistinguishable" multi-anyon states that contain an anyon a at point x_1, anyon b at point x_2, etc., and that can be obtained from a single anyon t by applying a unitary operator supported in a finite region around t. Here, $N_t^{abc...}$ denotes the fusion multiplicity of t in the fusion product $a \times b \times c \cdots$. Also, when we say that these states are "locally indistinguishable" we mean that they satisfy

$$\langle \mu' | O | \mu \rangle = (\text{const.}) \cdot \delta_{\mu\mu'} \tag{3.116}$$

where O is any local operator, and where we are using the abbreviation

$$|\mu\rangle \equiv |a_{x_1}, b_{x_2}, c_{x_3}, ...; t; \mu\rangle \tag{3.117}$$

As in the Abelian case, it is useful to give a precise definition of the multi-anyon states in terms of the single anyon states: we define the multi-anyon states to be the set of *all* states that have the same expectation values as the ground state for local operators supported away from all the anyons, and the same expectation values as $|a_{x_1}\rangle$ for local operators near x_1, the same expectation values as $|b_{x_2}\rangle$ for local operators near x_2, and so on. That is, the multi-anyon states are characterized by the fact that

$$\langle ..., a_x, ...; t; \mu | O | ..., a_x, ...; t; \mu \rangle = \langle a_x | O | a_x \rangle \tag{3.118}$$

for every operator O supported in the neighborhood of a single anyon a_x.

With this setup, we are now ready to define movement operators. For any anyon a and any pair of points x, x', we say that $M^a_{x'x}$ is a "movement operator" if it obeys two conditions:

first,

$$M^a_{x'x}|a_x\rangle \propto |a_{x'}\rangle \tag{3.119}$$

where the proportionality constant is a $U(1)$ phase; second, $M^a_{x'x}$ is supported in a neighborhood of the interval containing x and x'. As in the Abelian case, the second condition, together with (3.118), guarantees that $M^a_{x'x}$ has a similar effect on any multi-anyon state of the form $|..., a_x, ...\rangle$ that does not contain any other anyons between x and x':

$$M^a_{x'x}|..., a_x, ...; t; \mu\rangle = \sum_{\mu'} V^{\mu'}_{\mu} |..., a_{x'}, ...; t; \mu'\rangle \tag{3.120}$$

where $V^{\mu'}_{\mu}$ is a unitary matrix.

We now move on to define splitting operators. First, we fix two (well-separated) points on the line, '1' and '2.' Let a, b be any pair of anyons and let c be any anyon that appears in the product $a \times b$ with multiplicity $N^{ab}_c \geq 1$. We say that a collection of operators $\{S^{ab}_{c,\mu}\}$, where $\mu = 1, ..., N^{ab}_c$, are "splitting operators" if $S^{ab}_{c,\mu}$ satisfies two conditions: first,

$$S^{ab}_{c,\mu}|c_1\rangle = \sum_{\mu'} Q^{\mu'}_{\mu} |a_1, b_2; c; \mu'\rangle, \tag{3.121}$$

where $Q^{\mu'}_{\mu}$ is a unitary matrix; second, $S^{ab}_{c,\mu}$ is supported in the neighborhood of the interval $[1, 2]$. As in the Abelian case, the second condition guarantees that the splitting operators have a similar effect when applied to any multi-anyon state of the form $|..., c_1, ...\rangle$, as long as the other anyons are located far from $[1, 2]$: that is,

$$S^{ab}_{c,\mu}|..., c_1, ...; t; \nu\rangle = \sum_{\lambda} W^{\lambda}_{\mu\nu}|..., a_1, b_2, ...; t; \lambda\rangle \tag{3.122}$$

for some complex coefficients, $W^{\lambda}_{\mu\nu}$. These coefficients are guaranteed to have the orthonor-

mality property

$$\sum_{\lambda}(W^{\lambda}_{\mu\nu})^* W^{\lambda}_{\mu'\nu'} = \delta_{\mu\mu'}\delta_{\nu\nu'} \tag{3.123}$$

An equivalent way to say this is that the states $S^{ab}_{c,\mu}|..., c_1, ...; t; \nu\rangle$ are orthonormal.

For any choice of movement and splitting operators, we define a corresponding F-symbol as follows. First, starting with a single anyon d at position 1, we apply two different sequences of movement and splitting operations:

$$\begin{aligned} |1, e, \mu, \nu\rangle &= M^b_{12} M^a_{01} S^{ab}_{e,\mu} M^c_{32} S^{ec}_{d,\nu} |d_1\rangle \\ |2, f, \kappa, \lambda\rangle &= M^c_{32} S^{bc}_{f,\kappa} M^f_{12} M^a_{01} S^{af}_{d,\lambda} |d_1\rangle \end{aligned} \tag{3.124}$$

These two processes are shown in Figure 3.15. Next, we consider the collection of states $\{|1, e, \mu, \nu\rangle\}$. By construction, all of these states contain anyons a, b, c at positions $0, 1, 3$. In fact, the collection of states $\{|1, e, \mu, \nu\rangle\}$ forms an orthonormal basis for the topologically degenerate subspace spanned by $\{|a_0, b_1, c_3; d; \sigma\rangle : \sigma = 1, ..., N^{abc}_d\}$. The same is true for the second collection of states, $\{|2, f, \kappa, \lambda\rangle\}$. It follows that the overlaps between these two collections of states form a unitary matrix. The F-symbol is defined to be this unitary matrix:

$$(F^{abc}_{def})^{\kappa\lambda}_{\mu\nu} = \langle 2, f, \kappa, \lambda | 1, e, \mu, \nu\rangle \tag{3.125}$$

3.6.4 Checking the definition of F

As in the Abelian case, we need to check two properties of F to establish that our definition is sensible: (i) different choices of anyon states and movement and splitting operators give the same F up to a gauge transformation; and (ii) F obeys the pentagon identity (3.114). In this section, we prove property (i). As for property (ii), this follows from arguments that

are almost identical to those in the Abelian case, discussed in Appendix 7.1.

To prove property (i), we first consider how F transforms if we change the splitting and movement operators by a transformation of the form

$$\begin{aligned} M^a_{x'x} &\to e^{i\theta^a_{x'x}} M^a_{x'x} \\ S^{ab}_{c,\mu} &\to \sum_{\mu'} (\beta^{ab}_c)^{\mu'}_{\mu} S^{ab}_{c,\mu'} \end{aligned} \tag{3.126}$$

where $(\beta^{ab}_c)^{\mu'}_{\mu}$ is an $N^{ab}_c \times N^{ab}_c$ unitary matrix and $\theta^a_{x'x} \in \mathbb{R}$. Substituting (3.126) into the definition of F (3.125), it is easy to see that F changes by a gauge transformation with

$$(\alpha^{ab}_c)^{\mu'}_{\mu} = (\beta^{ab}_c)^{\mu'}_{\mu} \cdot e^{i\theta^b_{12}} \tag{3.127}$$

Next, consider the more general situation where M and S are changed in an arbitrary way (for a fixed choice of single[6] anyon states $|a_x\rangle$). Denoting the new movement and splitting operators by

$$M^a_{x'x} \to \tilde{M}^a_{x'x}, \qquad S^{ab}_{c,\mu} \to \tilde{S}^{ab}_{c,\mu}, \tag{3.128}$$

it follows from the definition that

$$\begin{aligned} \tilde{M}^a_{x'x} |..., a_x, ...; t; \mu\rangle &= \sum_{\mu'} T^{\mu'}_{\mu} \cdot M^a_{x'x} |..., a_x, ...; t; \mu'\rangle \\ \tilde{S}^{ab}_{c,\mu} |..., c_1, ...; t; \nu\rangle &= \sum_{\mu'\nu'} U^{\mu'\nu'}_{\mu\nu} S^{ab}_{c,\mu'} |..., c_1, ...; t; \nu'\rangle \end{aligned}$$

where $T^{\mu'}_{\mu}$ and $U^{\mu'\nu'}_{\mu\nu}$ are unitary matrices. These matrices are highly constrained: first,

6. Fixing the single anyon states guarantees that the *subspace* of locally indistinguishable multi-anyon states is also fixed.

the topological degeneracy property (3.116) implies that $T_\mu^{\mu'} = T\delta_\mu^{\mu'}$ for some phase factor T, and likewise, $U_{\mu\nu}^{\mu'\nu'} = U_\mu^{\mu'}\delta_\nu^{\nu'}$ for some unitary matrix $U_\mu^{\mu'}$. Next, since both movement operators are supported in a neighborhood of the interval containing x and x', it follows from property (3.118) that T can only depend on a, x, x'. Likewise, $U_\mu^{\mu'}$ can only depend on a, b, c. Putting this all together, we conclude that

$$\begin{aligned}\tilde{M}^a_{x'x}|..., a_x, ...; t; \mu\rangle &= e^{i\theta_{x'x}(a)} M^a_{x'x}|..., a_x, ...; t; \mu\rangle \\ \tilde{S}^{ab}_{c,\mu}|..., c_1, ...; t; \nu\rangle &= \sum_{\mu'} (\beta_c^{ab})_\mu^{\mu'} S^{ab}_{c,\mu'}|..., c_1, ...; t; \nu\rangle\end{aligned}$$

for some real-valued $\theta_{xx'}(a)$ and some unitary matrix $(\beta^{ab_c})_\mu^{\mu'}$. Substituting these relations into (3.125), we again see that F changes by a gauge transformation (3.112) with α given by (3.127).

To complete our proof of property (i), we need to check that F changes at most by a gauge transformation if we choose different anyon states $|a_x\rangle$. This can established using nearly identical arguments to the Abelian case (see Sec. 5.3.5).

3.6.5 Abstract definition of R

We now explain the abstract definition of R in the case of non-Abelian anyons [74, 112]. As always, the basic idea is to compare two different physical processes (Fig. 3.16). In one process, an anyon, c, splits into two anyons a, b, with a on the left and b on the right, and then a, b are exchanged in the counterclockwise direction; the other process, c is splits into a, b with b on the left and a on the right, without any subsequent exchange. If the fusion multiplicity N_c^{ab} is larger than 1, then are multiple ways to split c into a, b. Therefore, we label the two splittings by additional indices μ, ν, which run from 1 to N_c^{ab}. Denoting the two final states by $|1, \nu\rangle$ and $|2, \mu\rangle$, it is clear, by the same logic as in Sec. 3.6.2, that these two sets of states are related by a unitary matrix. The R-symbol $(R_c^{ab})_\nu^\mu$ is defined to be

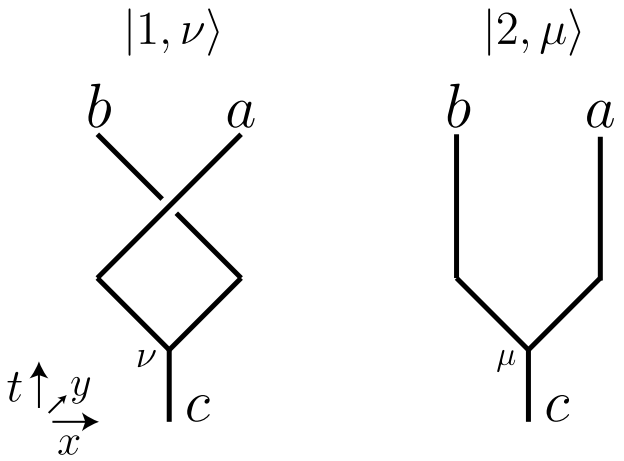

Figure 3.16: Two processes in which an anyon c splits into anyons a, b. The inner product of the final states $|1,\nu\rangle, |2,\mu\rangle$, defines the non-Abelian R-symbol.

this unitary matrix:

$$|1,\nu\rangle = \sum_{\mu} (R_c^{ab})_\nu^\mu |2,\mu\rangle \tag{3.129}$$

Similarly to the Abelian case, two properties of the R-symbol follow from this definition. First, R is only well-defined up to gauge transformations of the form

$$(R_c^{ab})_\nu^\mu \to \sum_{\mu'\nu'} (R_c^{ab})_{\nu'}^{\mu'} (\alpha_c^{ab})_\nu^{\nu'} (\alpha_{ba}^c)_{\mu'}^\mu \tag{3.130}$$

where $(\alpha_c^{ab})_\mu^{\mu'}$ is the same family of unitary matrices of dimension $N_c^{ab} \times N_c^{ab}$ that appears in the gauge transformation for F (3.112). (As before, we use the notation $\alpha_{ab}^c \equiv (\alpha_c^{ab})^{-1}$ to denote the inverse matrix).

The second property of the R-symbol is that it obeys the hexagon equations. In the

non-Abelian case, these take the form

$$\sum_{\mu'\kappa}(R_e^{ab})_\mu^{\mu'}(F_{def}^{bac})_{\mu'\lambda'}^{\kappa\lambda}(R_f^{ac})_\kappa^{\kappa'} = \sum_{g\sigma\tau\tau'}(F_{deg}^{abc})_{\mu\lambda'}^{\sigma\tau}(R_d^{ag})_\tau^{\tau'}(F_{dgf}^{bca})_{\sigma\tau'}^{\kappa'\lambda}$$
$$\sum_{\mu'\kappa}(R_{ba}^{e})_\mu^{\mu'}(F_{def}^{bac})_{\mu'\lambda'}^{\kappa\lambda}(R_{ca}^{f})_\kappa^{\kappa'} = \sum_{g\sigma\tau\tau'}(F_{deg}^{abc})_{\mu\lambda'}^{\sigma\tau}(R_{ga}^{d})_\tau^{\tau'}(F_{dgf}^{bca})_{\sigma\tau'}^{\kappa'\lambda} \tag{3.131}$$

where we use the notation $R_{bc}^{a} \equiv (R_a^{bc})^{-1}$ to denote the inverse matrix. These equations follow from the same reasoning as in the Abelian case.

3.6.6 Microscopic definition of R

The microscopic definition of the R-symbol for non-Abelian anyon theories is similar to the one in the Abelian case. The first step is to choose a representative anyon state $|a_x\rangle$ for each anyon a and each point x. As in the Abelian case, we include both the usual anyon states $|a_x\rangle$, where the position x is located on the x-axis, as well as an additional collection of anyon states $\{|a_Y\rangle\}$ for some specific point Y that has a negative y-coordinate (Fig. 3.11a).

We then use the same notation for multi-anyon states as in Sec. 3.5.2: we label them as $|a_{x_1}, b_{x_2}, c_{x_3}, ...; t; \mu\rangle$ where $a, b, c, ...$ are the different anyons in the state and $x_1, x_2, x_3, ...$ are their well-separated positions, ordered according to their x-coordinate. Also, as in the Abelian case, we introduce two additional movement operators M_{Y1}^a and M_{1Y}^a which move an anyon a from point 1 to point Y and vice-versa.

To define R, consider the initial state $|c_1\rangle$, i.e. the state with a single anyon c at position 1. Starting with this state, we apply two different sequences of movement and splitting

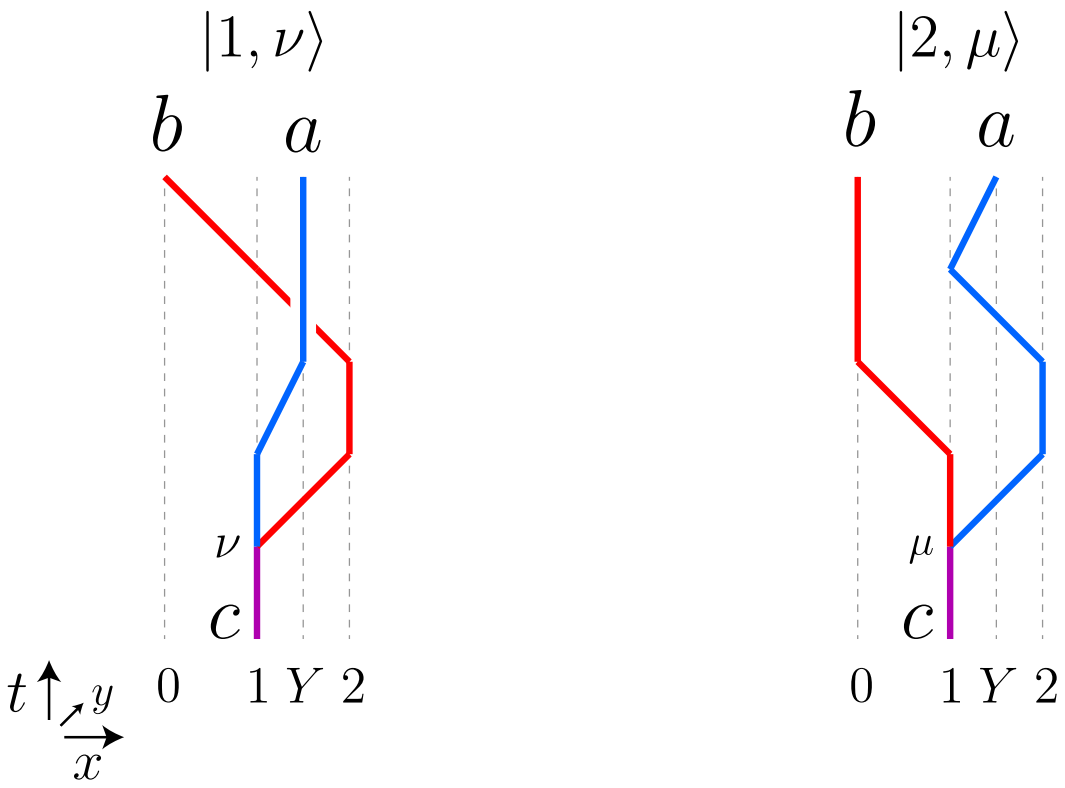

Figure 3.17: The two processes that are compared in the microscopic definition of the non-Abelian R-symbol.

operators, denoting the final states by $|1,\nu\rangle$ and $|2,\mu\rangle$:

$$\begin{aligned} |1,\nu\rangle &= M_{01}^{b} M_{12}^{b} M_{Y1}^{a} S_{c,\nu}^{ab} |c_1\rangle \\ |2,\mu\rangle &= M_{Y1}^{a} M_{12}^{a} M_{01}^{b} S_{c,\mu}^{ba} |c_1\rangle \end{aligned} \tag{3.132}$$

These two processes are shown in Figure 3.17. By construction, the final states, $|1,\nu\rangle, |2,\mu\rangle$, produced by these processes both contain anyons a, b at positions $Y, 0$, and form an orthonormal basis for the subspace of two anyon states at these positions. It follows that $|1,\nu\rangle$ and $|2,\mu\rangle$ are related by a unitary matrix. We define $(R_c^{ab})_\nu^\mu$ to be this unitary matrix:

$$(R_c^{ab})_\nu^\mu = \langle 2,\mu|1,\nu\rangle \tag{3.133}$$

3.6.7 Checking the definition of R

We need to check two properties of R to show that our definition is sensible: (i) different choices of anyon states and movement and splitting operators give the same R up to a gauge transformation (3.130); and (ii) R obeys the hexagon equations (3.131). In this section, we prove property (i). As for property (ii), this follows from arguments that are almost identical to those in the Abelian case discussed in Appendix 7.2.

The first step in proving property (i) is to consider how R transforms if we replace the movement and splitting operators by

$$\begin{aligned} M^a_{x'x} &\to e^{i\theta^a_{x'x}} M^a_{x'x} \\ S^{ab}_{c,\mu} &\to \sum_{\mu'} (\beta^{ab}_c)^{\mu'}_{\mu} S^{ab}_{c,\mu'} \end{aligned} \tag{3.134}$$

where $(\beta^{ab}_c)^{\mu'}_{\mu}$ is an $N^{ab}_c \times N^{ab}_c$ unitary matrix and $\theta^a_{x'x} \in \mathbb{R}$. Substituting this into (3.132-3.133) we conclude that R changes by a gauge transformation (3.130) with

$$(\alpha^{ab}_c)^{\mu'}_{\mu} = (\beta^{ab}_c)^{\mu'}_{\mu} \cdot e^{i\theta^b_{12}} \tag{3.135}$$

Importantly, the above expression for α is the same as in Eq. (3.127): thus, the F and R-symbols undergo gauge transformations generated by the *same* α, as desired.

Next, consider the more general situation where the movement and splitting operators are changed in an arbitrary way (again for a fixed choice of single anyon states $|a_x\rangle$). Denoting the new movement and splitting operators by

$$M^a_{x'x} \to \tilde{M}^a_{x'x}, \qquad S^{ab}_{c,\mu} \to \tilde{S}^{ab}_{c,\mu}, \tag{3.136}$$

the same arguments as in the previous section imply that

$$\tilde{M}^a_{x'x}|..., a_x, ...; t; \mu\rangle = e^{i\theta_{x'x}(a)} M^a_{x'x}|..., a_x, ...; t; \mu\rangle$$
$$\tilde{S}^{ab}_{c,\mu}|..., c_1, ...; t; \nu\rangle = \sum_{\mu'} (\beta^{ab}_c)^{\mu'}_{\mu} S^{ab}_{c,\mu'}|..., c_1, ...; t; \nu\rangle$$

for some real-valued $\theta_{xx'}(a)$ and some unitary matrix $(\beta^{ab_c})^{\mu'}_{\mu}$. Substituting these relations into (3.132-3.133), we again see that R changes by a gauge transformation with α given by (3.127).

At this point we have almost proved property (i): all that remains is show that different representative anyon states $|a_x\rangle$ lead to the same R, up to a gauge transformation. This result follows from the same argument as in the Abelian case (Sec. 3.5.3).

3.7 Conclusion

In this paper, we have proposed microscopic definitions of both the F-symbol and the R-symbol. These definitions are quite general: they apply to arbitrary bosonic or fermionic many-body systems with local interactions and an energy gap. We have also shown that our definitions obey the pentagon and hexagon equations, thereby providing a microscopic derivation of these fundamental constraints.

Throughout this paper, we have emphasized that our definitions provide concrete procedures for *computing* anyon data from microscopic models. It is natural to wonder: can we go a step further and turn these procedures into experimental protocols? In other words, do our definitions provide a way to *measure* F and R?

The answer to this question is 'yes,' at least in principle. For example, consider the Abelian F-symbol $F(a, b, c)$. To measure this quantity, one could first prepare an initial state of the form $\frac{1}{\sqrt{2}}|(abc)_1\rangle \otimes (|\uparrow\rangle + |\downarrow\rangle)$, where $|(abc)_1\rangle$ denotes an anyon state, and $|\uparrow\rangle, |\downarrow\rangle$ are (orthogonal) states of an ancilla qubit. Next, one could perform the sequence of movement

and splitting operations in process '1' (3.11), with each operation conditioned on the ancilla qubit being in the state $|\uparrow\rangle$, followed by the operations in process '2,' each conditioned on the ancilla qubit being in the state $|\downarrow\rangle$.[7] This sequence of operations produces the final state $\frac{1}{\sqrt{2}}(|1\rangle \otimes |\uparrow\rangle + |2\rangle \otimes |\downarrow\rangle)$. Finally, by measuring the expectation values $\langle\sigma^x\rangle$ and $\langle\sigma^y\rangle$ for the ancilla qubit, one could extract the real and imaginary parts of $\langle 2|1\rangle = F(a,b,c)$. A similar scheme could be used to measure R; thus, in principle one can measure the *complete* set of anyon data. These schemes also generalize easily to the non-Abelian case.

That said, these schemes, both theoretical and experimental, suffer from a serious limitation: they assume a detailed microscopic understanding of anyon excitations. An important problem is to find other methods of extracting a complete set of anyon data that do not require as much information about the underlying many-body system. For example, several authors have proposed methods for computing various pieces of anyon data from a ground state wave function alone[148, 87, 75, 169, 170, 106, 167, 137, 49]; it would be interesting if one could develop methods of this kind for the F-symbol or R-symbol.

Another interesting direction would be to consider many-body systems with *symmetries*. These systems are characterized by a richer set of data that describes both the topological properties of anyon excitations as well as how they transform under the symmetries [7, 133, 132, 80]. A natural extension of this work would be to find microscopic definitions and measurement schemes for this "symmetry-enriched" data.

7. Here, we assume that the movement and splitting operators are chosen so that they are *unitary*.

ACKNOWLEDGMENTS

We thank R. Mong for useful discussions. K.K. and M.L. acknowledge the support of the Kadanoff Center for Theoretical Physics at the University of Chicago. This research was supported in part by NSF DMR-1254741 as well as the Simons Foundation through the "Ultra-Quantum Matter" Simons Collaboration.

CHAPTER 4

MICROSCOPIC DEFINITIONS OF BOSONIC SPT DATA FROM BOUNDARY THEORIES

This chapter is reprinted with permission from:

Kyle Kawagoe and Michael Levin. Anomalies in bosonic symmetry-protected topological edge theories: Connection to F symbols and a method of calculation. Phys. Rev. B, 104:115156, Sep 2021.

Abstract

We describe a systematic procedure for determining the identity of a 2D bosonic symmetry protected topological (SPT) phase from the properties of its edge excitations. Our approach applies to general bosonic SPT phases with either unitary or antiunitary symmetries, and with either continuous or discrete symmetry groups, with the only restriction being that the symmetries must be on-site. Concretely, our procedure takes a bosonic SPT edge theory as input, and produces an element ω of the cohomology group $H^3(G, U_T(1))$. This element $\omega \in H^3(G, U_T(1))$ can be interpreted as either a label for the bulk 2D SPT phase or a label for the anomaly carried by the SPT edge theory. The basic idea behind our approach is to compute the F-symbol associated with domain walls in a symmetry broken edge theory; this domain wall F-symbol is precisely the anomaly we wish to compute. We demonstrate our approach with several SPT edge theories including both lattice models and continuum field theories.

4.1 Introduction

A gapped quantum many-body system belongs to a nontrivial "symmetry-protected topological" (SPT) phase if it has two properties: (i) the ground state is unique and short-range

entangled[1]; and (ii) it is not possible to adiabatically connect the system to another system with a trivial (product-state) ground state without breaking one or more global symmetries [110, 40, 24, 120, 25, 28]. Famous examples of SPT phases include the 2D and 3D topological insulators [53, 114] and the 1D Haldane spin-1 chain [50].

The most important physical property of nontrivial SPT phases is that these systems support robust gapless boundary modes. These boundary modes are "protected" in the sense that they cannot be gapped out without breaking one or more global symmetries [66, 164, 162, 26, 84, 39] or, in the case of 3D or higher dimensional systems, introducing topological order on the boundary [139, 100, 30, 144, 14].

A basic question is how to determine the identity of an SPT phase from the properties of its boundary modes. This "bulk-boundary correspondence" is largely understood for non-interacting fermionic SPTs. For example, in the case of 2D time-reversal symmetric insulators, one can determine whether the bulk phase is a trivial insulator or a topological insulator based on whether there are an even or odd number of Kramers pairs of edge modes. Similar formulas expressing bulk invariants in terms of boundary modes are known for other non-interacting fermion SPTs [53, 114]. The interacting case, however, is less understood, especially in two and higher dimensions. This paper seeks to address the interacting problem in the case of 2D bosonic SPT phases with on-site (i.e. non-spatial) symmetries. We ask: how can one determine the identity of a 2D bosonic SPT phase from its (1D) edge modes?

To make this question more concrete, let us recall the conjectured cohomology classification of 2D bosonic SPT phases [28]. According to this classification, there is a one-to-one correspondence between 2D bosonic SPT phases with on-site symmetry group G and elements of the cohomology group $H^3(G, U_T(1))$. Our problem is thus to compute an element $\omega \in H^3(G, U_T(1))$ from a bosonic SPT edge theory. This element $\omega \in H^3(G, U_T(1))$ can be interpreted as describing the *anomaly* carried by the edge theory.

1. A state $|\Psi\rangle$ is "short-range entangled" if it can be transformed into a product state by local unitary transformation, i.e. a unitary of the form $U = \mathcal{T} \exp(-i \int_0^T H(t)dt)$ where H is a local Hermitian operator.

Significant progress on this problem has been made in previous work. In a pioneering paper, Chen, Liu, and Wen [26] showed how to compute the anomaly $\omega \in H^3(G, U(1))$ for any bosonic SPT edge theory whose symmetries are represented by matrix product unitary operators. Later, in another important advance, Else and Nayak [39] introduced a method for computing anomalies based on the idea of spatially restricting symmetry operators. This symmetry restriction method applies to any SPT edge theory whose symmetries are local unitary transformations, i.e. of the form $U = \mathcal{T} \exp(-i \int_0^T H(t)dt)$ for some local Hermitian operator H. In another line of research, several authors have presented approaches for determining anomalies in SPT edge theories with conformal symmetry, using orbifold [129, 18, 135, 91] or orientifold constructions [57], though it is not obvious how to extend the latter approaches to general symmetry groups.

One limitation of the approaches introduced in Ref. [26], [39] is that they do not apply to SPT edge theories with antiunitary symmetries except in special cases [39]. Another limitation is that they require that the symmetries take a particular form – either a matrix product operator or a local unitary transformation. A priori there could be edge theories where the symmetries cannot be written in these forms, or it may be difficult to write explicitly.

In this paper, we present an alternative approach for computing anomalies in bosonic SPT edge theories, which addresses these issues. Unlike previous work, our approach applies to general bosonic SPT edge theories with both unitary and antiunitary symmetries. Our only restriction is that the underlying 2D symmetry must be on-site.

The basic idea behind our approach is simple. First, we choose an edge Hamiltonian that spontaneously[2] breaks all the symmetries on the edge and opens up an energy gap. Such a Hamiltonian has a collection of degenerate ordered ground states related to one another by symmetry transformations. The elementary excitations are domain walls between the

2. Alternatively, we can break the symmetry explicitly rather than spontaneously. See Sec. 4.7 for details.

different ground states. These domain walls can be fused together to form new domain walls, much like anyon excitations in 2D topological systems. This allows one to define an "F-symbol" that describes the phase difference associated with fusing domain walls in different orders. This domain wall F-symbol is precisely the anomaly we wish to compute: we show that F is naturally an element of $H^3(G, U_T(1))$, and that F depends only on the edge theory and not on other details. Some care is required to compute F, but we describe a concrete procedure for performing this computation using the formalism of Ref. [69]. We note that the connection between domain wall F-symbols and anomalies was also alluded to in Ref. [117] in the context of a $\mathbb{Z}_2$ SPT edge theory.

This paper is organized as follows. In Sec. 5.2 we explain the basic setup for our problem. Then, in Sec. 4.3, we present our anomaly computation procedure in the simplest case: SPT edge theories with discrete unitary symmetry groups. We illustrate our procedure with several (discrete unitary) examples in Sec. 5.4. In Sec. 4.5, we discuss the connection between our procedure and the symmetry restriction approach of Ref. [39], and we prove that the two approaches agree with one another in cases where both are applicable. In Sec. 5.5 we consider the general case of SPT edge theories with both unitary and antiunitary symmetries, and we show that the same procedure works in this case. Sec. 4.7 discusses how to extend our approach to the case of *continuous* symmetries. Finally, we give our conclusions in Sec. 5.6. Technical details are discussed in the Appendix.

4.2 Setup

We begin by defining what we mean by an "edge theory", or more precisely, a bosonic SPT edge theory. At an intuitive level, a bosonic SPT edge theory is a collection of data that describes the low energy edge excitations of an SPT phase. More specifically, a bosonic SPT edge theory consists of three pieces of data:

1. A Hilbert space $\mathcal{H}$.

2. A complete list of "local operators" $\{\mathcal{O}\}$ acting in $\mathcal{H}$.

3. A collection of (unitary or anti-unitary) symmetry transformations $\{U^g : g \in G\}$ acting on $\mathcal{H}$.

Each of these pieces of data has a simple physical interpretation: the Hilbert space $\mathcal{H}$ describes the subspace of low energy edge excitations; the list $\{\mathcal{O}\}$ describes the low energy projection of local operators in the original 2D system; and the $\{U^g\}$ operators describe how the edge excitations transform under the symmetry.

In order to qualify as a valid bosonic SPT edge theory, we require that the above data is physically *realizable* as the edge of some 2D SPT Hamiltonian with on-site symmetries. That is, we require the existence of a 2D Hamiltonian H_{2D} that belongs to an SPT phase with (on-site) symmetry group G and that has the following properties:

1. The Hilbert space $\mathcal{H}$ is isomorphic to the subspace of low energy edge excitations of H_{2D}.

2. The operators $\{\mathcal{O}\}$ correspond to local operators of the 2D system, projected into this low energy subspace.

3. The $\{U^g\}$ transformations describe how the low energy subspace transforms under the symmetries in G.

See Secs. 5.4, 4.6.4, 4.7.2 for examples of bosonic SPT edge theories. In general, bosonic SPT edge theories can be described using either continuum fields or lattice degrees of freedom and our results apply equally well to both cases.

With this background, we can now state our main result, (summarized in Fig. 4.1): we describe a systematic procedure that takes a bosonic SPT edge theory as input, and that outputs an element ω of the cohomology group $H^3(G, U_T(1))$ (see Sec. 5.5.1 for a definition). As explained in the introduction, the element $\omega \in H^3(G, U_T(1))$ can be interpreted in two

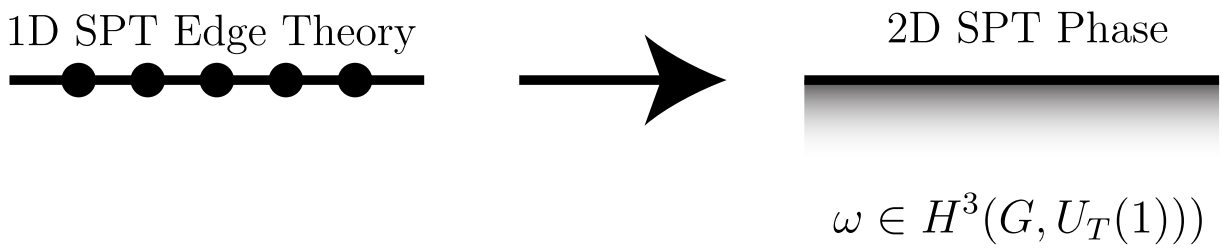

Figure 4.1: Schematic picture for our main result: we describe a procedure that takes a 1D bosonic SPT edge theory as input, and produces as output an element $\omega \in H^3(G, U_T(1))$. This element ω can be interpreted as either a label for the bulk 2D SPT phase or the anomaly carried by the edge theory.

equivalent ways: ω can be thought of as either a label for the bulk 2D SPT phase or a label for the *anomaly* carried by the SPT edge theory. Thus, depending on one's point of view, our procedure provides a systematic method for computing either the bulk 2D SPT phase or the anomaly associated with a given edge theory.

4.3 Discrete unitary symmetries

4.3.1 Outline of procedure

In this section, we outline our procedure in the case where the symmetry group G is discrete and unitary.

We start by reviewing the definition of the cohomology group $H^3(G, U(1))$, since this is the group that describes the output of our procedure in the case of discrete unitary symmetries. The cohomology group $H^3(G, U(1))$ consists of equivalence classes of functions $\omega : G \times G \times G \to U(1)$ obeying the condition

$$\frac{\omega(g,h,k)\omega(g,hk,l)\omega(h,k,l)}{\omega(gh,k,l)\omega(g,h,kl)} = 1. \tag{4.1}$$

Any function ω obeying (5.7) is called a "cocycle." The equivalence relation between different

coycles is defined as follows: $\omega \equiv \omega'$ if ω'/ω is a "coboundary," i.e.

$$\frac{\omega'(g,h,k)}{\omega(g,h,k)} = \frac{\nu(gh,k)\nu(g,h)}{\nu(g,hk)\nu(h,k)} \tag{4.2}$$

for some function $\nu : G \times G \to U(1)$. We will see that the output of our procedure is a cocycle ω, which is uniquely defined up to multiplication by a coboundary (4.2); in this way, our procedure produces an element of $H^3(G, U(1))$.

With this background, we now move on to explain our procedure. The first step in our procedure is to choose an (edge) Hamiltonian H that acts within the Hilbert space $\mathcal{H}$. The Hamiltonian H can be arbitrary as long as it has three properties: (i) H is local, i.e. H is built out of the local operators $\{\mathcal{O}\}$ from Sec. 5.2; (ii) H has an energy gap; and (iii) H breaks the G-symmetry spontaneously and completely.[3]

An important aspect of the Hamiltonian H is that it has multiple degenerate ground states due to the spontaneously broken symmetry. More specifically, H has $|G|$ degenerate, short-range correlated ground states, which are permuted amongst themselves by the symmetry transformations. These ground states can be naturally labeled by group elements, $g \in G$. To do this, we pick one of the degenerate ground states and denote it by $|\Omega; 1\rangle$. We then label the other states by $\{|\Omega; g\rangle\}$ where $|\Omega; g\rangle$ is defined by

$$|\Omega; g\rangle = U^g |\Omega; 1\rangle \tag{4.3}$$

By construction, $U^g|\Omega; h\rangle = |\Omega; gh\rangle$.

Having found the ground states of H, the next step in our procedure is to construct domain wall excitations. We give a precise definition of domain wall excitations in Sec. 4.3.2, but roughly speaking a domain wall excitation is a state in $\mathcal{H}$ that "looks like" one ground

3. Actually, such a Hamiltonian is not strictly necessary for our procedure: all that we really need is a single (edge) state $|\Psi\rangle$ that *explicitly* breaks all symmetries. See Sec. 4.7 for more details.

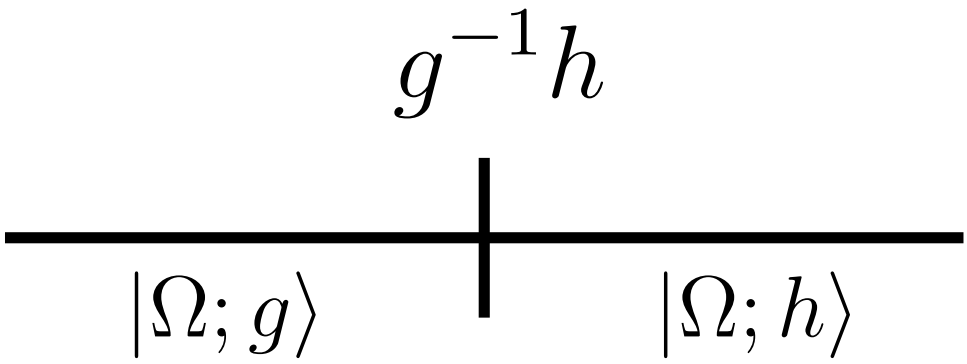

Figure 4.2: A domain wall excitation: a state that shares the same local expectation values as one ground state $|\Omega; g\rangle$ to the left of some point x, and another ground state $|\Omega; h\rangle$ to the right of x. We label such a domain wall by the group element $g^{-1}h$.

state $|\Omega; g\rangle$ to the left of some point x, and like another ground state $|\Omega; h\rangle$ to the right of x, and that interpolates between the two ground states in some arbitrary way in the vicinity of x (Fig. 5.1). Like the ground states, these domain wall excitations can be naturally labeled by group elements: in particular, we will label a domain wall with the above structure with the group element $g^{-1}h$. An important property of this labeling is that it is invariant under any global symmetry transformation U^k: under such a transformation, $|\Omega; g\rangle \to |\Omega; kg\rangle$ and $|\Omega; h\rangle \to |\Omega; kh\rangle$ so $g^{-1}h \to (kg)^{-1}(kh) = g^{-1}h$.

Like other topological defects, domain walls cannot be created or annihilated individually. Instead, the most basic process that one can perform on domain walls is to combine them together in a process called "fusion": if one has a g type domain wall located nearby and to the left of an h type domain wall, then one can convert this pair of domain walls into a single gh type domain wall by applying a local operator acting on both domain walls. This process is shown in Fig. 5.2. Alternatively, one can perform the reverse ("splitting") process and apply a local operator that turns a gh type domain wall into a g type domain wall to the left of an h type domain wall.

This ability to fuse or split domain walls allows us to define an "F-symbol" for these excitations. The F-symbol is usually discussed in the context of 2D anyon theories [74, 112],

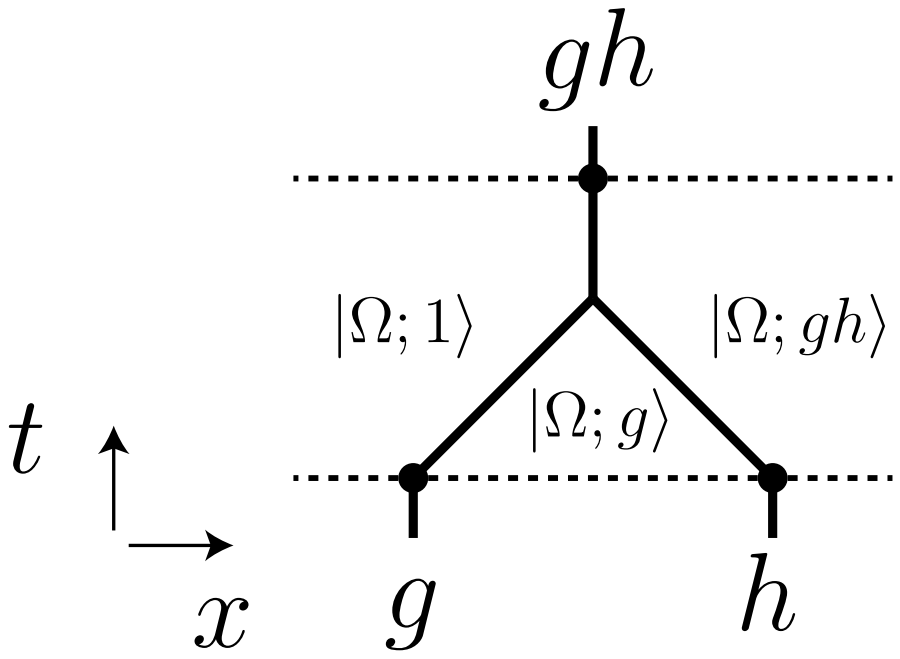

Figure 4.3: Spacetime diagram of fusion of a g and h domain wall into a gh domain wall. The initial state consists of three different ground states $|\Omega;1\rangle, |\Omega;g\rangle, |\Omega;gh\rangle$ in three different regions, separated by domain walls g, h. During the fusion process, the $|\Omega;g\rangle$ region disappears and we are left only with the $|\Omega;1\rangle, |\Omega;gh\rangle$ regions separated by a gh domain wall. Reversing the arrow of time corresponds to a "splitting" operation.

but it is a more general concept that can be defined for any point-like mobile defects. In particular, we can sensibly define an F-symbol for domain walls in 1D edge theories. The basic idea is to consider two different physical processes in which a domain wall of type ghk splits into three domain walls of types g, h, k (Fig. 4.4). In one process, ghk splits into gh and k, and then gh splits into g and h; in the other process, ghk splits into g and hk and then hk splits into h and k. By construction, the final states $|1\rangle, |2\rangle$ produced by these processes contain the same domain walls, g, h, k, at the same three positions. Therefore, the two final states $|1\rangle, |2\rangle$ must be the same up to a phase. The F-symbol, $F(g, h, k)$, is the phase difference between the two states:

$$|1\rangle = F(g, h, k)|2\rangle. \tag{4.4}$$

The final step in our procedure is to compute this F-symbol for domain wall excitations. This F-symbol defines our cocycle $\omega \in H^3(G, U(1))$:

$$\omega(g,h,k) \equiv F(g,h,k) \tag{4.5}$$

To justify Eq. 5.16, we need to explain why $F(g,h,k)$ is an element of $H^3(G,U(1))$. This follows from two important properties of F which we prove in Sec. 4.3.3. The first property is that F satisfies a non-trivial constraint, known as the "pentagon identity":

$$F(g,h,k)F(g,hk,l)F(h,k,l) = F(gh,k,l)F(g,h,kl) \tag{4.6}$$

To understand the origin of this identity, consider the 5 processes shown in Fig. 4.5. Notice that the final states produced by these processes, namely $\{|1\rangle, ..., |5\rangle\}$, are all the same up to a phase. We can compute the phase difference between states $|1\rangle$ and $|5\rangle$ in two different ways. In the first way, we compute the relative phases between $(|1\rangle, |2\rangle)$, $(|2\rangle, |3\rangle)$, and $(|3\rangle, |5\rangle)$ using (5.15); in the second way, we compute the relative phases between $(|1\rangle, |4\rangle)$ and $(|4\rangle, |5\rangle)$. Demanding consistency between the two calculations gives the pentagon identity (5.17).

The second property of F is that is has an inherent ambiguity: it is only well-defined up to transformations of the form

$$F(g,h,k) \to F(g,h,k)\frac{\nu(gh,k)\nu(g,h)}{\nu(g,hk)\nu(h,k)} \tag{4.7}$$

where $\nu(g,h) \in U(1)$. To understand where this ambiguity comes from, it is helpful to think about the physical processes in Fig. 4.4 as being implemented by a sequence of two "splitting operators" applied to an initial state $|ghk_1\rangle$. The key point is that the phases of these splitting operators are arbitrary. If we multiply the four splitting operators by four

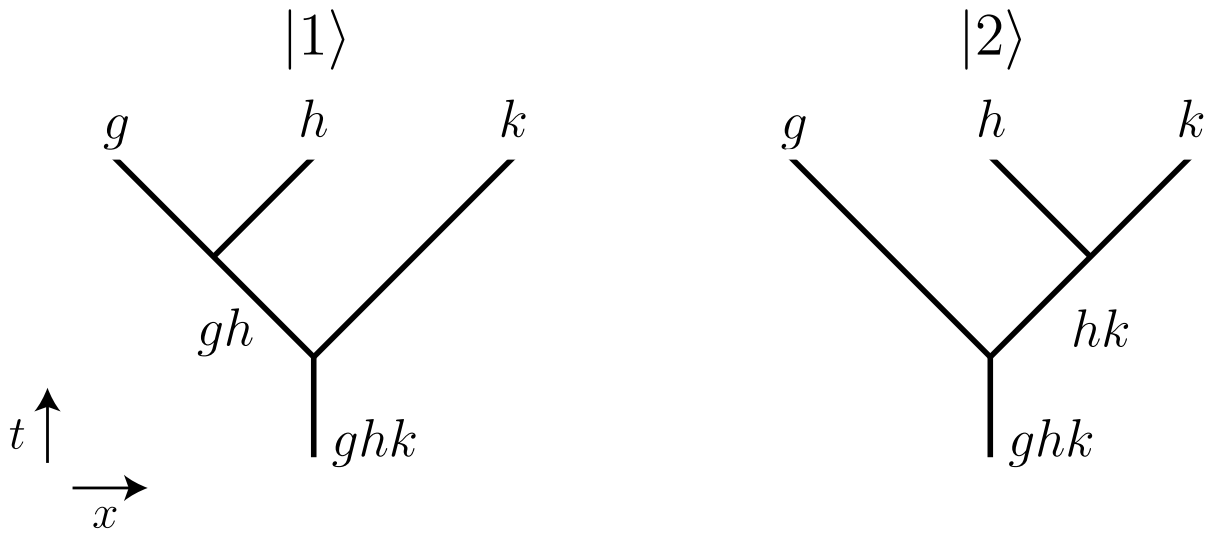

Figure 4.4: Spacetime diagrams for two processes in which a domain wall ghk splits into domain walls g, h, k. The final states, $|1\rangle, |2\rangle$, are equal up to the $U(1)$ phase, $F(g, h, k)$.

phases, $\nu(gh, k), \nu(g, h), \nu(g, hk), \nu(h, k)$, this changes F by exactly the above transformation (5.20). We will call the transformations in (5.20) "gauge transformations."

Comparing the above properties of F to the definition of $H^3(G, U(1))$, we can see that the pentagon identity (5.17) is identical to the cocycle condition (5.7), while the ambiguity (5.20) is equivalent to the equivalence relation (4.2) on cocycles. Hence, F naturally an element of $H^3(G, U(1))$, as we claimed earlier.

4.3.2 Microscopic definition of F-symbol for domain walls

In this section, we give precise, operational definitions of domain wall states and their associated F-symbols. These definitions are essential for making our procedure a useful calculational tool; they are also important for putting our procedure on a firm foundation. We note that these definitions closely parallel the microscopic definition of the anyonic F-symbol that was given in Ref. [69] in the context of anyon theories.

To begin, let ℓ be a distance that is much greater than the correlation length ξ of the system. The length scale ℓ will play an important role in the following discussion. In

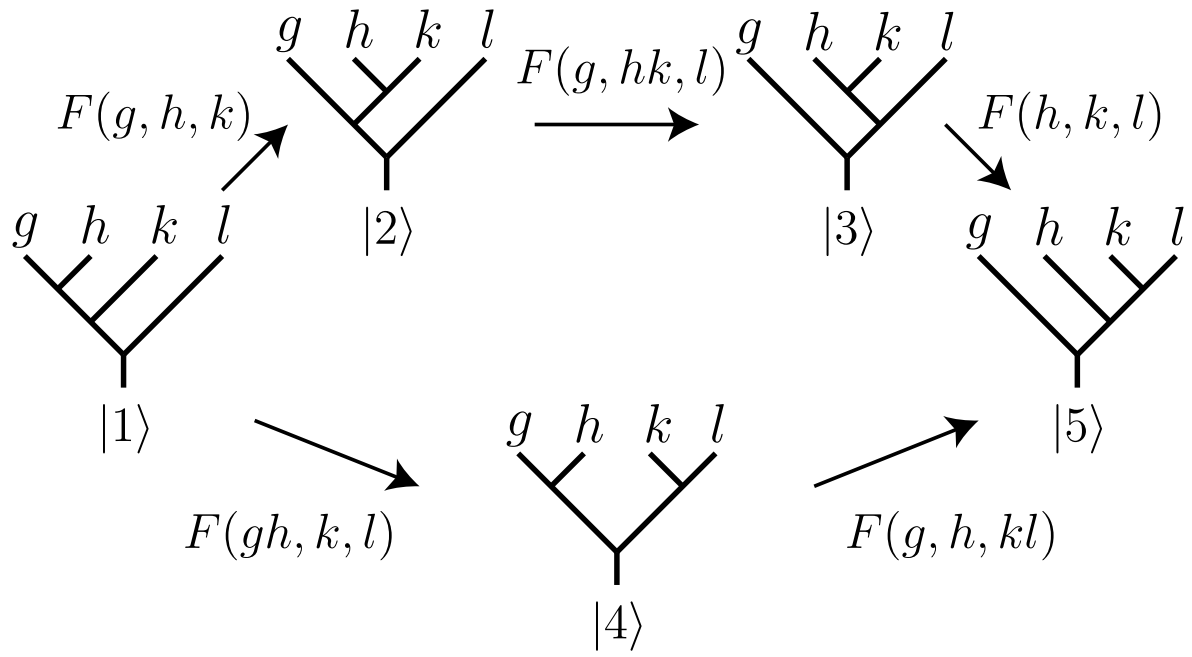

Figure 4.5: The pentagon identity: consistency requires that the product of the three F-symbols on the upper path is equal to the product of the two F-symbols on the lower path.

particular, we will only consider states in which domain wall excitations are separated by distances of at least ℓ, and we will neglect finite size effects of order $e^{-\ell/\xi}$.

We define domain wall states as follows. For each point x on the edge, we choose a state that has the same expectation values as $|\Omega; 1\rangle$ for local operators $\{\mathcal{O}\}$ supported to the left of $x - \ell$ and the same expectation values as $|\Omega; g\rangle$ for local operators $\{\mathcal{O}\}$ to the right of $x + \ell$. We denote this state by $|g_x\rangle$. In our language, the state $|g_x\rangle$ describes a single domain wall of "type g" at position x. Note that the definition of $|g_x\rangle$ involves an arbitrary choice of a state: we will show that our results do not depend on this choice.

Next, for each domain wall state $|g_x\rangle$, we define a collection of symmetry partner states $|g_x; h\rangle$, with $h \in G$, by

$$|g_x; h\rangle = U^h |g_x\rangle \tag{4.8}$$

By construction, $|g_x; h\rangle$ has the same expectation values as $|\Omega; h\rangle$ for local operators sup-

ported to the left of $x - \ell$ and the same expectation values as $|\Omega; hg\rangle$ for local operators to the right of $x + \ell$.

We now introduce *multi*-domain wall states. Let $x_1 < x_2 < ... < x_n$ be well-separated (i.e. having a spacing of at least ℓ) and pick group elements $g^{(1)}, g^{(2)}, ..., g^{(n)} \in G$. We will use the notation $|g^{(1)}_{x_1}, g^{(2)}_{x_2}, ...\rangle$ to denote the multi-domain wall state that has a domain wall of type $g^{(i)}$ at each location x_i and that has the same expectation values as $|\Omega; 1\rangle$ for local operators supported to the left of all the domain walls. More precisely, we define $|g^{(1)}_{x_1}, g^{(2)}_{x_2}, ...\rangle$ to be the unique state with the following two properties: first, for any local operator $\mathcal{O}$ supported near one domain wall x_i,

$$\langle g^{(1)}_{x_1}, g^{(2)}_{x_2}, ...|\mathcal{O}|g^{(1)}_{x_1}, g^{(2)}_{x_2}, ...\rangle = \langle g^{(i)}_{x_i}; g_L|\mathcal{O}|g^{(i)}_{x_i}; g_L\rangle \tag{4.9}$$

where g_L is the product of all domain wall types to the left of $\mathcal{O}$:

$$g_L = g^{(1)} \cdots g^{(i-1)} \tag{4.10}$$

Second, for any operator $\mathcal{O}$ supported away from the domain walls,

$$\langle g^{(1)}_{x_1}, g^{(2)}_{x_2}, ...|\mathcal{O}|g^{(1)}_{x_1}, g^{(2)}_{x_2}, ...\rangle = \langle \Omega; g_L|\mathcal{O}|\Omega; g_L\rangle \tag{4.11}$$

where g_L is again the product of domain wall types to the left of $\mathcal{O}$. These two properties imply that multidomain wall states have a structure like that in Fig. 4.6.

An important corollary of Eq. 4.9, which we will need below, is that for any operator $\mathcal{O}$ that is supported near a domain wall g at point x and is invariant under all the symmetries (i.e. $U^h \mathcal{O} (U^h)^{-1} = \mathcal{O}$), the following identity holds:

$$\langle ..., g_x, ...|\mathcal{O}|..., g_x, ...\rangle = \langle g_x|\mathcal{O}|g_x\rangle \tag{4.12}$$

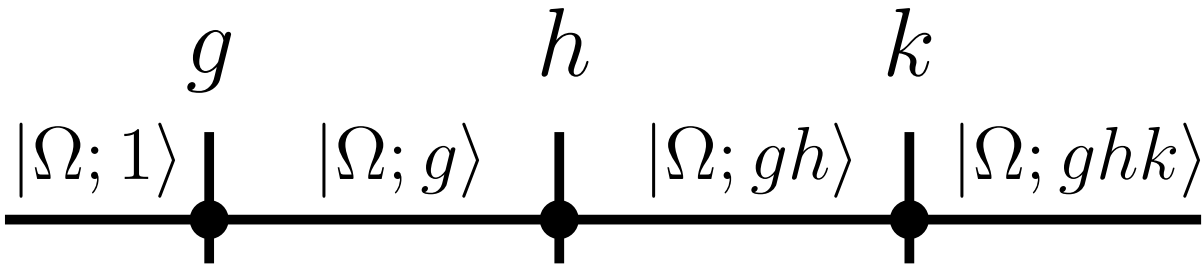

Figure 4.6: A multi-domain wall state $|g_x, h_{x'}, k_{x''}\rangle$ consisting of a g-type, h-type, and k-type domain wall at positions x, x', x''. The domain walls separate four regions which share the same local expectation values as the four ground states $|\Omega; 1\rangle, |\Omega; g\rangle, |\Omega; gh\rangle, |\Omega; ghk\rangle$.

Now that we have fixed our definitions of domain wall states, the next step is to define *movement* operators for these domain walls. Given any group element $g \in G$, and any pair of points, x, x', we say that $M^g_{x'x}$ is a movement operator if it satisfies three conditions: (i) $M^g_{x'x}$ obeys

$$M^g_{x'x}|g_x\rangle \propto |g_{x'}\rangle \tag{4.13}$$

where the proportionality constant is a $U(1)$ phase; (ii) $M^g_{x'x}$ is invariant under all the symmetries, i.e.

$$U^h M^g_{x'x}(U^h)^{-1} = M^g_{x'x} \tag{4.14}$$

and (iii) $M^g_{x'x}$ is *local* in the sense that it is supported in the neighborhood of the interval containing x, x'.

Here, the symmetry condition (5.36) is important because it guarantees that the analog of Eq. 5.35 holds for any (single) domain wall state $|g_x; h\rangle$:

$$M^g_{x'x}|g_x; h\rangle \propto |g_{x'}; h\rangle \tag{4.15}$$

Likewise, the locality condition is important because it guarantees that the analog of Eq. 5.35

holds for any multi-domain wall state of the form $|..., g_x, ...\rangle$: that is,

$$M^g_{x'x}|..., g_x, ...\rangle \propto |..., g_{x'}, ...\rangle \tag{4.16}$$

as long as the other domain walls in $|..., g_x, ...\rangle$ are well-separated from the interval containing x and x'. Again the constant of proportionality is a $U(1)$ phase.

To derive Eq. 5.38 from Eq. 5.35, consider the expectation value of any local operator, $\mathcal{O}$, supported in the neighborhood of $[x, x']$ (or $[x', x]$ if $x' < x$), in the two states $|..., g_{x'}, ...\rangle$ and $M^g_{x'x}|..., g_x, ...\rangle$. Using (4.9) and (5.37), we can see that $\mathcal{O}$ has the same expectation value in the two states, $|..., g_{x'}, ...\rangle$ and $M^g_{x'x}|..., g_x, ...\rangle$:

$$\begin{aligned}\langle ..., g_{x'}, ...|\mathcal{O}|..., g_{x'}, ...\rangle &= \langle g_{x'}; g_L|\mathcal{O}|g_{x'}; g_L\rangle \\ &= \langle g_x; g_L|(M^g_{x'x})^\dagger \mathcal{O} M^g_{x'x}|g_x; g_L\rangle \\ &= \langle ..., g_x, ...|(M^g_{x'x})^\dagger \mathcal{O} M^g_{x'x}|..., g_x, ...\rangle \end{aligned} \tag{4.17}$$

The two states, $|..., g_{x'}, ...\rangle$ and $M^g_{x'x}|..., g_x, ...\rangle$ also share the same expectation values for local operators supported away from the interval $[x, x']$ (or $[x', x]$) by virtue of the short ranged correlations of these states. Therefore, by the uniqueness property of our domain wall states, we obtain Eq. 5.38.

In addition to the movement operators, we also define *splitting* operators for our domain walls. Fix two well-separated points on the line, which we will call '1' and '2'. For any pair of domain walls g, h, we say that $S(g, h)$ is a splitting operator if it satisfies three conditions: (i) $S(g, h)$ satisfies

$$S(g, h)|gh_1\rangle \propto |g_1, h_2\rangle \tag{4.18}$$

where the proportionality constant is a $U(1)$ phase; (ii) $S(g, h)$ is invariant under all the symmetries U^k; (iii) $S(g, h)$ is supported in the neighborhood of the interval $[1, 2]$.

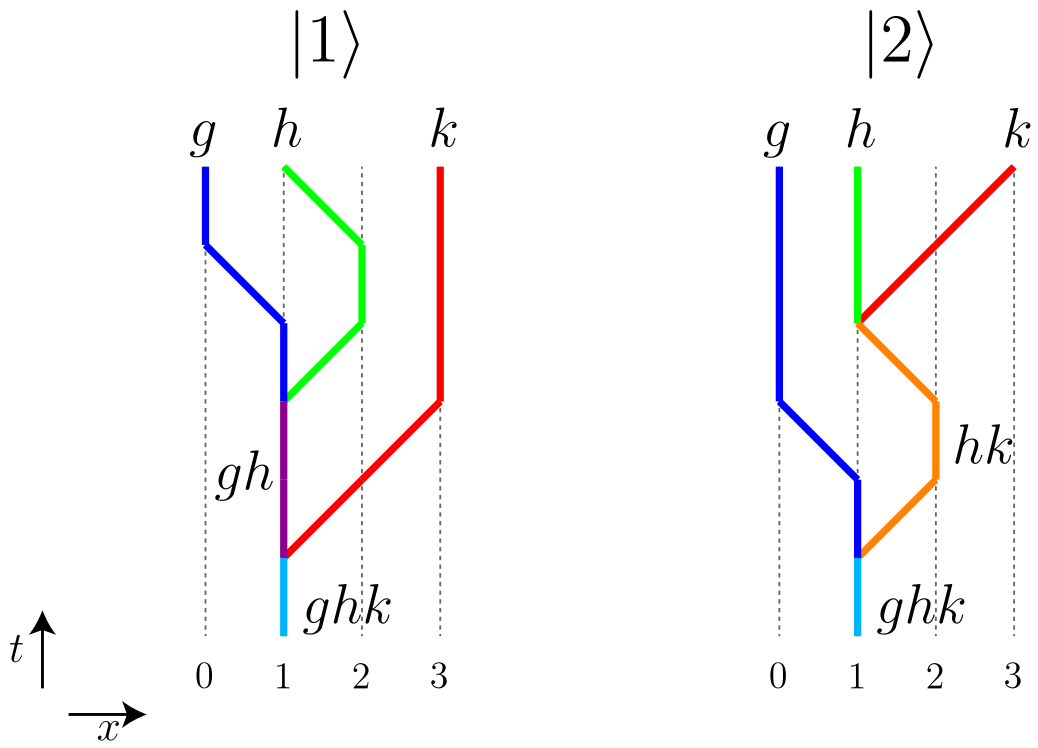

Figure 4.7: The two processes that are compared in the microscopic definition of the domain wall F-symbol. Starting from an initial state $|ghk_1\rangle$, movement and splitting operators are applied sequentially to obtain final states $|1\rangle$ and $|2\rangle$ on the left and right, respectively. States $|1\rangle, |2\rangle$ are both proportional to $|g_0, h_1, k_3\rangle$. The x-axis is the position on the edge and the t-axis shows operator ordering.

Just as before, it can be shown that these conditions guarantee that the splitting operators can be applied to any multi-domain wall state of the form $|..., gh_1, ...\rangle$ provided that the other domain walls are located far from the interval $[1, 2]$:

$$S(g, h)|..., gh_1, ...\rangle \propto |..., g_1, h_2, ...\rangle \tag{4.19}$$

where the proportionality constant is a $U(1)$ phase. Note that, unlike the movement operators, we only define splitting operators that act on a *single* interval $[1, 2]$ on the x-axis.

With this setup, we are now ready to define the F-symbol. The first step is to fix some choice of domain wall states, $|g_x\rangle$, and some choice of movement and splitting operators, $M^g_{x'x}, S(g, h)$. Next, consider the initial state $|ghk_1\rangle$, i.e. the state with a single domain

wall ghk at position 1. We then apply two different sequences of movement and splitting operators to $|ghk_1\rangle$, denoting the final states by $|1\rangle$ and $|2\rangle$:

$$\begin{aligned} |1\rangle &= M_{12}^{h} M_{01}^{g} S(g,h) M_{32}^{k} S(gh,k) |ghk_1\rangle \\ |2\rangle &= M_{32}^{k} S(h,k) M_{12}^{hk} M_{01}^{g} S(g,hk) |ghk_1\rangle \end{aligned} \tag{4.20}$$

These two processes are shown in Fig. 4.7. By construction, the final states $|1\rangle, |2\rangle$ produced by these processes both contain domain walls g, h, k at positions $0, 1, 3$, respectively. In particular, this means that $|1\rangle, |2\rangle$ are the same up to a phase. We define the F-symbol, $F(g,h,k)$, to be this phase difference:

$$F(g,h,k) = \langle 2|1\rangle \tag{4.21}$$

4.3.3 Checking the microscopic definition

To show that our microscopic definition is correct, we need to establish two properties of F: (i) F is well-defined in the sense that different choices of domain wall states and movement and splitting operators give the same F up to a gauge transformation (5.20); and (ii) F obeys the pentagon equation (5.17). We prove property (ii) in Appendix 7.1; the goal of this section is to prove property (i).

As a warm-up, let us see how F transforms if we only change the *phase* of the movement and splitting operators. That is, suppose we replace

$$M_{x'x}^{g} \to e^{i\theta_{x'x}(g)} M_{x'x}^{g}, \quad S(g,h) \to e^{i\phi(g,h)} S(g,h) \tag{4.22}$$

for some real-valued θ, ϕ. Substituting these transformations into (4.20-4.21) gives

$$F(g,h,k) \to F(g,h,k)\frac{e^{i\phi(gh,k)}e^{i\phi(g,h)}e^{i\theta_{12}(h)}}{e^{i\phi(g,hk)}e^{i\phi(h,k)}e^{i\theta_{12}(hk)}} \tag{4.23}$$

Crucially, this transformation is identical to a coboundary transformation (5.20) with

$$\nu(g,h) = e^{i[\phi(g,h)+\theta_{12}(h)]} \tag{4.24}$$

This is exactly what we want: different phase choices lead to the same F, up to a coboundary, or gauge transformation.

With this warm-up, we are now ready to consider the general case where we change the movement and splitting operators in an arbitrary way:

$$M^{g}_{x'x} \to M'^{g}_{x'x}, \qquad S(g,h) \to S'(g,h) \tag{4.25}$$

To analyze this case, we note that the definition of movement and splitting operators implies that

$$\begin{aligned} M'^{g}_{x'x}|g_x\rangle &= e^{i\theta_{x'x}(g)}M^{g}_{x'x}|g_x\rangle \\ S'(g,h)|gh_1\rangle &= e^{i\phi(g,h)}S(g,h)|gh_1\rangle \end{aligned} \tag{4.26}$$

for some real valued $\theta_{x'x}(g)$ and $\phi(g,h)$. Likewise, for *multi*-domain wall states,

$$M'^{g}_{x'x}|...,g_x,...\rangle = \omega_1 \cdot M^{g}_{x'x}|...,g_x,...\rangle \tag{4.27}$$

$$S'(g,h)|...,gh_1,...\rangle = \omega_2 \cdot S(g,h)|...,gh_1,...\rangle \tag{4.28}$$

for some $U(1)$ phases ω_1, ω_2.

To proceed further, we need to find the relationship between the multi-domain wall phases

ω_1, ω_2 and the single domain wall phases $e^{i\theta_x}$ and $e^{i\phi(g,h)}$. To do this, we multiply the two sides of (5.70) by $\langle ..., g_x, ...|(M^g_{x'x})^\dagger$ and then use property (5.34) to derive

$$\begin{aligned}\omega_1 &= \langle ..., g_x, ...|(M^g_{x'x})^\dagger M'^g_{x'x}|..., g_x, ...\rangle \\ &= \langle g_x|(M^g_{x'x})^\dagger M'^g_{x'x}|g_x\rangle \\ &= e^{i\theta_{x'x}(g)}\end{aligned} \tag{4.29}$$

By the same reasoning, $\omega_2 = e^{i\phi(g,h)}$. We conclude that

$$\begin{aligned}M'^g_{x'x}|..., g_x, ...\rangle &= e^{i\theta_{x'x}(g)} M^g_{x'x}|..., g_x, ...\rangle \\ S'(g,h)|..., gh_1, ...\rangle &= e^{i\phi(g,h)} S(g,h)|..., gh_1, ...\rangle\end{aligned} \tag{4.30}$$

We are now finished: substituting the above relations (5.73) into (4.20), we again see that F changes by a gauge transformation with ν given by (5.66).

So far, we have shown that different choices of movement and splitting operators lead to the same F, up to a gauge transformation. Next, we need to check that different choices of edge Hamiltonians and domain wall states also lead to the same F, up to a gauge transformation. To investigate this issue, consider two choices of edge Hamiltonians, H and H', with ground states $\{|\Omega; g\rangle\}$ and $\{|\Omega; g\rangle'\}$ respectively. It seems reasonable to assume that H and H' can be adiabatically connected, i.e. there exists an interpolating Hamiltonian H_s, with $0 \leq s \leq 1$ with $H_0 = H$ and $H_1 = H'$ such that H_s is local, gapped, and breaks the G-symmetry spontaneously and completely. Assuming the existence of such an interpolation, it then follows from the quasi-adiabatic continuation construction [54] that there exists a G-invariant, "locality preserving" unitary transformation W that connects the two sets of ground states: that is,

$$\{|\Omega; g\rangle'\} = \{W|\Omega; g\rangle\} \tag{4.31}$$

Here, when we say W is "locality preserving", we mean that it has the following property: for any local operator $\mathcal{O}$, the operator $W\mathcal{O}W^{-1}$ is also local and is supported near $\mathcal{O}$.

Comparing Eq. 5.98 with our labeling scheme (5.11), we deduce that the two sets of ground states are related by

$$|\Omega; g\rangle' = WU^k|\Omega; g\rangle \tag{4.32}$$

for some $k \in G$.

Next, consider the implications of Eq. (5.99) for domain wall states. Applying WU^k to a multi-domain wall state $|g^{(1)}_{x_1}, g^{(2)}_{x_2}, g^{(3)}_{x_3}, ...\rangle$ for H, we see that the state $WU^k|g^{(1)}_{x_1}, g^{(2)}_{x_2}, g^{(3)}_{x_3}, ...\rangle$ is a valid multi-domain wall state for H'. Let us compare this state to the "primed" domain wall state, which we denote by $|g^{(1)}_{x_1}, g^{(2)}_{x_2}, g^{(3)}_{x_3}, ...\rangle'$. There is no reason that the two states must agree microscopically, but it is reasonable to assume that they can be transformed into one another by a G-invariant locality preserving unitary. Assuming this is the case, it follows that there exists a G-invariant locality preserving unitary V such that

$$|g^{(1)}_{x_1}, g^{(2)}_{x_2}, g^{(3)}_{x_3}, ...\rangle' = VU^k|g^{(1)}_{x_1}, g^{(2)}_{x_2}, g^{(3)}_{x_3}, ...\rangle \tag{4.33}$$

With Eq. (5.100), we are now in a position to compare the F-symbols for the two choices of domain wall states. First, we observe that we are free to choose the movement and splitting operators for the states $|g^{(1)}_{x_1}, g^{(2)}_{x_2}, g^{(3)}_{x_3}, ...\rangle'$ however we like, changing F by, at most, a gauge transformation. The simplest choice that is consistent with (5.100) is

$$M'^{g}_{x'x} = VM^{g}_{x'x}V^{-1}, \quad S'(g,h) = VS(g,h)V^{-1} \tag{4.34}$$

With this choice, it is clear that $|1'\rangle = VU^k|1\rangle$, and $|2'\rangle = VU^k|2\rangle$. It follows that $F' = \langle 2'|1'\rangle = \langle 2|1\rangle = F$. Thus, we conclude that F doesn't depend on the choice of the edge

Hamiltonian or the choice of domain wall states. This completes the proof of property (i) above.

4.4 Examples with discrete unitary symmetries

In this section, we present several examples illustrating our method of calculating anomalies in bosonic SPT edge theories.

4.4.1 Lattice edge theory for $\mathbb{Z}_2$ SPT phase

We start with one of the simplest non-trivial examples: a lattice edge theory for the bosonic SPT phase with symmetry group $G = \mathbb{Z}_2$. This edge theory was introduced in Refs. [26, 84].

Edge theory

We begin by reviewing the structure of the edge theory. As explained in Sec 5.2, an edge theory consists of three pieces of data: (1) a Hilbert space $\mathcal{H}$; (2) a set of local operators $\{\mathcal{O}\}$ that act in $\mathcal{H}$; and (3) a collection of symmetry transformations $\{U^g : g \in G\}$ acting within $\mathcal{H}$.

The Hilbert space $\mathcal{H}$ for the $\mathbb{Z}_2$ SPT edge theory couldn't be simpler: the Hilbert space is equivalent to a one-dimensional spin-1/2 chain, with spins living on integer lattice sites $n \in \mathbb{Z}$. A complete orthonomal basis for this Hilbert space can be obtained by considering σ^z eigenstates of the form

$$|..., \alpha_{-1}, \alpha_0, \alpha_1, ...\rangle, \qquad \alpha_n \in \{+, -\} \tag{4.35}$$

where

$$\sigma^z_n |..., \alpha_{-1}, \alpha_0, \alpha_1, ...\rangle = \alpha_n |..., \alpha_{-1}, \alpha_0, \alpha_1, ...\rangle \tag{4.36}$$

The local operators $\{\mathcal{O}\}$ in the $\mathbb{Z}_2$ SPT edge theory are the usual local operators in a spin-1/2 chain, namely products of Pauli spin operators $\{\sigma_n^x, \sigma_n^y, \sigma_n^z\}$ acting on a collection of nearby lattice sites.

We now move on to the symmetry transformations U^g. Denoting the symmetry group by $\mathbb{Z}_2 = \{1, s\}$, we only need to discuss the symmetry operator U^s, since $U^1 = \mathbb{1}$. Denoting $U^s \equiv U$ for brevity, we can describe the symmetry operator U by how it acts on the Pauli spin operators [84]:

$$\begin{aligned} U\sigma_j^x U^{-1} &= -\sigma_{j-1}^z \sigma_j^x \sigma_{j+1}^z \\ U\sigma_j^y U^{-1} &= \sigma_{j-1}^z \sigma_j^y \sigma_{j+1}^z \\ U\sigma_j^z U^{-1} &= -\sigma_j^z \end{aligned} \tag{4.37}$$

We can also write down an explicit formula for U [84]:

$$U = -\prod_j i^{\frac{1-\sigma_j^z\sigma_{j+1}^z}{2}} \prod_j \sigma_j^x \tag{4.38}$$

Note that we will not need the above formula (4.38) to compute the anomaly: our approach only requires knowing the transformation laws for local operators (4.37).

Calculating the anomaly

We now proceed to compute the anomaly associated with the edge theory described above. As we explained in Sec. 4.3.1, the first step in calculating the anomaly is to choose a gapped (edge) Hamiltonian that breaks the $\mathbb{Z}_2$ symmetry spontaneously and completely. We use an Ising Hamiltonian

$$H = -J \sum_i \sigma_i^z \sigma_{i+1}^z \tag{4.39}$$

with $J > 0$.

To see that this Hamiltonian spontaneously breaks the symmetry note that σ^z is odd under the symmetry (4.38) and has a non-zero expectation value in the two degenerate ground states $|+,+,...,+\rangle$ and $|-,-,...,-\rangle$. Following the notation in Sec. 4.3.1. we denote these ground states by

$$\begin{aligned} |\Omega;1\rangle &= |+,+,...,+\rangle \\ |\Omega;s\rangle &= |-,-,...,-\rangle \end{aligned} \tag{4.40}$$

The next step is to define domain wall states. Since the symmetry group is $\mathbb{Z}_2$, there is only one non-trivial domain wall state that we need to construct. Denoting this state by $|s_n\rangle$ where n is the location of the domain wall, we define

$$|s_n\rangle = |...,+,+,(+)_n,-,-,-,...\rangle \tag{4.41}$$

Here we use the notation $(+)_n$ to indicate that the corresponding '+' is the state of the nth spin, so that the '-' that follows is the state of the $(n+1)$st spin. Notice that (5.110) implies a particular convention for labeling domain wall locations: a domain wall is at "position n" if the nth and $(n+1)$st spins are anti-aligned. (This will also hold for the multi-domain wall states.) Likewise, we define the trivial or "no-domain" wall state $|1_n\rangle$ in the obvious way:

$$|1_n\rangle = |...,+,(+)_n,+,...\rangle \tag{4.42}$$

Next we construct movement and splitting operators for these domain walls. We will start by constructing the movement operators. We define the movement operator between

n and $n+1$ by

$$\begin{aligned} M^s_{(n+1)n} &= \sigma^+_{n+1} + U\sigma^+_{n+1}U^{-1} \\ &= \sigma^+_{n+1} - \sigma^z_n\sigma^-_{n+1}\sigma^z_{n+2} \end{aligned} \tag{4.43}$$

where the second equality follows from (4.37). Let us check that $M^s_{(n+1)n}$ obeys all the required conditions, i.e. $M^s_{(n+1)n}$ is local, $\mathbb{Z}_2$ symmetric, and has the correct action on domain walls. Locality and $\mathbb{Z}_2$ symmetry are obvious since $M^s_{(n+1)n}$ is explicitly symmetrized. As for the action on domain walls, this is easy to verify:

$$\begin{aligned} M^s_{(n+1)n}|s_n\rangle &= \sigma^+_{n+1}|..., +, +, (+)_n, -, -, -, ...\rangle \\ &= |..., +, +, (+)_n, +, -, -, ...\rangle \\ &= |s_{n+1}\rangle \end{aligned} \tag{4.44}$$

We define the reverse movement operator in a similar fashion:

$$\begin{aligned} M^s_{n(n+1)} &= \left(M^s_{(n+1)n}\right)^\dagger \\ &= \sigma^-_{n+1} - \sigma^z_n\sigma^+_{n+1}\sigma^z_{n+2} \end{aligned} \tag{4.45}$$

As for the splitting operators, we define $S(s,s)$ as

$$\begin{aligned} S(s,s) &= \sigma^-_2 + U\sigma^-_2U^{-1} \\ &= \sigma^-_2 - \sigma^z_1\sigma^+_2\sigma^z_3 \end{aligned} \tag{4.46}$$

Again let us check that $S(s,s)$ is a valid splitting opreator. Clearly $S(s,s)$ is local and $\mathbb{Z}_2$

symmetric. To see that it has the correct action on domain walls note that

$$\begin{aligned} S(s,s)|1_1\rangle &= \sigma_2^-|...,(+)_1,+,+,...\rangle \\ &= |...,(+)_1,-,+,...\rangle \\ &\propto |s_1,s_2\rangle \end{aligned} \tag{4.47}$$

where $|s_1,s_2\rangle$ denotes the state with two domain walls at positons 1 and 2.

Moving on to the other splitting operators, we define $S(1,s)$ as

$$S(1,s) = M_{21}^s = \sigma_2^+ - \sigma_1^z\sigma_2^-\sigma_3^z \tag{4.48}$$

Also, we define the movement operator $M_{n'n}^1$ and the splitting operators $S(s,1), S(1,1)$ as

$$M_{n'n}^1 = S(s,1) = S(1,1) = \mathbb{1} \tag{4.49}$$

(The reason we can set these operators equal to the identity is that none of these operators are supposed to change the location of any nontrivial domain walls, e.g. $S(s,1)$ is defined by the condition $S(s,1)|s_1\rangle = |s_1,1_2\rangle$, and similarly for the other operators).

With these operator definitions in place, we are now ready to calculate $F(s,s,s)$. Using Eq. 4.20, we have

$$|1\rangle = M_{12}^s M_{01}^s S(s,s) M_{32}^s S(1,s)|s_1\rangle \tag{4.50}$$

We now simplify this expression, working from right to left. First, we note that

$$\begin{aligned} S(1,s)|s_1\rangle &= (\sigma_2^+ - \sigma_1^z\sigma_2^-\sigma_3^z)|s_1\rangle \\ &= \sigma_2^+|s_1\rangle \end{aligned}$$

since $\sigma_1^z \sigma_2^- \sigma_3^z |s_1\rangle = 0$. Likewise,

$$M_{32}^s \sigma_2^+ |s_1\rangle = \sigma_3^+ \sigma_2^+ |s_1\rangle$$

since the second term in M_{32}^s, i.e. $(-\sigma_2^z \sigma_3^- \sigma_4^z)$, annihilates $\sigma_2^+ |s_1\rangle$. Proceeding in this way, we can drop either the first or second term in each of the movement and splitting operators. The final result is:

$$\begin{aligned} |1\rangle &= (-\sigma_1^z \sigma_2^+ \sigma_3^z) \sigma_1^- \sigma_2^- \sigma_3^+ \sigma_2^+ |s_1\rangle \\ &= |..., +, (-)_1, +, +, -, ...\rangle \end{aligned} \tag{4.51}$$

where the second equality follows from $|s_1\rangle = |..., +, (+)_1, -, -, -, ...\rangle$. Following the same logic, we obtain

$$\begin{aligned} |2\rangle &= M_{32}^s S(s,s) M_{12}^1 M_{01}^s S(s,1) |s_1\rangle \\ &= \sigma_3^+ (-\sigma_1^z \sigma_2^+ \sigma_3^z) \sigma_1^- |s_1\rangle \\ &= -|..., +, (-)_1, +, +, -, ...\rangle \end{aligned} \tag{4.52}$$

Comparing these two expressions, we see that $|1\rangle = -|2\rangle$, so that

$$F(s,s,s) = \langle 2|1\rangle = -1 \tag{4.53}$$

More generally, one can check that all other values of F are 1 for this model, i.e. $F(g,h,k) = 1$ for all other choices of $g, h, k \in \{1, s\}$.

Having computed F, the next question is to determine whether F corresponds to a trivial or non-trivial cocycle, i.e. a trivial or non-trivial element of $H^3(G, U(1)) = \mathbb{Z}_2$. To answer

this question, we compute the following gauge invariant quantity:

$$F(s,s,s)F(s,1,s) = -1 \tag{4.54}$$

Since this quantity is different from 1, it follows that F is a nontrivial cocycle. We conclude that our edge theory describes the boundary of the non-trivial bosonic SPT phase with $\mathbb{Z}_2$ symmetry. This conclusion is consistent with the original microscopic derivation of this edge theory [26, 84].

4.4.2 Chiral boson edge theory for $\mathbb{Z}_2$ SPT phase

We now present an example involving a *continuum* edge theory for the $\mathbb{Z}_2$ bosonic SPT phase (the same SPT phase as in the previous example). This edge theory was introduced in Ref. [84].

Edge theory

We begin by reviewing the continuum $\mathbb{Z}_2$ SPT edge theory. This edge theory is a chiral boson edge theory consisting of two conjugate fields θ, ϕ obeying the commutation relations

$$[\theta(x), \partial_y \phi(y)] = 2\pi i \delta(x-y) \tag{4.55}$$

with all other commutators vanishing.

Again, to define the edge theory, we need to specify three pieces of data: (1) a Hilbert space $\mathcal{H}$; (2) a set of local operators $\{\mathcal{O}\}$ that act in $\mathcal{H}$; and (3) a collection of symmetry transformations $\{U^g : g \in G\}$ acting within $\mathcal{H}$. The Hilbert space $\mathcal{H}$ is the usual infinite dimensional representation of the above algebra (4.55). The local operators $\{\mathcal{O}\}$ in this edge theory consist of arbitrary derivatives and/or products of the operators $\{e^{\pm i\theta}, e^{\pm i\phi}\}$.

To complete the edge theory, we need to specify the $\mathbb{Z}_2$ symmetry transformation, $U \equiv$

U^s, where $\mathbb{Z}_2 = \{1, s\}$. This transformation acts as [84]

$$\begin{aligned} U\theta U^{-1} &= \theta - \pi \\ U\phi U^{-1} &= \phi - \pi \end{aligned} \tag{4.56}$$

We can see that this is a $\mathbb{Z}_2$ symmetry since the fields θ, ϕ are only defined modulo 2π.

We can also write out an explicit formula for U, though we will not need it for our computation below [84]:

$$U = e^{-\frac{i}{2}\int_{-\infty}^{\infty} dy[\partial_y\theta(y)+\partial_y\phi(y)]} \tag{4.57}$$

Calculating the anomaly

We now proceed to calculate the anomaly in the above edge theory. The first step is to choose a gapped Hamiltonian that breaks the $\mathbb{Z}_2$ symmetry spontaneously and completely. We will use the Hamiltonian

$$H = H_0 - \int dx V \cos(2\theta) \tag{4.58}$$

where H_0 is the usual free boson Hamiltonian:

$$H_0 = \int dx \frac{1}{4\pi}[v_\theta(\partial_x\theta)^2 + v_\phi(\partial_x\phi)^2]$$

for some velocities $v_\theta, v_\phi > 0$.

When V is sufficiently large, the above Hamiltonian H has all the required properties. In that regime, the cosine term locks θ to one of two values: $\theta = 0$ and $\theta = \pi$, spontaneously breaking the $\mathbb{Z}_2$ symmetry (5.131) and opening up an energy gap.

For simplicity, we will consider the limit $V \to \infty$ in what follows. In this limit, the two

ground states of H are *eigenstates* of $e^{i\theta(x)}$. Following our standard labeling scheme, we denote these ground states by $|\Omega;1\rangle$ and $|\Omega;s\rangle$, where

$$\begin{aligned} e^{i\theta(x)}|\Omega;1\rangle &= |\Omega;1\rangle \\ e^{i\theta(x)}|\Omega;s\rangle &= -|\Omega;s\rangle \end{aligned} \tag{4.59}$$

for all x.

The next step is to construct domain wall states $|s_x\rangle$, that interpolate spatially between the two ground states, $|\Omega;1\rangle$ and $|\Omega;s\rangle$. We define $|s_x\rangle$ by

$$|s_x\rangle = a_x^\dagger|\Omega;1\rangle \tag{4.60}$$

where

$$a_x^\dagger = e^{-\frac{i}{2}\int_x^\infty dy\ \partial_y\phi(y)} \tag{4.61}$$

Here $a_x^\dagger$ is a (non-local) creation operator for a domain wall at postion x. To see that $|s_x\rangle$ is a valid domain wall state, note that $|s_x\rangle$ obeys

$$e^{i\theta(x')}|s_x\rangle = \mathrm{sgn}(x-x')|s_x\rangle \tag{4.62}$$

(This follows from the fact that $a_x^\dagger$ anticommutes with $e^{i\theta(x')}$ for $x' > x$). Likewise, we define the no-domain wall state $|1_x\rangle$ to be $|1_x\rangle = |\Omega;1\rangle$.

Now that we have defined domain wall states, the next step is to construct movement and splitting operators for these domain walls. First, we define the movement operator $M^s_{x'x}$

by

$$M^s_{x'x} = e^{\frac{i}{2}\int_x^{x'} dy\ \partial_y \phi(y)} \tag{4.63}$$

This is a valid movement operator because it is local and $\mathbb{Z}_2$ symmetric and it obeys $M^s_{x'x}|s_x\rangle \propto |s_{x'}\rangle$ since $M^s_{x'x} a^\dagger_x \propto a^\dagger_{x'}$.

Next, we define the splitting operator $S(s,s)$ by

$$\begin{aligned} S(s,s) &= M^s_{21} e^{i[\phi(1)-\theta(1^-)]} \\ &= e^{\frac{i}{2}\int_1^2 dy\ \partial_y\phi(y)} e^{i[\phi(1)-\theta(1^-)]} \end{aligned} \tag{4.64}$$

Here, $\theta(1^-)$ is shorthand for $\theta(1-\epsilon)$ where ϵ is a small positive number.

To see that this is a valid splitting operator, note that $S(s,s)$ is local, it is $\mathbb{Z}_2$ symmetric, and furthermore

$$\begin{aligned} S(s,s)|1_1\rangle &= e^{\frac{i}{2}\int_1^2 dy\ \partial_y\phi(y)} e^{i[\phi(1)-\theta(1^-)]}|\Omega;1\rangle \\ &\propto e^{\frac{i}{2}\int_1^2 dy\ \partial_y\phi(y)} e^{i\phi(1))}|\Omega;1\rangle \\ &\propto a_2^\dagger a_1^\dagger |\Omega;1\rangle \\ &\propto |s_1,s_2\rangle \end{aligned} \tag{4.65}$$

Here, the second equality follows from $e^{-i\theta(1^-)}|\Omega;1\rangle = |\Omega;1\rangle$, while the third equality follows from the definition of $a^\dagger_x$ (5.136). Readers may wonder why we include the factor of $e^{-i\theta(1^-)}$ in the definition $S(s,s)$ given that $e^{-i\theta(1^-)}$ acts trivially on $|\Omega;1\rangle$: the reason for including this factor of $e^{-i\theta(1^-)}$ is that, without it, $S(s,s)$ would be *odd*, not even, under the $\mathbb{Z}_2$ symmetry. Furthermore, the reason that we use $e^{-i\theta(1^-)}$ rather than say, $e^{-i\theta(1)}$ is that this choice will regularize some of the commutators that we calculate below. (We could equally well choose $e^{-i\theta(1^+)}$ and we would arrive at the same result.)

Moving on to the other splitting operators, we define

$$S(1,s) = M^s_{21} \tag{4.66}$$

Also we define

$$M^1_{x'x} = S(s,1) = S(1,1) = 1 \tag{4.67}$$

With these operators in hand, we are now ready to compute $F(s,s,s)$. Using (4.20), we have

$$\begin{aligned} |1\rangle &= M^s_{12} M^s_{01} M^s_{21} e^{i[\phi(1)-\theta(1^-)]} M^s_{32} M^s_{21} |s_1\rangle \\ |2\rangle &= M^s_{32} M^s_{21} e^{i[\phi(1)-\theta(1^-)]} M^s_{01} |s_1\rangle \end{aligned} \tag{4.68}$$

In order to compare these expressions, we need to reorder the operators within them. We do this using the following commutation relations, which can be derived from the Baker-Campbell-Hausdorff formula:

$$\begin{aligned} e^{i[\phi(1)-\theta(1^-)]} M^s_{x1} &= (-1)^{\Theta(1-x)} M^s_{x1} e^{i[\phi(1)-\theta(1^-)]} \\ [M^s_{x'x}, M^s_{y'y}] &= 0 \end{aligned} \tag{4.69}$$

where $\Theta(x)$ denotes the Heaviside step function. With these formulas and the identity $M^s_{xx'} = (M^s_{x'x})^{-1}$, we can rewrite $|1\rangle$ as:

$$|1\rangle = -M^s_{32} M^s_{21} e^{i[\phi(1)-\theta(1^-)]} M^s_{01} |s_1\rangle \tag{4.70}$$

Therefore, $|1\rangle = -|2\rangle$ and hence

$$F(s,s,s) = \langle 2|1\rangle = -1 \tag{4.71}$$

In the same way, one can check that all other values of F are 1 for this model, i.e. $F(g,h,k) = 1$, for all other choices of $g,h,k \in \{1,s\}$.

Comparing with the previous example, we see that the two F's are identical. Therefore, just as in that example, we conclude that F is a non-trivial cocycle, and the corresponding edge theory describes the boundary of the non-trivial $\mathbb{Z}_2$ SPT phase. This result is consistent with the original derivation of this edge theory [84].

4.4.3 SPT lattice edge theory with symmetry group G

We now generalize the example in Sec. 4.4.1 to a large class of lattice edge theories with a finite unitary symmetry group G. A similar class of edge theories was studied in Ref. [39] and we will mostly follow their notation here.

Edge theory

As before, to define the edge theory, we need to specify three pieces of data: (1) a Hilbert space $\mathcal{H}$; (2) a set of local operators $\{\mathcal{O}\}$ that act in $\mathcal{H}$; and (3) a collection of symmetry transformations $\{U^g : g \in G\}$ acting within $\mathcal{H}$.

We begin by describing the Hilbert space $\mathcal{H}$. This Hilbert space is equivalent to a one-dimensional spin chain where each spin can be in $|G|$ different states. We label these states by group elements, $|g\rangle$, $g \in G$. In this notation, the basis states for the Hilbert space are of the form

$$|..., \alpha_{-1}, \alpha_0, \alpha_1, ...\rangle, \qquad \alpha_n \in G \tag{4.72}$$

The local operators $\{\mathcal{O}\}$ in this edge theory are the usual local operators in a spin chain – i.e. products of single site operators acting on a collection of neighboring sites. In particular, there are two basic types of single site operators, from which all other operators can be built. The first operator, P_n^g, is a projection operator that projects onto states with $\alpha_n = g$, i.e.

$$P_n^g|..., \alpha_{n-1}, \alpha_n, \alpha_{n+1}, ...\rangle = \delta_{\alpha_n,g}|..., \alpha_{n-1}, g, \alpha_{n+1}, ...\rangle \tag{4.73}$$

The second operator, R_n^g is a unitary operator that performs right multiplication by g on the nth spin:

$$R_n^g|..., \alpha_{n-1}, \alpha_n, \alpha_{n+1}, ...\rangle = |..., \alpha_{n-1}, \alpha_n g, \alpha_{n+1}, ...\rangle \tag{4.74}$$

To complete the edge theory, we need to describe the symmetry transformations U^g. We start by writing down an explicit formula for U^g. This formula is a product of two terms:

$$U^g = N^g X^g \tag{4.75}$$

where X^g acts by left multiplication by g on every site,

$$X^g|..., \alpha_{-1}, \alpha_0, \alpha_1, ...\rangle = |..., g\alpha_{-1}, g\alpha_0, g\alpha_1, ...\rangle, \tag{4.76}$$

while N^g is a phase factor that is diagonal in the $|\alpha\rangle$ basis:

$$N^g|\alpha\rangle = e^{i\mathcal{N}^{(1)}(g)[\alpha]}|\alpha\rangle \tag{4.77}$$

Here we are using the abbreviation $|\alpha\rangle \equiv |..., \alpha_{-1}, \alpha_0, \alpha_1, ...\rangle$. The term in the exponent,

$\mathcal{N}^{(1)}(g)$, is a functional of the configuration α of the form

$$\mathcal{N}^{(1)}(g)[\alpha] = \sum_n \Phi_n^g(\alpha_{n-1}, \alpha_n, \alpha_{n+1}) \tag{4.78}$$

for some real valued Φ_n^g that depends on *triplets* of neighboring spins. We note that the above functional form is not essential for our method – we could equally well consider generalizations of Φ_n^g that act on any finite number of nearby spins.

An alternative, and more local, way to describe the symmetry transformations U^g is to specify how these transformations act on local operators – specifically P_n^h and R_n^h. In this description, the symmetry transformation is defined by

$$\begin{aligned} U^g P_n^h (U^g)^{-1} &= P_n^{gh} \\ U^g R_n^h (U^g)^{-1} &= R_n^h W_n^{g,h} \end{aligned} \tag{4.79}$$

where $W_n^{g,h}$ is an unitary operator of the form

$$W_n^{g,h} = \sum_{a,b,c \in G} \Theta_n^{g,h}(a,b,c) P_{n-1}^a P_n^b P_{n+1}^c \tag{4.80}$$

and where $\Theta_n^{g,h}(a,b,c)$ is a $U(1)$ phase. (Again, our method does not require this particular functional form of $\Theta_n^{g,h}$ and we could consider generalizations that act on any finite number of nearby spins). In the calculation that follows, we only use the latter, more local, description of the symmetry transformation given in Eqs. 4.79-4.80.

Calculating the anomaly

The first step is to choose an edge Hamiltonian that breaks the G-symmetry spontaneously and completely. We choose

$$H = -J \sum_n \sum_g P_n^g P_{n+1}^g \tag{4.81}$$

Note that H has a "ferromagnetic" interaction that favors states in which neighboring spins are in the same state $|g\rangle$. As a result, it is easy to see that this Hamiltonian has $|G|$ degenerate ground states of the form $|..., g, g, g, ...\rangle$ where $g \in G$. We will label these states by

$$|\Omega; g\rangle = |..., g, g, g, ...\rangle \tag{4.82}$$

We now turn to the definition of the domain wall state $|g_n\rangle$. We define $|g_n\rangle$ by

$$|g_n\rangle = |..., 1, 1, (1)_n, g, g, g, ...\rangle \tag{4.83}$$

Here the notation $(1)_n$ signifies that this '1' is the state of the nth spin, so that the 'g' that follows is the state of the $(n+1)$st spin and so on. Similarly to Sec. 4.4.1, the domain wall at location n sits between sites n and $n+1$.

Having defined the domain wall states, the next step is to construct movement and splitting operators. We define the movement operator between n and $n+1$ by

$$M_{n+1,n}^g = \sum_{k \in G} U^k R_{n+1}^{g^{-1}} P_{n+1}^g (U^k)^{-1} \tag{4.84}$$

To see that $M_{n+1,n}^g$ is a valid movement operator notice that it is local and G-symmetric by

construction. Furthermore, it has the correct action on domain wall states:

$$\begin{aligned} M^g_{(n+1)n}|g_n\rangle &= \sum_{k\in G} U^k R^{g^{-1}}_{n+1} P^g_{n+1} (U^k)^{-1} |..., (1)_n, g, g, ...\rangle \\ &= R^{g^{-1}}_{n+1} |..., (1)_n, g, g, ...\rangle \\ &= |..., (1)_n, 1, g, ...\rangle \\ &= |g_{n+1}\rangle \end{aligned} \tag{4.85}$$

Here the second equality follows from noting that all the terms in the sum vanish except for $k = 1$. Similarly, we define the reverse movement operator by

$$M^g_{n(n+1)} = \left(M^g_{(n+1)n}\right)^\dagger \tag{4.86}$$

Following a similar calculation to before, one can check that this is a valid movement operator.

Moving on to splitting operators, we define $S(g, h)$ by

$$S(g,h) = \sum_{k\in G} U^k R_2^{h^{-1}} P_2^{gh} (U^k)^{-1} \tag{4.87}$$

Again, $S(g, h)$ is local and G-symmetric by construction. We now show that it has the correct action on domain wall states:

$$\begin{aligned} S(g,h)|gh_1\rangle &= \sum_{k\in G} U^k R_2^{h^{-1}} P_2^{gh} (U^k)^{-1} |..., (1)_1, gh, gh, ...\rangle \\ &= R_2^{h^{-1}} |..., (1)_1, gh, gh, ...\rangle \\ &= |..., (1)_1, g, gh, ...\rangle \\ &= |g_1, h_2\rangle \end{aligned} \tag{4.88}$$

Again, the second equality follows from noting that all the terms in the sum vanish except for $k = 1$.

We are now ready to calculate $F(g, h, k)$. Using (4.20), we have

$$\begin{aligned}|1\rangle =& M_{12}^{h} M_{01}^{g} S(g,h) M_{32}^{k} S(gh,k) |ghk_1\rangle \\ =& (U^g R_2^h [U^g]^{-1}) \cdot R_1^g \cdot R_2^{h^{-1}} \\ & \cdot (U^{gh} R_3^{k^{-1}} [U^{gh}]^{-1}) \cdot R_2^{k^{-1}} |ghk_1\rangle \end{aligned} \tag{4.89}$$

Here, to derive the second equality, notice that whenever a movement or splitting operator acts on a domain wall state, only one value of k gives a nonzero contribution; Eq. 4.89 follows by keeping this one nonvanishing term for each movement and splitting operator.

To proceed further, we use the transformation law for R_n^h in Eqs. 4.79-4.80 to derive

$$\begin{aligned}|1\rangle =& (R_2^h W_2^{g,h}) \cdot R_1^g \cdot R_2^{h^{-1}} \cdot (R_3^{k^{-1}} W_3^{gh,k^{-1}}) \cdot R_2^{k^{-1}} |ghk_1\rangle \\ =& \Theta_2^{g,h}(g,g,gh) \cdot \Theta_3^{gh,k^{-1}}(gh, ghk, ghk) \\ & \cdot |..., 1, (g)_1, gh, gh, ghk, ...\rangle \end{aligned} \tag{4.90}$$

where the second equality follows from $|ghk_1\rangle = |..., 1, (1)_1, ghk, ghk, ghk, ...\rangle$. By the same reasoning, we have

$$\begin{aligned}|2\rangle =& M_{32}^{k} S(h,k) M_{12}^{hk} M_{01}^{g} S(g,hk) |ghk_1\rangle \\ =& (U^{gh} R_3^{k^{-1}} [U^{gh}]^{-1}) \cdot (U^g R_2^{k^{-1}} [U^g]^{-1}) \\ & \cdot (U^g R_2^{hk} [U^g]^{-1}) \cdot R_1^g \cdot R_2^{(hk)^{-1}} |ghk_1\rangle \\ =& (R_3^{k^{-1}} W_3^{gh,k^{-1}}) \cdot (R_2^h W_2^{g,h}) \cdot R_1^g \cdot R_2^{(hk)^{-1}} |ghk_1\rangle \\ =& \Theta_3^{gh,k^{-1}}(gh, ghk, ghk) \cdot \Theta_2^{g,h}(g,g,ghk) \\ & \cdot |..., 1, (g)_1, gh, gh, ghk, ...\rangle \end{aligned} \tag{4.91}$$

Taking the inner product between $|1\rangle$ and $|2\rangle$, we see that the $\Theta_3^{gh,k^{-1}}(gh, ghk, ghk)$ factors cancel out, leaving

$$F(g,h,k) = \langle 2|1\rangle = \frac{\Theta_2^{g,h}(g,g,gh)}{\Theta_2^{g,h}(g,g,ghk)} \tag{4.92}$$

where we are using the fact that $\Theta_n^{g,h}$ is a $U(1)$ phase.

4.5 Connection with symmetry restriction method for computing anomalies

As we mentioned earlier, in Ref. [39], Else and Nayak showed how to compute anomalies in a large class of SPT edge theories using restricted symmetry operators. It is natural to wonder how our F-symbol based approach is related to this symmetry restriction approach. In this section we derive a connection between the two approaches by explicitly showing that the two approaches give identical results in cases where both methods are applicable.

4.5.1 Review of symmetry restriction method

We begin by reviewing the symmetry restriction method [39]. This method applies to SPT edge theories with a discrete unitary symmetry group G and with the property that the symmetry operators $\{U^g, g \in G\}$ are local unitary transformations.[4] Here, by a "local unitary transformation", we mean that U^g can be generated by the time evolution of a local Hermitian operator over a finite period of time T: $U^g = \mathcal{T}\exp[-i\int_0^T dt H(t)]$.

The symmetry restriction method proceeds as follows. Consider an edge theory of the above kind, with symmetry operators U^g. To compute the anomaly associated with this edge theory, the first step is to choose a large interval $I = [a, b]$, and then choose a "restriction"

4. This method also applies to continuous symmetries and some antiunitary symmetries; we focus on discrete unitary symmetries for simplicity.

of U^g to I, which we will denote by U_I^g. Here, when we say that U_I^g is a restriction of U^g to I, we mean U_I^g has two properties: (i) U_I^g is a local unitary transformation supported in a neighborhood of I, and (ii) for any operator $\mathcal{O}$ that is supported in I,

$$U_I^g \mathcal{O} (U_I^g)^{-1} = U^g \mathcal{O} (U^g)^{-1} \tag{4.93}$$

Note that the existence of such a U_I^g is guaranteed by the fact that U^g is a local unitary transformation, but U_I^g is not unique.

Next, define an operator $\Omega_I(g,h)$ by

$$\Omega_I(g,h) = U_I^g U_I^h (U_I^{gh})^{-1} \tag{4.94}$$

By construction $\Omega_I(g,h)$ is a local unitary transformation that is supported near a, b – the endpoints of I. It follows that we can factor $\Omega_I(g,h)$ as a product

$$\Omega_I(g,h) = \Omega_a(g,h)\Omega_b(g,h) \tag{4.95}$$

where $\Omega_a(g,h)$ and $\Omega_b(g,h)$ are unitary operators supported near a and b, respectively.[5]

The operator $\Omega_a(g,h)$ (or equivalently $\Omega_b(g,h)$) is the key to computing the anomaly. In particular, Ref. [39] showed that Ω_a and Ω_b obey the following operator identities:

$$\begin{aligned} \Omega_a(g,h)\Omega_a(gh,k) &= \omega(g,h,k) U_I^g \Omega_a(h,k) (U_I^g)^{-1} \Omega_a(g,hk) \\ \Omega_b(g,h)\Omega_b(gh,k) &= \\ &\omega^{-1}(g,h,k) U_I^g \Omega_b(h,k) (U_I^g)^{-1} \Omega_b(g,hk) \end{aligned} \tag{4.96}$$

5. Readers may notice that there is a phase ambiguity in $\Omega_a(g,h)$, $\Omega_b(g,h)$, i.e. we can replace $\Omega_a(g,h) \to \Omega_a(g,h)\nu(g,h)$, and $\Omega_b(g,h) \to \Omega_b(G,h)\nu^{-1}(g,h)$ where $\nu(g,h)$ is a $U(1)$ phase. This ambiguity is related to the fact that the quantity $\omega(g,h,k)$ is only well-defined up to a coboundary.

where $\omega(g,h,k) \in H^3(G,U(1))$ is the anomaly carried by the SPT edge theory. Thus, if we know $\Omega_a(g,h)$ (or equivalently $\Omega_b(g,h)$), we can immediately compute the anomaly by comparing the left and right hand sides of Eq. 4.96.

Putting this all together, the symmetry restriction method involves the following steps: one first computes the restricted symmetry operator U_I^g, and then the associated operators $\Omega_I(g,h)$ and $\Omega_a(g,h)$. One then computes the anomaly $\omega(g,h,k)$ using Eq. 4.96 above.

4.5.2 F-symbol computation

We now show how to compute the F-symbol for the above class of edge theories, i.e. edge theories with a finite unitary symmetry group G and with the property that the symmetry operators $\{U^g, g \in G\}$ are local unitary transformations. Our goal will be to show that $F(g,h,k) = \omega(g,h,k)$.

Consider any edge theory of the above type. To compute the F-symbol for such an edge theory, the first step is to choose an edge Hamiltonian that breaks the symmetry spontaneously and completely and opens up a gap. We then label the $|G|$ degenerate ground states by $\{|\Omega; g\rangle\}$ where

$$|\Omega; g\rangle = U^g|\Omega; 1\rangle \tag{4.97}$$

The next step is to define domain wall states. We will do this using restricted symmetry operators, in order to facilitate a comparison with Ref. [39]. To begin, we choose a point Y that is far to the right of the region where we will be manipulating domain walls. This point Y can be thought of as playing a similar role to $+\infty$, but it will be important for our purposes that Y is finite. Next, for every point $x < Y$, we choose a unitary operator U_x^g that is a restriction of U^g to the interval $[x,Y]$, where this restriction is defined as in Eq. 4.93 above. In addition, we require that the U_x^g are chosen so that they obey the following matching

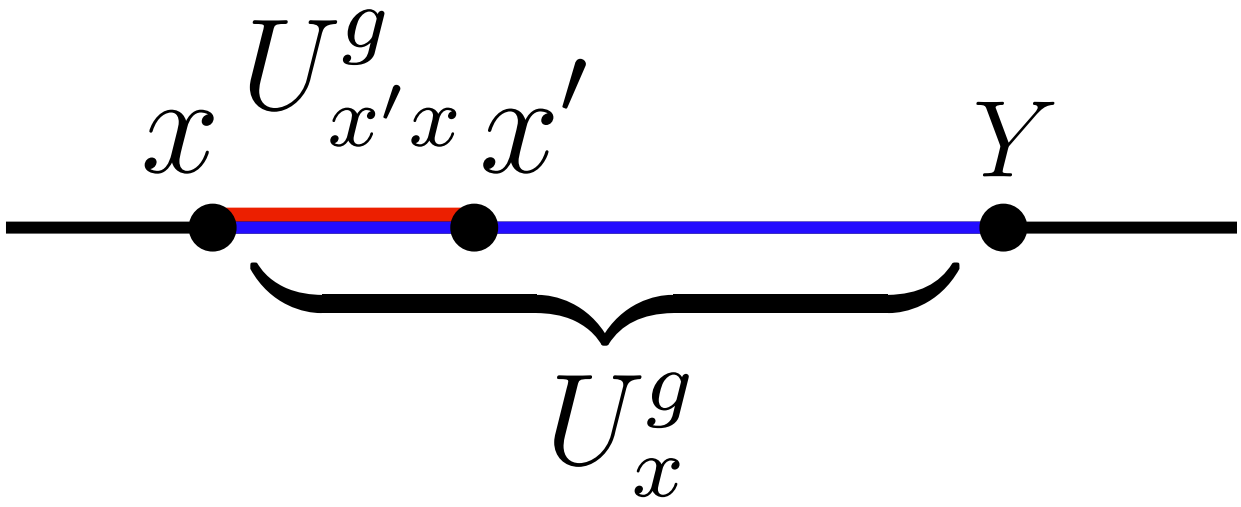

Figure 4.8: Regions of support for the operators $U^g_{x'x}$ and U^g_x: the operator U^g_x is supported in the interval $[x, Y]$ shown in blue, while $U^g_{x'x}$ is supported in the interval $[x, x']$ shown in red.

condition: for any two points $x < x'$ the operators U^g_x and $U^g_{x'}$ have the same action except in the neighborhood of the interval $[x, x']$. Equivalently, we will require that the operator

$$U^g_{x'x} \equiv U^g_{x'}(U^g_x)^{-1} \tag{4.98}$$

is supported in a neighborhood of the interval $[x, x']$ (see Fig. 4.8). One can show that it is always possible to choose U^g_x in this way, given our assumption that U^g are local unitary transformations.

Having defined U^g_x, we now define (single) domain wall states $|g_x\rangle$ by

$$|g_x\rangle = U^g_x|\Omega; 1\rangle \tag{4.99}$$

By construction $U^g_x|\Omega; 1\rangle$ contains a type g domain wall at x and a type g^{-1} domain wall at Y, so one could view $U^g_x|\Omega; 1\rangle$ as a *two* domain wall state. However, we will view $U^g_x|\Omega; 1\rangle$ as a single domain wall state. We can do this because (i) the point Y is far away from the region of interest, and (ii) the g^{-1} domain wall at Y takes the same form independent of

x: for any x, x' the two states $U^g_x|\Omega;1\rangle$ and $U^g_{x'}|\Omega;1\rangle$ have the same local expectation values near Y, due to our assumption (4.98). Actually, the above definition of $|g_x\rangle$ is no different than the one given in e.g. Eq. 4.60 where we set $Y = +\infty$, except that we are now calling attention to the point Y because it will be useful for proving that our formalism matches that of Else and Nayak.

Now that we have defined domain wall states, the next step is to construct splitting and movement operators. To this end, notice that the operator $U^g_{x'x}$ defined in Eq. (4.98) obeys

$$U^g_{x'x}|g_x\rangle = |g_{x'}\rangle \tag{4.100}$$

Given this observation, we can construct a movement operator $M^g_{x'x}$ by appropriately symmetrizing $U^g_{x'x}$:

$$M^g_{x'x} = \sum_{k\in G} U^k U^g_{x'x} P^g_{x'} (U^k)^{-1}, \qquad x' > x \tag{4.101}$$

Here $P^g_{x'}$ is a projection operator that projects onto states that share the same local expectation values as $|\Omega;g\rangle$ in the neighborhood of x'. More precisely, $P^g_{x'}$ is a Hermitian operator that is supported in the neighborhood of x' and that has the property that $P^g_{x'}|\Omega;h\rangle = \delta_{gh}|\Omega;g\rangle$. For the models discussed in Sec. 4.4.3, $P^g_{x'}$ can be defined is the same way as the operator P^g_n (4.73). In more general systems, it may be necessary to take the neighborhood around x' to be of order ξ to construct a projector $P^g_{x'}$ of this kind. In any case, we will take the existence of this projection operator as an assumption.

To see that $M^g_{x'x}$ is a valid movement operator, note that it is local and G-symmetric by construction. Furthermore, it has the correct action on domain walls:

$$M^g_{x'x}|g_x\rangle = U^g_{x'x}|g_x\rangle = |g_{x'}\rangle \tag{4.102}$$

Similarly, we define the reverse movement operator by

$$M^g_{xx'} = (M^g_{x'x})^\dagger, \qquad x' > x \tag{4.103}$$

In order to construct splitting operators, we first define a unitary operator $\Omega(g,h)$ by

$$\Omega(g,h) = U^g_1 U^h_1 (U^{gh}_1)^{-1} \tag{4.104}$$

By construction $\Omega(g,h)$ is a local unitary operator that is supported near 1 and Y, so we can factor $\Omega(g,h)$ as

$$\Omega(g,h) = \Omega_1(g,h)\Omega_Y(g,h) \tag{4.105}$$

where $\Omega_1(g,h)$ and $\Omega_Y(g,h)$ are unitary operators supported near 1 and Y, respectively. (Note that Eqs. 4.104-4.105 are essentially the same as Eqs. 4.94-4.95, with $I = [1,Y]$).

With this notation, we define the splitting operator $S(g,h)$ by

$$S(g,h) = \sum_{k\in G} U^k U^g_1 U^h_{21} (U^g_1)^{-1} \Omega_1(g,h) P^{gh}_2 (U^k)^{-1}. \tag{4.106}$$

Again, it is easy to see that $S(g,h)$ is G-symmetric and supported in a neighborhood around $[1,2]$. To see that it has the correct action on domain wall states, note that

$$\begin{aligned} S(g,h)|gh_1\rangle &= U^g_1 U^h_{21} (U^g_1)^{-1} \Omega_1(g,h)|gh_1\rangle \\ &= \Omega_Y(g,h)^{-1} U^g_1 U^h_{21} (U^g_1)^{-1} \Omega(g,h)|gh_1\rangle \\ &= \Omega_Y(g,h)^{-1} U^g_1 U^h_2 |\Omega;1\rangle \\ &\propto |g_1,h_2\rangle. \end{aligned} \tag{4.107}$$

Here, the last equality follows from observing that the state $\Omega_Y(g,h)^{-1} U^g_1 U^h_2 |\Omega;1\rangle$ has the

Figure 4.9: The points that are relevant to the calculation of $F(g,h,k)$ and $\omega(g,h,k)$: the operators that are used to calculate $F(g,h,k)$ are supported in a neighborhood of $[0,3]$, whereas the operators used to calculate $\omega(g,h,k)$ are supported in a small neighborhood around the point Y, far to the right of 3. We connect the two calculations using the identity $\Omega_1(g,h) = \Omega_Y^{-1}(g,h)\Omega(g,h)$.

same local expectation values as $|g_1\rangle$ near $x = 1$ and the same local expectation values as $U^g|h_2\rangle$ near $x = 2$, and the same local expectation values as $U^g|\Omega;1\rangle$ in the region between $x = 1$ and $x = 2$. (We don't have to worry about the expectaton values away from $[1,2]$ since the locality of $S(g,h)$ guarantees that $S(g,h)|gh_1\rangle$ has the correct expectation values away from $[1,2]$).

Now that we have defined movement and splitting operators, we can compute the F-symbol using Eqs. 4.20-4.21, i.e.

$$F(g,h,k) = \langle 2|1\rangle, \tag{4.108}$$

where

$$\begin{aligned} |1\rangle &= M_{12}^h M_{01}^g S(g,h) M_{32}^k S(gh,k)|ghk_1\rangle \\ |2\rangle &= M_{32}^k S(h,k) M_{12}^{hk} M_{01}^g S(g,hk)|ghk_1\rangle \end{aligned} \tag{4.109}$$

4.5.3 Comparing results with Else and Nayak

We now show $F(g,h,k) = \omega(g,h,k)$ where $F(g,h,k)$ is defined in Eq. 4.108 and $\omega(g,h,k)$ is defined in Eq. 4.96.

To prove this equality, we use the fact that $\Omega_1(g,h) = \Omega_Y^{-1}(g,h)\Omega(g,h)$. Substituting

this identity into the definition of $S(g,h)$ and simplifying gives

$$S(g,h) = \sum_{k\in G} U^k \Omega_Y^{-1}(g,h) U_1^g U_2^h (U_1^{gh})^{-1} P_2^{gh} (U^k)^{-1} \tag{4.110}$$

The basic idea of the proof is to substitute (4.110) into (4.109) and then simplify the resulting expressions for $|1\rangle, |2\rangle$. After this substitution, we will then separate out all the Ω_Y factors. These Ω_Y factors will naturally form combinations like those in Eq. 4.96, which will allow us to derive a direct connection between the F-symbol $F(g,h,k)$ and the cocycle $\omega(g,h,k)$ (see Fig. 4.9).

Following this plan, we first simplify $|1\rangle$ as follows:

$$\begin{aligned}
|1\rangle &= M_{12}^h M_{01}^g S(g,h) M_{32}^k S(gh,k) |ghk_1\rangle \\
&= M_{12}^h M_{01}^g S(g,h) M_{32}^k \Omega_Y^{-1}(gh,k) U_1^{gh} U_2^k (U_1^{ghk})^{-1} |ghk_1\rangle \\
&= \Omega_Y^{-1}(gh,k) M_{12}^h M_{01}^g S(g,h) M_{32}^k U_1^{gh} U_2^k |\Omega; 1\rangle \\
&= \Omega_Y^{-1}(gh,k) M_{12}^h M_{01}^g S(g,h) U_1^{gh} U_3^k |\Omega; 1\rangle \\
&= [\Omega_Y^{-1}(gh,k) \Omega_Y^{-1}(g,h)] M_{12}^h M_{01}^g U_1^g U_2^h U_3^k |\Omega; 1\rangle \\
&= [\Omega_Y^{-1}(gh,k) \Omega_Y^{-1}(g,h)] U_0^g U_1^h U_3^k |\Omega; 1\rangle
\end{aligned} \tag{4.111}$$

Here, the second and fifth equalities follow from substituting (4.110), while the third equality follows from the fact that $\Omega_Y(gh,k)$ is supported near Y and therefore commutes with all the movement and splitting operators. Likewise, the fourth and sixth equalities follow from the fact that $[M_{x'x}^g, U_y^h] = 0$ as long as $y \notin [x,x']$, which in turn follows from the fact that the movement operators are G-symmetric.

We can simplify $|2\rangle$ in a similar manner:

$$\begin{aligned}
|2\rangle &= M_{32}^{k} S(h,k) M_{12}^{hk} M_{01}^{g} S(g,hk)|ghk_1\rangle \\
&= \Omega_Y^{-1}(g,hk) M_{32}^{k} S(h,k) M_{12}^{hk} M_{01}^{g} U_1^{g} U_2^{hk}|\Omega;1\rangle \\
&= \Omega_Y^{-1}(g,hk) M_{32}^{k} S(h,k) U_0^{g} U_1^{hk}|\Omega;1\rangle \\
&= \Omega_Y^{-1}(g,hk) M_{32}^{k} U_0^{g} S(h,k) U_1^{hk}|\Omega;1\rangle \\
&= [\Omega_Y^{-1}(g,hk) U_0^{g} \Omega_Y^{-1}(h,k) (U_0^{g})^{-1}] M_{32}^{k} U_0^{g} U_1^{h} U_2^{k}|\Omega;1\rangle \\
&= [\Omega_Y^{-1}(g,hk) U_0^{g} \Omega_Y^{-1}(h,k) (U_0^{g})^{-1}] U_0^{g} U_1^{h} U_3^{k}|\Omega;1\rangle \\
&= [\Omega_Y^{-1}(g,hk) U_1^{g} \Omega_Y^{-1}(h,k) (U_1^{g})^{-1}] U_0^{g} U_1^{h} U_3^{k}|\Omega;1\rangle
\end{aligned} \tag{4.112}$$

where the last line is obtained the fact that $\Omega_Y^{-1}(h,k)$ is supported near Y. To make contact with (4.96), notice that the inverse of the second equation in (4.96) with $I = [1, Y]$ gives the following operator identity:

$$\begin{aligned}
&\Omega_Y^{-1}(gh,k)\Omega_Y^{-1}(g,h) = \\
&\qquad \omega(g,h,k)\Omega_Y^{-1}(g,hk) U_1^{g} \Omega_Y^{-1}(h,k) (U_1^{g})^{-1}
\end{aligned} \tag{4.113}$$

Comparing this identity with the bracketed expressions in Eqs. 4.111 and 4.112, we conclude that

$$|1\rangle = \omega(g,h,k)|2\rangle \tag{4.114}$$

Hence,

$$F(g,h,k) = \langle 2|1\rangle = \omega(g,h,k), \tag{4.115}$$

as we wished to show.

4.6 Discrete antiunitary symmetries

So far we have focused on the case where the symmetry group G is *unitary*. In this section, we consider the more general case where G contains both unitary and antiunitary symmetry transformations.

4.6.1 Cohomology group

We start by reviewing the cohomology group $H^3(G, U_T(1))$. This group is important because it describes the output of our procedure in the general antiunitary case.

First, we explain the meaning of "$U_T(1)$." This symbol denotes the group $U(1)$ with a particular G-module structure, which is defined as follows: for any $g \in G$ and $\omega = e^{i\theta} \in U(1)$, the action of g on ω is given by

$$g\omega = \begin{cases} \omega^* & g \text{ antiunitary} \\ \omega & g \text{ unitary} \end{cases} \tag{4.116}$$

In other words, antiunitary symmetries act on $U(1)$ by complex conjugation, while unitary symmetries act trivially.

Just like the unitary case, the cohomology group $H^3(G, U_T(1))$ consists of equivalence classes of functions $\omega : G \times G \times G \to U(1)$ obeying a "cocycle" condition. However, the cocycle condition takes a modified form, namely

$$\frac{\omega(g,h,k)\omega(g,hk,l)[g\omega(h,k,l)]}{\omega(gh,k,l)\omega(g,h,kl)} = 1 \tag{4.117}$$

where $g\omega$ denotes the group action (4.116). The equivalence relation/coboundary transfor-

mation is also modified: we say that $\omega \sim \omega'$ if

$$\frac{\omega'(g,h,k)}{\omega(g,h,k)} = \frac{\nu(gh,k)\nu(g,h)}{\nu(g,hk)[g\nu(h,k)]} \tag{4.118}$$

where $\nu(g,h) \in U(1)$ and, again, $g\nu$ denotes the group action (4.116).

4.6.2 Outline of procedure

The procedure for computing anomalies in the general case is exactly the same as the unitary case. As before, the first step is to choose an (edge) Hamiltonian H that breaks the G-symmetry spontaneously and completely. This Hamiltonian H has $|G|$ ground states which we label by $|\Omega; g\rangle$. The next step is to define domain wall states $|g_x\rangle$, and corresponding domain wall movement and splitting operators, $M^g_{x'x}$ and $S(g,h)$. Again, we use exactly the same definitions as in Sec. 4.3.2.

The last step is to compute the F-symbol for the domain walls, $F(g,h,k)$. Again, we use the same definition as before, namely $F(g,h,k) = \langle 2|1\rangle$ where states $|1\rangle$ and $|2\rangle$ are defined as in Eq. 4.20.

The only new element in the antiunitary case involves the structure of the F-symbol. In particular, in the general antiunitary case, one can show that F obeys the *modified* cocycle condition (4.117), and is well-defined up to the *modified* coboundary transformation (5.155). As a result, F is naturally an element of the cohomology group $H^3(G, U_T(1))$. For a derivation of the modified cocycle condition, see Appendix 7.1; we discuss the modified coboundary transformation in the next subsection.

4.6.3 Checking the microscopic definition

In this section, we show that different choices of domain wall states or movement and splitting operators give the same F up to the coboundary transformation (5.155). This result, together

with the derivation of the cocycle condition discussed in Appendix 7.4, guarantees that our procedure produces a well-defined element of $H^3(G, U_T(1))$.

A key result which we will need in our derivation is the following identity, which generalizes Eq. 5.34. Let $\mathcal{O}$ be any operator that is invariant under all the symmetries and is supported near a domain wall g at point x. We claim that

$$\langle ..., g_x, ... | \mathcal{O} | ..., g_x, ... \rangle = g_L \langle g_x | \mathcal{O} | g_x \rangle \tag{4.119}$$

where g_L is the product of all domain walls to the left of x, and where the expression on the right hand side is defined by the group action (4.116). To derive this identity, note that

$$\begin{aligned} \langle ..., g_x, ... | \mathcal{O} | ..., g_x, ... \rangle &= \langle g_x; g_L | \mathcal{O} | g_x; g_L \rangle \\ &= \langle U^{g_L} g_x | \mathcal{O} | U^{g_L} g_x \rangle \\ &= g_L \langle g_x | \mathcal{O} | g_x \rangle \end{aligned} \tag{4.120}$$

Here, the first equality follows from (4.9), while the second equality follows from the definition, $|g_x; g_L\rangle = U^{g_L} |g_x\rangle$. The third equality follows from the fact that $\mathcal{O}$ commutes with U^{g_L} together with the defining property of unitary/anti-unitary operators, namely $\langle U^g v | U^g w \rangle = g \langle v | w \rangle$.

With Eq. (4.119) in hand, we are now ready to show that F is well-defined up to the coboundary transformation (5.155). To start, let us see how F transforms if we change the movement and splitting operators:

$$M^g_{x'x} \to M'^g_{x'x}, \qquad S(g,h) \to S'(g,h) \tag{4.121}$$

Similarly to the unitary case, the definition of movement and splitting operators implies that

$$\begin{aligned} M'^{g}_{x'x}|g_x\rangle &= e^{i\theta_{x'x}(g)} M^{g}_{x'x}|g_x\rangle \\ S'(g,h)|gh_1\rangle &= e^{i\phi(g,h)} S(g,h)|gh_1\rangle \end{aligned} \tag{4.122}$$

for some real valued $\theta_{x'x}(g)$ and $\phi(g,h)$. Likewise, for the multi-domain wall states,

$$M'^{g}_{x'x}|..., g_x, ...\rangle = \omega_1 \cdot M^{g}_{x'x}|..., g_x, ...\rangle \tag{4.123}$$

$$S'(g,h)|..., gh_1, ...\rangle = \omega_2 \cdot S(g,h)|..., gh_1, ...\rangle \tag{4.124}$$

for some $U(1)$ phases, ω_1, ω_2. To find the relation between ω_1, ω_2 and $e^{i\theta_{x'x}(g)}, e^{i\phi(g,h)}$, we multiply both sides of Eq. (5.162) by $\langle..., g_x, ...|(M^{g}_{x'x})^\dagger$, and then we apply (4.119) to derive

$$\begin{aligned} \omega_1 &= \langle..., g_x, ...|(M^{g}_{x'x})^\dagger M'^{g}_{x'x}|..., g_x, ...\rangle \\ &= g_{L,x}\langle g_x|(M^{g}_{x'x})^\dagger M'^{g}_{x'x}|g_x\rangle \\ &= g_{L,x} e^{i\theta_{x'x}(g)} \end{aligned} \tag{4.125}$$

where $g_{L,x}$ is the product of all domain walls to the left of x. By the same reasoning,

$$\omega_2 = g_{L,1} e^{i\phi(g,h)} \tag{4.126}$$

where $g_{L,1}$ is the product of all domain walls to the left of the point 1.

Substituting (5.164) and (5.165) into (5.162-5.163), we derive

$$\begin{aligned} M'^{g}_{x'x}|..., g_x, ...\rangle &= (g_{L,x} e^{i\theta_{x'x}(g)}) M^{g}_{x'x}|..., g_x, ...\rangle \\ S'(g,h)|..., gh_1, ...\rangle &= (g_{L,1} e^{i\phi(g,h)}) S(g,h)|..., gh_1, ...\rangle \end{aligned} \tag{4.127}$$

Next, plugging (5.166) into the definition of F (4.20-4.21), we obtain

$$F'(g,h,k) = F(g,h,k)\frac{e^{i\phi(g,h)}e^{i\phi(gh,k)}\left(ge^{i\theta_{12}(g)}\right)}{\left(ge^{i\phi(h,k)}\right)e^{i\phi(g,hk)}\left(ge^{i\theta_{12}(hk)}\right)} \tag{4.128}$$

Crucially, this transformation matches the modified coboundary transformation (5.155) with

$$\nu(g,h) = e^{i\phi(g,h)}\left(ge^{i\theta_{12}(h)}\right) \tag{4.129}$$

This is exactly what we want: different choices of movement and splitting operators lead to the same F, up to a modified coboundary transformation.

To complete the argument we also need to check that different choices of edge Hamiltonians and domain wall states lead to the same F, up to a coboundary transformation. Both properties follow by exactly the same reasoning as in the unitary case so we will not repeat it here.

4.6.4 Example: chiral boson edge theory for $\mathbb{Z}_2 \times \mathbb{Z}_2^T$ SPT phase

We now illustrate our general antiunitary procedure in an example. The example we consider is a continuum edge theory for a $\mathbb{Z}_2 \times \mathbb{Z}_2^T$ bosonic SPT phase, discussed in Ref. [94]. Here $\mathbb{Z}_2$ denotes a unitary symmetry and $\mathbb{Z}_2^T$ denotes an antiunitary symmetry.

Edge theory

Similarly to the example discussed in Sec. 4.4.2, the edge theory is a chiral boson theory with two fields θ, ϕ obeying the commutation relations

$$[\theta(x), \partial_y\phi(y)] = 2\pi i\delta(x-y)$$

with all other commutators vanishing. As in Sec. 4.4.2, the Hilbert space $\mathcal{H}$ is the usual infinite dimensional representation of the above algebra and the local operators in the edge theory are given by arbitrary derivatives and products of the elementary operators $\{e^{\pm i\theta}, e^{\pm i\phi}\}$.

In order to define the symmetry transformations, we first introduce some notation: we denote the elements of G by $\{1, s, t, st\}$, where s is the (unitary) generator of $\mathbb{Z}_2$ and t is the (antiunitary) generator of $\mathbb{Z}_2^T$. Likewise, we denote the $\mathbb{Z}_2 \times \mathbb{Z}_2^T$ symmetry transformations by $\{U^1, U^s, U^t, U^{st}\}$. It suffices to specify the action of the two generators U^s, U^t. These generators act on θ, ϕ as follows:

$$\begin{aligned} U^s\theta(U^s)^{-1} &= \theta \\ U^s\phi(U^s)^{-1} &= \phi - \pi \end{aligned} \tag{4.130}$$

and

$$\begin{aligned} U^t\theta(U^t)^{-1} &= \theta - \pi \\ U^t\phi(U^t)^{-1} &= -\phi \end{aligned} \tag{4.131}$$

(Here, U^s is unitary while U^t is antiunitary).

Calculating the anomaly

To calculate the anomaly we need to choose an edge Hamiltonian that breaks the symmetry completely. We will do this in a slightly roundabout way: we will first introduce some auxiliary degrees of freedom into our edge theory. We will then break the symmetry of this enlarged edge theory. This approach will simplify our calculation.

To begin, consider the following chiral boson theory described by two fields $\bar{\theta}, \bar{\phi}$ obeying

commutation relations

$$[\bar{\theta}(x), \partial_y \bar{\phi}(y)] = 2\pi i \delta(x-y)$$

with all other commutators vanishing. We assume that the symmetry acts on $\bar{\theta}, \bar{\phi}$ in the following way:

$$\begin{aligned} U^s \bar{\theta} (U^s)^{-1} &= \bar{\theta} \\ U^s \bar{\phi} (U^s)^{-1} &= \bar{\phi} - \pi \\ U^t \bar{\theta} (U^t)^{-1} &= \bar{\theta} \\ U^t \bar{\phi} (U^t)^{-1} &= -\bar{\phi} \end{aligned} \tag{4.132}$$

A crucial aspect of the $\bar{\theta}, \bar{\phi}$ chiral boson theory is that it is *not* anomalous – that is, it can be realized by a one dimensional lattice boson system with on-site $\mathbb{Z}_2 \times \mathbb{Z}_2^T$ symmetry. One way to see this is to note that the above chiral boson theory is the standard low energy description of the 1D XXZ spin chain model where the $\mathbb{Z}_2^T$ symmetry U^t is complex conjugation in the σ^z basis, and the $\mathbb{Z}_2$ symmetry U^s is the $\mathbb{Z}_2$ subgroup of the $U(1)$ symmetry of the XXZ model. Another way to see that the $\bar{\theta}, \bar{\phi}$ theory is not anomalous is to note that it can be gapped without breaking any the symmetries, for example by the Hamiltonian $H = H_{aux} - \int dx\ V \cos(\bar{\theta})$, where H_{aux} is defined below.

Now, since the $\bar{\theta}, \bar{\phi}$ theory is not anomalous, we can add it to our edge theory without changing anything. (Physically, this corresponds to attaching a strictly 1D wire onto the edge of the SPT phase of interest). After enlarging our edge theory in this way, we then choose an edge Hamiltonian that breaks the $\mathbb{Z}_2 \times \mathbb{Z}_2^T$ symmetry spontaneously and completely and

opens up a gap. A Hamiltonian that does the job is

$$H = H_0 + H_{aux} - \int dx\ V[\cos(2\theta) + \cos(2\bar{\phi})] \tag{4.133}$$

where H_0, H_{aux} are the usual free boson Hamiltonians,

$$H_0 = \int dx \frac{1}{4\pi}[v_\theta(\partial_x\theta)^2 + v_\phi(\partial_x\phi)^2]$$
$$H_{aux} = \int dx \frac{1}{4\pi}[v_{\bar{\theta}}(\partial_x\bar{\theta})^2 + v_{\bar{\phi}}(\partial_x\bar{\phi})^2]$$

for some velocities $v_\theta, v_\phi, v_{\bar{\theta}}, v_{\bar{\phi}} > 0$.

For V large and positive, the two cosine terms lock θ and $\bar{\phi}$ to one of two values $0, \pi$, spontaneously breaking the $\mathbb{Z}_2 \times \mathbb{Z}_2^T$ symmetry (4.130-4.132) and opening up an energy gap.

We can now see the advantage of introducing the auxiliary fields $\bar{\theta}, \bar{\phi}$: these fields allow us to break the symmetry *completely* in a simple way. If we dropped these fields, along with the corresponding cosine term, $\cos(2\bar{\phi}(x))$, then the first term $V\cos(2\theta(x))$ would only break the $\mathbb{Z}_2^T$ symmetry and would leave the $\mathbb{Z}_2$ symmetry intact. Of course, we could also break the symmetry completely without introducing $\bar{\theta}, \bar{\phi}$, e.g. with a Hamiltonian of the form $H = H_0 + \int dx V\cos(4\phi)$, but this leads to a more complicated calculation.

Turning back to the calculation, we now discuss the ground states of H. As in the example in Sec. 4.4.2, we will take the limit $V \to \infty$ for simplicity. In this limit, the four ground states of H are eigenstates of $e^{i\theta(x)}$ and $e^{i\bar{\phi}(x)}$ with eigenvalues ± 1. We define $|\Omega; 1\rangle$ to be the state with eigenvalues $+1$:

$$e^{i\theta(x)}|\Omega; 1\rangle = |\Omega; 1\rangle$$
$$e^{i\bar{\phi}(x)}|\Omega; 1\rangle = |\Omega; 1\rangle \tag{4.134}$$

We then define the other ground states by $|\Omega; g\rangle = U^g|\Omega; 1\rangle$, which corresponds to the

following eigenvalue assignments (given Eqs. 4.130-4.132):

$$e^{i\theta(x)}|\Omega;g\rangle = e^{i2\pi\lambda(g)}|\Omega;g\rangle$$
$$e^{i\bar{\phi}(x)}|\Omega;g\rangle = e^{i2\pi\mu(g)}|\Omega;g\rangle \tag{4.135}$$

where

$$\lambda(g) = \begin{cases} 0 & g = 1, s \\ 1/2 & g = t, st \end{cases} \tag{4.136}$$

and

$$\mu(g) = \begin{cases} 0 & g = 1, t \\ 1/2 & g = s, st \end{cases} \tag{4.137}$$

Next we define domain wall states $|g_x\rangle$ by:

$$|g_x\rangle = (a_x^g)^\dagger|\Omega;1\rangle \tag{4.138}$$

where the operators $(a_x^g)^\dagger$ are defined as

$$(a_x^g)^\dagger = e^{-i\int_x^\infty dy\ (\lambda(g)\partial_y\phi(y)+\mu(g)\partial_y\bar{\theta}(y))} \tag{4.139}$$

To see that $|g_x\rangle$ is a valid domain wall state, note that

$$e^{i\theta(x')}|g_x\rangle = \begin{cases} |g_x\rangle & x' < x \\ e^{i2\pi\lambda(g)}\ |g_x\rangle & x' > x \end{cases}$$

and

$$e^{i\bar{\phi}(x')}|g_x\rangle = \begin{cases} |g_x\rangle & x' < x \\ e^{i2\pi\mu(g)}\ |g_x\rangle & x' > x \end{cases}$$

by the commutation relations between θ, ϕ and $\bar{\theta}, \bar{\phi}$.

The next step is to define movement and splitting operators. We define the movement operator $M^g_{x'x}$, for $x' > x$, by

$$M^g_{x'x} = \sum_{k\in G} U^k X^g_{x'x} P^g_{x'} (U^k)^{-1}, \qquad x' > x \tag{4.140}$$

where

$$X^g_{x'x} = e^{i\int_x^{x'} dy\ (\lambda(g)\partial_y\phi(y) + \mu(g)\partial_y\bar{\theta}(y))} \tag{4.141}$$

and

$$P^g_{x'} = \frac{(1 + e^{i\theta(x')}e^{-i2\pi\lambda(g)})(1 + e^{i\bar{\phi}(x')}e^{-i2\pi\mu(g)})}{4} \tag{4.142}$$

Here $P^g_{x'}$ should be thought of as a local ground state projection operator, supported near x'. The defining property of this operator is that it leaves invariant the state $|\Omega; g\rangle$ and annihilates the other ground states: that is, $P^g_{x'}|\Omega; h\rangle = \delta_{gh}|\Omega; g\rangle$.

To see that $M^g_{x'x}$ is a valid movement operator, note that it is local and $\mathbb{Z}_2 \times \mathbb{Z}_2^T$ symmetric by construction. We can also see that it has the correct action on domain wall states:

$$M^g_{x'x}|g_x\rangle = X^g_{x'x}|g_x\rangle = |g_{x'}\rangle \tag{4.143}$$

Here, the first equality follows from the observation that only the $k = 1$ term in (4.140) gives

a nonzero result when acting on $|g_x\rangle$, while the second equality follows from the fact that $X^g_{x'x}(a^g_x)^\dagger = (a^g_{x'})^\dagger$.

Likewise, we define the reverse movement operator by

$$M^g_{xx'} = (M^g_{x'x})^\dagger, \qquad x' > x \tag{4.144}$$

Moving on to splitting operators, we define $S(g,h)$ by

$$S(g,h) = \sum_{k\in G} U^k U^g X^h_{21} (U^g)^{-1} C(g,h) P_2^{gh} (U^k)^{-1} \tag{4.145}$$

where

$$C(g,h) = e^{i[p(g,h)\phi(1) + q(g,h)\bar{\theta}(1)]} \tag{4.146}$$

and

$$\begin{aligned} p(g,h) &= \lambda(g) + \lambda(h) - \lambda(gh) \\ q(g,h) &= \mu(g) + \sigma(g)\mu(h) - \mu(gh) \end{aligned} \tag{4.147}$$

Here $\sigma(g) = \pm 1$ depending on whether g is unitary or antiunitary, i.e. $\sigma(g) = 1 - 4\lambda(g)$.

To see that $S(g,h)$ is a valid splitting operator, notice that it is local and $\mathbb{Z}_2 \times \mathbb{Z}_2^T$ symmetric by construction. We can also check that $S(g,h)$ has the correct action on domain walls:

$$\begin{aligned} S(g,h)|gh_1\rangle &= U^g X^h_{21} (U^g)^{-1} C(g,h) |gh_1\rangle \\ &\propto U^g (a^h_2)^\dagger (U^g)^{-1} (a^g_1)^\dagger |\Omega; 1\rangle \\ &\propto |g_1, h_2\rangle \end{aligned} \tag{4.148}$$

Here, the first equality follows from the fact that only the $k = 1$ term in (4.145) gives a nonzero result when acting on $|gh_1\rangle$, while the second equality follows from the definition of $(a_x^g)^\dagger$. The third equality follows by noting that $U^g(a_2^h)^\dagger(U^g)^{-1}(a_1^g)^\dagger|\Omega;1\rangle$ has the same local expectation values as $|g_1\rangle$ near $x = 1$, and the same local expectation values as $U^g|h_2\rangle$ near $x = 2$, and the same local expectation values as $U^g|\Omega;1\rangle$ between $x = 1$ and $x = 2$.

With these operators defined, we are ready to compute $F(g, h, k)$. From equation 4.20,

$$\begin{aligned}
|1\rangle &= [U^g X_{12}^h (U^g)^{-1}] \cdot X_{01}^g \cdot [U^g X_{21}^h (U^g)^{-1}] \\
&\quad \cdot C(g,h) \cdot [U^{gh} X_{32}^k X_{21}^k (U^{gh})^{-1}] \cdot C(gh,k)|ghk_1\rangle \\
|2\rangle &= [U^{gh} X_{32}^k X_{21}^k (U^{gh})^{-1}] \cdot [U^g C(h,k)(U^g)^{-1}] \\
&\quad \cdot [U^g X_{12}^{hk} (U^g)^{-1}] \cdot X_{01}^g \cdot [U^g X_{21}^{hk} (U^g)^{-1}] \\
&\quad \cdot C(g,hk)|ghk_1\rangle
\end{aligned} \tag{4.149}$$

In order to compare these two states, we note that all the operators in the above products commute with one another. Using this commutativity together with the identity $X_{xx'}^\alpha = (X_{x'x}^\alpha)^{-1}$, we can rewrite our states as:

$$\begin{aligned}
|1\rangle &= X_{01}^g U^{gh} X_{32}^k X_{21}^k (U^{gh})^{-1} \\
&\quad \cdot C(g,h)C(gh,k)|ghk_1\rangle \\
|2\rangle &= X_{01}^g U^{gh} X_{32}^k X_{21}^k (U^{gh})^{-1} \\
&\quad \cdot U^g C(h,k)(U^g)^{-1} C(g,hk)|ghk_1\rangle
\end{aligned} \tag{4.150}$$

Next, using the definition (4.146) and the symmetry action, one can check that

$$\begin{aligned}
&C(g,h)C(gh,k)|ghk_1\rangle = \\
&\quad e^{i2\pi\mu(g)p(h,k)} U^g C(h,k)(U^g)^{-1} C(g,hk)|ghk_1\rangle
\end{aligned} \tag{4.151}$$

We conclude that $|1\rangle = e^{i2\pi\mu(g)p(h,k)}|2\rangle$ so that

$$F(g,h,k) = \langle 2|1\rangle = e^{i2\pi\mu(g)p(h,k)} \tag{4.152}$$

Having computed F, the next question is to determine whether F is a trivial or nontrivial cocycle, i.e. a trivial or non-trivial element of $H^3(G, U_T(1))$. To answer this question, we compute the following two gauge invariant combinations of F:

$$\begin{aligned} F(s,s,s)F(s,1,s) &= 1 \\ \chi_s(t,t)\chi_s(1,t) &= -1 \end{aligned} \tag{4.153}$$

where

$$\chi_g(h,k) = \frac{F(g,h,k)F(h,k,g)}{F(h,g,k)} \tag{4.154}$$

Given that the second quantity is different from 1, it follows that F is a nontrivial cocycle. (Both quantities are 1 for a trivial cocycle). We conclude that our edge theory describes the boundary of one of the three nontrivial SPT phases within the $\mathcal{H}(\mathbb{Z}_2 \times \mathbb{Z}_2^T, U(1)_T) = \mathbb{Z}_2 \times \mathbb{Z}_2$ classification [28], which is consistent with the original analysis of Ref. [94].

4.7 Continuous symmetries

4.7.1 Outline of procedure

So far we have presented a procedure for computing anomalies for SPT edge theories with a discrete symmetry group G. We now discuss how to generalize this procedure to edge theories with *continuous* symmetries.

The main obstruction to applying our procedure in the continuous case has to do with the

definition of domain wall states. Recall that in the discrete case we construct domain walls as follows: first, we choose an (edge) Hamiltonian that breaks the symmetry spontaneously and completely and opens up an energy gap at the edge. Such a Hamiltonian has a collection of degenerate ground states, which we label by $|\Omega; g\rangle$. We then define domain wall excitations to be states that have the same local expectation values as one ground state, $|\Omega; g\rangle$, in some large interval, and the same local expectation values as another ground state $|\Omega; h\rangle$ in a neighboring large interval. The problem with applying this scheme to continuous symmetries is that it is impossible to both break a continuous symmetry *and* open up an energy gap: spontaneously breaking a continuous symmetry always leads to gapless Goldstone modes.

The key to overcoming this problem is to recognize that we don't actually need a Hamiltonian with spontaneous symmetry breaking and an energy gap: this symmetry-breaking Hamiltonian provides a nice physical context for thinking about domain wall states – our main objects of interest – but it isn't strictly necessary for our procedure. From an operational point of view, all that we need is a single (edge) state $|\Psi\rangle$ with two properties: (i) $|\Psi\rangle$ breaks the symmetry explicitly and completely – i.e. is not invariant under any of the symmetry transformations; and (ii) $|\Psi\rangle$ is the unique ground state of a gapped, local Hamiltonian. (The latter condition is important to guarantee that $|\Psi\rangle$ has various locality properties like short-range correlations). Once we have such a state, we denote it by $|\Psi\rangle \equiv |\Omega; 1\rangle$ and then define $|\Omega; g\rangle$ by

$$|\Omega; g\rangle = U^g |\Omega; 1\rangle \tag{4.155}$$

Having defined the $|\Omega; g\rangle$ states, we then define our domain wall states and calculate $F(g, h, k)$ exactly as before. This modified procedure works equally well for either continuous or discrete symmetry groups.

One subtlety that appears in the continuous symmetry case is that SPT phases with continuous symmetry groups are conjectured to be classified by the *Borel* cohomology group

$\mathcal{H}^3_{\mathcal{B}}(G, U_T(1))$ [28]. This means that if we want to interpret $F(g,h,k)$ as a label for a bulk SPT phase, we need to show that $F(g,h,k) \in \mathcal{H}^3_{\mathcal{B}}(G, U_T(1))$. This amounts to showing that (i) $F(g,h,k)$ is a Borel measurable 3-cocycle, and (ii) $F(g,h,k)$ is well-defined up to multiplication by the coboundary of a Borel measurable 2-cocycle. Neither of these properties are obvious from our definition of F. Indeed, if we do not impose any additional constraints on the splitting operators $S(g,h)$ and the movement operators $M^g_{x'x}$, then we can only show weaker versions of (i) and (ii) that do not include the Borel measurability constraints. In this paper, we will not attempt to fill in this gap, but we expect that both properties (i) and (ii) follow naturally if the splitting operators $S(g,h)$ and movement operators $M^g_{x'x}$ are chosen so that their dependence on $g, h \in G$ is not too discontinuous; for example, it may be enough to require that the matrix elements of $S(g,h)$ and $M^g_{x'x}$ are piecewise continuous as a function of g and h. We will see evidence for this conjecture in the next example: there we will see that a reasonable choice of splitting and movement operators leads to a Borel measurable $F(g,h,k)$.

4.7.2 Example: chiral boson edge theory for bosonic IQH phase

We now demonstrate our approach with an example: an edge theory for the bosonic integer quantum Hall state – a nontrivial bosonic SPT phase with $U(1)$ symmetry. This edge theory was introduced in Ref. [94].

Edge theory

Like the examples discussed in Sec. 4.4.2 and Sec. 4.6.4, the edge theory we consider is a chiral boson edge theory with two fields θ, ϕ obeying the commutation relations

$$[\theta(x), \partial_y \phi(y)] = 2\pi i \delta(x-y)$$

with all other commutators vanishing. As in the previous examples, the local operators in the edge theory are given by arbitrary products and derivatives of the elementary operators $\{e^{\pm i\theta}, e^{\pm i\phi}\}$ and the Hilbert space $\mathcal{H}$ is the usual infinite dimensional representation of the above algebra.

To complete the edge theory, we need to specify the $U(1)$ symmetry transformation. Denoting these transformations by U^α, where $\alpha \in [0, 2\pi)$, the symmetry action is given by:

$$\begin{aligned} U^\alpha \theta (U^\alpha)^{-1} &= \theta - \alpha \\ U^\alpha \phi (U^\alpha)^{-1} &= \phi - \alpha \end{aligned} \tag{4.156}$$

We note that this edge theory reduces to the one discussed in Sec. 4.4.2 if we restrict to the $\mathbb{Z}_2$ subgroup of $U(1)$.

Calculating the anomaly

The first step in calculating the anomaly is to choose a state $|\Psi\rangle \equiv |\Omega; 0\rangle$[6] that (i) breaks the $U(1)$ symmetry completely and (ii) is the unique ground state of a gapped local Hamiltonian. To this end, we define $|\Omega; 0\rangle$ to be the (unique) simultaneous eigenstate of the operators $e^{i\theta(x)}$ with eigenvalue 1:

$$e^{i\theta(x)} |\Omega; 0\rangle = |\Omega; 0\rangle \tag{4.157}$$

for all x. To see that $|\Omega; 0\rangle$ has the required properties, note that it breaks the $U(1)$ symmetry defined in (4.156), and furthermore it is the unique ground state of the (gapped) Hamiltonian $H_0 - \int dx\ V \cos(\theta)$ in the limit $V \to \infty$, where $H_0 = \int dx \frac{1}{4\pi}[v_\theta (\partial_x \theta)^2 + v_\phi (\partial_x \phi)^2]$.

After choosing $|\Omega; 0\rangle$, we then define the remaining vacuum states $|\Omega; \alpha\rangle$ to be symmetry

6. We denote the identity element by 0 since we are using additive notation.

partners of $|\Omega;0\rangle$.

$$|\Omega;\alpha\rangle = U^{\alpha}|\Omega;0\rangle \tag{4.158}$$

By construction $|\Omega;\alpha\rangle$ is a simultaneous eigenstate of $e^{i\theta(x)}$ with eigenvalue $e^{i\alpha}$:

$$e^{i\theta(x)}|\Omega;\alpha\rangle = e^{i\alpha}|\Omega;\alpha\rangle \tag{4.159}$$

The next step is to define domain wall states $|\alpha_x\rangle$ that spatially interpolate between the two states, $|\Omega;0\rangle$ and $|\Omega;\alpha\rangle$. We define

$$|\alpha_x\rangle = (a_x^{\alpha})^{\dagger}|\Omega;1\rangle \tag{4.160}$$

where $(a_x^{\alpha})^{\dagger}$ is defined by

$$(a_x^{\alpha})^{\dagger} = e^{-i\frac{\alpha}{2\pi}\int_x^{\infty} dy\ \partial_y\phi(y)} \tag{4.161}$$

We can see that $|\alpha_x\rangle$ is a valid domain wall state since

$$e^{i\theta(x')}|\alpha_x\rangle = \begin{cases} |\alpha_x\rangle & x' < x \\ e^{i\alpha}\ |\alpha_x\rangle & x' > x \end{cases}$$

by the commutation relations between θ and ϕ.

Next, we define movement and splitting operators for the above domain walls. We define the movement operator by

$$M_{x'x}^{\alpha} = e^{i\frac{\alpha}{2\pi}\int_x^{x'} dy\ \partial_y\phi(y)} \tag{4.162}$$

To see that this is a valid movement operator, note that $M^{\alpha}_{x'x}$ is local and $U(1)$ symmetric by construction. Also, $M^{\alpha}_{x'x}$ has the correct action on domain walls: $M^{\alpha}_{x'x}|\alpha_x\rangle \propto |\alpha_{x'}\rangle$ since $M^{\alpha}_{x'x}(a^{\alpha}_x)^\dagger \propto (a^{\alpha}_{x'})^\dagger$.

Moving on to splitting operators, we define $S(\alpha,\beta)$ by

$$\begin{aligned} S(\alpha,\beta) &= M^{\beta}_{21} C(\alpha,\beta) \\ &= e^{i\frac{\beta}{2\pi}\int_1^2 dy\ \partial_y\phi(y)} C(\alpha,\beta) \end{aligned} \tag{4.163}$$

where $C(\alpha,\beta)$ denotes the operator

$$C(\alpha,\beta) = e^{\frac{i}{2\pi}(\alpha+\beta-[\alpha+\beta])(\phi(1)-\theta(1^-))} \tag{4.164}$$

Here we use the symbol $[x]$ to denote the unique number in $[0,2\pi)$ that is equal to x modulo 2π. Also, the notation $\theta(1^-)$ is shorthand for $\theta(1-\epsilon)$ where ϵ is a small positive number. (It is important to carefully distinguish between $\theta(1^-)$ and $\theta(1^+)$ because we will be applying this operator to a domain wall state with a θ domain wall at $x=1$.)

To see that $S(\alpha,\beta)$ is a valid splitting operator, notice that it is local and $U(1)$ symmetric by construction. We can also see that $S(\alpha,\beta)$ has the correct action on domain walls:

$$\begin{aligned} S(\alpha,\beta)|[\alpha+\beta]_1\rangle &= M^{\beta}_{21} C(\alpha,\beta)|[\alpha+\beta]_1\rangle \\ &= M^{\beta}_{21} e^{\frac{i}{2\pi}(\alpha+\beta-[\alpha+\beta])\phi(1)}|[\alpha+\beta]_1\rangle \\ &\propto (a^{\beta}_2)^\dagger (a^{\alpha}_1)^\dagger |\Omega;1\rangle \\ &\propto |\alpha_1,\beta_2\rangle \end{aligned} \tag{4.165}$$

Here, the second equality follows from the fact that $e^{i\theta(1^-)}|[\alpha+\beta]_1\rangle = |[\alpha+\beta]_1\rangle$, while the third equality follows from the definition of $(a^{\alpha}_x)^\dagger$. The last equality follows from the fact that the state $(a^{\beta}_2)^\dagger(a^{\alpha}_1)^\dagger|\Omega;1\rangle$ has the same expectation values for local operators as

$|\alpha_1, \beta_2\rangle$.

With these operators defined, we are ready to compute $F(\alpha, \beta, \gamma)$. From equation 4.20,

$$\begin{aligned}
|1\rangle =& M_{12}^{\beta} M_{01}^{\alpha} M_{21}^{\beta} C(\alpha, \beta) M_{32}^{\gamma} M_{21}^{\gamma} \\
& \cdot C([\alpha+\beta], \gamma) |[\alpha+\beta+\gamma]_1\rangle \\
|2\rangle =& M_{32}^{\gamma} M_{21}^{\gamma} C(\beta, \gamma) M_{12}^{[\beta+\gamma]} M_{01}^{\alpha} M_{21}^{[\beta+\gamma]} \\
& \cdot C(\alpha, [\beta+\gamma]) |[\alpha+\beta+\gamma]_1\rangle
\end{aligned} \tag{4.166}$$

In order to compare these two states, we will reorder the operators with the following identities derived using the Baker-Campbell-Hausdorff formula:

$$\begin{aligned}
M_{x'x}^{\alpha} M_{y'y}^{\beta} &= M_{y'y}^{\beta} M_{x'x}^{\alpha} \\
C(\beta, \gamma) M_{x1}^{\alpha} &= e^{-\frac{i\alpha}{2\pi}(\beta+\gamma-[\beta+\gamma])\Theta(1-x)} M_{x1}^{\alpha} C(\beta, \gamma)
\end{aligned} \tag{4.167}$$

where $\Theta(x)$ denotes the Heaviside step function. With these formulas and the identity $M_{xx'}^{\alpha} = (M_{x'x}^{\alpha})^{-1}$, we can rewrite our states as:

$$\begin{aligned}
|1\rangle &= M_{01}^{\alpha} M_{32}^{\gamma} M_{21}^{\gamma} C(\alpha, \beta) C([\alpha+\beta], \gamma) |[\alpha+\beta+\gamma]_1\rangle \\
|2\rangle &= e^{i\Gamma} M_{01}^{\alpha} M_{32}^{\gamma} M_{21}^{\gamma} C(\beta, \gamma) C(\alpha, [\beta+\gamma]) |[\alpha+\beta+\gamma]_1\rangle
\end{aligned} \tag{4.168}$$

where $\Gamma = -\frac{\alpha}{2\pi}(\beta+\gamma-[\beta+\gamma])$.

Next, using the definition (4.164), it is easy to check that

$$C(\alpha, \beta) C([\alpha+\beta], \gamma) = C(\beta, \gamma) C(\alpha, [\beta+\gamma]) \tag{4.169}$$

Substituting this identity into the above expression for $|1\rangle, |2\rangle$, we see that $|2\rangle = e^{i\Gamma}|1\rangle$. We

conclude that

$$F(\alpha,\beta,\gamma) = \langle 2|1\rangle = e^{\frac{i\alpha}{2\pi}(\beta+\gamma-[\beta+\gamma])} \tag{4.170}$$

Note that F is a piecewise continuous function of α, β, γ and is therefore Borel measurable. This is consistent with our conjecture that F will always be Borel measurable for piecewise continuous movement and splitting operators.

Having computed F, the next question is to determine whether F is a trivial or non-trivial cocycle. To answer this question, we compute the following gauge invariant quantity:

$$F(\pi,\pi,\pi)F(\pi,0,\pi) = -1 \tag{4.171}$$

Since this quantity is different from 1, it follows that F is a non-trivial cocycle. We conclude that our edge theory describes the boundary of a nontrivial bosonic SPT phase with $U(1)$ symmetry. This is consistent with previous work [94].

4.8 Conclusion

In this paper, we have presented a general procedure for calculating anomalies in (1D) bosonic SPT edge theories. Our procedure takes as input a bosonic SPT edge theory and produces as output an element $\omega \in H^3(G, U_T(1))$ describing the anomaly carried by the edge theory. An important feature of our procedure is that, unlike previous approaches, it applies to general bosonic SPT edge theories with both unitary and antiunitary symmetries, with the only restriction being that the underlying 2D symmetry must be on-site.

One class of SPT edge theories that we cannot analyze with our current approach are those with spatial symmetries such as translation or reflection symmetries [128, 134]. The problem is that, for these types of edge theories, it is impossible to construct movement and splitting operators with the two requirements that they are are local in space and also

invariant under all the symmetries. A potential hint for how to overcome this problem, at least in some cases, is the observation [128] that SPT phases with point group symmetries are closely connected to SPT phases with on-site symmetries in fewer spatial dimensions. This suggests that our method might be suitable for studying boundary theories of higher dimensional (e.g. 3D) SPT phases with point group symmetries.

Our anomaly calculation always starts by choosing an edge Hamiltonian that opens up a gap and breaks the symmetry on the edge completely. However, in some edge theories, it is possible to open up a gap by only breaking *some* of the symmetries. (A famous example is the 2D topological insulator: in this case the edge can be gapped by breaking time-reversal symmetry while preserving $U(1)$ charge conservation symmetry). It would be interesting to develop methods for computing anomalies in this partial symmetry-breaking scenario. In this case, domain walls have more structure: they can carry quantum numbers under the symmetry, in addition to their fusion properties. We expect that the anomaly is encoded in this more complicated set of data. This problem may be related to the decorated domain wall construction of Ref. [31].

Another interesting direction for future work would be to generalize our approach to (1D) *fermionic* SPT edge theories. The fermionic case is especially intriguing given that there are 2D fermionic SPT phases that are beyond [35] the supercohomology classification scheme [47]. Despite the complexity of 2D fermionic SPT phases, we expect that our basic approach is still applicable: that is, given any fermionic SPT edge theory, we can determine the identity of the corresponding 2D SPT phase by breaking the symmetry and then extracting the fusion rules and F-symbol of the domain walls at the edge.

ACKNOWLEDGMENTS

We thank Colin Aitken for useful discussions. K.K. and M.L. acknowledge the support of the Kadanoff Center for Theoretical Physics at the University of Chicago. This work was supported in part by the Simons Collaboration on Ultra-Quantum Matter, which is a grant from the Simons Foundation (651440, ML).

CHAPTER 5

MICROSCOPIC DEFINITIONS OF FERMIONIC SPT DATA FROM BOUNDARY THEORIES

Kawagoe, K., Levin, M. (2022). "Microscopic definitions of fermionic SPT data from boundary theories." Manuscript to be submitted for publication.

Abstract

We describe a systematic procedure for determining the identity of a 2D fermionic symmetry protected topological (SPT) phase from the properties of its microscopic boundary theory. This will follow from the fact that fermionic SPTs are classified by supercohomology and each fermionic SPT can be identified by its supercohomology data. We will show that this data can be concretely defined on the boundary of fermionic SPTs. The basic idea behind our approach is to determine the fusion rules and F-symbol of the domain walls in a symmetry broken boundary theory; this information can then be mapped on to the supercohomology data. We demonstrate our approach with several fermionic SPT edge theories including a field theory for the topological insulator.

5.1 Introduction

Topological insulators are gapped quantum many-body systems which have short-range entangled ground states. Despite this short-range entanglement, they have long lived low energy edge modes which are protected by charge conservation and time reversal symmetries. These symmetry protected edge modes actually encode topological information about the bulk theory via the so-called "bulk-boundary correspondence." In particular, one can determine whether the bulk phase is a trivial insulator or a topological insulator based on whether there are an even or odd number of Kramers pairs of edge modes, respectively.

Symmetry protected topological phases (SPT phases) of matter are a natural generalization of topological insulators. A gapped quantum many-body system belongs to a nontrivial SPT phase if it has two properties: (i) the ground state is unique and short-range entangled[1]; and (ii) it is not possible to adiabatically connect the system to another system with a trivial (product-state) ground state without breaking one or more global symmetries [110, 40, 24, 120, 25, 28]. Instead of insisting on charge conservation and time reversal symmetries, SPTs generalize the topological insulators by allowing for a generic symmetry group. These theories also admit low energy edge modes which are protected under the symmetry. Therefore, it natural to ask if we can extend the bulk boundary correspondence seen in topological insulators to SPTs.

Just as the number of Kramers pairs of edge modes diagnose the topological properties of the bulk of topological insulators, similar formulas expressing bulk invariants in terms of boundary modes are known for other non-interacting fermionic SPTs [53, 114]. Additionally, recent work on bosonic SPTs have also generated formulas for deriving the bulk invariants from their boundary theories [26, 39, 70]. The interacting fermionic case, however, is less understood, especially in two and higher dimensions. By extending our previous work on bosonic SPTs, this paper seeks to address the interacting problem in the case of 2D fermionic SPT phases with on-site (i.e. non-spatial) symmetries. Concisely, we ask: how can one determine the identity of a 2D fermionic SPT phase from the 1D theory of its edge modes?

We can make this question more concrete by recalling the recent work on the conjectured classification of fermionic SPTs in (2+1)D [68, 35, 47, 32, 8, 1]. According to this classification, is a one-to-one correspondence between certain fermionic SPTs and the "supercohomology data" which is a pair of functions (ρ, ν)[2] which we will describe in the main

1. A state $|\Psi\rangle$ is "short-range entangled" if it can be transformed into a fermionic product state by local unitary transformation, i.e. a unitary of the form $U = \mathcal{T}\exp(-i\int_0^T H(t)dt)$ where H is a local Hermitian operator.

2. Some authors call this pair (n_2, ν_3).

text. The pair (ρ, ν) has the interpretation of describing the anomaly on the boundary theory of a fermionic SPT. In this paper, we will use the general idea that F-symbols of domain walls on the boundary contain bulk topological information to calculate the bulk data in fermionic SPTs.

In the case of bosonic SPTs, this task has been thoroughly addressed [129, 18, 135, 57, 91, 26, 39, 70]. Despite this work on bosonic SPTs and the vast literature on the bulk boundary correspondence in non-interacting fermionic SPTs, there is very little work showing how to extract bulk topological information from the boundary theories of interacting fermionic SPTs. In a paper by Else and Nayak [39], the authors showed how to extract the supercohomology data in the case of fermionic SPTs in (2+1)D with unitary symmetries which can be restricted to a patch on the boundary. This symmetry restriction method applies to any SPT edge theory whose symmetries are local unitary transformations, i.e. of the form $U = \mathcal{T}\exp(-i\int_0^T H(t)dt)$ for some local Hermitian operator H. However, a priori there could be edge theories where the symmetries cannot be restricted, or it may be difficult to write them explicitly. Additionally, there is no published work describing how to extract this data from boundary theories when there are antiunitary symmetries.

In this paper, we present an approach for computing anomalies in fermionic SPT edge theories. Unlike previous work, our approach applies to general fermionc SPT edge theories with both unitary and antiunitary symmetries. Our only restriction is that the underlying 2D symmetry must be on-site.

The basic idea behind our approach is simple. First, we choose an edge Hamiltonian that spontaneously[3] breaks all the symmetries, except for fermion parity symmetry, on the edge and opens up an energy gap. Such a Hamiltonian has a collection of degenerate ordered ground states related to one another by symmetry transformations. The elementary excitations are domain walls between the different ground states. These domain walls can

3. Alternatively, we can break the symmetry explicitly rather than spontaneously for continuous symmetries.

be fused together to form new domain walls, much like anyon excitations in 2D topological systems. One interesting feature of fermionic SPTs, as opposed to bosonic SPTs, is that the fusion rules of the domain walls, in general, differ from the group law of the symmetry group. We will use this group law to define ρ. The fusion rules also allow one to define an "F-symbol" that describes the phase difference associated with fusing domain walls in different orders. This domain wall F-symbol is related to the quantity ν. Some care is required to compute F, but we describe a concrete procedure for performing this computation using the formalism of Refs. [69, 70] and then introduce some further restrictions to relate it to ν. In this way, we provide rigorous and practical definitions for the pair (ρ, ν) in the edge theory, thereby identifying the bulk fermionic SPT from its boundary theory.

This paper is organized as follows. In Sec. 5.2 we explain the basic setup of our problem. Then, in Sec. 5.3, we present our anomaly computation procedure in the simplest case: SPT edge theories with discrete unitary symmetry groups. We illustrate our procedure with several (discrete unitary) examples in Sec. 5.4. In Sec. 5.5 we consider the general case of SPT edge theories with both unitary and antiunitary symmetries, and we show that the same procedure works in this case. We apply the formalism in that section to the topological insulator. Finally, we give our conclusions in Sec. 5.6. Technical details are discussed in the Appendix.

5.2 Setup

We begin by defining what we mean by an "edge theory", or more precisely, a fermionic SPT edge theory. At an intuitive level, a fermionic SPT edge theory is a collection of data that describes the low energy edge excitations of an SPT phase. More specifically, a fermionic SPT edge theory consists of three pieces of data:

1. A Hilbert space $\mathcal{H}$.

2. A complete list of "local operators" $\{\mathcal{O}\}$ acting in $\mathcal{H}$, including fermion parity odd operators.

3. A collection of (unitary or anti-unitary) symmetry transformations $\{U^g : g \in G_0\}$ acting on $\mathcal{H}$. Here G_0 denotes the quotient group, $G_0 = G/\mathbb{Z}_2^F$.

Each of these pieces of data has a simple physical interpretation: the Hilbert space $\mathcal{H}$ describes the subspace of low energy edge excitations; the list $\{\mathcal{O}\}$ describes the low energy projection of local operators in the original 2D system; and the $\{U^g\}$ operators describe how the edge excitations transform under the symmetry.

In order to qualify as a valid fermionic SPT edge theory, we require that the above data is physically *realizable* as the edge of some 2D SPT Hamiltonian with on-site symmetries. That is, we require the existence of a 2D Hamiltonian H_{2D} that belongs to an SPT phase with (on-site) symmetry group G and that has the following properties:

1. The Hilbert space $\mathcal{H}$ is isomorphic to the subspace of low energy edge excitations of H_{2D}.

2. The operators $\{\mathcal{O}\}$ correspond to local operators of the 2D system, projected into this low energy subspace.

3. The $\{U^g\}$ transformations describe how the low energy subspace transforms under the symmetries in G.

See Secs. 5.4,5.5.4 for examples of fermionic SPT edge theories. In general, fermionic SPT edge theories can be described using either continuum fields or lattice degrees of freedom and our results apply equally well to both cases.

With this background, we can now state our main result: We describe a systematic procedure that takes a fermionic SPT edge theory as input, and that outputs two pieces of data, ρ, ν (see Sec. for details). As explained in the introduction, the pair (ρ, ν) can be

interpreted as either a label for the bulk 2D SPT phase or a label for the *anomaly* carried by the SPT edge theory. Thus, depending on one's point of view, our procedure provides a systematic method for computing either the bulk 2D SPT phase or the anomaly associated with a given edge theory.

5.3 Discrete unitary symmetries

5.3.1 Outline of procedure

In this section, we outline our procedure in the case where the symmetry group G is discrete and unitary and where none of the domain walls carry Majorana modes.

Review of fermionic symmetry groups

We begin by reviewing the structure of the symmetry group G. This structure can be understood most easily by thinking about the quotient group $G_0 = G/\mathbb{Z}_2^F$, where $\mathbb{Z}_2^F$ denotes the fermion parity subgroup. Intuitively, G_0 describes all the symmetries except for fermion parity.

A key point is that the elements of G can be parameterized as ordered pairs $[g, s]$ where $g \in G_0$ and $s \in \mathbb{Z}_2 = \{0, 1\}$. Here $g \in G_0$ labels the cosets of $\mathbb{Z}_2^F$ within G, while $s = 0, 1$ labels the two elements within each coset. Note that there is some arbitrariness in this labeling scheme: for each coset $g\mathbb{Z}_2^F$, we have the freedom to pick either element of the coset and label it by $[g, 0]$.

Suppose we choose a labeling scheme of this kind. Then the group multiplication on G takes the form

$$[g, 0] \cdot [h, 0] = [gh, \lambda(g, h)] \tag{5.1}$$

for some function $\lambda : G_0 \times G_0 \to \mathbb{Z}_2 = \{0, 1\}$. Associativity of multiplication guarantees that λ obeys the condition

$$\lambda(g, h) + \lambda(gh, k) = \lambda(h, k) + \lambda(g, hk) \tag{5.2}$$

Thus, λ is a "2-cocycle."

So far we have shown that the symmetry group G defines a quotient group $G_0 = G/\mathbb{Z}_2^F$ and a 2-cocycle $\lambda : G_0 \times G_0 \to \mathbb{Z}_2$. The reverse is also true: the quotient group G_0, together with a 2-cocycle λ, completely determines the full symmetry group G. In this construction, the group multiplication law in G given by $[g, s][h, t] = [gh, \lambda(g, h) + s + t]$; the group G is said to be the "$\mathbb{Z}_2$ extension of G_0 determined by λ.

In this paper we will use the latter point of view in describing symmetry groups: we will describe the symmetry group G by specifying the quotient group $G_0 = G/\mathbb{Z}_2^F$ and the 2-cocycle λ. Likewise, we will describe the symmetry transformations on the edge theory by focusing on the subset of transformations corresponding to group elements of the form $[g, 0]$ (where $g \in G_0$). We will use the abbreviation

$$U^g \equiv U^{[g,0]}, \quad g \in G_0 \tag{5.3}$$

Note every symmetry transformation can be constructed out of the U^g's and F, where F denotes the fermion parity operator. Note also that the U^g's obey the algebra

$$U^g U^h = U^{gh} F^{\lambda(g,h)} \tag{5.4}$$

in view of (5.1).

A comment about our labeling conventions: we will find it convenient to fix a labeling

convention in which $[1,0]$ corresponds to the identity element in G, and therefore

$$U^1 \equiv U^{[1,0]} = \mathbb{I} \tag{5.5}$$

and

$$\lambda(1,g) = 0 \tag{5.6}$$

Review of supercohomology data

Next we review the definitions of the super cohomology data since this will describe the output of our procedure in the case of discrete unitary symmetries in the absence of Majorana degrees of freedom. The super cohomology data consists of a pair of functions $\rho : G_0 \times G_0 \to \mathbb{Z}_2 = \{0,1\}$ and $\nu : G_0 \times G_0 \times G_0 \to U(1)$. This pair of functions (ρ, ν) obeys certain constraints and is well-defined up to a certain equivalence relation. The constraints are

$$\rho(g,h) + \rho(gh,k) = \rho(h,k) + \rho(g,hk) \tag{5.7}$$

and

$$\frac{\nu(g,h,k)\nu(g,hk,l)\nu(h,k,l)}{\nu(gh,k,l)\nu(g,h,kl)} = (-1)^{(\rho(g,h)+\lambda(g,h))\rho(k,l)}. \tag{5.8}$$

The equivalence relation is defined as follows: $(\rho,\nu) \sim (\rho',\nu')$ if

$$\rho'(g,h) - \rho(g,h) = \mu(g) + \mu(h) - \mu(gh) + s\lambda(g,h) \tag{5.9}$$

and

$$\frac{\nu'(g,h,k)}{\nu(g,h,k)} = \frac{\alpha(gh,k)\alpha(g,h)}{\alpha(g,hk)\alpha(h,k)} \cdot (-1)^{(\rho(g,h)+\lambda(g,h))\mu(k)+\mu(g)(\rho(h,k)+(d\mu)(h,k))} \cdot (-1)^{s(\rho(gh,k)\lambda(g,h)+\rho(g,hk)\lambda(h,k))} \tag{5.10}$$

for some function $\mu : G_0 \to \mathbb{Z}_2$ and $\alpha : G_0 \times G_0 \to U(1)$, and $s \in \mathbb{Z}_2$. Here, $(d\mu)(h,k) = \mu(h) + \mu(k) - \mu(hk)$.

We will see that the output of our procedure is a pair of functions (ρ, ν), which obeys the constraints (5.7-5.8) and is uniquely defined up to the transformations (5.9-5.10); in this way our procedure naturally produces the supercohomology data.

Our procedure

With this background, we now move on to explain our procedure. The first step in our procedure is to choose an (edge) Hamiltonian H that acts within the Hilbert space $\mathcal{H}$. The Hamiltonian H can be arbitrary as long as it has three properties: (i) H is built out of the local (fermion parity even) operators $\{\mathcal{O}\}$ from Sec. 5.2; (ii) H has an energy gap; and (iii) H breaks the G_0-symmetry spontaneously and completely.[4]

An important aspect of the Hamiltonian H is that it has multiple degenerate ground states due to the spontaneously broken symmetry. More specifically, H has $|G_0|$ degenerate, short-range correlated ground states, which are permuted amongst themselves by the symmetry transformations. These ground states can be naturally labeled by group elements, $g \in G_0$. To do this, we pick one of the degenerate ground states and denote it by $|\Omega; 1\rangle$. We

4. Actually, such a Hamiltonian is not strictly necessary for our procedure: all that we really need is a single (edge) state $|\Psi\rangle$ that *explicitly* breaks all symmetries in G_0. See Sec. 5.5.4 for more details.

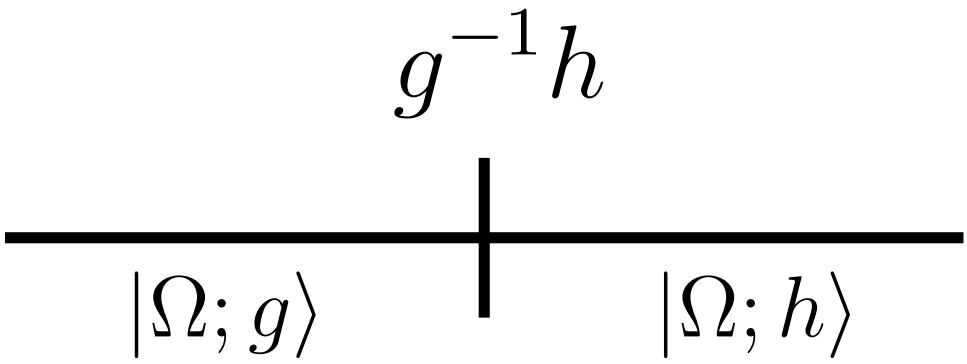

Figure 5.1: A domain wall excitation: a state that shares the same local expectation values as one ground state $|\Omega; g\rangle$ to the left of some point x, and another ground state $|\Omega; h\rangle$ to the right of x. We say that such a domain wall is $g^{-1}h$-type. This domain wall may be bare or decorated and denoted as $(g^{-1}h, 0)$ or $(g^{-1}h, 1)$, respectively.

then label the other states by $\{|\Omega; g\rangle\}$ with $g \in G_0$ where $|\Omega; g\rangle$ is defined by

$$|\Omega; g\rangle = U^g|\Omega; 1\rangle \tag{5.11}$$

By construction, $U^g|\Omega; h\rangle \propto |\Omega; gh\rangle$ (since the ground states have a definite fermion parity).

Having found the ground states of H, the next step in our procedure is to construct domain wall excitations. We give a precise definition of domain wall excitations in Sec. 5.3.2, but roughly speaking a domain wall excitation is a state in $\mathcal{H}$ that "looks like" one ground state $|\Omega; g\rangle$ to the left of some point x, and like another ground state $|\Omega; h\rangle$ to the right of x, and that interpolates between the two ground states in some arbitrary way in the vicinity of x (Fig. 5.1). Like the ground states, these domain wall excitations can be labeled by elements of G_0: in particular, we will label the above domain wall with the group element $g^{-1}h$. An important property of this labeling is that it is invariant under any global symmetry transformation U^k: under such a transformation, $|\Omega; g\rangle \to |\Omega; kg\rangle$ and $|\Omega; h\rangle \to |\Omega; kh\rangle$ so $g^{-1}h \to (kg)^{-1}(kh) = g^{-1}h$.

We now come to an important feature of fermionic SPT edge theories (in the absence of Majorana modes): for each group element $g \in G_0$ there are *two* topologically distinct species

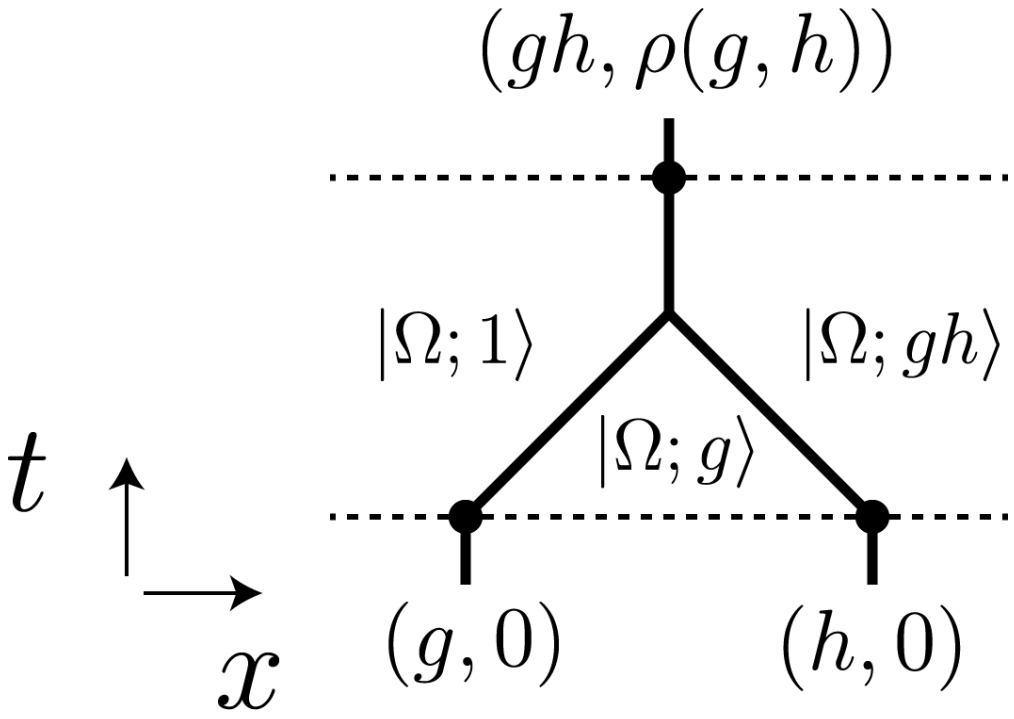

Figure 5.2: Spacetime diagram of fusion of a $(g,0)$ and $(h,0)$ domain wall into a $(gh,\rho(g,h))$ domain wall. The initial state consists of three different ground states $|\Omega;1\rangle, |\Omega;g\rangle, |\Omega;gh\rangle$ in three different regions, separated by domain walls $(g,0),(h,0)$. During the fusion process, the $|\Omega;g\rangle$ region disappears and we are left only with the $|\Omega;1\rangle, |\Omega;gh\rangle$ regions separated by a $(gh,\rho(g,h))$ domain wall. Reversing the arrow of time corresponds to a "splitting" operation.

of domain walls. These two domain wall species differ from one another by a local fermion – i.e. a local operator that carries odd fermion parity. We will label them by $(g,0)$ and $(g,1)$. Note that there is some arbitrariness in this labeling scheme: for each group element g, we are free to label either of the two domain walls by $(g,0)$ and the other by $(g,1)$. We denote the collection of domain walls by $D = \{(g,s)\}$.

At this point, we introduce an abbreviated notation which will be useful below: we use bold symbols like $\boldsymbol{a}$ to denote ordered pairs of the form $\boldsymbol{a} = (g,s)$, where $g \in G_0$ and $s \in \mathbb{Z}_2 = \{0,1\}$. With this notation, we can talk about domain walls $\boldsymbol{a}, \boldsymbol{b} \in D$, rather than $(g,s),(h,t)$, etc.

An important aspect of domain walls is that they can be combined them together in a

process called "fusion": if one has an $\boldsymbol{a}$ domain wall located nearby and to the left of a $\boldsymbol{b}$ domain wall, then one can convert this pair of domain walls into a single $\boldsymbol{c}$ domain wall by applying a local (fermion parity even) operator acting on both domain walls. We will denote these fusion rules by

$$\boldsymbol{a} \times \boldsymbol{b} = \boldsymbol{c} \quad \text{or} \quad \boldsymbol{ab} = \boldsymbol{c}. \tag{5.12}$$

These fusion rules have a G_0-graded structure: if $\boldsymbol{a}, \boldsymbol{b}$ are of type g, h then $\boldsymbol{c}$ is of type gh (Fig. 5.2). In particular, this means that the fusion rules take the form

$$(g, 0) \times (h, 0) = (gh, \rho(g, h)) \tag{5.13}$$

for some function $\rho : G_0 \times G_0 \to \mathbb{Z}_2 = \{0, 1\}$. More generally, the fusion rules are given by

$$(g, s) \times (h, t) = (gh, \rho(g, h) + s + t) \tag{5.14}$$

These fusion rules endow the set of domain walls D with a *group* structure. More specifically, the domain wall group D is a $\mathbb{Z}_2$ extension of G_0 – just like the symmetry group G.[5] The function ρ, defined in (5.13), is the first piece of super cohomology data. Thus, from an operational point of view, we can extract the first piece of super cohomology data by studying the fusion rules of the domain wall excitations.

To extract the second piece of cohomology data, ν, we need to consider the "F-symbol" for these excitations. The basic idea is to consider two different physical processes in which a domain wall of type $\boldsymbol{abc} \in D$ splits into three domain walls $\boldsymbol{a}, \boldsymbol{b}, \boldsymbol{c} \in D$ (Fig. 5.3). (Here, splitting is the opposite of fusion). In one process, $\boldsymbol{abc}$ splits into $\boldsymbol{ab}$ and $\boldsymbol{c}$, and then $\boldsymbol{ab}$ splits into $\boldsymbol{a}$ and $\boldsymbol{b}$; in the other process, $\boldsymbol{abc}$ splits into $\boldsymbol{a}$ and $\boldsymbol{bc}$ and then $\boldsymbol{bc}$ splits into

5. Though both groups are $\mathbb{Z}_2$ extensions, $D \neq G$ in general since $\rho \neq \lambda$.

$\boldsymbol{b}$ and $\boldsymbol{c}$. By construction, the final states $|1\rangle, |2\rangle$ produced by these processes contain the same domain walls, $\boldsymbol{a}, \boldsymbol{b}, \boldsymbol{c}$, at the same three positions. Therefore, the two final states $|1\rangle, |2\rangle$ must be the same up to a phase. The F-symbol, $F(\boldsymbol{a}, \boldsymbol{b}, \boldsymbol{c})$, is the phase difference between the two states:

$$|1\rangle = F(\boldsymbol{a}, \boldsymbol{b}, \boldsymbol{c})|2\rangle. \tag{5.15}$$

This F-symbol defines the second piece of super cohomology data:

$$\nu(g, h, k) \equiv F((g, 0), (h, 0), (k, 0)) \tag{5.16}$$

To complete this discussion, we need to explain why (ρ, ν) obey the constraints (5.7-5.8) and are well-defined up to the transformation (5.9-5.10). is a supercocycle. We begin with the constraint on ρ (5.7): this constraint follows immediately from the fact that the fusion product is associative. Next, consider the constraint on ν (5.8). This constraint comes from the fact that the F-symbol obeys the "pentagon identity":

$$F(\boldsymbol{a}, \boldsymbol{b}, \boldsymbol{c})F(\boldsymbol{a}, \boldsymbol{bc}, \boldsymbol{d})F(\boldsymbol{b}, \boldsymbol{c}, \boldsymbol{d}) = F(\boldsymbol{ab}, \boldsymbol{c}, \boldsymbol{d})F(\boldsymbol{a}, \boldsymbol{b}, \boldsymbol{cd}) \tag{5.17}$$

In addition, one can show that different F-symbols are related to one another via:

$$\begin{aligned} F((g, s), (h, t), (k, r)) = F((g, 0), (h, 0), (k, 0)) \\ \cdot (-1)^{(\rho(g,h)+\lambda(g,h))r} \end{aligned} \tag{5.18}$$

Combining (5.17) and (5.18) together with the fusion rules (5.14), it follows immediately that ν obeys the constraint (5.8).

Although understanding (5.18) will take more work, we can get an intuitive understanding of the pentagon identity immediately. Consider the 5 processes shown in Fig. 7.1. Notice

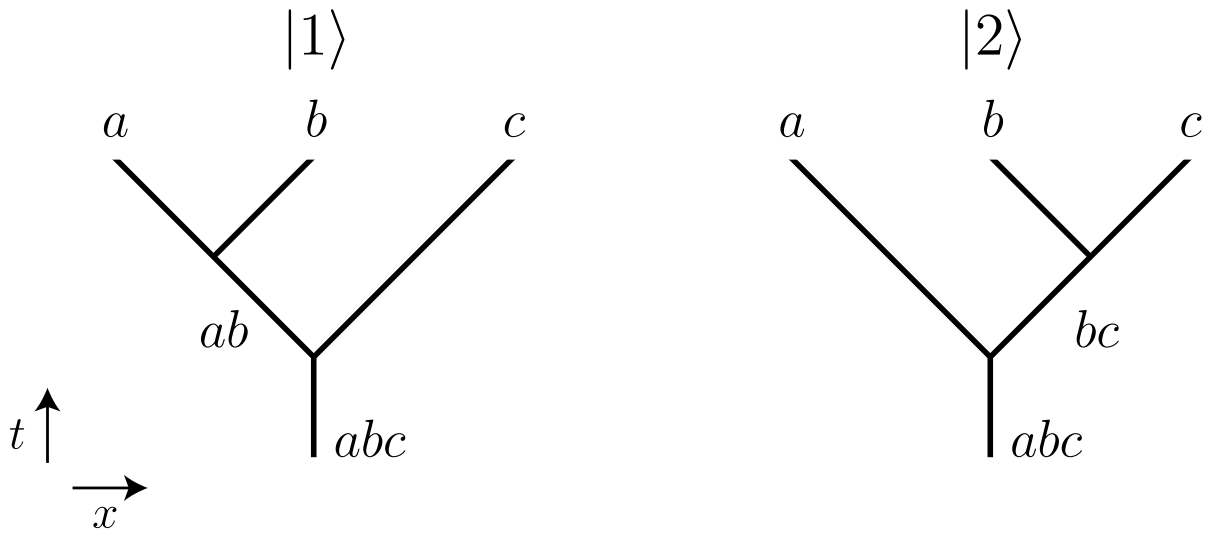

Figure 5.3: Spacetime diagrams for two processes in which a domain wall $\boldsymbol{abc}$ splits into domain walls $\boldsymbol{a}, \boldsymbol{b}, \boldsymbol{c}$. The final states, $|1\rangle, |2\rangle$, are equal up to the $U(1)$ phase, $F(\boldsymbol{a}, \boldsymbol{b}, \boldsymbol{c})$.

that the final states produced by these processes, namely $\{|1\rangle, ..., |5\rangle\}$, are all the same up to a phase. We can compute the phase difference between states $|1\rangle$ and $|5\rangle$ in two different ways. In the first way, we compute the relative phases between $(|1\rangle, |2\rangle)$, $(|2\rangle, |3\rangle)$, and $(|3\rangle, |5\rangle)$ using (5.15); in the second way, we compute the relative phases between $(|1\rangle, |4\rangle)$ and $(|4\rangle, |5\rangle)$. Demanding consistency between the two calculations gives the pentagon identity (5.17).

We now want to understand the ambiguity in ρ and ν. We begin with ρ. Recall that we made an arbitrary choice as to which domain wall to call $(g, 0)$ and $(g, 1)$. Suppose we rename the domain walls according to $(g, s) \to (g, s + \mu(g))$ where $\mu : G_0 \to \mathbb{Z}_2$. Then

$$\rho(g, h) \to \rho(g, h) + \mu(g) + \mu(h) - \mu(gh) \tag{5.19}$$

This explains the first term in (5.9). The second term in (5.9) takes more work but the basic picture is that it comes from stacking a 1D Kitaev chain onto the edge theory.

We now discuss the ambiguity in ν. To do so, we first consider the ambiguity in F.

Naively, one might expect that F has an ambiguity of the form

$$F(\boldsymbol{a},\boldsymbol{b},\boldsymbol{c}) \to F(\boldsymbol{a},\boldsymbol{b},\boldsymbol{c})\frac{\alpha(\boldsymbol{ab},\boldsymbol{c})\alpha(\boldsymbol{a},\boldsymbol{b})}{\alpha(\boldsymbol{a},\boldsymbol{bc})\alpha(\boldsymbol{b},\boldsymbol{c})} \tag{5.20}$$

where $\alpha : D \times D \to U(1)$. To understand where this ambiguity comes from, it is helpful to think about the physical processes in Fig. 5.3 as being implemented by a sequence of two "splitting operators" applied to an initial state with a $\boldsymbol{abc}$ domain wall. The key point is that the phases of these splitting operators are arbitrary. If we multiply the four splitting operators by four phases, $\nu(\boldsymbol{ab},\boldsymbol{c}), \nu(\boldsymbol{a},\boldsymbol{b}), \nu(\boldsymbol{a},\boldsymbol{bc}), \nu(\boldsymbol{b},\boldsymbol{c})$, this changes F by exactly the above transformation (5.20).

However, the ambiguity in F is not as severe as (5.20). The reason is that the $(g,0)$ and $(g,1)$ domain walls are related to one another by a local fermion operator; therefore we can also relate the splitting operators associated with $(g,0)$ and $(g,1)$ using local fermion operators. Consequently, we can choose splitting operators so that the phases of related splitting operators are locked together. This results in restricting the α transformation so that $\alpha((g,s),(h,t))$ depends only on g,h and is independent of s,t. Hence we can write $\alpha((g,s),(h,t)) \equiv \alpha(g,h)$. These "restricted gauge transformations" lead to an ambiguity in F of the form

$$\begin{aligned} F((g,s),(h,t),(k,r)) \to\ & F((g,s),(h,t),(k,r)) \\ & \cdot \frac{\alpha(gh,k)\alpha(g,h)}{\alpha(g,hk)\alpha(h,k)} \end{aligned} \tag{5.21}$$

In particular, if we specialize to the case $s = t = r = 0$, then the ambiguity is of the form

$$\begin{aligned} F((g,0),(h,0),(k,0)) \to\ & F((g,0),(h,0),(k,0)) \\ & \cdot \frac{\alpha(gh,k)\alpha(g,h)}{\alpha(g,hk)\alpha(h,k)} \end{aligned} \tag{5.22}$$

This ambiguity explains the first term in (5.10). To understand the second term, we need to consider the effect of relabeling domain walls, $(g, s) \to (g, s + \mu(g))$. Under this transformation, one can show that F changes as

$$\begin{aligned} &F((g,0),(h,0),(k,0)) \to F((g,0),(h,0),(k,0)) \\ &\cdot (-1)^{(\rho(g,h)+\lambda(g,h))\mu(k)+\mu(g)(\rho(h,k)+(d\mu)(h,k))} \end{aligned} \tag{5.23}$$

This explains the second term in (5.10).

5.3.2 Microscopic definition of domain walls

In this section, we give precise, operational definitions of domain wall states. We note that these definitions closely parallel the microscopic definition of the domain walls that was given in Ref. [70] in the context of bosonic SPTs.

To begin, let ℓ be a distance that is much greater than the correlation length ξ of the system. The length scale ℓ will play an important role in the following discussion. In particular, we will only consider states in which domain wall excitations are separated by distances of at least ℓ, and we will neglect finite size effects of order $e^{-\ell/\xi}$.

We define domain wall states as follows. For each point x on the edge, we choose a state that has the same expectation values as $|\Omega; 1\rangle$ for local operators $\{\mathcal{O}\}$ supported to the left of $x - \ell$ and the same expectation values as $|\Omega; g\rangle$ for $g \in G_0$ for local operators $\{\mathcal{O}\}$ to the right of $x + \ell$. We denote this state by $|(g, 0)_x\rangle$. In our language, the state $|(g, 0)_x\rangle$ describes a single domain wall of "type $(g, 0)$" at position x. We require that these domain wall states are constructed so that $|(g, 0)_x\rangle$ has the same fermion parity for every position x. More precisely, we require that for every x and x', there exists a fermion parity even operator supported in the neighborhood of the interval containing x and x' such that $|(g, 0)_x\rangle = \mathcal{O}|(g, 0)_{x'}\rangle$. Note that the definition of $|(g, 0)_x\rangle$ involves an arbitrary choice of a

state: we will show that our results do not depend on this choice.

So far we have defined the $(g, 0)$ domain wall states. We now define the $(g, 1)$ states. To this end, we choose, for each position x, a local unitary operator γ_x that is supported near the point x and has odd fermion parity. We then define the domain wall state $|(g, 1)_x\rangle$ by

$$|(g, 1)_x\rangle = \gamma_x |(g, 0)_x\rangle \tag{5.24}$$

Next, for each domain wall state $|\boldsymbol{a}_x\rangle$ with $\boldsymbol{a} = (g, s)$, we define a collection of symmetry partner states $|\boldsymbol{a}_x; h\rangle$, with $h \in G_0$, by

$$|\boldsymbol{a}_x; h\rangle \propto U^h |\boldsymbol{a}_x\rangle \tag{5.25}$$

By construction, $|\boldsymbol{a}_x; h\rangle$ has the same expectation values as $|\Omega; h\rangle$ for local operators supported to the left of $x - \ell$ and the same expectation values as $|\Omega; hg\rangle$ for local operators to the right of $x + \ell$.

We now introduce *multi*-domain wall states. Let $x_1 < x_2 < ... < x_n$ be well-separated (i.e. having a spacing of at least ℓ) and pick group elements $g^{(1)}, g^{(2)}, ..., g^{(n)} \in G_0$. We will use the notation $|(g^{(1)}, 0)_{x_1}, (g^{(2)}, 0)_{x_2}, ...\rangle$ to denote the multi-domain wall state that has a domain wall of type $(g^{(i)}, 0)$ at each location x_i and that has the same expectation values as $|\Omega; 1\rangle$ for local operators supported to the left of all the domain walls. More precisely, we define $|(g^{(1)}, 0)_{x_1}, (g^{(2)}, 0)_{x_2}, ...\rangle$ to be the unique state with the following two properties: first, for any local operator $\mathcal{O}$ supported near one domain wall x_i,

$$\begin{aligned} &\langle (g^{(1)}, 0)_{x_1}, (g^{(2)}, 0)_{x_2}, ... | \mathcal{O} | (g^{(1)}, 0)_{x_1}, (g^{(2)}, 0)_{x_2}, ... \rangle \\ &\qquad = \langle (g^{(i)}, 0)_{x_i}; g_L | \mathcal{O} | (g^{(i)}, 0)_{x_i}; g_L \rangle \end{aligned} \tag{5.26}$$

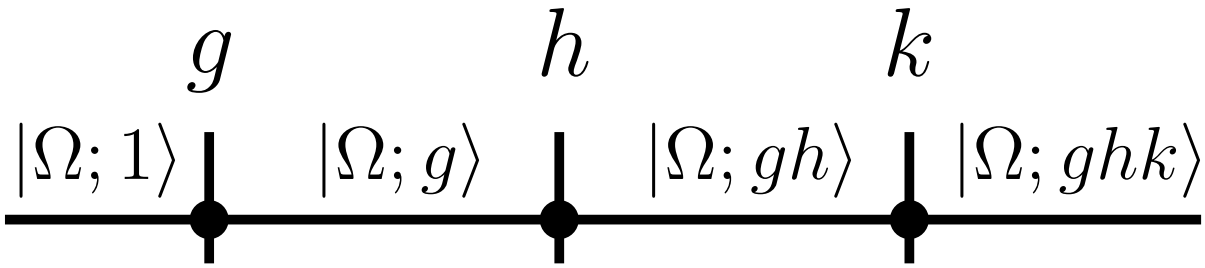

Figure 5.4: A multi-domain wall state consisting of a g-type, h-type, and k-type domain wall. The domain walls separate four regions which share the same local expectation values as the four ground states $|\Omega; 1\rangle, |\Omega; g\rangle, |\Omega; gh\rangle, |\Omega; ghk\rangle$.

where g_L is the product

$$g_L = g^{(1)} \cdots g^{(i-1)} \tag{5.27}$$

Second, for any operator $\mathcal{O}$ supported away from the domain walls,

$$\begin{aligned} &\langle (g^{(1)}, 0)_{x_1}, (g^{(2)}, 0)_{x_2}, ... | \mathcal{O} | (g^{(1)}, 0)_{x_1}, (g^{(2)}, 0)_{x_2}, ... \rangle \\ &\qquad = \langle \Omega; g_L | \mathcal{O} | \Omega; g_L \rangle \end{aligned} \tag{5.28}$$

where g_L is again the product of the $g^{(j)}$'s to the left of $\mathcal{O}$. These two properties imply that multi-domain wall states have a structure like that in Fig. 5.4.

We now define general multi-domain wall states (as opposed to the "bare" multi-domain wall states defined above) as follows: Again, let $x_1 < x_2 < ... < x_n$ be well-separated points and pick group elements $g^{(1)}, g^{(2)}, ..., g^{(n)} \in G_0$. This time, we will also choose $s^{(1)}, s^{(2)}, ..., s^{(n)} \in \{0, 1\}$. We define the general multi-domain wall state $|(g^{(1)}, s^{(1)})_{x_1}, (g^{(2)}, s^{(2)})_{x_2}, ...\rangle$

by

$$|(g^{(1)}, s^{(1)})_{x_1},(g^{(2)}, s^{(2)})_{x_2}, ...\rangle = \prod_i \left({}^{g_L^{(i)}}\gamma_{x_i} \right)^{s^{(i)}} |(g^{(1)}, 0)_{x_1}, (g^{(2)}, 0)_{x_2}, ...\rangle \tag{5.29}$$

where

$${}^{h}\gamma_x = U^h \gamma_x \left(U^h\right)^{-1}, \tag{5.30}$$

and

$$g_L^{(i)} = g^{(1)} \cdots g^{(i-1)}. \tag{5.31}$$

Importantly, the above definition ensures that the general multi-domain wall states have the same structure as the bare multi-domain wall states. Let $\boldsymbol{a}^{(i)} = (g^{(i)}, s^{(i)})$. Then $|\boldsymbol{a}^{(1)}_{x_1}, \boldsymbol{a}^{(2)}_{x_2}, ...\rangle$ is the unique state with the following two properties: first, for any local operator $\mathcal{O}$ supported near one domain wall x_i,

$$\langle \boldsymbol{a}^{(1)}_{x_1}, \boldsymbol{a}^{(2)}_{x_2}, ...|\mathcal{O}|\boldsymbol{a}^{(1)}_{x_1}, \boldsymbol{a}^{(2)}_{x_2}, ...\rangle = \langle \boldsymbol{a}^{(i)}_{x_i}; g_L|\mathcal{O}|\boldsymbol{a}^{(i)}_{x_i}; g_L\rangle \tag{5.32}$$

where g_L is the product of the G_0 component of all domain walls to the left of $\mathcal{O}$ (5.27). Second, for any operator $\mathcal{O}$ supported away from the domain walls,

$$\langle \boldsymbol{a}^{(1)}_{x_1}, \boldsymbol{a}^{(2)}_{x_2}, ...|\mathcal{O}|\boldsymbol{a}^{(1)}_{x_1}, \boldsymbol{a}^{(2)}_{x_2}, ...\rangle = \langle \Omega; g_L|\mathcal{O}|\Omega; g_L\rangle \tag{5.33}$$

where g_L is again the product of the G_0 component of domain wall types to the left of $\mathcal{O}$. We prove this statement in Appendix 7.6.

An important corollary of Eq. 5.32, which we will need below, is that for any operator $\mathcal{O}$

that is supported near a domain wall $\boldsymbol{a}$ at point x and is invariant under all the symmetries (i.e. $U^h\mathcal{O}(U^h)^{-1} = \mathcal{O}$), the following identity holds:

$$\langle ..., \boldsymbol{a}_x, ...|\mathcal{O}|..., \boldsymbol{a}_x, ...\rangle = \langle \boldsymbol{a}_x|\mathcal{O}|\boldsymbol{a}_x\rangle \tag{5.34}$$

5.3.3 Microscopic definition of domain wall F-symbol

In this section, we give a precise definition of the F-symbol for domain walls. The first step is to define *movement* operators for domain walls. Given any domain wall type $\boldsymbol{a} \in D$, and any pair of points, x, x', we say that $M^{\boldsymbol{a}}_{x'x}$ is a movement operator if it satisfies three conditions: (i) $M^{\boldsymbol{a}}_{x'x}$ obeys

$$M^{\boldsymbol{a}}_{x'x}|\boldsymbol{a}_x\rangle \propto |\boldsymbol{a}_{x'}\rangle \tag{5.35}$$

where the proportionality constant is a $U(1)$ phase; (ii) $M^{\boldsymbol{a}}_{x'x}$ is invariant under all the symmetries, i.e.

$$U^h M^{\boldsymbol{a}}_{x'x}(U^h)^{-1} = M^{\boldsymbol{a}}_{x'x} \tag{5.36}$$

and (iii) $M^{\boldsymbol{a}}_{x'x}$ is *local* in the sense that it is supported in the neighborhood of the interval containing x, x' and has even fermion parity.

Here, the symmetry condition (5.36) is important because it guarantees that the analog of Eq. 5.35 holds for any (single) domain wall state $|\boldsymbol{a}_x; h\rangle$:

$$M^{\boldsymbol{a}}_{x'x}|\boldsymbol{a}_x; h\rangle \propto |\boldsymbol{a}_{x'}; h\rangle \tag{5.37}$$

Likewise, the locality condition is important because it guarantees that the analog of Eq. 5.35 holds for any multi-domain wall state of the form $|..., \boldsymbol{a}_x, ...\rangle$: that is,

$$M^{\boldsymbol{a}}_{x'x}|..., \boldsymbol{a}_x, ...\rangle \propto |..., \boldsymbol{a}_{x'}, ...\rangle \tag{5.38}$$

as long as the other domain walls in $|..., \boldsymbol{a}_x, ...\rangle$ are well-separated from the interval containing x and x'. Again the constant of proportionality is a $U(1)$ phase.

To derive Eq. 5.38 from Eq. 5.35, consider the expectation value of any local operator, $\mathcal{O}$, supported in the neighborhood of $[x, x']$ (or $[x', x]$ if $x' < x$), in the two states $|..., \boldsymbol{a}_{x'}, ...\rangle$ and $M^{\boldsymbol{a}}_{x'x}|..., \boldsymbol{a}_x, ...\rangle$. Using (5.32) and (5.37), we can see that $\mathcal{O}$ has the same expectation value in the two states, $|..., \boldsymbol{a}_{x'}, ...\rangle$ and $M^{\boldsymbol{a}}_{x'x}|..., \boldsymbol{a}_x, ...\rangle$:

$$\begin{aligned}\langle ..., \boldsymbol{a}_{x'}, ...|\mathcal{O}|..., \boldsymbol{a}_{x'}, ...\rangle &= \langle \boldsymbol{a}_{x'}; g_L|\mathcal{O}|\boldsymbol{a}_{x'}; g_L\rangle \\ &= \langle \boldsymbol{a}_x; g_L|(M^{\boldsymbol{a}}_{x'x})^\dagger \mathcal{O} M^{\boldsymbol{a}}_{x'x}|\boldsymbol{a}_x; g_L\rangle \\ &= \langle ..., \boldsymbol{a}_x, ...|(M^{\boldsymbol{a}}_{x'x})^\dagger \mathcal{O} M^{\boldsymbol{a}}_{x'x}|..., \boldsymbol{a}_x, ...\rangle \end{aligned} \tag{5.39}$$

The two states, $|..., \boldsymbol{a}_{x'}, ...\rangle$ and $M^{\boldsymbol{a}}_{x'x}|..., \boldsymbol{a}_x, ...\rangle$ also share the same expectation values for local operators supported away from the interval $[x, x']$ (or $[x', x]$) by virtue of the short ranged correlations of these states. Therefore, by the uniqueness property of our domain wall states, we obtain Eq. 5.38.

In addition to the movement operators, we also define *splitting* operators for our domain walls. Fix two well-separated points on the line, which we will call '1' and '2'. For any pair of domain walls $\boldsymbol{a}, \boldsymbol{b} \in D$, we say that $S(\boldsymbol{a}, \boldsymbol{b})$ is a splitting operator if it satisfies three conditions: (i) $S(\boldsymbol{a}, \boldsymbol{b})$ satisfies

$$S(\boldsymbol{a}, \boldsymbol{b})|\boldsymbol{a}\boldsymbol{b}_1\rangle \propto |\boldsymbol{a}_1, \boldsymbol{b}_2\rangle \tag{5.40}$$

where the proportionality constant is a $U(1)$ phase; (ii) $S(\boldsymbol{a}, \boldsymbol{b})$ is invariant under all the symmetries U^g; (iii) $S(\boldsymbol{a}, \boldsymbol{b})$ is supported in the neighborhood of the interval $[1, 2]$ and has even fermion parity.

Just as before, it can be shown that these conditions guarantee that the splitting operators can be applied to any multi-domain wall state of the form $|..., \boldsymbol{a}\boldsymbol{b}_1, ...\rangle$ provided that the other

domain walls are located far from the interval $[1, 2]$:

$$S(\boldsymbol{a}, \boldsymbol{b})|..., \boldsymbol{a}\boldsymbol{b}_1, ...\rangle \propto |..., \boldsymbol{a}_1, \boldsymbol{b}_2, ...\rangle \tag{5.41}$$

where the proportionality constant is a $U(1)$ phase. Note that, unlike the movement operators, we only define splitting operators that act on a *single* interval $[1, 2]$ on the x-axis.

The last step is to restrict the phases of the movement and splitting operators in a canonical way. Let $\boldsymbol{a}$ be a type-g domain wall (i.e. $\boldsymbol{a} = (g, s)$ for some s). First, notice that it follows immediately from our definitions that

$$M^{\boldsymbol{a}}_{x'x}|\boldsymbol{a}_x\rangle \propto \gamma_{x'}^{\sigma(\boldsymbol{a})} \widetilde{M}^g_{x'x} \gamma_x^{-\sigma(\boldsymbol{a})} |\boldsymbol{a}_x\rangle \tag{5.42}$$

where

$$\widetilde{M}^g_{x'x} = M^{(g,0)}_{x'x} \tag{5.43}$$

and where we define $\sigma : D \to \mathbb{Z}_2 = \{0, 1\}$ by

$$\sigma(\boldsymbol{a}) = s \quad \text{for } \boldsymbol{a} = (g, s) \tag{5.44}$$

Since we are free to adjust the phase of the movement operator, we require that this proportionality is an equality. That is, we require that

$$M^{\boldsymbol{a}}_{x'x}|\boldsymbol{a}_x\rangle = \gamma_{x'}^{\sigma(\boldsymbol{a})} \widetilde{M}^g_{x'x} \gamma_x^{-\sigma(\boldsymbol{a})} |\boldsymbol{a}_x\rangle \tag{5.45}$$

We may impose a similar constraint on the splitting operators. Let $\boldsymbol{a}, \boldsymbol{b}$ be type-g and

type-h domain walls respectively. We know that

$$S(\boldsymbol{a},\boldsymbol{b})|\boldsymbol{a}\boldsymbol{b}_1\rangle \propto \gamma_1^{\sigma(\boldsymbol{a})}({}^g\gamma_2)^{\sigma(\boldsymbol{b})}\widetilde{S}(g,h)\gamma_1^{-\sigma(\boldsymbol{a}\boldsymbol{b})}|\boldsymbol{a}\boldsymbol{b}_1\rangle \tag{5.46}$$

where

$$\widetilde{S}(g,h) = S((g,0),(h,0))\gamma_1^{\rho(g,h)} \tag{5.47}$$

and where ${}^g\gamma_x$ is defined as in (5.30). Again, by adjusting the phase of the splitting operators, we can require this proportionality to be an equality:

$$S(\boldsymbol{a},\boldsymbol{b})|\boldsymbol{a}\boldsymbol{b}_1\rangle = \gamma_1^{\sigma(\boldsymbol{a})}({}^g\gamma_2)^{\sigma(\boldsymbol{b})}\widetilde{S}(g,h)\gamma_1^{-\sigma(\boldsymbol{a}\boldsymbol{b})}|\boldsymbol{a}\boldsymbol{b}_1\rangle \tag{5.48}$$

We will refer to $\widetilde{M}^g_{x'x}$ and $\widetilde{S}(g,h)$ as "bare" movement and splitting operators. We use this terminology because we can construct the usual movement and splitting operators $M^{\boldsymbol{a}}_{x'x}, S(\boldsymbol{a},\boldsymbol{b})$ by multiplying (or "dressing") the bare operators $\widetilde{M}^g_{x'x}, \widetilde{S}(g,h)$ by appropriate fermion operators γ_x (see Eqs. 5.45, 5.48 above).

With this setup, we are now ready to define the F-symbol. The first step is to fix some choice of domain wall states, $|\boldsymbol{a}_x\rangle$, and some choice of movement and splitting operators, $M^{\boldsymbol{a}}_{x'x}, S(\boldsymbol{a},\boldsymbol{b})$. Next, consider the initial state $|\boldsymbol{a}\boldsymbol{b}\boldsymbol{c}_1\rangle$, i.e. the state with a single domain wall $\boldsymbol{abc}$ at position 1. We then apply two different sequences of movement and splitting operators to $|\boldsymbol{a}\boldsymbol{b}\boldsymbol{c}_1\rangle$, denoting the final states by $|1\rangle$ and $|2\rangle$:

$$\begin{aligned}
|1\rangle &= M^{\boldsymbol{b}}_{12}M^{\boldsymbol{a}}_{01}S(\boldsymbol{a},\boldsymbol{b})M^{\boldsymbol{c}}_{32}S(\boldsymbol{a}\boldsymbol{b},\boldsymbol{c})|\boldsymbol{a}\boldsymbol{b}\boldsymbol{c}_1\rangle \\
|2\rangle &= M^{\boldsymbol{c}}_{32}S(\boldsymbol{b},\boldsymbol{c})M^{\boldsymbol{b}\boldsymbol{c}}_{12}M^{\boldsymbol{a}}_{01}S(\boldsymbol{a},\boldsymbol{b}\boldsymbol{c})|\boldsymbol{a}\boldsymbol{b}\boldsymbol{c}_1\rangle
\end{aligned} \tag{5.49}$$

These two processes are shown in Fig. 5.5. By construction, the final states $|1\rangle, |2\rangle$ produced by these processes both contain domain walls $\boldsymbol{a},\boldsymbol{b},\boldsymbol{c}$ at positions $0,1,3$, respectively. In

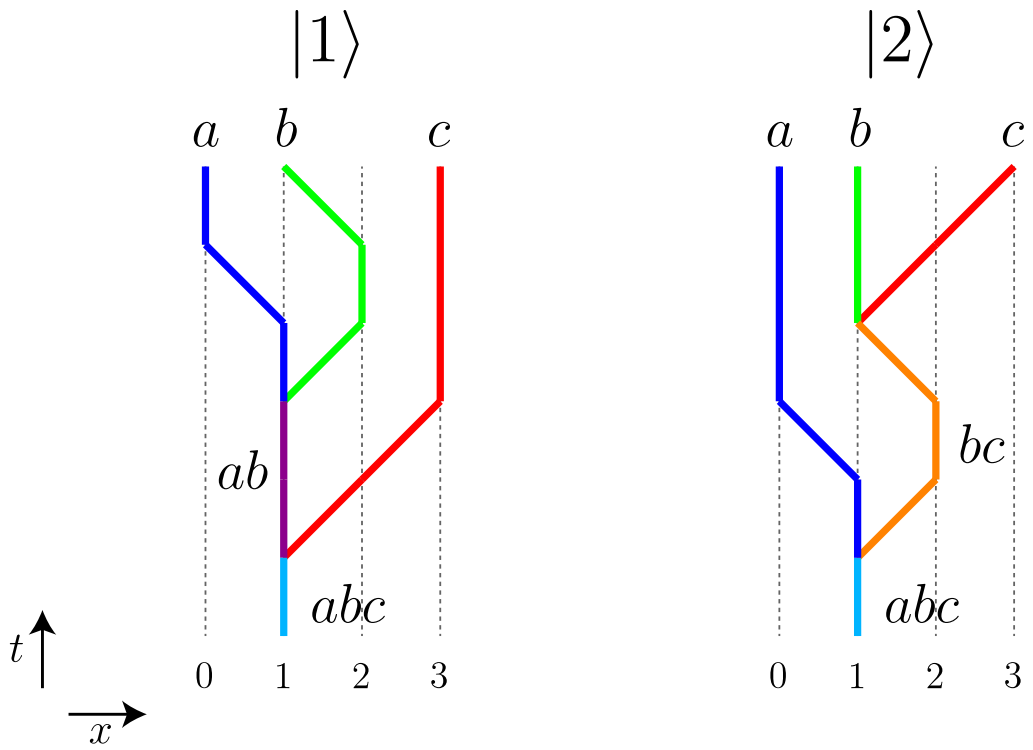

Figure 5.5: The two processes that are compared in the microscopic definition of the domain wall F-symbol. Starting from an initial state $|\boldsymbol{abc}_1\rangle$, movement and splitting operators are applied sequentially to obtain final states $|1\rangle$ and $|2\rangle$ on the left and right, respectively. States $|1\rangle, |2\rangle$ are both proportional to $|\boldsymbol{a}_0, \boldsymbol{b}_1, \boldsymbol{c}_3\rangle$. The x-axis is the position on the edge and the t-axis shows operator ordering.

particular, this means that $|1\rangle, |2\rangle$ are the same up to a phase. We define the F-symbol, $F(\boldsymbol{a}, \boldsymbol{b}, \boldsymbol{c})$, to be this phase difference:

$$F(\boldsymbol{a}, \boldsymbol{b}, \boldsymbol{c}) = \langle 2|1\rangle \tag{5.50}$$

5.3.4 The bare F-symbol and its relation to the usual F-symbol

In this section, we define a function $\widetilde{F} : G_0 \times G_0 \times G_0 \to U(1)$ which we call the "bare" F-symbol. We show that $\widetilde{F}$ is closely related to the standard F-symbol F, and that it is a useful tool for computing ν efficiently.

Let $g, h, k \in G_0$. To define $\widetilde{F}(g,h,k)$, consider the domain wall state $|(ghk,0)_1\rangle$ – that is, the state with a single domain wall $(ghk,0)$ at position 1. Starting from this initial state, we construct two states $|\widetilde{1}\rangle, |\widetilde{2}\rangle$ by applying two different sequences of *bare* movement and splitting operators, similarly to (5.49):

$$\begin{aligned} |\widetilde{1}\rangle &= \widetilde{M}^h_{12}\widetilde{M}^g_{01}\widetilde{S}(g,h)\widetilde{M}^k_{32}\widetilde{S}(gh,k)|(ghk,0)_1\rangle \\ |\widetilde{2}\rangle &= \widetilde{M}^k_{32}[{}^g\widetilde{S}(h,k)]\widetilde{M}^{hk}_{12}\widetilde{M}^g_{01}\widetilde{S}(g,hk)|(ghk,0)_1\rangle \end{aligned} \tag{5.51}$$

Here ${}^g\widetilde{S}(h,k)$ is defined by

$${}^g\widetilde{S}(h,k) = U^g\widetilde{S}(g,h)(U^g)^{-1} \tag{5.52}$$

We then define

$$\widetilde{F}(g,h,k) = \langle\widetilde{2}|\widetilde{1}\rangle \tag{5.53}$$

Our main result is that F is related to $\widetilde{F}$ via

$$F((g,s),(h,t),(k,r)) = (-1)^{(\rho(g,h)+\lambda(g,h))r}\widetilde{F}(g,h,k) \tag{5.54}$$

To understand the implications of this equation, note that in the special case where $s = t = r = 0$ it reduces to

$$F((g,0),(h,0),(k,0)) = \widetilde{F}(g,h,k) \tag{5.55}$$

It follows that we can compute ν directly from $\widetilde{F}$:

$$\nu(g,h,k) = \widetilde{F}(g,h,k) \tag{5.56}$$

This method for computing ν is more efficient than computing $F((g,0),(h,0),(k,0))$ since the definition of $\widetilde{F}$ involves fewer movement and splitting operators. We will use this method in all of the examples in Sec. 5.4.

Another important consequence of (5.54) is that

$$\begin{aligned} F((g,s),(h,t),(k,r)) = (-1)^{(\rho(g,h)+\lambda(g,h))r} \\ \cdot F((g,0),(h,0),(k,0)) \end{aligned}$$

This is the identity (5.18) that we claimed earlier, and that we used to derive the constraint on ν Eq. 5.8.

Our goal now is to relate F to $\widetilde{F}$ and derive (5.54). The first step is to better understand the relationship between the usual splitting operator S and the bare splitting operator $\widetilde{S}$. We know how S and $\widetilde{S}$ are related when acting on single domain wall states of the form $|\boldsymbol{a}\boldsymbol{b}_1\rangle$ (5.48). However, there is a slightly different relation when acting on the symmetry partner states $|\boldsymbol{a}\boldsymbol{b}_1;k\rangle$. To see this, let $\boldsymbol{a},\boldsymbol{b}$ be type g,h domain walls. Using the symmetry of $S(\boldsymbol{a},\boldsymbol{b})$, we have

$$\begin{aligned} S(\boldsymbol{a},\boldsymbol{b})|\boldsymbol{a}\boldsymbol{b}_1;k\rangle =& S(\boldsymbol{a},\boldsymbol{b})U^k|\boldsymbol{a}\boldsymbol{b}_1\rangle \\ =& U^k S(\boldsymbol{a},\boldsymbol{b})|\boldsymbol{a}\boldsymbol{b}_1\rangle \\ =& U^k \gamma_1^{\sigma(\boldsymbol{a})} ({}^g\gamma_2)^{\sigma(\boldsymbol{b})} \widetilde{S}(g,h) \gamma_1^{-\sigma(\boldsymbol{a}\boldsymbol{b})} |\boldsymbol{a}\boldsymbol{b}_1\rangle \\ =& [U^k \gamma_1^{\sigma(\boldsymbol{a})} (U^k)^{-1}] \cdot [U^k ({}^g\gamma_2)^{\sigma(\boldsymbol{b})} (U^k)^{-1}] \cdot [U^k \widetilde{S}(g,h) (U^k)^{-1}] \\ & \cdot [U^k \gamma_1^{-\sigma(\boldsymbol{a}\boldsymbol{b})} (U^k)^{-1}] \cdot U^k |\boldsymbol{a}\boldsymbol{b}_1\rangle \\ =& (-1)^{\lambda(k,g)\sigma(\boldsymbol{b})} \cdot ({}^k\gamma_1)^{\sigma(\boldsymbol{a})} \cdot ({}^{kg}\gamma_2)^{\sigma(\boldsymbol{b})} \cdot [{}^k\widetilde{S}(g,h)] \cdot ({}^k\gamma_1)^{-\sigma(\boldsymbol{a}\boldsymbol{b})} \cdot U^k |\boldsymbol{a}\boldsymbol{b}_1\rangle \\ =& (-1)^{\lambda(k,g)\sigma(\boldsymbol{b})} ({}^k\gamma_1)^{\sigma(\boldsymbol{a})} ({}^{kg}\gamma_2)^{\sigma(\boldsymbol{b})} [{}^k\widetilde{S}(g,h)] ({}^k\gamma_1)^{-\sigma(\boldsymbol{a}\boldsymbol{b})} |\boldsymbol{a}\boldsymbol{b}_1;k\rangle \end{aligned} \tag{5.57}$$

Here the third equality follows from (5.48); in the fifth equality, we used the identity

$$U^k({}^g\gamma_2)(U^k)^{-1} = (-1)^{\lambda(k,g)} \cdot ({}^{kg}\gamma_2) \tag{5.58}$$

which follows from the fact that $U^k U^g = U^{kg} F^{\lambda(k,g)}$. From (5.57), we can now deduce the relationship between between S and $\widetilde{S}$ when acting on *multi*-domain wall states. Consider a state $|..., \boldsymbol{a}\boldsymbol{b}_1, ...\rangle$, where $\boldsymbol{a}, \boldsymbol{b}$ are type g, h domain walls, and the product of all the domain wall types to the left of $\boldsymbol{a}$ is g_L as in Eqs. 5.26 and 5.27. Then:

$$S(\boldsymbol{a}, \boldsymbol{b})|..., \boldsymbol{a}\boldsymbol{b}_1, ...\rangle = (-1)^{\lambda(g_L,g)\sigma(\boldsymbol{b})}({}^{g_L}\gamma_1)^{\sigma(\boldsymbol{a})}({}^{g_L g}\gamma_2)^{\sigma(\boldsymbol{b})}[{}^{g_L}\widetilde{S}(g,h)]({}^{g_L}\gamma_1)^{-\sigma(\boldsymbol{a}\boldsymbol{b})}|..., \boldsymbol{a}\boldsymbol{b}_1, ...\rangle \tag{5.59}$$

One way to derive (5.59) from (5.57) is to consider the inner product between the left and right hand sides of (5.59). This inner product is 1 by (5.32) and (5.57).

Next we derive the relationship between M and $\widetilde{M}$ when acting on multi-domain wall states, thereby generalizing (5.45). Following the same logic as above, it is straightforward to show that

$$M^{\boldsymbol{a}}_{x'x}|..., \boldsymbol{a}_x, ...\rangle = ({}^{g_L}\gamma_{x'})^{\sigma(\boldsymbol{a})}\widetilde{M}^g_{x'x}({}^{g_L}\gamma_x)^{-\sigma(\boldsymbol{a})}|..., \boldsymbol{a}_x, ...\rangle \tag{5.60}$$

where $\boldsymbol{a}$ is a type g domain wall and g_L is the product of all the domain wall types to the left of $\boldsymbol{a}$.

We are now ready to relate F to $\widetilde{F}$. To do this, we relate the two states $|1\rangle, |2\rangle$ to $|\widetilde{1}\rangle, |\widetilde{2}\rangle$.

First, we note that

$$\begin{aligned}
|1\rangle &= M_{12}^{\boldsymbol{b}} M_{01}^{\boldsymbol{a}} S(\boldsymbol{a},\boldsymbol{b}) M_{32}^{\boldsymbol{c}} S(\boldsymbol{ab},\boldsymbol{c})|\boldsymbol{abc}_1\rangle \\
&= \gamma_0^{\sigma(\boldsymbol{a})} ({}^g\gamma_1)^{\sigma(\boldsymbol{b})} \widetilde{M}_{12}^h \widetilde{M}_{01}^g \widetilde{S}(g,h) ({}^{gh}\gamma_3)^{\sigma(\boldsymbol{c})} \widetilde{M}_{32}^k \widetilde{S}(gh,k)|(ghk,0)_1\rangle \\
&= (-1)^{\rho(g,h)\sigma(\boldsymbol{c})} \gamma_0^{\sigma(\boldsymbol{a})} ({}^g\gamma_1)^{\sigma(\boldsymbol{b})} ({}^{gh}\gamma_3)^{\sigma(\boldsymbol{c})} \widetilde{M}_{12}^h \widetilde{M}_{01}^g \widetilde{S}(g,h) \widetilde{M}_{32}^k \widetilde{S}(gh,k)|(ghk,0)_1\rangle \\
&= (-1)^{\rho(g,h)\sigma(\boldsymbol{c})} \gamma_0^{\sigma(\boldsymbol{a})} ({}^g\gamma_1)^{\sigma(\boldsymbol{b})} ({}^{gh}\gamma_3)^{\sigma(\boldsymbol{c})} |\widetilde{1}\rangle
\end{aligned} \tag{5.61}$$

Here the factor of $(-1)^{\rho(g,h)\sigma(\boldsymbol{c})}$ in the third equality comes from commuting $({}^{gh}\gamma_3)^{\sigma(\boldsymbol{c})}$ past $\widetilde{S}(g,h)$, whose fermion parity is $\rho(g,h)$. We have also used the fact that ${}^1\widetilde{S}(g,h) = \widetilde{S}(g,h)$ since $U^1 = \mathbb{I}$, and that $\lambda(1,g) = 1$ (5.6).

Similarly, we have

$$\begin{aligned}
|2\rangle &= M_{32}^{\boldsymbol{c}} S(\boldsymbol{b},\boldsymbol{c}) M_{12}^{\boldsymbol{bc}} M_{01}^{\boldsymbol{a}} S(\boldsymbol{a},\boldsymbol{bc})|\boldsymbol{abc}_1\rangle \\
&= (-1)^{\lambda(g,h)\sigma(\boldsymbol{c})} \gamma_0^{\sigma(\boldsymbol{a})} ({}^g\gamma_1)^{\sigma(\boldsymbol{b})} ({}^{gh}\gamma_3)^{\sigma(\boldsymbol{c})} \widetilde{M}_{32}^k [{}^g\widetilde{S}(h,k)] \widetilde{M}_{12}^{hk} \widetilde{M}_{01}^g \widetilde{S}(g,hk)|(ghk,0)_1\rangle \\
&= (-1)^{\lambda(g,h)\sigma(\boldsymbol{c})} \gamma_0^{\sigma(\boldsymbol{a})} ({}^g\gamma_1)^{\sigma(\boldsymbol{b})} ({}^{gh}\gamma_3)^{\sigma(\boldsymbol{c})} |\widetilde{2}\rangle
\end{aligned} \tag{5.62}$$

Therefore,

$$\langle 2|1\rangle = (-1)^{(\rho(g,h)+\lambda(g,h))r} \langle\widetilde{2}|\widetilde{1}\rangle \tag{5.63}$$

The desired identity (5.54) now follows immediately from the definition of F and $\widetilde{F}$.

5.3.5 Checking the microscopic definition

To show that our microscopic definition of F is correct, we need to establish two properties of F: (i) F is well-defined in the sense that different choices of domain wall states and movement and splitting operators give the same F up to the two transformations (5.21,5.23); and (ii) F obeys the pentagon identity (5.17). We prove property (ii) in Appendix 7.7; the goal of

this section is to prove property (i).

Choice of movement and splitting operators

As a warm-up, let us see how F transforms if we only change the *phase* of the movement and splitting operators. That is, suppose we replace

$$\begin{aligned} M^{(g,s)}_{x'x} &\to e^{i\theta_{x'x}(g)} M^{(g,s)}_{x'x}, \\ S((g,s),(h,t)) &\to e^{i\phi(g,h)} S((g,s),(h,t)) \end{aligned} \tag{5.64}$$

for some real-valued θ, ϕ. Note that the above phases $\theta_{x'x}(g), \phi(g,h)$ only depend on the G_0 component of the domain wall types so as to stay consistent with our phase conventions in Eqs. (5.45) and (5.48).

Substituting these transformations into (5.49-5.50) gives

$$\begin{aligned} F((g,s),(h,t),(k,r)) \to F((g,s),(h,t),(k,r)) \\ \cdot \frac{e^{i\phi(gh,k)} e^{i\phi(g,h)} e^{i\theta_{12}(h)}}{e^{i\phi(g,hk)} e^{i\phi(h,k)} e^{i\theta_{12}(hk)}} \end{aligned} \tag{5.65}$$

Crucially, this transformation is identical to the restricted gauge transformation (5.21) with

$$\alpha(g,h) = \phi(g,h) + \theta_{12}(h) \tag{5.66}$$

This is exactly what we want: different phase choices lead to the same F, up to a restricted gauge transformation (5.21).

With this warm-up, we are now ready to consider the general case where we change the movement and splitting operators in an arbitrary way:

$$M^{\boldsymbol{a}}_{x'x} \to M'^{\boldsymbol{a}}_{x'x}, \qquad S(\boldsymbol{a},\boldsymbol{b}) \to S'(\boldsymbol{a},\boldsymbol{b}) \tag{5.67}$$

To analyze this case, we note that the definition of movement and splitting operators implies that

$$\begin{aligned} M'^{\boldsymbol{a}}_{x'x}|\boldsymbol{a}_x\rangle &= e^{i\theta_{x'x}(\boldsymbol{a})} M^{\boldsymbol{a}}_{x'x}|\boldsymbol{a}_x\rangle \\ S'(\boldsymbol{a},\boldsymbol{b})|\boldsymbol{a}\boldsymbol{b}_1\rangle &= e^{i\phi(\boldsymbol{a},\boldsymbol{b})} S(\boldsymbol{a},\boldsymbol{b})|\boldsymbol{a}\boldsymbol{b}_1\rangle \end{aligned} \tag{5.68}$$

for some real valued $\theta_{x'x}(\boldsymbol{a})$ and $\phi(\boldsymbol{a},\boldsymbol{b})$. In fact, using the constraint (5.45) we can see that $\theta_{x'x}(\boldsymbol{a})$ only depends on the G_0 component of $\boldsymbol{a}$: in other words $\theta_{x'x}(\boldsymbol{a})$ only depends on the group element g if a is of type g, so that $\theta_{x'x}(\boldsymbol{a}) \equiv \theta_{x'x}(g)$. Likewise, using (5.48), we can see that $\phi(\boldsymbol{a},\boldsymbol{b}) \equiv \phi(g,h)$ only depends on g,h where $\boldsymbol{a},\boldsymbol{b}$ are of type g,h. Hence,

$$\begin{aligned} M'^{\boldsymbol{a}}_{x'x}|\boldsymbol{a}_x\rangle &= e^{i\theta_{x'x}(g)} M^{\boldsymbol{a}}_{x'x}|\boldsymbol{a}_x\rangle \\ S'(\boldsymbol{a},\boldsymbol{b})|\boldsymbol{a}\boldsymbol{b}_1\rangle &= e^{i\phi(g,h)} S(\boldsymbol{a},\boldsymbol{b})|\boldsymbol{a}\boldsymbol{b}_1\rangle \end{aligned} \tag{5.69}$$

Now consider *multi*-domain wall states. In that case,

$$M'^{\boldsymbol{a}}_{x'x}|...,\boldsymbol{a}_x,...\rangle = \omega_1 \cdot M^{\boldsymbol{a}}_{x'x}|...,\boldsymbol{a}_x,...\rangle \tag{5.70}$$

$$S'(\boldsymbol{a},\boldsymbol{b})|...,\boldsymbol{a}\boldsymbol{b}_1,...\rangle = \omega_2 \cdot S(\boldsymbol{a},\boldsymbol{b})|...,\boldsymbol{a}\boldsymbol{b}_1,...\rangle \tag{5.71}$$

for some $U(1)$ phases ω_1, ω_2.

Let us try to find the relationship between the multi-domain wall phases ω_1, ω_2 and the single domain wall phases $e^{i\theta_{x'x}(g)}$ and $e^{i\phi(g,h)}$. To do this, we multiply the two sides of (5.70) by $\langle...,\boldsymbol{a}_x,...|(M^{\boldsymbol{a}}_{x'x})^\dagger$ and then use property (5.34) to derive

$$\begin{aligned} \omega_1 &= \langle...,\boldsymbol{a}_x,...|(M^{\boldsymbol{a}}_{x'x})^\dagger M'^{\boldsymbol{a}}_{x'x}|...,\boldsymbol{a}_x,...\rangle \\ &= \langle\boldsymbol{a}_x|(M^{\boldsymbol{a}}_{x'x})^\dagger M'^{\boldsymbol{a}}_{x'x}|\boldsymbol{a}_x\rangle \\ &= e^{i\theta_{x'x}(g)} \end{aligned} \tag{5.72}$$

By the same reasoning, $\omega_2 = e^{i\phi(g,h)}$. We conclude that

$$\begin{aligned} M'^{\boldsymbol{a}}_{x'x}|..., \boldsymbol{a}_x, ...\rangle &= e^{i\theta_{x'x}(g)} M^{\boldsymbol{a}}_{x'x}|..., \boldsymbol{a}_x, ...\rangle \\ S'(\boldsymbol{a}, \boldsymbol{b})|..., \boldsymbol{a}\boldsymbol{b}_1, ...\rangle &= e^{i\phi(g,h)} S(\boldsymbol{a}, \boldsymbol{b})|..., \boldsymbol{a}\boldsymbol{b}_1, ...\rangle \end{aligned} \tag{5.73}$$

Substituting these relations into (5.49) and using the same logic as before, we see that F again changes by a restricted gauge transformation (5.21) with α given by (5.66).

for some real-valued θ, ϕ. Substituting these relations into (5.49) and using the same logic as before, we see that $\widetilde{F}$, and therefore ν, changes by a gauge transformation with α given by (5.66).

Choice of fermion operators

In this section, we analyze how a change in the fermion operators γ_x affects F. More specifically, we consider the special case where we replace $\gamma_x \to \gamma'_x$ but we do not change the domain wall states (up to a phase). That is, we assume

$$\gamma'_x|(g,0)_x\rangle = e^{i\theta_x(g)}\gamma_x|(g,0)_x\rangle \tag{5.74}$$

for some real valued $\theta_x(g)$. In Sec. 5.3.5 we consider the more general case where the domain wall can change by more than just a phase.

To understand how the F-symbol changes under such a replacement, note that we are free to choose the movement and splitting operators M', S' however we like, since different choices only change F by at most a gauge transformation according to Sec. 5.3.5. A particularly

convenient choice is

$$\begin{aligned} M'^{(g,0)}_{x'x} &= M^{(g,0)}_{x'x} \\ S'((g,0),(h,0)) &= e^{-i\rho(g,h)\theta_1(gh)} S((g,0),(h,0)) \end{aligned} \tag{5.75}$$

Here, the reason we include the phase factor in the definition of S' is that it leads to a particularly simple relation between $\widetilde{S}'$ and $\widetilde{S}$, namely

$$\begin{aligned} \widetilde{S}'(g,h)|(gh,0)_1\rangle &= S'((g,0),(h,0))\gamma_1'^{\rho(g,h)}|(gh,0)_1\rangle \\ &= S((g,0),(h,0))\gamma_1^{\rho(g,h)}|(gh,0)_1\rangle \\ &= \widetilde{S}(g,h)|(gh,0)_1\rangle \end{aligned} \tag{5.76}$$

Note that the crucial step is the second equality where the phase factor in $S'((g,0),(h,0))$ cancels the phase factor coming from γ_1'.

As usual, the above relation between $\widetilde{S}'$ and $\widetilde{S}$ also extends to multi-domain wall states:

$$\widetilde{S}'(g,h)|...,(gh,0)_1,...\rangle = \widetilde{S}(g,h)|...,(gh,0)_1,...\rangle \tag{5.77}$$

To derive (5.77) from (5.76), we take the inner product of both sides of (5.77) and then use (5.34).

So far we have shown that the splitting operators $\widetilde{S}'$ and $\widetilde{S}$ have the same action on domain wall states. Likewise, for the movement operators, we have

$$\widetilde{M}'^{g}_{x'x} = \widetilde{M}^{g}_{x'x} \tag{5.78}$$

Given (5.77) and (5.78), it then follows from the definition of $\widetilde{F}$ that

$$\widetilde{F}'(g,h,k) = \widetilde{F}(g,h,k) \tag{5.79}$$

and hence

$$F'((g,0),(h,0),(k,0)) = F((g,0),(h,0),(k,0)) \tag{5.80}$$

Thus, replacing $\gamma_x \to \gamma'_x$ has no effect on F.

Choice of bare and decorated domain walls

In this section, we work out how F transforms if we change our labeling convention for domain walls. More precisely, consider a new set of "primed" domain wall states $|\boldsymbol{a}_x\rangle'$, defined by

$$|\boldsymbol{a}_x\rangle' = |\pi(\boldsymbol{a})_x\rangle \tag{5.81}$$

where π is a mapping of the form

$$\pi(g,s) = (g, s + \mu(g)) \tag{5.82}$$

for some $\mu : G_0 \to \mathbb{Z}_2$. Our goal is to understand the relationship between the F-symbols for the "primed" states and "unprimed" states.

The first step is to choose fermion operators and movement and splitting operators for the "primed" domain walls. For the fermion operators, the simplest choice is

$$\gamma'_x |(g,0)_x\rangle' = |(g,1)_x\rangle' \tag{5.83}$$

Next, we need to choose movement and splitting operators, M' and S'. We begin by defining the movement operator M'. To do this, we first define

$$M'^{(g,0)}_{yx} = M^{\pi(g,0)}_{yx} \tag{5.84}$$

With this definition, we can then work out the relationship between $\widetilde{M}'$ and $\widetilde{M}$ when acting on a single domain wall state:

$$\begin{aligned}\widetilde{M}'^{g}_{yx}|(g,0)_x\rangle' &= M'^{(g,0)}_{yx}|(g,0)_x\rangle' \\ &= M^{\pi(g,0)}_{yx}|(g,0)_x\rangle' \\ &= \gamma_y^{\mu(g)}\widetilde{M}^{g}_{yx}\gamma_x^{-\mu(g)}|(g,0)_x\rangle'\end{aligned} \tag{5.85}$$

Next, we can relate M' and M when acting on a single domain wall state:

$$\begin{aligned}M'^{\boldsymbol{a}}_{yx}|\boldsymbol{a}_x\rangle' &= \gamma_y'^{\sigma(\boldsymbol{a})}\widetilde{M}'^{g}_{yx}\gamma_x'^{-\sigma(\boldsymbol{a})}|\boldsymbol{a}_x\rangle' \\ &= \gamma_y'^{\sigma(\boldsymbol{a})}\gamma_y^{\mu(g)}\widetilde{M}^{g}_{yx}\gamma_x^{-\mu(g)}\gamma_x'^{-\sigma(\boldsymbol{a})}|\boldsymbol{a}_x\rangle'\end{aligned} \tag{5.86}$$

Now it is easy to check that

$$\gamma_x^{-\mu(g)}\gamma_x'^{-\sigma(\boldsymbol{a})}|\boldsymbol{a}_x\rangle' = \gamma_x^{-\sigma(\pi(\boldsymbol{a}))}|\boldsymbol{a}_x\rangle' \tag{5.87}$$

Substituting this into the right hand side of (5.86) gives

$$\begin{aligned}M'^{\boldsymbol{a}}_{yx}|\boldsymbol{a}_x\rangle' &= \gamma_x^{\sigma(\pi(\boldsymbol{a}))}\widetilde{M}^{g}_{yx}\gamma_x^{-\sigma(\pi(\boldsymbol{a}))}|\boldsymbol{a}_x\rangle' \\ &= M^{\pi(\boldsymbol{a})}_{yx}|\boldsymbol{a}_x\rangle'\end{aligned} \tag{5.88}$$

Next consider the splitting operator S'. Like M', we first define $S'((g,0),(h,0))$ and then

work out its implications for more general splitting operators. Specifically, we define

$$S'((g,0),(h,0)) = S(\pi(g,0),\pi(h,0)) \tag{5.89}$$

We can then relate $\widetilde{S}'$ and $\widetilde{S}$:

$$\begin{aligned}
\widetilde{S}'(g,h)|(gh,0)_1\rangle' &= S'((g,0),(h,0))|(gh,\rho'(g,h))_1\rangle' \\
&= S(\pi(g,0),\pi(h,0))|(gh,\rho'(g,h))_1\rangle' \\
&= \gamma_1^{\mu(g)}(\gamma_2^g)^{\mu(h)}\widetilde{S}(g,h)\gamma_1^{-\mu(gh)}|(gh,0)_1\rangle'
\end{aligned} \tag{5.90}$$

Likewise, we can relate S' to S:

$$\begin{aligned}
S'(\boldsymbol{a},\boldsymbol{b})|\boldsymbol{a}\boldsymbol{b}_1\rangle' &= \gamma_1'^{\sigma(\boldsymbol{a})}({}^g\gamma_2')^{\sigma(\boldsymbol{b})}\widetilde{S}'(g,h)\gamma_1'^{-\sigma(\boldsymbol{a}\boldsymbol{b})}|\boldsymbol{a}\boldsymbol{b}_1\rangle' \\
&= \gamma_1'^{\sigma(\boldsymbol{a})}({}^g\gamma_2')^{\sigma(\boldsymbol{b})}\gamma_1^{\mu(g)}({}^g\gamma_2)^{\mu(h)}\widetilde{S}(g,h)\gamma_1^{-\mu(gh)}\gamma_1'^{-\sigma(\boldsymbol{a}\boldsymbol{b})}|\boldsymbol{a}\boldsymbol{b}_1\rangle' \\
&= (-1)^{\sigma(\boldsymbol{b})\mu(g)}\gamma_1'^{\sigma(\boldsymbol{a})}\gamma_1^{\mu(g)}({}^g\gamma_2')^{\sigma(\boldsymbol{b})}({}^g\gamma_2)^{\mu(h)}\widetilde{S}(g,h)\gamma_1^{-\mu(gh)}\gamma_1'^{-\sigma(\boldsymbol{a}\boldsymbol{b})}|\boldsymbol{a}\boldsymbol{b}_1\rangle'
\end{aligned} \tag{5.91}$$

Here the factor of $(-1)^{\sigma(\boldsymbol{b})\mu(g)}$ in the third line comes from commuting $\gamma_1^{\mu(g)}$ past $({}^g\gamma_2')^{\sigma(\boldsymbol{b})}$. To proceed further, we substitute (5.87) into the right hand side of (5.91) to obtain

$$S'(\boldsymbol{a},\boldsymbol{b})|\boldsymbol{a}\boldsymbol{b}_1\rangle' = (-1)^{\sigma(\boldsymbol{b})\mu(g)}S(\pi(\boldsymbol{a}),\pi(\boldsymbol{b}))|\boldsymbol{a}\boldsymbol{b}_1\rangle' \tag{5.92}$$

As usual, the relationship between M', S' and M, S generalizes to multi-domain wall

states, i.e.

$$M'^{\boldsymbol{a}}_{yx}|..., \boldsymbol{a}_x, ...\rangle' = M^{\pi(\boldsymbol{a})}_{yx}|..., \boldsymbol{a}_x, ...\rangle' \tag{5.93}$$

$$S'(\boldsymbol{a}, \boldsymbol{b})|..., \boldsymbol{a}\boldsymbol{b}_1, ...\rangle' = (-1)^{\sigma(\boldsymbol{b})\mu(g)} S(\pi(\boldsymbol{a}), \pi(\boldsymbol{b}))|..., \boldsymbol{a}\boldsymbol{b}_1, ...\rangle' \tag{5.94}$$

Substituting (5.94) into the definition of F, we deduce that

$$F'(\boldsymbol{a}, \boldsymbol{b}, \boldsymbol{c}) = (-1)^{\sigma(\boldsymbol{b}\boldsymbol{c})\mu(g)+\sigma(\boldsymbol{c})\mu(h)+\sigma(\boldsymbol{c})\mu(gh)+\sigma(\boldsymbol{b})\mu(g)} F(\pi(\boldsymbol{a}), \pi(\boldsymbol{b}), \pi(\boldsymbol{c})) \tag{5.95}$$

where the four phase factors come from the four splitting operators that appear in the inner product $\langle 2|1\rangle$. We can simplify further if we specialize to the case $\boldsymbol{a} = (g, 0)$, $\boldsymbol{b} = (h, 0)$, and $\boldsymbol{c} = (k, 0)$. In that case,

$$\sigma(\boldsymbol{b}) = \sigma(\boldsymbol{c}) = 0, \qquad \sigma(\boldsymbol{b}\boldsymbol{c}) = \rho(h, k) + d\mu(h, k) \tag{5.96}$$

where $d\mu(h, k) = \mu(h) + \mu(k) - \mu(hk)$. Hence,

$$\begin{aligned} F'((g, 0), (h, 0), (k, 0)) &= (-1)^{(\rho(h,k)+d\mu(h,k))\mu(g)} F((g, \mu(g)), (h, \mu(h)), (k, \mu(k)) \\ &= (-1)^{(\rho(h,k)+d\mu(h,k))\mu(g)+(\rho(g,h)+\lambda(g,h))\mu(k)} F((g, 0), (h, 0), (k, 0)) \end{aligned} \tag{5.97}$$

This is exactly what we want: when we relabel domain walls F changes by the transformation (5.23).

Choice of domain wall states

So far, we have shown that different choices of movement and splitting operators lead to the same ν, up to a gauge transformation. Next, we need to check that different choices of edge Hamiltonians and domain wall states also lead to the same ν, up to a gauge transforma-

tion. To investigate this issue, consider two choices of edge Hamiltonians, H and H', with ground states $\{|\Omega; g\rangle\}$ and $\{|\Omega; g\rangle'\}$ respectively. For now, assume that H and H' can be adiabatically connected, i.e. there exists an interpolating Hamiltonian H_s, with $0 \leq s \leq 1$ with $H_0 = H$ and $H_1 = H'$ such that H_s is local, gapped, and breaks the G-symmetry spontaneously and completely. Assuming the existence of such an interpolation, it then follows from the quasi-adiabatic continuation construction [54] that there exists a G-invariant, "locality preserving" unitary transformation W that connects the two sets of ground states: that is,

$$\{|\Omega; g\rangle'\} = \{W|\Omega; g\rangle\} \tag{5.98}$$

Here, when we say W is "locality preserving", we mean that it has the following property: for any local operator $\mathcal{O}$, the operator $W\mathcal{O}W^{-1}$ is also local and is supported near $\mathcal{O}$.

Comparing Eq. 5.98 with our labeling scheme (5.11), we deduce that the two sets of ground states are related by

$$|\Omega; g\rangle' = WU^k|\Omega; g\rangle \tag{5.99}$$

for some $k \in G$.

To proceed with our analysis, we will make the additional assumption that Eq. (5.99) can be extended from ground states to (multi-)domain wall states. That is, we assume that, for any two choices of domain wall states, there exists a G-invariant, locality preserving unitary transformation W such that

$$|g_{x_1}^{(1)}, g_{x_2}^{(2)}, g_{x_3}^{(3)}, ...\rangle' = WU^k|g_{x_1}^{(1)}, g_{x_2}^{(2)}, g_{x_3}^{(3)}, ...\rangle \tag{5.100}$$

This assumption is reasonable as long as the domain wall positions $x_1, x_2, ...$ are well-

separated.

With Eq. (5.100), we are now in a position to compare the F-symbols for the two choices of domain wall states. First, we observe that we are free to choose the movement and splitting operators for the states $|g_{x_1}^{(1)}, g_{x_2}^{(2)}, g_{x_3}^{(3)}, ...\rangle'$ however we like, changing F by, at most, a gauge transformation. The simplest choice that is consistent with (5.100) is

$$M'^{g}_{x'x} = W M^{g}_{x'x} W^{-1}, \quad S'(g,h) = W S(g,h) W^{-1} \tag{5.101}$$

With this choice, it is clear that $|1'\rangle = WU^k|1\rangle$, and $|2'\rangle = WU^k|2\rangle$. It follows that $F' = \langle 2'|1'\rangle = \langle 2|1\rangle = F$. Thus, we conclude that F doesn't depend on the choice of the edge Hamiltonian or the choice of domain wall states. This completes the proof of property (i) above.

Previously, we assumed that we may adiabatically interpolate between our two edge Hamiltonians. However, there is one more case to consider. It may be the case that before this interpolation may take place, we must stack a 1D Kitaev chain with symmetry G on the boundary. In Appendix 7.8, we will show that this results in a change

$$\begin{aligned} \rho(g,h) &\to \rho(g,h) + \lambda(g,h) \\ \nu(g,h,k) &\to \nu(g,h,k). \end{aligned} \tag{5.102}$$

5.4 Examples

5.4.1 $\nu = 2$ lattice edge theory

In these notes we calculate the F-symbols for a $\nu = 2$ lattice model. We begin by defining our model along with the essential operators. This model should be thought of as the edge of an SPT.

Edge theory

We begin by describing the edge theory. As explained in Sec. 5.2, an edge theory consists of three pieces of data: (1) a Hilbert space $\mathcal{H}$; (2) a set of local operators $\{\mathcal{O}\}$ that act in $\mathcal{H}$; and (3) a collection of symmetry transformations $\{U^g : g \in G\}$ acting within $\mathcal{H}$.

The Hilbert space $\mathcal{H}$ for the $\nu = 2$ edge theory is described by a one-dimensional lattice with one spin-1/2 site and one fermion site in each unit cell. More specifically, we take the spin-1/2's to live on integer lattice sites $i \in \mathbb{Z}$, and we denote the corresponding Pauli operators by $\sigma_i^z, \sigma_i^y, \sigma_i^z$. Likewise, we take the the fermions to live on *half-integer* sites $i + 1/2$, $i \in \mathbb{Z}$, and we denote the corresponding creation/annihilation operators by $c_{i+1/2}^\dagger, c_{i+1/2}$. A complete orthonormal basis for this Hilbert space can be obtained by considering simultaneous eigenstates of the Pauli σ_i^z operators, and the fermion occupation numbers $N_{i+1/2} = c_{i+1/2}^\dagger c_{i+1/2}$. We denote these eigenstates by

$$|..., \alpha_{-1}, n_{-1/2}, \alpha_0, n_{1/2}, ...\rangle, \tag{5.103}$$

where $\alpha_i \in \{+, -\}$ denotes the eigenvalue of σ_i^z, and $n_{i+1/2} \in \{0, 1\}$ denotes the eigenvalue of $N_{i+1/2}$. The local operators $\{\mathcal{O}\}$ in the $\nu = 2$ lattice edge theory are the usual local operators, namely products of Pauli spin operators and/or fermion operators acting on a collection of nearby lattice sites.

We now move on to the symmetry transformations. We denote the symmetry group G_0 by $G_0 = \mathbb{Z}_2 = \{1, s\}$. In this notation, it suffices to specify the action of the $\mathbb{Z}_2$ symmetry transformation $U \equiv U^s$, as well as the fermion parity operator F. These operators act as

follows:

$$\begin{aligned} U\sigma_i^x U^{-1} &= -i\gamma^a_{i-1/2}\gamma^a_{i+1/2}\sigma_i^x f(\sigma^z_{i-1},\sigma^z_i,\sigma^z_{i+1}) \\ U\sigma_i^y U^{-1} &= i\gamma^a_{i-1/2}\gamma^a_{i+1/2}\sigma_i^y f(\sigma^z_{i-1},\sigma^z_i,\sigma^z_{i+1}) \\ U\sigma_i^z U^{-1} &= -\sigma_i^z \\ U\gamma^a_{i+1/2}U^{-1} &= -\sigma_i^z\sigma^z_{i+1}\gamma^a_{i+1/2} \\ U\gamma^b_{i+1/2}U^{-1} &= -\gamma^b_{i+1/2} \end{aligned} \tag{5.104}$$

where

$$f(\sigma^z_{i-1},\sigma^z_i,\sigma^z_{i+1}) = \frac{1}{2}(1+\sigma^z_{i-1}\sigma^z_{i+1} + i\sigma^z_{i-1}\sigma^z_i - i\sigma^z_i\sigma^z_{i+1}) \tag{5.105}$$

and

$$\gamma^a_{i+1/2} = c_{i+1/2} + c^\dagger_{i+1/2} \quad \gamma^b_{i+1/2} = i(c_{i+1/2} - c^\dagger_{i+1/2}) \tag{5.106}$$

In particular,

$$UN_{i+1/2}U^{-1} = N_{i+1/2}\sigma^z_i\sigma^z_{i+1} + \frac{1}{2}(1-\sigma^z_i\sigma^z_{i+1}) \tag{5.107}$$

Calculation of the anomaly

We now proceed to compute the anomaly associated with the edge theory described above. As we explained in Sec. 5.3.1 the first step in calculating the anomaly is to choose a gapped (edge) Hamiltonian that breaks the $\mathbb{Z}_2$ symmetry spontaneously and completely. We use the Hamiltonian

$$H = -J\sum_i \sigma^z_i\sigma^z_{i+1} + K\sum_i N_{i+1/2}(1+\sigma^z_i\sigma^z_{i+1}) \tag{5.108}$$

with $J, K > 0$.

To see that this Hamiltonian spontaneously breaks the $\mathbb{Z}_2$ symmetry note that σ^z_i is odd

under the symmetry (Eq. 5.104) and has a non-zero expectation value in the two degenerate ground states $|+,0,+,0...,+,0\rangle$ and $|-,0,-,0,...,-,0\rangle$. Following the notation in Sec. 5.3.2. we denote these ground states by

$$\begin{aligned} |\Omega;1\rangle &= |+,0,+,0,...,+,0\rangle \\ |\Omega;s\rangle &= |-,0,-,0,...,-,0\rangle \end{aligned} \tag{5.109}$$

The next step is to define domain wall states. Since the symmetry group is $G_0 = \mathbb{Z}_2$, there is only one non-trivial domain wall state that we need to construct. Denoting this state by $|s_i\rangle$ where i is the location of the domain wall, we define

$$|s_i\rangle = |...,+,0,(+)_i,0,-,0,-,...\rangle \tag{5.110}$$

Here we use the notation $(+)_i$ to indicate that the corresponding '+' is the state of the ith spin, so that the '-' that follows is the state of the $(i+1)$st spin. Notice that (5.110) implies a particular convention for labeling domain wall locations: a domain wall is at "position i" if the ith and $(i+1)$st spins are anti-aligned. (This will also hold for the multi-domain wall states.) Likewise, we define the trivial or "no-domain" wall state $|1_i\rangle$ in the obvious way:

$$|1_i\rangle = |...,+,0,(+)_i,0,+,0,+,...\rangle \tag{5.111}$$

For future reference, we note that the symmetry partners of the domain wall state $|s_i\rangle$

$$U|s_i\rangle \propto |...,-,0,(-)_i,1,+,0,+,...\rangle \tag{5.112}$$

Here, to see why the symmetry changes the occupation number $0 \to 1$ at the position of the domain wall, note that this follows from Eq. 5.107 above.

To proceed further, we need to define fermion operators γ_x. We define:

$$\gamma_i = \gamma^b_{i+3/2}, \tag{5.113}$$

(Here, the reason we define γ_i using $\gamma^b_{i+3/2}$ instead of the more "natural" choice $\gamma^b_{i+1/2}$ is that this will simplify our calculation below). We then define the other two types of domain wall states, $|\psi_i\rangle$ and $|(\psi s)_i\rangle$ as in Eq. 5.24:

$$|\psi_i\rangle \equiv \gamma_i|1_i\rangle, \quad |(\psi s)_i\rangle \equiv \gamma_i|s_i\rangle \tag{5.114}$$

At this point we have defined all four types of domain wall states. The next step is to find their fusion rules. The most interesting fusion rule is $s \times s$. To compute this fusion product, note that the two domain wall state $|s_1, s_2\rangle$ is proportional to

$$|s_1, s_2\rangle \propto |..., (+)_1, 0, -, 1, +, 0, +, ...\rangle \tag{5.115}$$

in view of (5.110) and (5.112). Comparing this state with

$$|\psi_1\rangle \propto |..., (+)_1, 0, +, 1, +, 0, +, ...\rangle \tag{5.116}$$

we can see that $|s_1, s_2\rangle \propto \sigma_2^-|\psi_1\rangle$. In particular, since σ_2^- is a local, fermion parity even operator, we conclude that $s \times s = \psi$. As for the other fusion rules, e.g. $s \times 1$, and 1×2, etc., it is easy to see that these are all trivial. We conclude that

$$\rho(s, s) = 1 \tag{5.117}$$

with $\rho(g, h) = 0$ for all other choices of $g, h \in G_0$.

Next we construct movement and splitting operators for these domain walls. First, we

define the movement operators $M^s_{(i+1)i}$ by

$$M^s_{(i+1)i} = \sigma^+_{i+1} + U\sigma^+_{i+1}U^{-1} \tag{5.118}$$

To see that this is a valid movement operator, note that $M^s_{(i+1)i}$ is local, $\mathbb{Z}_2$ and fermion parity symmetric, and it has the correct action on domain wall states:

$$\begin{aligned} M^s_{(i+1)i}|s_i\rangle &= \sigma^+_{i+1}|..., +, 0, (+)_i, 0, -, 0, -, ...\rangle \\ &= |..., +, 0, (+)_i, 0, +, 0, -, ...\rangle \\ &= |s_{i+1}\rangle \end{aligned} \tag{5.119}$$

Likewise, we define the reverse movement operator by

$$\begin{aligned} M^s_{i(i+1)} &= (M^s_{(i+1)i})^\dagger \\ &= \sigma^-_{i+1} + U\sigma^-_{i+1}U^{-1} \end{aligned} \tag{5.120}$$

Moving on to the splitting operators, we define

$$S(s,s) = \sigma^-_2 + U\sigma^-_2 U^{-1} \tag{5.121}$$

Again let us check that $S(s,s)$ is a valid splitting operator. Clearly $S(s,s)$ is local and $\mathbb{Z}_2$ symmetric. To see that it has the correct action on domain walls note that

$$\begin{aligned} S(s,s)|\psi_1\rangle &\propto \sigma^-_2|..., (+)_1, 0, +, 1, +, 0, +, ...\rangle \\ &\propto |..., (+)_1, 0, -, 1, +, 0, +, ...\rangle \\ &\propto |s_1, s_2\rangle \end{aligned} \tag{5.122}$$

As for the other splitting operators, we define

$$S(1,s) = M^s_{21} = \sigma_2^+ + U\sigma_2^+ U^{-1} \tag{5.123}$$

Also, we define

$$M^1_{i'i} = S(s,1) = S(1,1) = 1 \tag{5.124}$$

(Here we can set these operators equal to the identity because none of these operators are supposed to change the position of any nontrivial domain walls. For example, $S(s,1)$ is defined by the condition $S(s,1)|s_1\rangle = |s_1, 1_2\rangle$ and similarly for the other operators).

We are now ready to compute the bare movement and splitting operators:

$$\begin{aligned}
\widetilde{S}(s,s) &= (\sigma_2^- + U\sigma_2^- U^{-1})\gamma^b_{5/2} \\
\widetilde{S}(1,s) &= \sigma_2^+ + U\sigma_2^+ U^{-1} \\
\widetilde{S}(s,1) &= \widetilde{S}(1,1) = 1 \\
\widetilde{M}^s_{x'x} &= \sigma^-_{i+1} + U\sigma^-_{i+1}U^{-1} \\
\widetilde{M}^1_{x'x} &= 1
\end{aligned} \tag{5.125}$$

We are now ready to calculate $\widetilde{F}(g,h,k)$. We start with $\widetilde{F}(s,s,s)$. Using (5.51), we have

$$|\widetilde{1}\rangle = \widetilde{M}^s_{12}\widetilde{M}^s_{01}\widetilde{S}(s,s)\widetilde{M}^s_{32}\widetilde{S}(1,s)|s_1\rangle \tag{5.126}$$

We now simplify this expression, working from right to left. First, we note that

$$\begin{aligned}
\widetilde{S}(1,s)|s_1\rangle &= (\sigma_2^+ + U\sigma_2^+ U^{-1})|s_1\rangle \\
&= \sigma_2^+|s_1\rangle
\end{aligned}$$

since $U\sigma_2^+U^{-1}|s_1\rangle = 0$. Likewise,

$$\widetilde{M}^s_{32}\sigma_2^+|s_1\rangle = \sigma_3^+\sigma_2^+|s_1\rangle$$

since the second term in M^s_{32}, i.e. $U\sigma_3^-U^{-1}$, annihilates $\sigma_2^+|s_1\rangle$. Proceeding in this way, we can drop either the first or second term in each of the movement and splitting operators. The final result is:

$$\begin{aligned}|\widetilde{1}\rangle &= (U\sigma_2^-U^{-1})\sigma_1^-(\sigma_2^-\gamma^b_{5/2})\sigma_3^+\sigma_2^+|s_1\rangle \\ &= \gamma^a_{3/2}\gamma^a_{5/2}\gamma^b_{5/2}|...,+,0,(-)_1,0,+,0,+,0,-,...\rangle \end{aligned} \tag{5.127}$$

where the second equality follows from $|s_1\rangle = |...,+,0,(+)_1,0,-,0,-,0,-,...\rangle$.

By the same logic,

$$\begin{aligned}|\widetilde{2}\rangle &= \widetilde{M}^s_{32}(U\widetilde{S}(s,s)U^{-1})\widetilde{M}^1_{12}\widetilde{M}^s_{01}\widetilde{S}(s,1)|s_1\rangle \\ &= \sigma_3^+(U\sigma_2^-\gamma^b_{5/2}U^{-1})\sigma_1^-|s_1\rangle \\ &= i\gamma^a_{3/2}\gamma^a_{5/2}\gamma^b_{5/2}|...,+,0,(-)_1,0,+,0,+,0,-,...\rangle \end{aligned} \tag{5.128}$$

Comparing these two expressions, we conclude that $|\widetilde{1}\rangle = -i|\widetilde{2}\rangle$ so that

$$\widetilde{F}(s,s,s) = \langle\widetilde{2}|\widetilde{1}\rangle = -i \tag{5.129}$$

In the same way, one can check that $\widetilde{F}(g,h,k) = 1$ for all other choices of $g,h,k \in \{1,s\}$.

5.4.2 $\nu = 2$ chiral boson edge theory

We now present an example involving a *continuum* edge theory for the $\nu = 2$ $\mathbb{Z}_2$ fermionic SPT phase (the same SPT phase as in the previous example).

Edge theory

We begin by reviewing the continuum edge theory for the $\nu = 2$ SPT phase. This edge theory consists of two counterpropagating chiral boson modes described by fields ϕ_1, ϕ_2 obeying the commutation relations

$$\begin{aligned} [\phi_1(x), \partial_y \phi_1(y)] &= -2\pi i \delta(x-y) \\ [\phi_2(x), \partial_y \phi_2(y)] &= 2\pi i \delta(x-y) \end{aligned} \tag{5.130}$$

with all other commutators vanishing. Here we are using a normalization convention where $e^{\pm i\phi_1}$ and $e^{\pm i\phi_2}$ are the fermion creation and annihilation operators on each mode.

As before, to define the edge theory, we need to specify three pieces of data: (1) a Hilbert space $\mathcal{H}$; (2) a set of local operators $\{\mathcal{O}\}$ that act in $\mathcal{H}$; and (3) a collection of symmetry transformations $\{U^g : g \in G\}$ acting within $\mathcal{H}$. The Hilbert space $\mathcal{H}$ is the usual infinite dimensional representation of the above algebra (5.130). The local operators $\{\mathcal{O}\}$ in this edge theory consist of arbitrary derivatives and/or products of the fermion creation/annihilation operators $\{e^{\pm i\phi_1}, e^{\pm i\phi_2}\}$.

To complete the edge theory, we need to specify the symmetry transformations. Let us denote the symmetry group G_0 by $G_0 = \mathbb{Z}_2 = \{1, s\}$. In this notation, it suffices to specify the action of the $\mathbb{Z}_2$ symmetry transformation $U \equiv U^s$:

$$\begin{aligned} U\phi_1 U^{-1} &= \phi_1 - \pi \\ U\phi_2 U^{-1} &= \phi_2 \end{aligned} \tag{5.131}$$

We can also write out an explicit formula for U, though we will not need it for our

computation below:

$$U = e^{\frac{i}{2}\int_{-\infty}^{\infty} dy \partial_y \phi_1(y)} \tag{5.132}$$

Calculating the anomaly

We now go ahead and calculate the anomaly in this edge theory. The first step is to choose a Hamiltonian that breaks the $\mathbb{Z}_2$ symmetry spontaneously and completely. We will use the Hamiltonian

$$H = H_0 - \int dx V \cos(2(\phi_1 + \phi_2)) \tag{5.133}$$

where

$$H_0 = \int dx \frac{1}{4\pi}[v_1(\partial_x \phi_1)^2 + v_2(\partial_x \phi_2)^2]$$

for some velocities $v_1, v_2 > 0$.

For V sufficiently large and positive, the cosine term locks $\phi_1 + \phi_2$ to one of two values: $\phi_1 + \phi_2 = 0$ and $\phi_1 + \phi_2 = \pi$, spontaneously breaking the $\mathbb{Z}_2$ symmetry (5.131) and opening up an energy gap.

For simplicity, we will consider the limit $V \to \infty$ in what follows. In this limit, the two ground states of H are *eigenstates* of $e^{i(\phi_1(x)+\phi_2(x))}$. Following our standard labeling scheme, we denote these ground states by $|\Omega; 1\rangle$ and $|\Omega; s\rangle$, where

$$\begin{aligned} e^{i(\phi_1(x)+\phi_2(x))}|\Omega; 1\rangle &= |\Omega; 1\rangle \\ e^{i(\phi_1(x)+\phi_2(x))}|\Omega; s\rangle &= -|\Omega; s\rangle \end{aligned} \tag{5.134}$$

for all x.

The next step is to construct domain wall states $|s_x\rangle$, which interpolate spatially between

the two ground states, $|\Omega;1\rangle$ and $|\Omega;s\rangle$. We define $|s_x\rangle$ by

$$|s_x\rangle = a_x^\dagger |\Omega;1\rangle \tag{5.135}$$

where

$$a_x^\dagger = e^{-\frac{i}{2}\int_x^\infty dy\ \partial_y \phi_1(y)} \tag{5.136}$$

Here $a_x^\dagger$ is a (non-local) creation operator for a domain wall at position x. To see that $|s_x\rangle$ is a valid domain wall state, note that $|s_x\rangle$ obeys

$$e^{i(\phi_1(x')+\phi_2(x'))}|s_x\rangle = \mathrm{sgn}(x-x')|s_x\rangle \tag{5.137}$$

(This follows from the fact that $a_x^\dagger$ anticommutes with $e^{i\phi_1(x')}$ for $x' > x$). Likewise, we define the no-domain wall state $|1_x\rangle$ to be $|1_x\rangle = |\Omega;1\rangle$.

To proceed further, we need to define fermion operators γ_x. We define:

$$\gamma_x = e^{-i\phi_2(x)}. \tag{5.138}$$

We then define the other two types of domain wall states, $|\psi_x\rangle$, and $|(\psi s)_x\rangle$ as in Eq. 5.24:

$$|\psi_x\rangle \equiv \gamma_x|1_x\rangle, \qquad |(\psi s)_x\rangle \equiv \gamma_x|s_x\rangle \tag{5.139}$$

Now that we have defined domain wall states, the next step is to find their fusion rules. In this case, the only non-trivial fusion rule is $s \times s$, which one can check gives $s \times s = \psi$. We conclude that

$$\rho(s,s) = 1 \tag{5.140}$$

Likewise, $\rho(g,h) = 0$ for all other choices of $g, h \in G_0$.

Next, we construct movement and splitting operators for these domain walls. First, we define the movement operator $M^s_{x'x}$ by

$$M^s_{x'x} = e^{\frac{i}{2}\int_x^{x'} dy\ \partial_y \phi_1(y)} \tag{5.141}$$

This is a valid movement operator because it is local and $\mathbb{Z}_2 \times \mathbb{Z}_2^F$ symmetric and it obeys $M^s_{x'x}|s_x\rangle \propto |s_{x'}\rangle$ since $M^s_{x'x} a^\dagger_x \propto a^\dagger_{x'}$.

We must also define splitting operators. First, we define the splitting operator $S(s,s)$ by

$$\begin{aligned} S(s,s) &= M^s_{21} \\ &= e^{\frac{i}{2}\int_1^2 dy\ \partial_y \phi_1(y)} \end{aligned} \tag{5.142}$$

To see that this is a valid splitting operator, note that $S(s,s)$ is local, $\mathbb{Z}_2 \times \mathbb{Z}_2^F$ symmetric and furthermore

$$\begin{aligned} S(s,s)|\psi_1\rangle &= e^{\frac{i}{2}\int_1^2 dy\ \partial_y \phi_1(y)} e^{-i\phi_2(1)} |\Omega; 1\rangle \\ &\propto e^{\frac{i}{2}\int_1^2 dy\ \partial_y \phi_1(y)} e^{i\phi_1(1)} |\Omega; 1\rangle \\ &\propto a_2^\dagger a_1^\dagger |\Omega; 1\rangle \\ &\propto |s_1, s_2\rangle \end{aligned} \tag{5.143}$$

Here, the second equality follows from $e^{i(\phi_1(1)+\phi_2(1))}|\Omega;1\rangle = |\Omega;1\rangle$, while the third equality follows from the definition of $a_x^\dagger$ (5.136).

Moving on to the other splitting operators, we define

$$S(1,s) = M^s_{21} \tag{5.144}$$

Also we define

$$M^1_{x'x} = S(s,1) = S(1,1) = 1 \tag{5.145}$$

This gives us the bare movement and splitting operators

$$\begin{aligned}
\widetilde{S}(s,s) &= M^s_{21} e^{-i\phi_2(1)} \\
\widetilde{S}(1,s) &= M^s_{21} \\
\widetilde{S}(s,1) &= \widetilde{S}(1,1) = 1 \\
\widetilde{M}^s_{x'x} &= M^s_{21} \\
\widetilde{M}^1_{x'x} &= 1
\end{aligned} \tag{5.146}$$

With these operators in hand, we are now ready to compute $\widetilde{F}(s,s,s)$. Using (5.51), we have

$$\begin{aligned}
|\widetilde{1}\rangle &= M^s_{12} M^s_{01} M^s_{21} e^{-i\phi_2(1)} M^s_{32} M^s_{21} |s_1\rangle \\
|\widetilde{2}\rangle &= M^s_{32} (U M^s_{21} e^{-i\phi_2(1)} U^{-1}) M^s_{01} |s_1\rangle
\end{aligned} \tag{5.147}$$

In order to compare these expressions, we need to reorder the operators within them. We do this using the following commutation relations, which can be derived from the Baker-Campbell-Hausdorff formula:

$$\begin{aligned}
M^s_{01} M^s_{21} &= e^{i\pi/4} M^s_{21} M^s_{01} \\
[M^s_{x'x}, e^{-i\phi_2(1)}] &= 0
\end{aligned} \tag{5.148}$$

With these formulas, along with the identity $M^s_{xx'} = (M^s_{x'x})^{-1}$, we can rewrite $|\widetilde{1}\rangle$ as:

$$|\widetilde{1}\rangle = e^{i\pi/2} M^s_{32} M^s_{21} e^{-i\phi_2(1)} M^s_{01} |s_1\rangle \tag{5.149}$$

Likewise, we can simplify $|\widetilde{2}\rangle$ as:

$$|\widetilde{2}\rangle = -M^s_{32} M^s_{21} e^{-i\phi_2(1)} M^s_{01} |s_1\rangle \tag{5.150}$$

Therefore, $|\widetilde{1}\rangle = -i|\widetilde{2}\rangle$ and hence

$$\widetilde{F}(s,s,s) = \langle\widetilde{2}|\widetilde{1}\rangle = -i \tag{5.151}$$

In the same way, one can check that all other values of $\widetilde{F}$ are 1 for this model, i.e. $\widetilde{F}(g,h,k) = 1$, for all other choices of $g,h,k \in \{1,s\}$.

5.5 Antiunitary symmetries

So far we have focused on the case where the symmetry group G is *unitary*. In this section, we consider the more general case where G contains both unitary and antiunitary symmetry transformations. When we introduce this formalism, we will assume that the group is discrete, but we will have to make a slight modification for our example which has a continuous symmetry group.

5.5.1 Supercohomology data

We start by reviewing the structure of the symmetry group and the supercohomology data for systems with antiunitary symmetries.

As in the unitary case, we think of the symmetry group G as a $\mathbb{Z}_2$ extension of $G_0 = G/\mathbb{Z}_2^F$. We label the elements of of G as ordered pairs $[g,s]$ where $g \in G_0$ and $s \in \mathbb{Z}_2 = \{0,1\}$.

The group multiplication law is again described by a 2-cocycle $\lambda : G_0 \times G_0 \to \mathbb{Z}_2$ and is of the form given in (Eq. 5.1). As before we focus on symmetry transformations corresponding to group elements of the form $[g, 0]$ ($g \in G_0$) and we use the abbreviation $U^g \equiv U^{[g,0]}$. These transformations obey the same same algebra (Eq. 5.4) as in the unitary case. We again use a labeling convention where $U^1 \equiv \mathbb{I}$, and where $\lambda(1, g) = 0$.

One new element in the general case is that some elements of G correspond to antiunitary symmetries while others correspond to unitary symmetries. This notion of unitary/antiunitary group elements can be naturally extended to elements of the quotient group $G_0 = G/\mathbb{Z}_2^F$ (since fermion parity is a unitary symmetry).

Relatedly, in the general case, it is useful to define a group action of G_0 on $U(1)$ as follows: for any $g \in G_0$ and $\omega = e^{i\theta} \in U(1)$, the action of g on ω is given by

$$g\omega = \begin{cases} \omega^* & g \text{ antiunitary} \\ \omega & g \text{ unitary} \end{cases} \tag{5.152}$$

In other words, antiunitary elements of G_0 act on $U(1)$ by complex conjugation, while unitary elements of G_0 act trivially.

Just like the unitary case, the supercohomology data consists of a pair of functions $\rho : G_0 \times G_0 \to \mathbb{Z}_2$ and $\nu : G_0 \times G_0 \times G_0 \to U(1)$. As before, this pair of functions (ρ, ν) obeys certain constraints and is well-defined up to a certain equivalence relation. However, these constraints take a modified form, namely

$$\begin{aligned} \rho(g, h) + \rho(gh, k) &= \rho(h, k) + \rho(g, hk) \\ \frac{\nu(g, h, k)\nu(g, hk, l)[g\nu(h, k, l)]}{\omega(gh, k, l)\nu(g, h, kl)} &= (-1)^{(\rho(g,h)+\lambda(g,h))\rho(k,l)} \end{aligned} \tag{5.153}$$

where $g\nu$ denotes the group action (5.152). The equivalence relation is also modified: we

say that $(\rho, \nu) \sim (\rho', \nu')$ if

$$\rho'(g,h) - \rho(g,h) = \mu(g) + \mu(h) - \mu(gh) + s\lambda(g,h) \tag{5.154}$$

and

$$\begin{aligned}\frac{\nu'(g,h,k)}{\nu(g,h,k)} &= \frac{\alpha(gh,k)\alpha(g,h)}{\alpha(g,hk)[g\alpha(h,k)]} \\ &\quad \cdot (-1)^{(\rho(g,h)+\lambda(g,h))\mu(k)+\mu(g)(\rho(h,k)+(d\mu)(h,k))}\end{aligned} \tag{5.155}$$

for some function $\mu : G_0 \to \mathbb{Z}_2$ and $\alpha : G_0 \times G_0 \to U(1)$, and $s \in \mathbb{Z}_2$. As before, $(d\mu)(h,k) = \mu(h) + \mu(k) - \mu(hk)$, and $g\alpha$ denotes the group action (5.152).

5.5.2 Outline of procedure

The procedure for computing anomalies in the general case is exactly the same as the unitary case. As before, the first step is to choose an (edge) Hamiltonian H that breaks the G_0-symmetry spontaneously and completely. This Hamiltonian H has $|G_0|$ ground states which we label by $|\Omega; g\rangle$ with $g \in G_0$. The next step is to define domain wall states, fermion operators γ_x, and domain wall movement and splitting operators, $M^{\boldsymbol{a}}_{x'x}$ and $S(\boldsymbol{a}, \boldsymbol{b})$. Again, we use exactly the same definitions as in Sec. 5.3.3.

The last step is to compute the F-symbol for the domain walls. We use the same definition as before, namely $F(\boldsymbol{a}, \boldsymbol{b}, \boldsymbol{c}) = \langle 2|1\rangle$ where states $|1\rangle$ and $|2\rangle$ are defined as in Eq. 5.49. We then compute $\nu(g,h,k)$ from F just as before, namely using $\nu(g,h,k) = F((g,0),(h,0),(k,0)$ or $\nu(g,h,k) = \widetilde{F}(g,h,k)$ where $\widetilde{F}$ is defined as in Sec. 5.3.4.

The only new element in the antiunitary case involves the properties of the F-symbol. In particular, in the general antiunitary case, one can show that F obeys a *modified* pentagon

identity

$$F(\boldsymbol{a},\boldsymbol{b},\boldsymbol{c})F(\boldsymbol{a},\boldsymbol{bc},\boldsymbol{d})[gF(\boldsymbol{b},\boldsymbol{c},\boldsymbol{d})] = F(\boldsymbol{ab},\boldsymbol{c},\boldsymbol{d})F(\boldsymbol{a},\boldsymbol{b},\boldsymbol{cd}) \tag{5.156}$$

where $\boldsymbol{a},\boldsymbol{b},\boldsymbol{c},\boldsymbol{d}$ are type g,h,k,l domain walls respectively. The ambiguity in F is also modified in the antiunitary case: while the relabeling transformation (Eq. 5.97) remains the same as before, the gauge transformations associated with the movement and splitting operators are now of the form

$$\begin{aligned} F((g,s),(h,t),(k,r)) \to F((g,s),(h,t),(k,r)) \\ \cdot \frac{\alpha(gh,k)\alpha(g,h)}{\alpha(g,hk)[g\alpha(h,k)]} \end{aligned} \tag{5.157}$$

As in the unitary case, the modified pentagon identity and gauge transformations for F imply the modified constraints and ambiguities in ν (Eqs. 5.153 and 5.155).

For a derivation of the modified pentagon identity, see Appendix 7.7; we discuss the modified gauge transformation in the next subsection.

5.5.3 Checking the microscopic definition

In this section, we show that different choices of movement and splitting operators give the same F up to the modified gauge transformation (5.157). These results, together with the derivation of the twisted pentagon identity discussed in Appendix 7.7, guarantee that our procedure produces well-defined supercohomology data.

A key result which we will need in our derivation is the following identity, which generalizes Eq. 5.34. Let $\mathcal{O}$ be any operator that is invariant under all the symmetries and is supported near a domain wall $\boldsymbol{a}$ at point x. We claim that

$$\langle ..., \boldsymbol{a}_x, ... | \mathcal{O} | ..., \boldsymbol{a}_x, ... \rangle = g_L \langle \boldsymbol{a}_x | \mathcal{O} | \boldsymbol{a}_x \rangle \tag{5.158}$$

where g_L is the product of all G_0 components of domain walls to the left of x, and where the expression on the right hand side is defined by the group action (5.152). To derive this identity, note that

$$\begin{aligned}\langle ..., \boldsymbol{a}_x, ...|\mathcal{O}|..., \boldsymbol{a}_x, ...\rangle &= \langle \boldsymbol{a}_x; g_L|\mathcal{O}|\boldsymbol{a}_x; g_L\rangle \\ &= \langle U^{g_L}\boldsymbol{a}_x|\mathcal{O}|U^{g_L}\boldsymbol{a}_x\rangle \\ &= g_L\langle \boldsymbol{a}_x|\mathcal{O}|\boldsymbol{a}_x\rangle \end{aligned} \tag{5.159}$$

Here, the first equality follows from Eq. 5.29, while the second equality follows from the definition, $|\boldsymbol{a}_x; g_L\rangle = U^{g_L}|\boldsymbol{a}_x\rangle$. The third equality follows from the fact that $\mathcal{O}$ commutes with U^{g_L} together with the defining property of unitary/anti-unitary operators, namely $\langle U^g v|U^g w\rangle = g\langle v|w\rangle$.

With Eq. (5.158) in hand, we are now ready to show that different choices of movement and splitting operators lead to the same F up to the transformation (5.157). Suppose we change the movement and splitting operators in an arbitrary way:

$$M^{\boldsymbol{a}}_{x'x} \to M'^{\boldsymbol{a}}_{x'x}, \qquad S(\boldsymbol{a}, \boldsymbol{b}) \to S'(\boldsymbol{a}, \boldsymbol{b}) \tag{5.160}$$

Similarly to the unitary case, the definition of movement and splitting operators implies that

$$\begin{aligned} M'^{\boldsymbol{a}}_{x'x}|\boldsymbol{a}_x\rangle &= e^{i\theta_{x'x}(g)} M^{\boldsymbol{a}}_{x'x}|\boldsymbol{a}_x\rangle \\ S'(\boldsymbol{a}, \boldsymbol{b})|\boldsymbol{a}\boldsymbol{b}_1\rangle &= e^{i\phi(g,h)} S(\boldsymbol{a}, \boldsymbol{b})|\boldsymbol{a}\boldsymbol{b}_1\rangle \end{aligned} \tag{5.161}$$

where $\theta_{x'x}(g)$ and $\phi(g, h)$ are real valued functions. Notice that these functions are functions of elements of G_0, not D due to our phase fixing conventions Eqns. 5.45,5.48. Likewise, for

the multi-domain wall states,

$$M'^{\boldsymbol{a}}_{x'x}|..., \boldsymbol{a}_x, ...\rangle = \omega_1 \cdot M^{\boldsymbol{a}}_{x'x}|..., \boldsymbol{a}_x, ...\rangle \tag{5.162}$$

$$S'(\boldsymbol{a}, \boldsymbol{b})|..., \boldsymbol{a}\boldsymbol{b}_1, ...\rangle = \omega_2 \cdot S(\boldsymbol{a}, \boldsymbol{b})|..., \boldsymbol{a}\boldsymbol{b}_1, ...\rangle \tag{5.163}$$

for some $U(1)$ phases, ω_1, ω_2. To find the relation between ω_1, ω_2 and $e^{i\theta_{x'x}(g)}, e^{i\phi(g,h)}$, we multiply both sides of Eq. (5.162) by $\langle ..., \boldsymbol{a}_x, ...|(M^{\boldsymbol{a}}_{x'x})^\dagger$, and then we apply (5.158) to derive

$$\begin{aligned}
\omega_1 &= \langle ..., \boldsymbol{a}_x, ...|(M^{\boldsymbol{a}}_{x'x})^\dagger M'^{\boldsymbol{a}}_{x'x}|..., \boldsymbol{a}_x, ...\rangle \\
&= g_{L,x}\langle \boldsymbol{a}_x|(M^{\boldsymbol{a}}_{x'x})^\dagger M'^{\boldsymbol{a}}_{x'x}|\boldsymbol{a}_x\rangle \\
&= g_{L,x}e^{i\theta_{x'x}(g)}
\end{aligned} \tag{5.164}$$

where $g_{L,x}$ is the product of all of the G_0 components of domain walls to the left of x. By the same reasoning,

$$\omega_2 = g_{L,1}e^{i\phi(g,h)} \tag{5.165}$$

where $g_{L,1}$ is the product of all G_0 parts of domain walls to the left of the point 1.

Substituting (5.164) and (5.165) into (5.162-5.163), we derive

$$\begin{aligned}
M'^{\boldsymbol{a}}_{x'x}|..., \boldsymbol{a}_x, ...\rangle &= (g_{L,x}e^{i\theta(g)_{x'x}})M^{\boldsymbol{a}}_{x'x}|..., \boldsymbol{a}_x, ...\rangle \\
S'(\boldsymbol{a}, \boldsymbol{b})|..., \boldsymbol{a}\boldsymbol{b}_1, ...\rangle &= (g_{L,1}e^{i\phi(g,h)})S(\boldsymbol{a}, \boldsymbol{b})|..., \boldsymbol{a}\boldsymbol{b}_1, ...\rangle
\end{aligned} \tag{5.166}$$

Next, plugging (5.166) into the definition of F (5.49-5.50), we obtain

$$F'((g,s),(h,t),(k,r)) = F((g,s),(h,t),(k,r)) \cdot \frac{e^{i\phi(g,h)}e^{i\phi(gh,k)}\left(ge^{i\theta_{12}^{h}}\right)}{\left(ge^{i\phi(h,k)}\right)e^{i\phi(g,hk)}\left(ge^{i\theta_{12}^{hk}}\right)} \tag{5.167}$$

This transformation matches the restricted gauge transformation (5.157) with

$$\alpha(g,h) = e^{i\phi(g,h)}\left(ge^{i\theta_{12}^{h}}\right) \tag{5.168}$$

This is exactly what we want: different choices of movement and splitting operators lead to the same F up to the transformation (5.157).

5.5.4 Topological Insulator

Edge theory

Like the example from Sec. 5.4.2, the edge theory is a chiral boson edge theory with two counterpropagating chiral boson modes. These modes are described by two fields $\phi_\uparrow, \phi_\downarrow$ obeying the commutation relations

$$\begin{aligned}[\phi_\uparrow(x), \partial_y\phi_\uparrow(y)] &= 2\pi i\delta(x-y) \\ [\phi_\downarrow(x), \partial_y\phi_\downarrow(y)] &= -2\pi i\delta(x-y)\end{aligned} \tag{5.169}$$

with all other commutators of this form vanishing. As in Sec. 5.4.2, we are using a normalization convention where $e^{\pm i\phi_\uparrow}$ and $e^{\pm i\phi_\downarrow}$ are the fermion creation and annihilation operators on each mode. Also, as in Sec. 5.4.2, the local operators $\mathcal{O}$ in this edge theory consist of arbitrary derivatives and/or products of the fermion operators $\{e^{\pm i\phi_\uparrow}, e^{\pm i\phi_\downarrow}\}$.

To complete the edge theory, we need to specify the symmetry transformations. Before

doing that, we first review the structure of the symmetry group G and and the quotient $G_0 = G/\mathbb{Z}_2^F$. We start with G_0, and then define G as an appropriate $\mathbb{Z}_2$ extension of G_0. The group G_0 is generated by two types of group elements: $\{r_\alpha, t\}$ where the index α runs over the real numbers. Here, r_α can be thought of as the $U(1)$ symmetry transformation $e^{i\alpha Q}$, while t corresponds to the antiunitary time reversal transformation T. These group elements obey the following relations:

$$\begin{aligned} r_\alpha \cdot r_\beta = r_{\alpha+\beta}, \quad t \cdot r_\alpha = r_{-\alpha} \cdot t, \\ r_\pi = t^2 = 1, \end{aligned} \tag{5.170}$$

(Here, the reason why the third equation is correct is that we are discussing the group $G_0 = G/\mathbb{Z}_2^F$ so we effectively have $e^{i\pi Q} = T^2 = 1$).

A useful way to parameterize the elements of G_0 is to write each element $g \in G_0$ as a product $g = r_\alpha t^k$ where $0 \leq \alpha < \pi$ and $k \in \{0, 1\}$. One can check that this parameterization is one-to-one. This allows us to define three real valued functions on G_0 which will be useful below:

$$\sigma(g) = (-1)^k, \quad \tau(g) = \frac{k}{2}, \quad \mu(g) = \frac{\alpha}{\pi}, \tag{5.171}$$

Note that $\sigma(g) = \pm 1$, depending on whether g is unitary or antiunitary.

With this notation, the symmetry group G is given by the $\mathbb{Z}_2$ extension of G_0 defined by

$$\lambda(g, h) = p(g, h) + q(g, h) \tag{5.172}$$

where

$$\begin{aligned} p(g,h) &= \tau(g) + \tau(h) - \tau(gh) \\ q(g,h) &= \mu(g) + \sigma(g)\mu(h) - \mu(gh) \end{aligned} \tag{5.173}$$

While these formulas may look complicated, they follow straightforwardly from the fact that, in the symmetry group G, the fermion parity operator is identified with t^2 and r_π.

Having defined the relevant symmetry groups, we are now ready to describe the symmetry transformations U^g. For this purpose, it suffices to describe the action of the generators U^{r_α} and U^t on the basic fields $\phi_\uparrow, \phi_\downarrow$. Denoting these operators by $U^\alpha \equiv U^{r_\alpha}$ and $T \equiv U^t$ for brevity, we have

$$\begin{aligned} U^\alpha \phi_\uparrow (U^\alpha)^{-1} &= \phi_\uparrow + \alpha \\ U^\alpha \phi_\downarrow (U^\alpha)^{-1} &= \phi_\downarrow - \alpha \\ T \phi_\uparrow T^{-1} &= \phi_\downarrow \\ T \phi_\downarrow T^{-1} &= \phi_\uparrow - \pi \end{aligned} \tag{5.174}$$

Calculation of anomalies

The first step to calculating the anomaly is to choose an edge Hamiltonian that breaks the symmetry. However, since this is a continuous symmetry, we will break the symmetry explicitly rather than spontaneously in accordance with Ref. [70]. We will then identify the ground state with $|\Omega; 1\rangle$ and define the remaining $|\Omega; g\rangle$ by applying symmetry operators to $|\Omega; 1\rangle$. The rest of the formalism will be applied just as in the discrete case.

To find a symmetry broken state, we find it convenient to first introduce some auxiliary degrees of freedom into our edge theory. We will then break the symmetry of this enlarged edge theory.

To begin, consider the following chiral boson theory described by two fields θ, φ obeying commutation relations

$$[\theta(x), \partial_y \varphi(y)] = 2\pi i \delta(x-y)$$

We assume that the symmetry acts on θ, φ in the following way:

$$\begin{aligned} U^\alpha \theta (U^\alpha)^{-1} &= \theta - 2\alpha \\ U^\alpha \varphi (U^\alpha)^{-1} &= \varphi \\ T\theta T^{-1} &= -\theta \\ T\varphi T^{-1} &= \varphi \end{aligned} \tag{5.175}$$

Importantly, the θ, φ chiral boson theory is *not* anomalous – that is, it can be realized by a one dimensional lattice boson system with on-site symmetry. One way to see this is to note that the above chiral boson theory is the standard low energy description of the 1D XXZ spin chain model where T is complex conjugation in the σ^z basis, and U^α is the $U(1)$ symmetry of the XXZ model. Alternatively, we can see that the θ, φ theory is not anomalous since it can be gapped without breaking any the symmetries, for example by the Hamiltonian $H = H_{aux} - \int dx\ V \cos(\varphi)$, where H_{aux} is defined below.

Now, since the θ, φ theory is not anomalous, we can add it to our edge theory without the anomaly. After enlarging our edge theory in this way, we then choose an edge Hamiltonian that breaks the symmetry spontaneously and completely and opens up a gap. A Hamiltonian that does the job is

$$H = H_0 + H_{aux} - \int dx (V_1 \cos(\phi_\uparrow + \phi_\downarrow) + V_2 \cos(\theta)) \tag{5.176}$$

where H_0, H_{aux} are the usual free boson Hamiltonians,

$$H_0 = \int dx \frac{v}{4\pi}[(\partial_x \phi_\uparrow)^2 + (\partial_x \phi_\downarrow)^2]$$
$$H_{aux} = \int dx \frac{1}{4\pi}[v_\theta (\partial_x \theta)^2 + v_\varphi (\partial_x \varphi)^2]$$

for some velocities $v, v_\theta, v_\varphi > 0$.

For V_1 sufficiently large and positive, the first cosine term locks $\phi_\uparrow + \phi_\downarrow = 0$, explicitly breaking the $\mathbb{Z}_2^T$ symmetry. For large enough $V_2 > 0$, the second cosine term locks $\theta = 0$ and explicitly breaks the $U(1)/\mathbb{Z}_2^F$ symmetry. These terms open up an energy gap.

For simplicity, we will consider the limit $V_{1,2} \to \infty$ in what follows. In this limit, the ground state of H is an *eigenstate* of the operators $e^{i(\phi_\uparrow(x)+\phi_\downarrow(x))}, e^{i\theta(x)}$. Following our standard labeling scheme, we denote this ground state by $|\Omega; 1\rangle$ where

$$e^{i(\phi_\uparrow(x)+\phi_\downarrow(x))}|\Omega; 1\rangle = |\Omega; 1\rangle$$
$$e^{i\theta(x)}|\Omega; 1\rangle = |\Omega; 1\rangle \tag{5.177}$$

Having defined $|\Omega; 1\rangle$, we then define the other "vacuum states" $|\Omega; g\rangle$ to be symmetry partners of $|\Omega; 1\rangle$:

$$|\Omega; g\rangle = U^g |\Omega; 1\rangle. \tag{5.178}$$

By construction, $|\Omega; g\rangle$ is a simultaneous eigenstate of $e^{i(\phi_\uparrow(x)+\phi_\downarrow(x))}$ and $e^{i\theta(x)}$:

$$e^{i(\phi_\uparrow(x)+\phi_\downarrow(x))}|\Omega; g\rangle = e^{i2\pi\tau(g)}|\Omega; g\rangle$$
$$e^{i\theta(x)}|\Omega; g\rangle = e^{i2\pi\mu(g)}|\Omega; g\rangle \tag{5.179}$$

From this, we may define the single domain wall states:

$$|g_x\rangle = (a_x^g)^\dagger |\Omega; 1\rangle \tag{5.180}$$

where

$$(a_x^g)^\dagger = e^{-i\int_x^\infty dy\ [\frac{1}{2}\tau(g)\partial_y(\phi_\uparrow - \phi_\downarrow) + \mu(g)\partial_y\varphi]} \tag{5.181}$$

To see that $|g_x\rangle$ is a valid domain wall state, note that

$$e^{i(\phi_\uparrow(x')+\phi_\downarrow(x')}|g_x\rangle = \begin{cases} |g_x\rangle & x' < x \\ e^{i2\pi\tau(g)}\ |g_x\rangle & x' > x \end{cases}$$

and

$$e^{i\theta(x')}|g_x\rangle = \begin{cases} |g_x\rangle & x' < x \\ e^{i2\pi\mu(g)}\ |g_x\rangle & x' > x \end{cases}$$

by the commutation relations between $\phi_\uparrow, \phi_\downarrow$ and θ, φ.

To proceed further, we need to define the fermion operators γ_x. We define:

$$\gamma_x = e^{i\phi_\uparrow(x)} \tag{5.182}$$

We then define the other types of domain wall states, $|(\psi g)_x\rangle$ as in Eq. 5.24

$$|(\psi g)_x\rangle = \gamma_x |g_x\rangle \tag{5.183}$$

Having defined domain wall states, the next step is to find their fusion rules. To this

end, note that the two domain wall state takes the form

$$|g_1, h_2\rangle \propto U^g (a_2^h)^\dagger (U^g)^{-1} (a_1^g)^\dagger |\Omega; 1\rangle \tag{5.184}$$

Expanding out these operators more explicitly gives

$$\begin{aligned} |g_1, h_2\rangle &= e^{-i\int_2^\infty dy\ [\frac{1}{2}\tau(h)\partial_y(\phi_\uparrow - \phi_\downarrow) + \sigma(g)\mu(h)\partial_y\varphi]} \\ &\quad \cdot e^{-i\int_1^\infty dy\ [\frac{1}{2}\tau(g)\partial_y(\phi_\uparrow - \phi_\downarrow) + \mu(g)\partial_y\varphi]} |\Omega; 1\rangle \\ &\propto e^{-i\int_2^\infty dy\ [\tau(h)\partial_y\phi_\uparrow + \sigma(g)\mu(h)\partial_y\varphi]} \\ &\quad \cdot e^{-i\int_1^\infty dy\ [\tau(g)\partial_y\phi_\uparrow + \mu(g)\partial_y\varphi]} |\Omega; 1\rangle \end{aligned} \tag{5.185}$$

Here the second line follows from the fact that $\partial_y(\phi_\uparrow + \phi_\downarrow)|\Omega; 1\rangle = 0$. At the same time, we have

$$\begin{aligned} |(gh)_1\rangle &\propto (a_1^{gh})^\dagger |\Omega; 1\rangle \\ &= e^{-i\int_1^\infty dy\ [\frac{1}{2}\tau(gh)\partial_y(\phi_\uparrow - \phi_\downarrow) + \mu(gh)\partial_y\varphi]} |\Omega; 1\rangle \\ &\propto e^{-i\int_1^\infty dy [\tau(gh)\partial_y\phi_\uparrow + \mu(gh)\partial_y\varphi]} |\Omega; 1\rangle \end{aligned} \tag{5.186}$$

Comparing $|g_1, h_2\rangle$ with $|(gh)_1\rangle$, we can see that

$$|g_1, h_2\rangle \propto O_{21} e^{ip(g,h)\phi_\uparrow(1) + q(g,h)\varphi(1)} |(gh)_2\rangle \tag{5.187}$$

where

$$O_{21} = e^{i\int_1^2 dy\ [\tau(h)\partial_y\phi_\uparrow + \sigma(g)\mu(h)\partial_y\varphi]} \tag{5.188}$$

Since O_{21} and $e^{i\varphi(1)}$ have even fermion parity while $e^{i\phi_\uparrow(1)}$ has odd fermion parity, we deduce that the two states have the same/opposite fermion parity depending on the parity of $q(g,h)$. Therefore, we conclude that

$$\rho(g,h) = p(g,h) \tag{5.189}$$

We now move on to construct movement and splitting operators. For notational convenience, we define the operator

$$X^g_{x'x} = e^{i\int_x^{x'} dy\ [\frac{1}{2}\tau(g)\partial_y(\phi_\uparrow - \phi_\downarrow) + \mu(g)\partial_y\varphi]} \tag{5.190}$$

From this, we define the movement operators $M^g_{x'x}$ for $g \in B$ and $x' > x$ as

$$M^g_{x'x} = \sum_{k=0}^{1} T^k X^g_{x'x} P^g_{x'} T^{-k}, \quad x' > x \tag{5.191}$$

where we define the projection operator

$$P^g_{x'} = \frac{1 + e^{i(\phi_\uparrow(x') + \phi_\downarrow(x'))} e^{-i2\pi\tau(g)}}{2} \tag{5.192}$$

To see that $M^g_{x'x}$ is a valid movement operator, note that it is local and symmetric by construction. Furthermore, it has the correct action on single domain wall states:

$$M^g_{x'x}|g_x\rangle = X^g_{x'x}|g_x\rangle = |g_{x'}\rangle \tag{5.193}$$

where the first equality follows from the fact that only the $k = 0$ term in (5.191) gives a nonzero result when acting on $|g_x\rangle$ and the second equality follows from the fact that $X^g_{x'x}(a^g_x)^\dagger = (a^g_{x'})^\dagger$.

Likewise, we define the reverse movement operator by

$$M^g_{x'x} = (M^g_{xx'})^\dagger, \quad x' < x \tag{5.194}$$

We now turn our attention to the splitting operators. For $g, h \in B$, define

$$S(g,h) = \sum_{k=0}^{1} T^k U^g X^h_{21} (U^g)^{-1} C(g,h) P_2^{gh} T^{-k} \tag{5.195}$$

where

$$C(g,h) = e^{iq(g,h)\varphi(1)} \tag{5.196}$$

We can see that $S(g,h)$ is symmetric in much the same way as the movement operator. We know that X^h_{21} and $C(g,h)$ are symmetric under U^α, $S(g,h)$ is fermion parity even, and that we have symmetrized over $\mathbb{Z}_2^T$. All that remains is to check that this splitting operator has the correct action on single domain wall states. To see this, note that

$$\begin{aligned} S(g,h) e^{ip(g,h)\phi_\uparrow(1)} |gh_1\rangle &= U^g X^h_{21} (U^g)^{-1} C(g,h) e^{ip(g,h)\phi_\uparrow(1)} |gh_1\rangle \\ &\propto U^g (a^h_2)^\dagger (U^g)^{-1} (a^g_1)^\dagger |\Omega; 1\rangle \\ &\propto |g_1, h_2\rangle \end{aligned} \tag{5.197}$$

Here, the first equality follows from the fact that only the $k = 1$ term in (5.195) gives a nonzero result when acting on $|gh_1\rangle$, while the second equality follows from the definition of $(a^g_x)^\dagger$. The third equality follows by noting that $U^g (a^h_2)^\dagger (U^g)^{-1} (a^g_1)^\dagger |\Omega; 1\rangle$ has the same local expectation values as $|g_1\rangle$ near $x = 1$, and the same local expectation values as $U^g |h_2\rangle$ near $x = 2$, and the same local expectation values as $U^g |\Omega; 1\rangle$ between $x = 1$ and $x = 2$.

All that remains to do before computing $\widetilde{F}(g,h,k)$ is to define $\widetilde{M}^g_{x'x}, \widetilde{S}(g,h)$. These are

defined as

$$\begin{aligned}\widetilde{M}^g_{x'x} &= M^g_{x'x} \\ \widetilde{S}(g,h) &= S(g,h)e^{ip(g,h)\phi_\uparrow(1)}\end{aligned} \tag{5.198}$$

for $g, h \in B$.

We are now ready to compute $\widetilde{F}(g,h,k)$. Using Eq. 5.51, we have

$$\begin{aligned}|\widetilde{1}\rangle &= [U^g X^h_{12}(U^g)^{-1}] \cdot X^g_{01} \cdot [U^g X^h_{21}(U^g)^{-1}] \\ &\quad \cdot \widetilde{C}(g,h) \cdot [U^{gh} X^k_{32} X^k_{21}(U^{gh})^{-1}] \cdot \widetilde{C}(g,hk)|(ghk)_1\rangle \\ |\widetilde{2}\rangle &= [U^{gh} X^k_{32}(U^{gh})^{-1}] \cdot [U^g U^h X^k_{21}(U^h)^{-1}\widetilde{C}(h,k)(U^g)^{-1}] \\ &\quad \cdot [U^g X^{hk}_{12}(U^g)^{-1}] \cdot X^g_{01} \cdot [U^g X^{hk}_{21}(U^g)^{-1}] \\ &\quad \cdot \widetilde{C}(g,hk)|(ghk)_1\rangle\end{aligned} \tag{5.199}$$

where $\widetilde{C}(g,h)$ is defined by

$$\begin{aligned}\widetilde{C}(g,h) &= C(g,h)e^{ip(g,h)\phi_\uparrow(1)} \\ &= e^{iq(g,h)\varphi(1)+ip(g,h)\phi_\uparrow(1)}\end{aligned} \tag{5.200}$$

We can simplify $|\widetilde{2}\rangle$ using the following identity which follows from the fact that $U^g U^h$ differs from U^{gh} by at most a fermion parity transformation, and that X^k_{21} has even fermion parity:

$$U^g U^h X^k_{21}(U^h)^{-1}(U^g)^{-1} = U^{gh} X^k_{21}(U^{gh})^{-1} \tag{5.201}$$

Using this identity, we can rewrite $|\widetilde{2}\rangle$ as

$$\begin{aligned}|\widetilde{2}\rangle &= [U^{gh}X^k_{32}X^k_{21}(U^{gh})^{-1}]\cdot[U^g\widetilde{C}(h,k)(U^g)^{-1}]\\ &\cdot[U^gX^{hk}_{12}(U^g)^{-1}]\cdot X^g_{01}\cdot[U^gX^{hk}_{21}(U^g)^{-1}]\\ &\cdot\widetilde{C}(g,hk)|(ghk)_1\rangle\end{aligned} \tag{5.202}$$

Next we use the fact that the $X^g_{xx'}$ operators commute with each other and their symmetry partners, together with identity $(X^\alpha_{xx'})^{-1}=X^\alpha_{x'x}$ to simplify these two states to:

$$\begin{aligned}|\widetilde{1}\rangle &= X^g_{01}\cdot\widetilde{C}(g,h)\cdot[U^{gh}X^k_{32}X^k_{21}(U^{gh})^{-1}]\\ &\cdot\widetilde{C}(gh,k)|(ghk)_1\rangle\\ |\widetilde{2}\rangle &= [U^{gh}X^k_{32}X^k_{21}(U^{gh})^{-1}]\cdot[U^g\widetilde{C}(h,k)(U^g)^{-1}]\\ &\cdot X^g_{01}\cdot\widetilde{C}(g,hk)|(ghk)_1\rangle\end{aligned} \tag{5.203}$$

In order to compare the two states, it is useful to reorder the operators so that all the X's are on the left. To do this, we use the following commutation relation, which follows from the Baker-Campbell-Hausdorff formula:

$$e^{in\phi_\uparrow(1)}X^g_{x1}=e^{-i\pi n\tau(g)\mathrm{sgn}(x-1)/2}X^g_{x1}e^{in\phi_\uparrow(1)} \tag{5.204}$$

Using this relation, we can rewrite these two states as

$$\begin{aligned}|\widetilde{1}\rangle &= e^{i\alpha}X^g_{01}U^{gh}X^k_{32}X^k_{21}(U^{gh})^{-1}\\ &\cdot\widetilde{C}(g,h)\widetilde{C}(g,hk)|(ghk)_1\rangle\\ |\widetilde{2}\rangle &= e^{i\beta}X^g_{01}U^{gh}X^k_{32}X^k_{21}(U^{gh})^{-1}\\ &\cdot U^g\widetilde{C}(h,k)(U^g)^{-1}\widetilde{C}(g,hk)|(ghk)_1\rangle\end{aligned} \tag{5.205}$$

where

$$\alpha = -\frac{\pi}{2}\tau(k)p(g,h), \quad \beta = \frac{\pi}{2}\tau(g)p(h,k) \tag{5.206}$$

Next, using the definition (5.200), one can check that

$$\begin{aligned}\widetilde{C}(g,h)\widetilde{C}(g,hk)|(ghk)_1\rangle = \\ e^{i\delta}U^g\widetilde{C}(h,k)(U^g)^{-1}\widetilde{C}(g,hk)|(ghk)_1\rangle\end{aligned} \tag{5.207}$$

where

$$\delta = \pi[\tau(g)p(h,k) + \mu(g)p(h,k)] \tag{5.208}$$

We conclude that $|\widetilde{1}\rangle = e^{i\delta+i\alpha-i\beta}|\widetilde{2}\rangle$ so that

$$\begin{aligned}\widetilde{F}(g,h,k) &= \langle\widetilde{2}|\widetilde{1}\rangle \\ &= e^{i\delta+i\alpha-i\beta} \\ &= e^{i\pi p(h,k)\mu(g)}\end{aligned} \tag{5.209}$$

Therefore, the data which describes the (2+1)D topological insulator is

$$\begin{aligned}\rho(g,h) = p(g,h) = \tau(g) + \tau(h) - \tau(gh) \\ \nu(g,h,k) = e^{i\pi p(h,k)\mu(g)}\end{aligned} \tag{5.210}$$

This completes the application of our formalism to a field theory of (2+1)D topological insulators.

5.6 Conclusion

In this paper, we have presented a general procedure for calculating anomalies in (1D) fermionic SPT edge theories which can be classified by supercohomology. Our procedure takes as input a fermionic SPT edge theory and produces as output a pair (ρ, ν) which specifies the anomaly carried by the edge theory. This data is enough to specify the bulk fermionic SPT on which this boundary theory can exist. An important feature of our procedure is that, unlike previous approaches[39], it applies to general fermionic SPT edge theories with both unitary and antiunitary symmetries. Although we have not presented it here, this can also be generalized to theories which go beyond the supercohomological classification[71]. One future direction is to show that this formalism can be applied to all beyond supercohomology phases of fermionic SPTs studied in Refs. [146, 147, 8, 1].

Another interesting direction for future work would be to generalize our approach to (1D) edge theories of general invertible phases [8, 1]. Since these theories, in general, have a non-zero central charge, our treatment of domain walls as gapped excitations would need to be modified. However, since the data associated with these phases are similar to the theories studied in this paper, we have hope that we could still define fusion rules and an F-symbol for some kind of domain walls on the boundary theory.

Furthermore, these invertible fermionic phases have been shown to be classified by their bosonic shadows [8]. These bosonic shadows are interesting to study in their own right because the bosonic shadows correspond to relatively simple SETs. In particular, they are $\mathbb{Z}_2$ topological orders which are enriched by G_0 symmetry. Understanding the microscopic definitions of the fermionic SPT data in this context could lead to microscopic definitions of all of the SET data. Progress on this problem has been made in Ref. [34].

Finally, spatial symmetries are beyond the reach of our current formalism. It is known that there are four, rather than two, SPTs with the symmetries of the topological insulator if one includes translation symmetry [66]. These extra phases include the weak topological

insulator. It would be interesting to see if our approach can be extended in some way to calculate the data required to identify fermionic SPTs with spatial symmetries [128, 134] from their boundary theories.

ACKNOWLEDGMENTS

The authors thank Maxim Metlitski and Robert Jones for sharing work which was unpublished at the time [65]. KK thanks Daniel Bulmash and Yu-An Chen for interesting discussions about fermionic SPTs.

CHAPTER 6

CONCLUSION

The connection between topological phases of matter and the "topological data" which describe and classify them is a prominent theme in modern condensed matter physics. In this dissertation, I have shown how we can understand the physical interpretation of this data by constructing their precise definitions in microscopic models of topological phases of matter. I have done this for intrinsic topological order as well as (2+1)D Symmetry Protected topological phases.

In the case of intrinsic topological order, I have shown how to extract the anyon data, particularly the F and R-symbols from a microscopic model. This allows us to give a physical interpretation of this data in any microscopic model, at least in principle.

In the case of SPT phases, I have shown how to calculate the topological data which classifies the bulk theory from a microscopic boundary theory. Since bosonic and fermionic SPTs have different classification schemes, I have shown how to do this in each case. In the bosonic case, this amounts to calculating the cocycle as the F-symbol of domain walls on the boundary. In the fermionic case, the fusion rules of boundary domain walls, and the F-symbol of those domain walls determine the data. This method is applicable for both unitary and antiunitary symmetries and for discrete symmetries as well as continuous symmetries. In an upcoming work [71], Michael Levin and I will extend this method to fermionic SPTs beyond supercohomology as well.

In the coming decade, we have a massive and exciting challenge ahead. We have a very good understanding of the classification of topological phases of matter in (2+1)D. We know how to write models of these phases of matter [88] and we know how to describe these phases of matter in the robust mathematical frameworks of category theory and cohomology [74, 75, 28]. Although there are a few remaining theoretical mysteries in the theory of (2+1)D topological phases, the majority of the work still do be done involves experimentation and

applications to quantum computation. However, in (3+1)D, we are faced with a grand array of new problems. In this case, it is unclear how to formulate all possible data associated with intrinsic topological phases. For example, we do not have a full classification of the braided fusion 2-categories which may be required to understand intrinsic topological order in (3+1)D [64, 77, 76].

Furthermore, the classification of fractonic phases of matter is wide open. Although we understand some specific constructions of fractons [113], and we know some of field theoretic principles that will be required to describe them [121, 122, 123], we lack a comprehensive understanding of the essential fractonic phases of matter that can exist. In a similar mode of thought as Ref. [104], we need to understand what type of math is most natural to complete the analogy of "symmetry breaking is to group theory as topological phases are to category theory as fractons are to ...."

I believe that there is also more work to be done along the lines of this thesis. That is, there is a general line of research to be performed which asks how to interpret pieces of topological data in terms of microscopic models, such as models of Symmetry Enriched Topological phases [80, 7, 132, 34], SPTs with spatial symmetries [128, 134, 97], or higher dimensional SPTs [28]. We can then use these microscopic definitions to better understand these theories. Fortunately, in these theories, there are proposals for how the topological data is structured. However, as I mentioned, there are many topological theories for which we still need a general framework. As these frameworks become known and better understood, we will progressively be able to ask more and more systems the question:

"What is this?"

CHAPTER 7

APPENDIX

7.1 Pentagon identity

In this appendix, we show that the Abelian F-symbol, defined in Eq. 3.12, satisfies the pentagon identity. Here, the main reason we focus on Abelian anyons is to simplify the presentation: the generalization to the non-Abelian case is straightforward.

The first step in the proof is to pick a nice phase convention for the movement operators $M^a_{x'x}$. Specifically, we choose the phases of the movement operators so that

$$\begin{aligned} M^a_{xx'} M^a_{x'x} |a_x\rangle &= |a_x\rangle \\ M^a_{x''x'} M^a_{x'x} |a_x\rangle &= M^a_{x''x} |a_x\rangle \end{aligned} \tag{7.1}$$

With this phase convention, our space-time diagrams satisfy the following "topological invariance" property: consider any process, P, composed out of a sequence of movement and splitting operators acting on an initial state

$$|i\rangle = |..., a_x, b_{x'}, c_{x''}, ...\rangle. \tag{7.2}$$

For any such process, we can draw a corresponding space-time diagram. Next, consider a second process, P', that acts on the same initial state, $|i\rangle$, and that leads to the same final configuration of anyons. Again, we can draw a corresponding space-time diagram. The topological invariance property says that if these two space-time diagrams can be continuously deformed into one another while fixing the endpoints, then the two processes produce the same final states with the same phases. That is,

$$P|i\rangle = P'|i\rangle \tag{7.3}$$

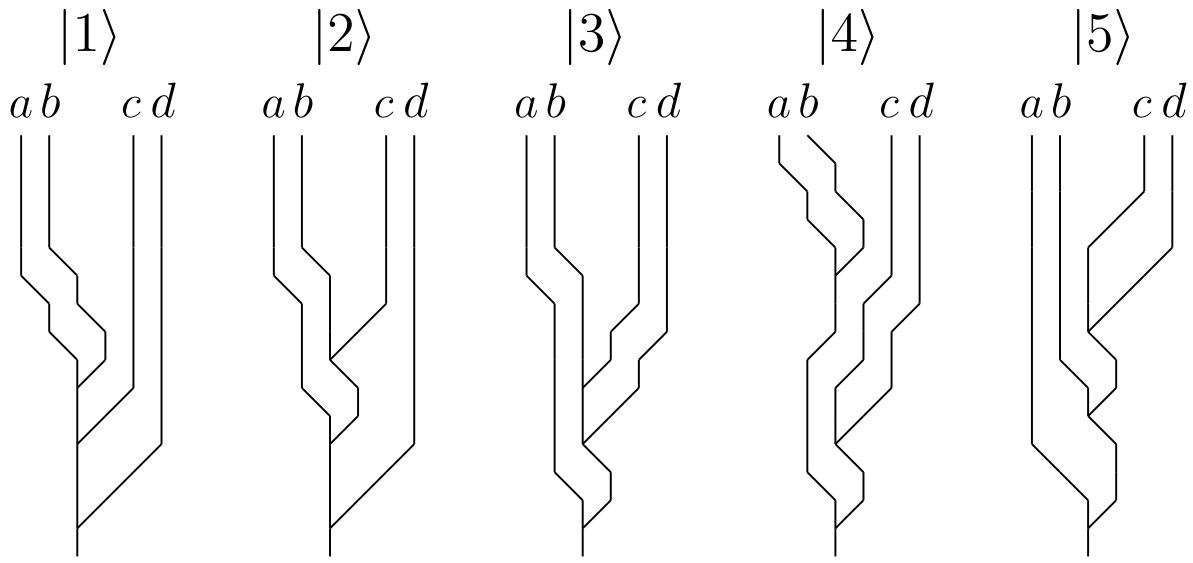

Figure 7.1: Five microscopic processes used to derive the pentagon identity.

We prove this result at the end of this section.

Using the above topological invariance property (7.33), it is easy to show that the F-symbol defined in (3.12) satisfies the pentagon identity. The proof follows the same line of reasoning as the argument in Sec. 3.3.1. Consider the five processes shown in Fig. 7.1. Let us denote the final states of these processes by $|1\rangle, |2\rangle, |3\rangle, |4\rangle, |5\rangle$. Notice that these states are the same up to a phase since they contain the same four anyons, a, b, c, d, at the same four points. The idea of the proof is to compute the relative phase between states $|1\rangle$ and $|5\rangle$ in two different ways. In the first calculation, we note that

$$\begin{aligned} |1\rangle &= F(a,b,c)|2\rangle \\ |2\rangle &= F(a,bc,d)|3\rangle \\ |3\rangle &= F(b,c,d)|5\rangle \end{aligned} \tag{7.4}$$

Here, the first relation follows by noting that the diagrams corresponding to $|1\rangle$ and $|2\rangle$ differ by a microscopic F-move (see Fig. 7.2). Likewise, the second relation follows in two steps (see Fig. 7.3): in the first step, we use topological invariance to redraw the space-time

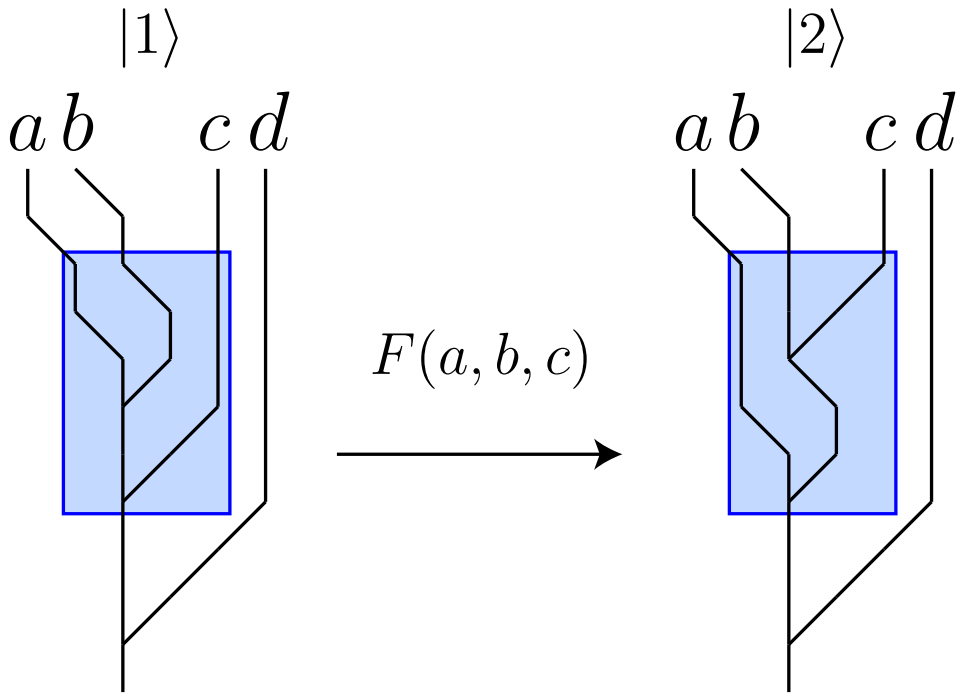

Figure 7.2: Graphical proof of $|1\rangle = F(a,b,c)|2\rangle$: the two processes are related by a microscopic F-move.

diagram corresponding to $|2\rangle$, while in the second step we related the modified diagram to $|3\rangle$ using an F-move. The third relation follows in a similar way (Fig. 7.4).

For the second calculation of the relative phase between $|1\rangle, |5\rangle$, we observe that

$$\begin{aligned} |1\rangle &= F(ab,c,d)|4\rangle \\ |4\rangle &= F(a,b,cd)|5\rangle \end{aligned} \tag{7.5}$$

Similarly to (7.4), both of these relations follow from the topological invariance property (7.33) together with the definition of F (3.12). (See Figs. 7.5-7.6 for graphical proofs). Combining (7.4) and (7.5), gives the desired pentagon identity:

$$F(a,b,c)F(a,bc,d)F(b,c,d) = F(ab,c,d)F(a,b,cd)$$

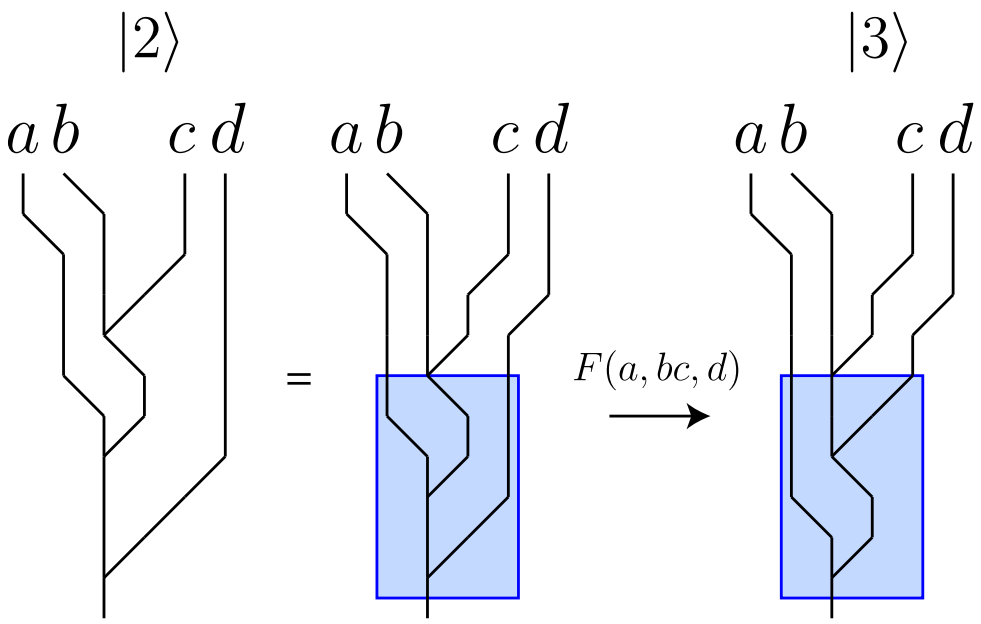

Figure 7.3: Graphical proof of $|2\rangle = F(a,bc,d)|3\rangle$. The first equality follows from topological invariance, while the second equality follows from a microscopic F-move.

To complete the argument, we now prove the topological invariance property (7.33). We begin by considering some special cases. First, we consider processes that (i) are composed only out of movement operators and (ii) return all anyons to their initial positions. We claim that any process, P, of this kind is equivalent to the identity operator in the sense that

$$P|i\rangle = |i\rangle \tag{7.6}$$

This claim follows from two properties of the movement operators. The first property is that movement operators commute when acting on non-overlapping intervals:

$$[M_{x_1x_2}, M_{x_3x_4}] = 0 \tag{7.7}$$

The second property is a multi-anyon generalization of (7.31) which follows from the locality

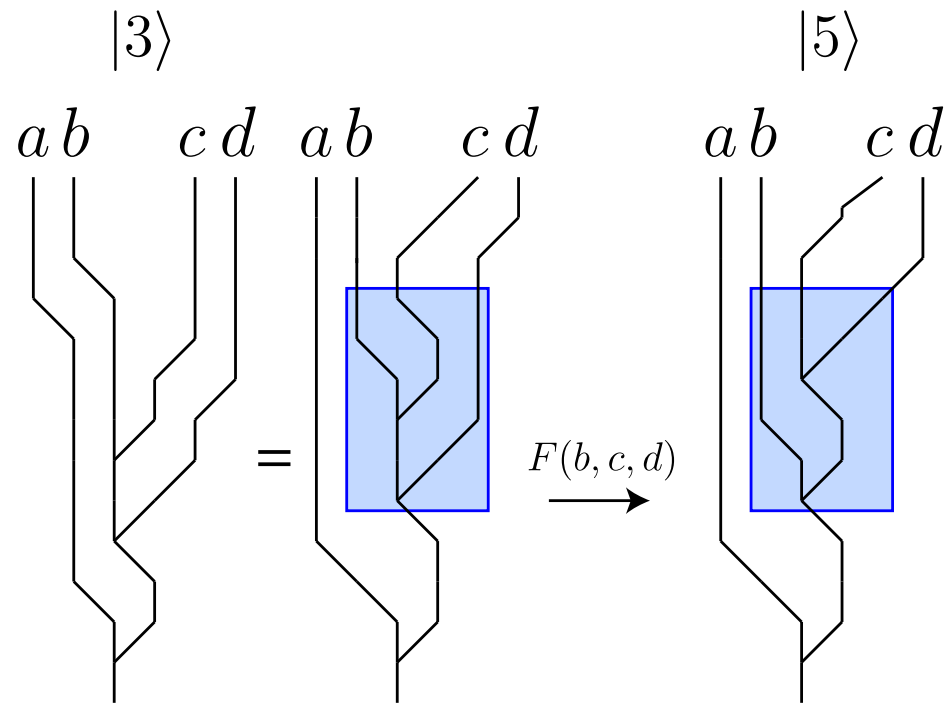

Figure 7.4: Graphical proof of $|3\rangle = F(b,c,d)|5\rangle$. The first equality follows from topological invariance, while the second follows from a microscopic F-move.

of the movement operators:

$$M^a_{xx'}M^a_{x'x}|...,a_x,...\rangle = |...,a_x,...\rangle \tag{7.8}$$

$$M^a_{x''x'}M^a_{x'x}|...,a_x,...\rangle = M^a_{x''x}|...,a_x,...\rangle \tag{7.9}$$

Here $|...,a_x,...\rangle$ is any multi-anyon state that does not have any additional anyons in the interval containing x, x' or x', x''.

To establish (7.6), it suffices to show that for any nontrivial process P, we can find a simpler process P' — i.e. a process with strictly fewer movement operators — such that $P|i\rangle = P'|i\rangle$. Once we establish the existence of P', Eq. (7.6) follows immediately since we can then simplify P repeatedly until we reduce it to the identity. To construct P', it is convenient to make two simplifying assumptions about P: (i) the positions x of the anyons are always integer-valued and (ii) all movements are of the form $M^a_{x'x}$, where $x' = x \pm 1$. (The

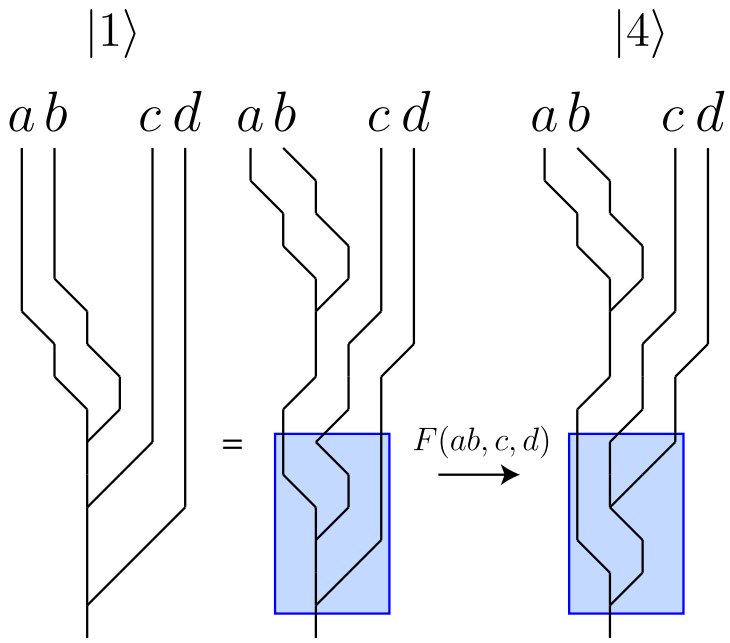

Figure 7.5: Graphical proof of $|1\rangle = F(b,c,d)|4\rangle$. The first equality follows from topological invariance, while the second follows from a microscopic F-move.

second assumption can be made without loss of generality given Eq. 7.9). Next, consider the leftmost anyon, a, with the property that, at some point during the process, a performs a movement to the right, i.e. $M^a_{x'x}$ with $x' > x$, followed later by a reverse movement $M^a_{xx'}$ with no movements of this anyon a in between. Since a is the *leftmost* anyon with this property, it is easy to see that there cannot be any movement operators that appear between $M^a_{x'x}$ and $M^a_{xx'}$ whose region of support overlaps the interval $[x, x']$. Therefore, we can use (7.7) to reorder the movement operators so that $M^a_{x'x}$ and $M^a_{xx'}$ appear one after the other. The two movement operators can then be removed from P using the identity (7.8). This gives the desired process P'. If there are *no* anyons with the above property, then we follow the same reasoning as above but we consider the *rightmost* anyon a that performs a movement to the *left*, i.e. $M^a_{x'x}$ with $x' < x$, followed later by a reverse movement $M^a_{xx'}$ with no movements of this anyon, a, in between. Again, this allows us to construct a simpler process P'.

Having established (7.6), the next step in the proof is to consider a slightly more general

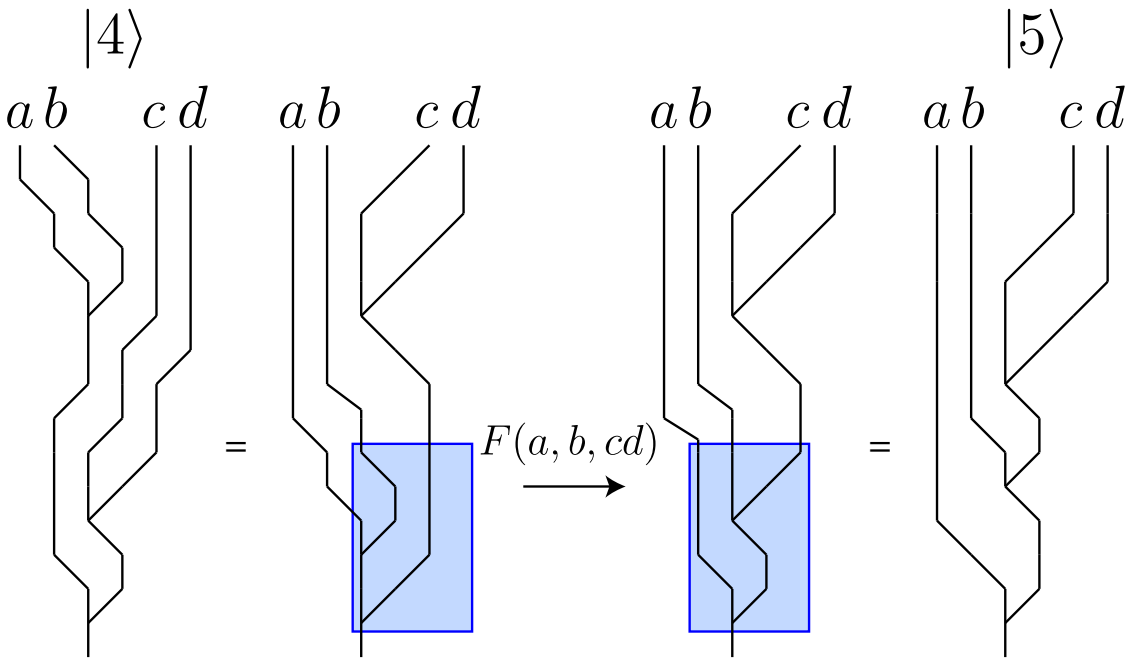

Figure 7.6: Graphical proof of $|4\rangle = F(b,c,d)|5\rangle$. The first and third equalities follow from topological invariance, while the second follows from a microscopic F-move.

set of processes: namely, processes that are composed out of movement operators but do not necessarily return the anyons to their initial positions. We claim that $P|i\rangle = P'|i\rangle$ for any two "movement-only" processes P, P' with the same initial state and same final configuration of anyons. To see this, consider the process $P^{inv}P'$, where P^{inv} is the inverse process to P — that is, the process obtained by reversing the order of the movement operators and replacing $M^a_{x'x} \to M^a_{xx'}$. By construction, $P^{inv}P'$ has the property that it returns all anyons to their original positions so we can use (7.6) to deduce that $P^{inv}P'|i\rangle = |i\rangle$. It then follows that $P|i\rangle = P'|i\rangle$, proving the claim.

We are now ready to consider general processes with both splitting and movement operators. We claim that $P|i\rangle = P'|i\rangle$ for any two processes P, P' whose spacetime diagrams can be continuously deformed into one another while fixing endpoints and preserving the time-ordered sequence of splittings. To prove this claim, it is useful to decompose P into a

product

$$P = P_1 S_1 P_2 S_2 \cdots \tag{7.10}$$

where $S_1, S_2, ...$ are splitting operators and $P_1, P_2, ...$ are movement-only processes. We decompose P' in a similar fashion, denoting the splitting operators by $S'_1, S'_2, ...$ and movement-only processes by $P'_1, P'_2, \cdots$. By assumption, $S_j = S'_j$ for every j. On the other hand $P_j \neq P'_j$ in general. Consider the special case where P_j and P'_j share the same initial anyon configuration and the same final anyon configuration for each j. In this case, it follows immediately that $P|i\rangle = P'|i\rangle$ using the above property of movement-only processes. Next, observe that the general case – where P_j and P'_j do not share the same initial and final anyon configurations – can always be reduced to this special case: given any P, P' obeying our assumption, it is not hard to construct modified processes, $\tilde{P}$ and $\tilde{P}'$ with $P|i\rangle = \tilde{P}|i\rangle$ and $P'|i\rangle = \tilde{P}'|i\rangle$ such that the corresponding movement-only processes, $\tilde{P}_j$ and $\tilde{P}'_j$, *do* share the same initial and final anyon configuration for each j. These modified processes $\tilde{P}$ and $\tilde{P}'$ can be obtained by inserting appropriate movement operators $M^a_{xx'}$ just before each splitting operator, along with their reverse movements $M^a_{x'x}$ just after the splitting operator, and using the fact that movement operators commute with splitting operators when acting on non-overlapping intervals.

At this point, we have *almost* proved the general topological invariance property (7.33), but we need one more result: we need to show that the *order* of splitting operators does not matter, i.e

$$S_L S_R |i\rangle = S_R S_L |i\rangle \tag{7.11}$$

where S_L and S_R are the two splitting processes shown in Fig. 7.7a. The identity (7.11),

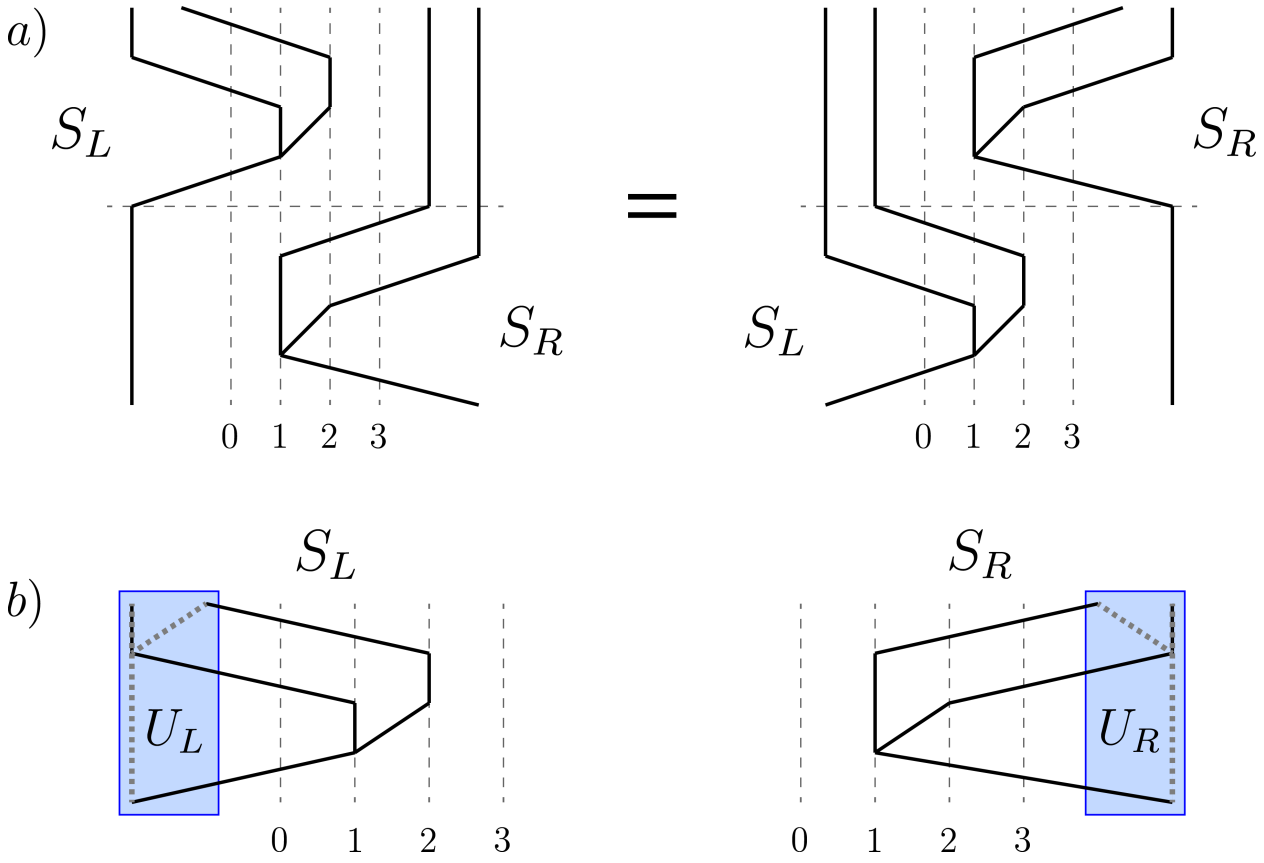

Figure 7.7: (a) Graphical representation of the identity (7.11). (b) Schematic representation of the two unitary operators U_L, U_R which are supported in the regions $x \leq 0$ and $x \geq 3$, respectively, and satisfy $U_L|i\rangle = S_L|i\rangle$ and $U_R|i\rangle = S_R|i\rangle$.

together with the claim in the previous paragraph implies topological invariance.[1]

To prove the identity (7.11), we note that neither $|i\rangle$ nor $S_L|i\rangle$ contain any anyons in the region $x > -1$, which means in particular that $|i\rangle$ and $S_L|i\rangle$ share the same expectation values for any operator supported in $x > 0$. It then follows from the properties of the Schmidt decomposition that there exists a unitary operator, U_L, supported in the complementary

1. Strictly speaking, to establish general topological invariance, one needs to prove a slight generalization of (7.11) in which S_L, S_R contain additional "spectator" anyon worldlines that do not participate in the splittings; however, this generalization of (7.11) can be proved using the same arguments as the special case (7.11).

region $x \leq 0$ such that

$$U_L|i\rangle = S_L|i\rangle \tag{7.12}$$

By the same reasoning, there exists a unitary operator, U_R, supported in the region $x \geq 3$ such that

$$U_R|i\rangle = S_R|i\rangle \tag{7.13}$$

Next, we observe that

$$[U_L, U_R] = [S_L, U_R] = [U_L, S_R] = 0 \tag{7.14}$$

since each pair of operators is supported on non-overlapping regions. Combining these identities, we derive

$$\begin{aligned} S_L S_R|i\rangle = S_L U_R|i\rangle = U_R S_L|i\rangle = U_R U_L|i\rangle = U_L U_R|i\rangle \\ S_R S_L|i\rangle = S_R U_L|i\rangle = U_L S_R|i\rangle = U_L U_R|i\rangle \end{aligned} \tag{7.15}$$

This proves the reordering identity (7.11) and completes our proof of the topological invariance property (7.33).

7.2 Hexagon equations

In this appendix, we show that our definitions of the Abelian F and R symbols obey the hexagon equations (3.87). Our proof closely follows the derivation of the pentagon identity given in Appendix 7.1 and like that derivation it is straightforward to generalize it to non-Abelian anyons.

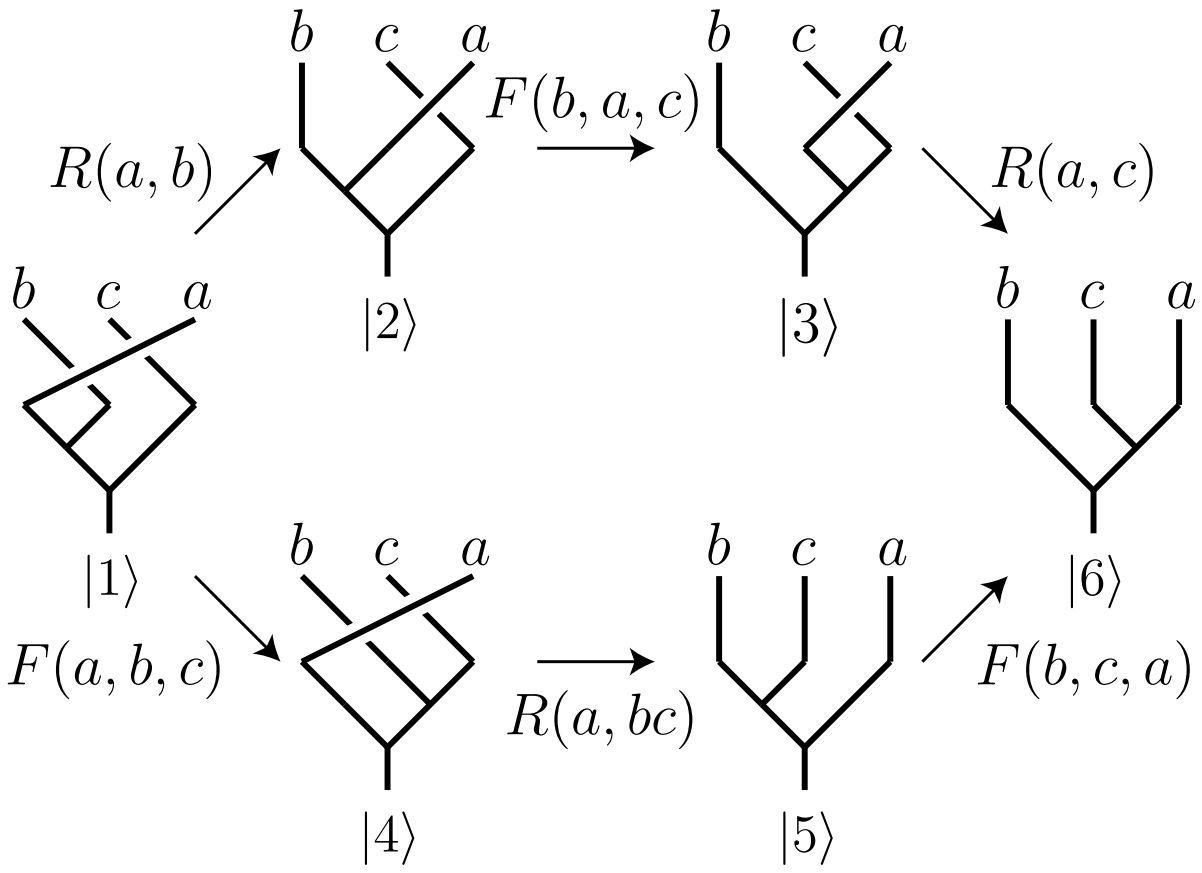

Figure 7.8: Graphical derivation of the first hexagon equation (3.87).

We will focus on the first hexagon equation since it is slightly easier to prove with our conventions. The first step of the proof is to construct *microscopic* processes that have the same structure as the six abstract processes shown in Fig. 7.8. This step is analogous to the first step of the proof in Appendix 7.1, in which we constructed the microscopic processes shown in Fig. 7.1. Just as in Fig. 7.1, we draw out explicit diagrams for these microscopic processes in Fig. 7.9. These processes are constructed so that they satisfy the following properties: (i) all six processes start in the same initial state and end with the same final particle positions; (ii) all anyon movements occur between either nearest neighbor integer points n and $n \pm 1$ or between 1 and Y; and (iii) each crossing in Fig. 7.8 is implemented, microscopically in Fig. 7.9, by a particle sitting at Y and another particle moving between 2 and 1.

Let us denote the final states produced by these six microscopic processes by $|1\rangle, ..., |6\rangle$. By construction, $|1\rangle, ..., |6\rangle$ have the same anyons in the same positions, so they only differ by a phase. The main idea of the proof is to compute the phase difference between $|1\rangle$ and $|6\rangle$ in two different ways. The first calculation proceeds along the top path of Figure 7.8: we claim that

$$\begin{aligned} |1\rangle &= R(a,b)|2\rangle \\ |2\rangle &= F(b,a,c)|3\rangle \\ |3\rangle &= R(a,c)|6\rangle \end{aligned} \tag{7.16}$$

Each of these three equalities follow from a property that we call "weak topological invariance." To state this property, let P, P' be any two processes composed out of movement and splitting operators, and suppose that P, P' start in the same initial state, $|i\rangle$, and end in the same anyon configuration. The weak topological invariance property states that $P|i\rangle = P'|i\rangle$ as long as the spacetime diagrams corresponding to P, P' – which we regard as decorated planar graphs – can be continuously deformed into one another while fixing the endpoints and preserving the time-ordered sequence of splittings and crossings.

Assuming weak topological invariance, which we will prove below, it is easy to derive the first equality in (7.16). The argument is similar to that in Fig. 7.6: one starts with the two microscopic processes P_1, P_2 that produce states $|1\rangle, |2\rangle$. One then constructs two modified processes P_1', P_2' whose spacetime diagrams are equivalent to P_1, P_2 according to weak topological invariance, and which are related to one another by a microscopic R-move. By weak topological invariance, we know that P_1', P_2' must produce the same final states as P_1, P_2. At the same time, since the P_1', P_2' are related to one another by a microscopic R-move, we know that their final states differ by $R(a,b)$; hence we deduce $|1\rangle = R(a,b)|2\rangle$. The other two equalities in (7.16) are derived similarly.

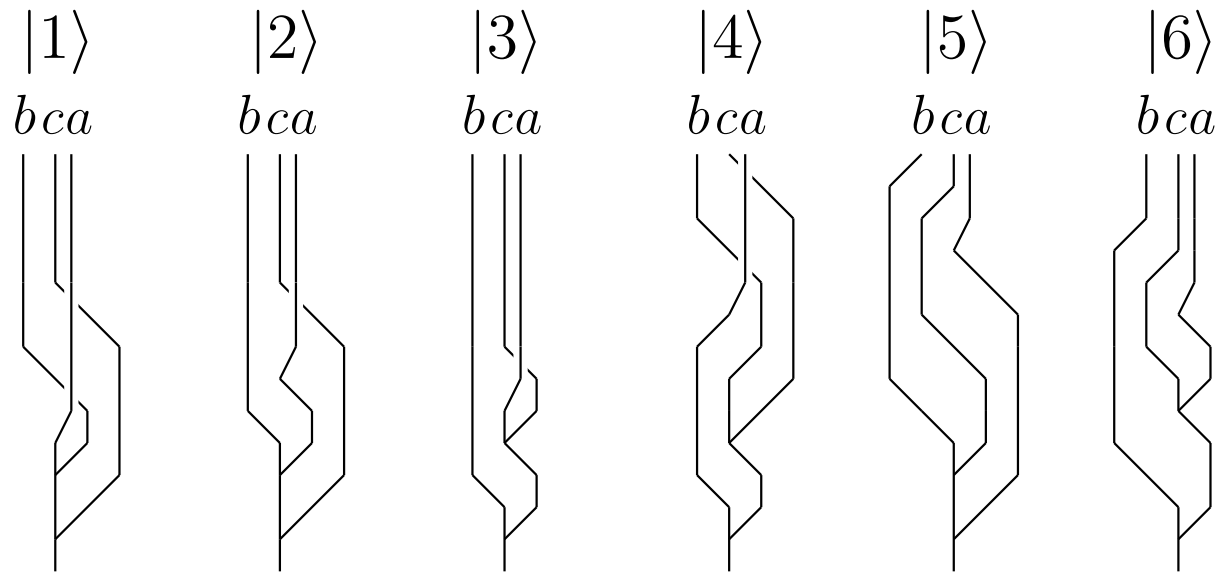

Figure 7.9: Six microscopic processes used to derive the first hexagon equation.

Next, we calculate the phase difference between $|1\rangle$ and $|6\rangle$ by going along the *bottom* path of figure 7.8. We claim that

$$\begin{aligned} |1\rangle &= F(a,b,c)|4\rangle \\ |4\rangle &= R(a,bc)|5\rangle \\ |5\rangle &= F(b,c,a)|6\rangle \end{aligned} \tag{7.17}$$

As in the previous calculation, the first and third equalities in (7.17) follow immediately from weak topological invariance. The second equality however requires an additional identity beyond weak topological invariance, namely the identity shown schematically in Figure 7.10. This identity, together with weak topological invariance, is sufficient to show $|4\rangle = R(a,bc)|5\rangle$.

Combining (7.16) and (7.17) gives the desired hexagon equation:

$$R(a,b)F(b,a,c)R(a,c) = F(a,b,c)R(a,bc)F(b,c,a)$$

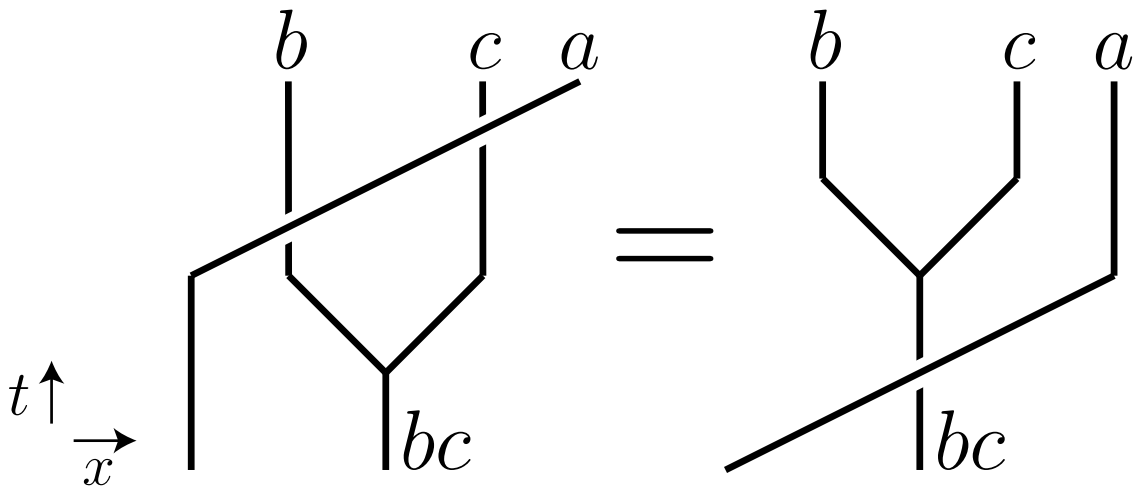

Figure 7.10: Graphical representation of the identity that is needed to relate states $|4\rangle$ and $|5\rangle$ in Fig. 7.8.

To complete the argument we need to establish two properties that we used above: (1) weak topological invariance and (2) the identity in Fig. 7.10. We begin by proving weak topological invariance.

As in Appendix 7.1, the first step of the proof is to consider the special class of processes that (i) are composed only out of movement operators; (ii) have spacetime diagrams that do not contain any crossings; and (iii) return all anyons to their initial positions. We claim that any process, P, of this kind obeys $P|i\rangle = |i\rangle$. The proof is virtually identical to the corresponding claim in Appendix 7.1, so we will not repeat it here.

The next step is to consider a slightly more general set of processes, namely processes that are composed out of movement operators and have spacetime diagrams without crossings, but do not necessarily return the anyons to their initial positions. We claim that $P|i\rangle = P'|i\rangle$ for any two processes of this kind. Again, the proof is the same as the corresponding claim in Appendix 7.1.

We are now ready to prove weak topological invariance. Suppose that P, P' are two processes that can be deformed into one another while fixing the endpoints and preserving the time-ordered sequence of splittings and crossings. We wish to show $P|i\rangle = P'|i\rangle$. Similarly

to Appendix 7.1, we decompose P into a product

$$P = P_1 V_1 P_2 V_2 \cdots \tag{7.18}$$

where $P_1, P_2, ...$ are movement-only processes without any crossings and where $V_1, V_2, ...$ are 'vertex operators' consisting of either a splitting operator $S(a, b)$ or a crossing operator (i.e. a movement operator M^a_{12} or M^a_{21} in the presence of a particle at position Y). We decompose P' in a similar fashion, denoting the movement-only processes by $P'_1, P'_2, ...$ and vertex operators by $V'_1, V'_2, \cdots$. By assumption, $V_j = V'_j$ for every j, but P_j and P'_j may be different. Consider the special case where P_j and P'_j share the same initial anyon configuration and the same final anyon configuration for each j. In this case, it follows immediately that $P|i\rangle = P'|i\rangle$ using the above property of movement-only processes. Next note that the general case – where P_j and P'_j do not share the same initial and final anyon configurations – can always be reduced to this special case: given any P, P' it is not hard to construct modified processes, $\tilde{P}$ and $\tilde{P}'$, with $P|i\rangle = \tilde{P}|i\rangle$ and $P'|i\rangle = \tilde{P}'|i\rangle$ such that the corresponding movement-only processes $\tilde{P}_j$ and $\tilde{P}'_j$ *do* share the same initial and final anyon configuration for each j. These modified processes $\tilde{P}, \tilde{P}'$ can be obtained in the same way as in Appendix 7.1, i.e. by inserting appropriate movement operators $M^a_{xx'}$ just before each splitting operator, along with their reverse movements $M^a_{x'x}$ just after the splitting operator, and using the fact that movement operators commute with splitting operators when acting on non-overlapping intervals.

All that remains is to prove the identity shown in Fig. 7.10. We will do this in two steps. First we will show that $|\Psi\rangle = |\Psi'\rangle$ where $|\Psi\rangle, |\Psi\rangle'$ are the two final states produced by the processes shown in Fig. 7.11a. Next we will show that $|\Psi'\rangle = |\Psi''\rangle$ where $|\Psi''\rangle$ is the final state produced by the second process in Fig. 7.12a. Taken together, these two equalities imply that $|\Psi\rangle = |\Psi''\rangle$. This last result is the microscopic analog of the identity in Fig. 7.10.

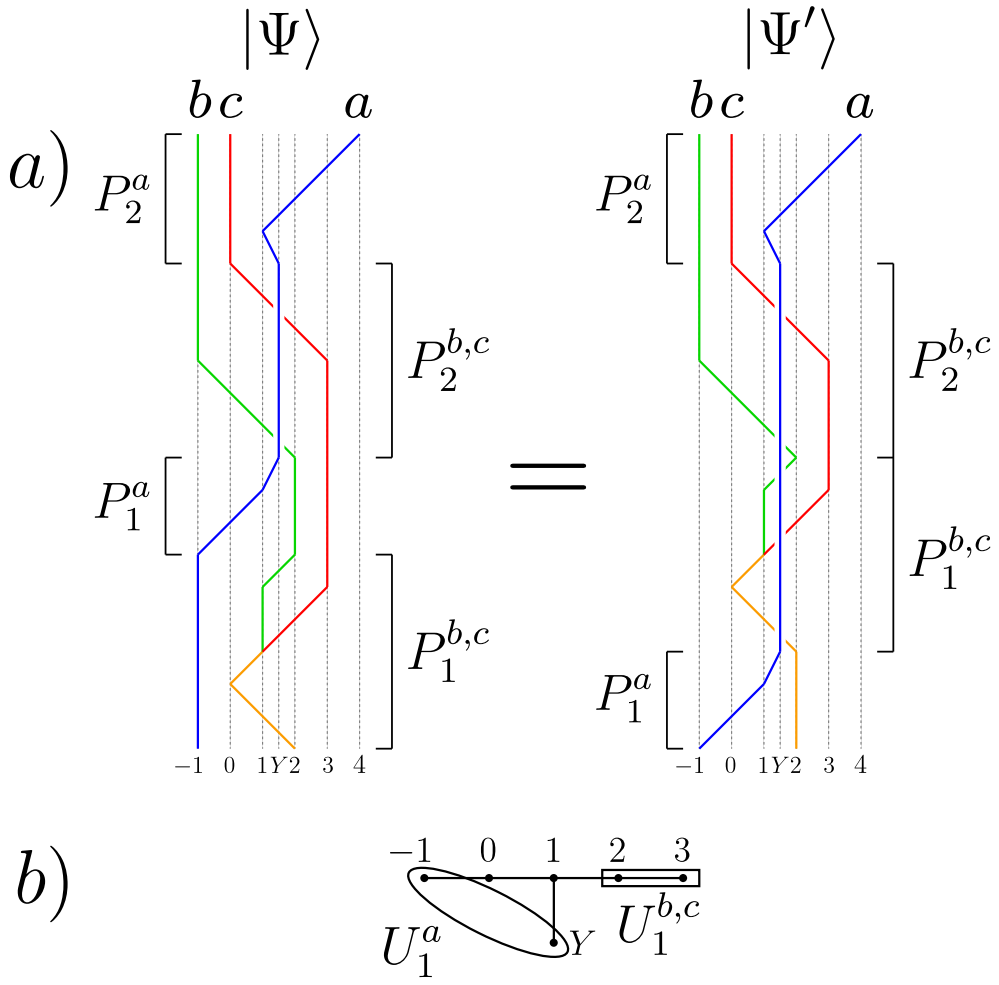

Figure 7.11: (a) The relation $|\Psi\rangle = |\Psi'\rangle$ is the first step in our proof of the identity in Fig. 7.10. (b) Regions of support of the operators $U_1^a, U_1^{b,c}$ used in proof of $|\Psi\rangle = |\Psi'\rangle$.

To prove $|\Psi\rangle = |\Psi'\rangle$, we note that

$$|\Psi\rangle = P_2^a P_2^{b,c} P_1^a P_1^{b,c} |i\rangle$$
$$|\Psi'\rangle = P_2^a P_2^{b,c} P_1^{b,c} P_1^a |i\rangle \tag{7.19}$$

where $|i\rangle$ is the initial state and $P_1^{b,c}, P_1^a, P_2^{b,c}, P_2^a$ are the processes shown in Fig. 7.11a. Given these two expressions, our problem reduces to showing that $P_1^a P_1^{b,c} |i\rangle = P_1^{b,c} P_1^a |i\rangle$. We prove this in the same way that we proved the identity (7.11) in Appendix 7.1. The first

step is to note that there exists a (unitary) operator, U_1^a, with a region of support, shown in Fig. 7.11b, such that $U_1^a|i\rangle = P_1^a|i\rangle$. Likewise, there exists a (unitary) operator, $U_1^{b,c}$, with a region of support shown in Fig. 7.11b, such that $U_1^{b,c}|i\rangle = P_1^{b,c}|i\rangle$. Given that these operators have non-overlapping regions of support we know that:

$$[U_1^a, U_1^{b,c}] = [P_1^a, U_1^{b,c}] = [U_1^a, P_1^{b,c}] = 0 \tag{7.20}$$

Combining these identities, the claim follows easily:

$$\begin{aligned} P_1^a P_1^{b,c}|i\rangle = P_1^a U_1^{b,c}|i\rangle = U_1^{b,c} P_1^a|i\rangle = U_1^{b,c} U_1^a|i\rangle \\ = U_1^a U_1^{b,c}|i\rangle = U_1^a P_1^{b,c}|i\rangle = P_1^{b,c} U_1^a|i\rangle = P_1^{b,c} P_1^a|i\rangle, \end{aligned}$$

To prove that $|\Psi'\rangle = |\Psi''\rangle$, we use similar reasoning. First we note that

$$\begin{aligned} |\Psi'\rangle &= P_2^a P_3^{b,c}(M_{01}^{bc} M_{12}^{bc} P_1^a)|i\rangle \\ |\Psi''\rangle &= P_3^{b,c} P_2^a (M_{01}^{bc} M_{12}^{bc} P_1^a)|i\rangle \end{aligned} \tag{7.21}$$

as one can see in Fig. 7.12a. Given these expressions, our problem is equivalent to showing that $P_2^a, P_3^{b,c}$ commute with each other when acting on the state $|m\rangle = M_{01}^{bc} M_{12}^{bc} P_1^a|i\rangle$. To show this commutation relation, we note that there exists a unitary operator, $U_3^{b,c}$, with a region of support shown in Fig. 7.12b, such that $U_3^{b,c}|m\rangle = P_3^{b,c}|m\rangle$. Likewise, there exists a unitary operator, U_2^a, with a region of support shown in Fig. 7.12b such that $U_2^a|m\rangle = P_2^a|m\rangle$. Using the same manipulations as above, the claim follows immediately:

$$\begin{aligned} P_2^a P_3^{b,c}|m\rangle = P_2^a U_3^{b,c}|m\rangle = U_1^{b,c} P_2^a|m\rangle = U_3^{b,c} U_2^a|m\rangle \\ = U_2^a U_3^{b,c}|m\rangle = U_2^a P_3^{b,c}|m\rangle = P_3^{b,c} U_2^a|m\rangle = P_3^{b,c} P_2^a|m\rangle, \end{aligned}$$

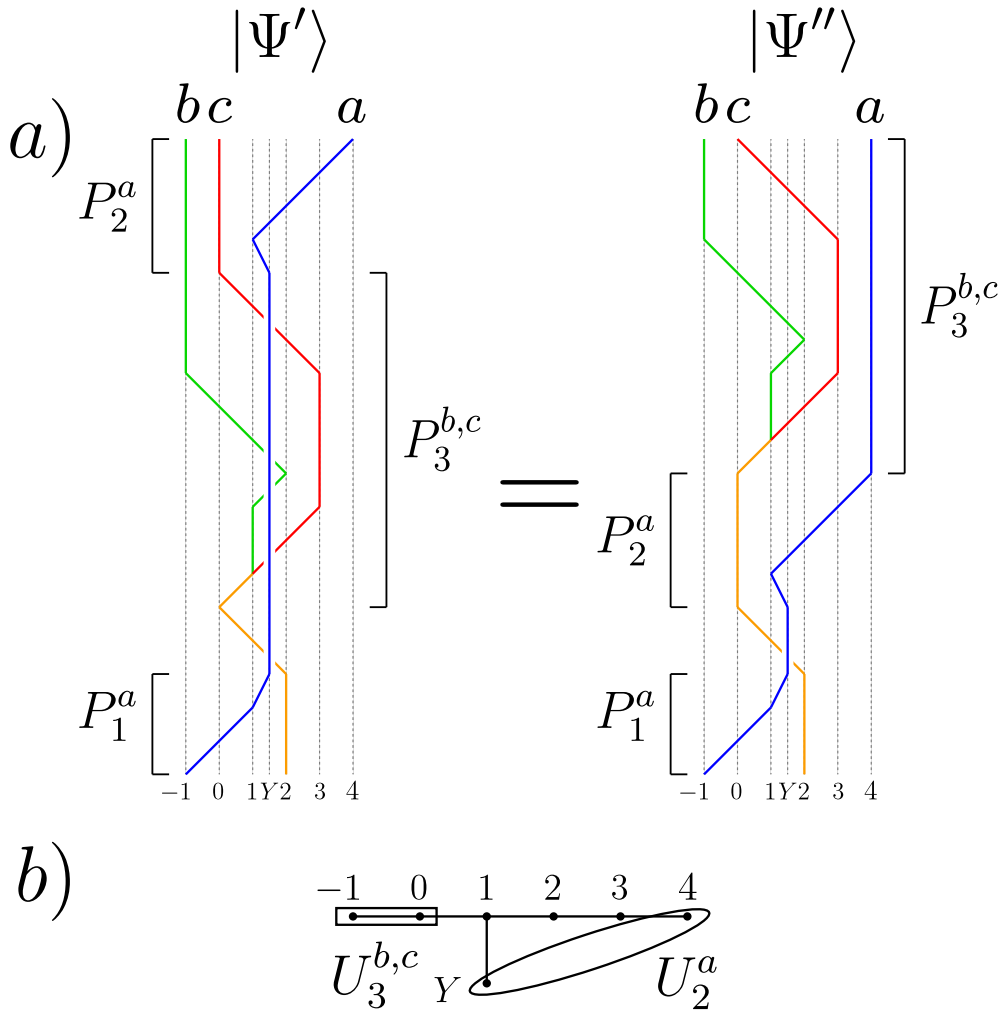

Figure 7.12: (a) The relation $|\Psi'\rangle = |\Psi''\rangle$ is the second step in our proof of the identity in Fig. 7.10. (b) Regions of support of the operators $U_2^a, U_3^{b,c}$ used in proof of $|\Psi'\rangle = |\Psi''\rangle$.

This completes the proof of the first hexagon equation.

7.3 Derivation of Eq. 3.46

In this appendix, we derive the identity (3.46) that we used in our analysis of the doubled semion model, that is:

$$S(s,s)|0\rangle \propto a_1^\dagger a_2^\dagger |0\rangle \tag{7.22}$$

where $S(s,s)$ is the splitting operator in the doubled semion model and $a_n^\dagger$ is the semion creation operator.

The derivation follows from straightforward algebra. First we write the semion creation operator $a_n^\dagger$ as a product

$$a_n^\dagger = W_n T_n U_n \tag{7.23}$$

where

$$\begin{aligned} W_n &= \prod_{m<n} \sigma^z_{m,L}\sigma^z_{m,R}, \\ T_n &= \prod_{m<n} (-1)^{\frac{1}{4}(1+\sigma^x_{m,L})(1-\sigma^x_{m,R})} \\ U_n &= \prod_{m<n} i^{\frac{1-\sigma^x_{m,U}}{2}} \end{aligned} \tag{7.24}$$

It follows that

$$\begin{aligned} a_1^\dagger a_2^\dagger &= (W_1T_1U_1)(W_2T_2U_2) \\ &= (W_1T_1W_2T_2)(U_1U_2) \\ &= (W_1W_2)(W_2T_1W_2T_2)(U_1U_2) \end{aligned} \tag{7.25}$$

where the second equality follows from the fact that the U_i operators commute with W_j, T_j.

Next, we note that

$$\begin{aligned} W_1W_2 &= \sigma^z_{1,L}\sigma^z_{1,R} \\ U_1U_2 &= i^{\frac{1-\sigma^x_{1,U}}{2}} \prod_{m<1} \sigma^x_{m,U} \end{aligned} \tag{7.26}$$

Also,

$$W_2 T_1 W_2 = \prod_{m<1} (-1)^{\frac{1}{4}(1-\sigma^x_{m,L})(1+\sigma^x_{m,R})}$$

so

$$W_2 T_1 W_2 T_2 = (-1)^{\frac{1}{4}(1+\sigma^x_{1,L})(1-\sigma^x_{1,R})} \prod_{m<1} \sigma^x_{m,L}\sigma^x_{m,R} \tag{7.27}$$

Substituting (7.26) and (7.27) into (7.25) gives

$$a_1^\dagger a_2^\dagger = \sigma^x_{0,R}\sigma^z_{1,L}\sigma^z_{1,R}(-1)^{\frac{1}{4}(1+\sigma^x_{1,L})(1-\sigma^x_{1,R})} i^{\frac{1-\sigma^x_{1,U}}{2}} \prod_{m<1} Q_m \tag{7.28}$$

where

$$Q_m \equiv \sigma^x_{m,L}\sigma^x_{m,U}\sigma^x_{m-1,R}. \tag{7.29}$$

denotes the Q_v operator on vertex m.

Acting both sides of (7.28) on the ground state $|0\rangle$ and using the fact that $Q_m|0\rangle = |0\rangle$, we obtain

$$a_1^\dagger a_2^\dagger |0\rangle = S(a,a)|0\rangle \tag{7.30}$$

as we wished to show.

7.4 Cocycle condition

In this appendix, we show that the domain wall F-symbol defined in (4.20-4.21) is a cocycle. More specifically, we show that F obeys Eq. 4.117 – the general cocycle condition for

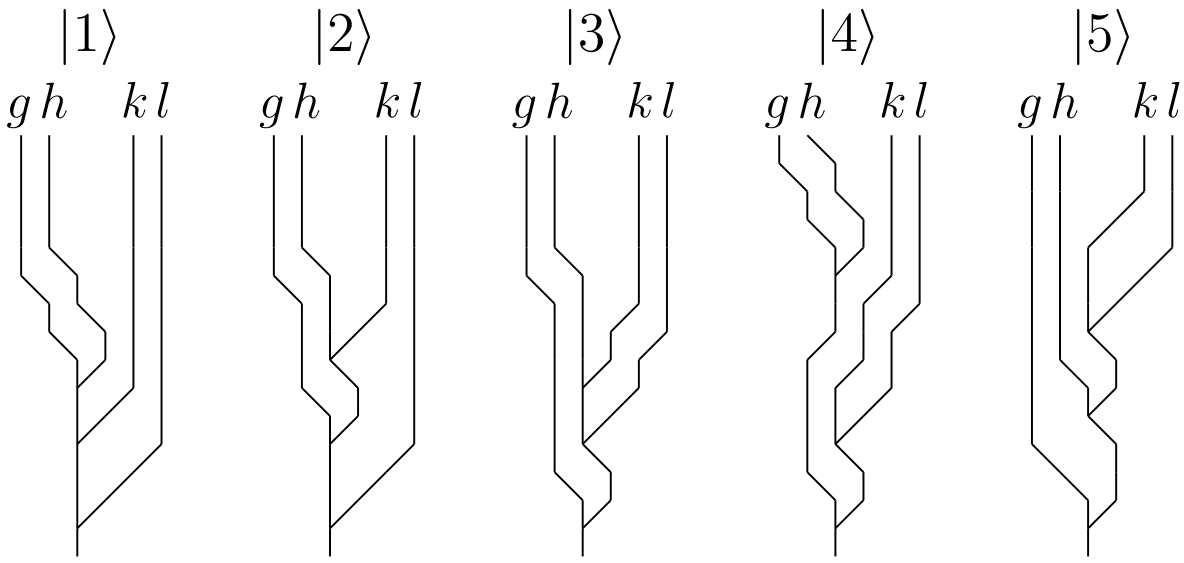

Figure 7.13: The five microscopic states used to prove the cocycle condition.

symmetry groups containing both unitary and antiunitary symmetries.

Our proof closely follows the derivation of the pentagon identity for anyonic F-symbols, presented in Appendix A of Ref. [69]. As in Ref. [69], the first step is to pick a nice phase convention for the movement operators $M^g_{x'x}$. Specifically, we choose the phases of the movement operators so that

$$\begin{aligned} M^g_{xx'} M^g_{x'x} |g_x\rangle &= |g_x\rangle \\ M^g_{x''x'} M^g_{x'x} |g_x\rangle &= M^g_{x''x} |g_x\rangle \end{aligned} \tag{7.31}$$

With this phase convention, it is possible to show that our space-time diagrams satisfy the following topological invariance property: consider any process, P, composed out of a sequence of movement and splitting operators acting on an initial state

$$|i\rangle = |..., g_x, h_{x'}, k_{x''}, ...\rangle. \tag{7.32}$$

For any such process, we can draw a corresponding space-time diagram. Next, consider a

second process, P', that acts on the same initial state, $|i\rangle$, and that leads to the same final state. Again, we can draw a corresponding space-time diagram. The topological invariance property says that if these two space-time diagrams can be continuously deformed into one another while fixing the endpoints, then the two processes produce the same final states with the same phases. That is,

$$P|i\rangle = P'|i\rangle \tag{7.33}$$

The proof of the topological invariance property (7.33) is identical to the one given in Appendix A of Ref. [69].

With the help of the topological invariance property (7.33), we will now show that the F-symbol defined in (4.20-4.21) satisfies the cocycle condition (4.117). Consider the five processes shown in Fig. 7.13. Let us denote the final states of these processes by $|1\rangle, |2\rangle, |3\rangle, |4\rangle, |5\rangle$. Notice that these states are the same up to a phase since they describe the same four domain walls in the same four positions. The idea of the proof is to compute the phase difference between state $|1\rangle$ and state $|5\rangle$ in two difference ways. More specifically, using the topological invariance property (7.33) we will show that

$$\begin{aligned} |1\rangle &= F(g,h,k)|2\rangle \\ |2\rangle &= F(g,hk,l)|3\rangle \\ |3\rangle &= g(F(h,k,l))|5\rangle \end{aligned} \tag{7.34}$$

and

$$\begin{aligned} |1\rangle &= F(gh,k,l)|4\rangle \\ |4\rangle &= F(g,h,kl)|5\rangle \end{aligned} \tag{7.35}$$

where the g action is defined as in Eq. 4.116. Putting this all together gives us the desired cocycle condition:

$$\frac{F(g,h,k)F(g,hk,l)[gF(h,k,l)]}{F(gh,k,l)F(g,h,kl)} = 1 \tag{7.36}$$

We now derive each of the above equations. To aid in the discussion, we define the operators

$$\begin{aligned}\mathcal{O}_1(g,h,k) &= M_{12}^h M_{01}^g S(g,h) M_{32}^k S(gh,k) \\ \mathcal{O}_2(g,h,k) &= M_{32}^k S(h,k) M_{12}^{hk} M_{01}^g S(g,hk)\end{aligned} \tag{7.37}$$

To derive the first equation, $|1\rangle = F(g,h,k)|2\rangle$, notice that processes 1 and 2 start in the same state $|ghkl_1\rangle$, and they also contain the same sequence of movement and splitting operators starting from the beginning of the process, leading up to the (intermediate) state $|ghk_1, l_4\rangle$. It is at that point that the two processes diverge: in process 1, the operator $\mathcal{O}_1(g,h,k)$ is applied while in process 2, the operator $\mathcal{O}_2(g,h,k)$ is applied. After that, the two processes again coincide. It follows that the phase difference between $|1\rangle$ and $|2\rangle$ comes entirely from the difference between $\mathcal{O}_1$ and $\mathcal{O}_2$. That is,

$$\begin{aligned}\langle 2|1\rangle &= \langle ghk_1, l_4|\mathcal{O}_2(g,h,k)^\dagger \mathcal{O}_1(g,h,k)|ghk_1, l_4\rangle \\ &= \langle ghk_1|\mathcal{O}_2(g,h,k)^\dagger \mathcal{O}_1(g,h,k)|ghk_1\rangle \\ &= F(g,h,k)\end{aligned} \tag{7.38}$$

where the second equality follows from (4.119) – one of the fundamental properties of multi-domain wall states.

The second equation, $|2\rangle = F(g,hk,l)|3\rangle$, follows from similar logic. In this case, we use the topological invariance property (7.33) to redraw process 2 so that it is identical to

process 3 except for an F-move at the very beginning of the process (see Fig. 20 of Ref. [69]). After this modification, the only difference between the two processes is that in process 2 the operator $\mathcal{O}_1(g, hk, l)$ is applied at the beginning, while in process 3, the operator $\mathcal{O}_2(g, hk, l)$ is applied. It then follows that

$$\begin{aligned}\langle 3|2\rangle &= \langle ghkl_1|\mathcal{O}_2(g, hk, l)^\dagger \mathcal{O}_1(g, hk, l)|ghkl_1\rangle \\ &= F(g, hk, l)\end{aligned} \tag{7.39}$$

The third equation, $|3\rangle = g(F(h, k, l))|5\rangle$ is the trickiest one, and the one that distinguishes the unitary and antiunitary cases. Again, we use the topological invariance property to redraw process 3 so that it differs from process 5 by a replacement $\mathcal{O}_1(h, k, l) \to \mathcal{O}_2(h, k, l)$ (see Fig. 21 of Ref. [69]). Hence

$$\begin{aligned}\langle 5|3\rangle &= \langle g_{-1}, hkl_1|\mathcal{O}_2(h, k, l)^\dagger \mathcal{O}_1(h, k, l)|g_{-1}, hkl_1\rangle \\ &= g\langle hkl_1|\mathcal{O}_2(h, k, l)^\dagger \mathcal{O}_1(h, k, l)|hkl_1\rangle \\ &= gF(g, h, k)\end{aligned} \tag{7.40}$$

where the second equation follows from (4.119). Note that the key difference between this equation and the others is that the F-move takes place to the right of the g domain wall; this is the origin of the g action.

The other two equations, $|1\rangle = F(gh, k, l)|4\rangle$ and $|4\rangle = F(g, h, kl)|5\rangle$, follow from similar reasoning. In both cases, the relevant processes can be related by topological invariance together with an appropriate F-move (see Figs. 22 and 23 of Ref. [69]). We then derive the

equations as before:

$$\begin{aligned}\langle 4|1\rangle &= \langle ghkl_1|\mathcal{O}_2(gh,k,l)^\dagger \mathcal{O}_1(gh,k,l)|ghkl_1\rangle \\ &= F(gh,k,l) \\ \langle 5|4\rangle &= \langle ghkl_1|\mathcal{O}_2(g,h,kl)^\dagger \mathcal{O}_1(g,h,kl)|ghkl_1\rangle \\ &= F(g,h,kl)\end{aligned} \tag{7.41}$$

This completes our derivation of the cocycle condition (4.117).

7.5 Connection to Tantivasadakarn-Vishwanath Model

We start by defining the Hilbert space and then define the low energy operators on the edge. Consider a triangle lattice. On each vertex, place a spin. On each triangle place a fermion with Majorana operators $\gamma, \widetilde{\gamma}$. On every edge on the boundary of the system place one Majorana degree of freedom η. On each vertex on the boundary, place three Majorana degrees of freedom λ, ξ, ζ. We can think of the pairs η, λ and ξ, ζ as forming two fermions per site on the edge.

Define the operator on the ith edge site

$$\begin{aligned}\overline{X}_i =& X_i Z_i CS^\dagger_{i-1,j} CS^\dagger_{j,k} CS^\dagger_{k,i+1} CZ_{i,j} CZ_{i,k} \\ & \eta_{i-1/2}^{g_{i-1}} \gamma_{(i-1,j,i)}^{g_{i-1}+g_j+1} \lambda_i \xi_i \zeta_i \gamma_{j,i,k}^{g_j+g_k+1} \gamma_{i,k,i+1}^{g_k+g_{i+1}+1} \eta_{i+1/2}^{g_{i+1}}\end{aligned} \tag{7.42}$$

Also define

$$\overline{\eta}_{i+1/2} = CZ_{i,i+1}\eta_{i+1/2} \quad \overline{\lambda}_{i+1/2} = Z_{i+1}\lambda_{i+1} \tag{7.43}$$

(Note, this may be inconsistent with the usual overline notation since we haven't at-

tempted to conjugate anything.)

The two new Majorana operators obey the usual relations and they commute with the $\overline{X}_i$ operator. Therefore, we will take these three to be our low energy operators. Lastly, we may constrain $i\xi\zeta = 1$ at this point since it commutes with the previous operators and with the symmetry.

If we rename

$$\overline{X} \to X \quad \overline{\eta} \to \gamma^a \quad \overline{\lambda} \to \gamma^b \tag{7.44}$$

then we recover the commutation relations described at the beginning of this document.

7.6 Uniqueness of decorated multi-domain wall states

In this Appendix, we prove that the decorated multi-domain wall states obey a uniqueness property to the bare multi-domain wall states. Pick group elements $g^{(1)}, g^{(2)}, ..., g^{(n)} \in G_0$ and $s^{(1)}, s^{(2)}, ..., s^{(n)} \in \mathbb{Z}_2$ and consider the state $|(g^{(1)}, s^{(1)})_{x_1}, (g^{(2)}, s^{(2)})_{x_2}, ...\rangle$ defined as

$$\begin{aligned} &|(g^{(1)}, s^{(1)})_{x_1}, (g^{(2)}, s^{(2)})_{x_2}, ...\rangle \\ &\qquad = \prod_i \left({}^{g_L^{(i)}}\gamma_{x_i} \right)^{s^{(i)}} |(g^{(1)}, 0)_{x_1}, (g^{(2)}, 0)_{x_2}, ...\rangle \end{aligned} \tag{7.45}$$

where ${}^{g}\gamma_x = U^{(g,0)}\gamma_x \left(U^{(g,0)}\right)^{-1}$, the left most operator in the product is the left most operator in the physical space, and

$$g_L^{(i)} = g^{(1)} \cdots g^{(i-1)}. \tag{7.46}$$

For ease of notation, we will write $g_L = g_L^{(i)}$ when we are referring to a particular domain wall i outside of a product.

We will prove that these are the unique states with the following two properties: first, for any local operator $\mathcal{O}$ supported near one domain wall x_i,

$$\begin{aligned}\langle (g^{(1)}, s^{(1)})_{x_1}, (g^{(2)}, s^{(2)})_{x_2}, ... | \mathcal{O} | (g^{(1)}, s^{(1)})_{x_1}, (g^{(2)}, s^{(2)})_{x_2}, ... \rangle \\ = \langle (g^{(i)}, s^{(i)})_{x_i}; g_L | \mathcal{O} | (g^{(i)}, s^{(i)})_{x_i}; g_L \rangle \end{aligned} \tag{7.47}$$

where g_L is the product of the G_0 component of all domain walls to the left of $\mathcal{O}$, as before.

Second, for any operator $\mathcal{O}$ supported away from the domain walls,

$$\begin{aligned}\langle (g^{(1)}, s^{(1)})_{x_1}, (g^{(2)}, s^{(2)})_{x_2}, ... | \mathcal{O} | (g^{(1)}, s^{(1)})_{x_1}, (g^{(2)}, s^{(2)})_{x_2}, ... \rangle \\ = \langle \Omega; g_L | \mathcal{O} | \Omega; g_L \rangle \end{aligned} \tag{7.48}$$

where g_L is again the product of the G_0 component of domain wall types to the left of $\mathcal{O}$.

First we will show that these two properties are met for the decorated multi-domain wall states, and then we will prove that these are the unique states with these two properties.

Let $\mathcal{O}$ be a local operators near the point x_i. Using Eqn. 5.26 and commuting fermion operators away from x_i past $\mathcal{O}$, we obtain

$$\begin{aligned}\langle \mathcal{O} \rangle &= \langle (g^{(1)}, 0)_{x_1}, (g^{(2)}, 0)_{x_2}, ... | \left(\gamma_{x_i}^{g_L}\right)^{-s^{(i)}} \mathcal{O} \left(\gamma_{x_i}^{g_L}\right)^{s^{(i)}} | (g^{(1)}, 0)_{x_1}, (g^{(2)}, 0)_{x_2}, ... \rangle \\ &= \langle (g^{(i)}, 0)_{x_i}; g_L | \left(\gamma_{x_i}^{g_L}\right)^{-s^{(i)}} \mathcal{O} \left(\gamma_{x_i}^{g_L}\right)^{s^{(i)}} | (g^{(i)}, 0)_{x_i}; g_L \rangle \\ &= \langle (g^{(i)}, s^{(i)})_{x_i}; g_L | \mathcal{O} | (g^{(i)}, s^{(i)})_{x_i}; g_L \rangle \end{aligned} \tag{7.49}$$

where the second equality is obtained from the relationship between bare and decorated single domain wall states. Similar reasoning can be used to show that the second property, where $\mathcal{O}$ is between domain walls, is also satisfied.

We now prove uniqueness. Let's say that we have some state $|\psi\rangle$ with the same expectation values of local operators as the decorated multidomain wall state $|(g^{(1)}, s^{(1)})_{x_1}, (g^{(2)}, s^{(2)})_{x_2}, ...\rangle$.

We will show that these states are the same by showing that

$$|(g^{(1)},0)_{x_1},(g^{(2)},0)_{x_2},...\rangle \propto \prod_i \left(g_L^{(i)}\gamma_{x_i}\right)^{-s^{(i)}}|\psi\rangle \tag{7.50}$$

Observe that for any local operator $\mathcal{O}$ near a particular x_i (recalling that we call $g_L = g_L^{(i)}$ when referring to a particular i), we have

$$\begin{aligned}
&\langle\psi|\prod_j \left(g_L^{(j)}\gamma_{x_j}\right)^{s^{(j)}} \mathcal{O} \prod_j \left(g_L^{(j)}\gamma_{x_j}\right)^{-s^{(j)}}|\psi\rangle \\
&= \langle\psi|\left(g_L\gamma_{x_i}\right)^{s^{(i)}} \mathcal{O}\left(g_L\gamma_{x_i}\right)^{-s^{(i)}}|\psi\rangle \\
&= \langle(g^{(i)},s^{(i)})_{x_i};g_L|\left(g_L\gamma_{x_i}\right)^{s^{(i)}} \mathcal{O}\left(g_L\gamma_{x_i}\right)^{-s^{(i)}}|(g^{(i)},s^{(i)})_{x_i};g_L\rangle \\
&= \langle(g^{(i)},0)_{x_i};g_L|\mathcal{O}|(g^{(i)},0)_{x_i};g_L\rangle
\end{aligned} \tag{7.51}$$

Similarly for local operators $\mathcal{O}$ between domain walls, one can show that

$$\begin{aligned}
&\langle\psi|\prod_j \left(g_L^{(j)}\gamma_{x_j}\right)^{s^{(j)}} \mathcal{O} \prod_j \left(g_L^{(j)}\gamma_{x_j}\right)^{-s^{(j)}}|\psi\rangle \\
&= \langle\Omega;g_L|\mathcal{O}|\Omega;g_L\rangle
\end{aligned} \tag{7.52}$$

Therefore, by the uniqueness of the bare multi-domain wall states, we know that

$$|(g^{(1)},0)_{x_1},(g^{(2)},0)_{x_2},...\rangle \propto \prod_i \left(\gamma_{x_i}^{g_L^{(i)}}(g^{(i)})\right)^{-s^{(i)}}|\psi\rangle \tag{7.53}$$

and therefore $|\psi\rangle$

$$|\psi\rangle \propto |(g^{(1)}, s^{(1)})_{x_1}, (g^{(2)}, s^{(2)})_{x_2}, ...\rangle \tag{7.54}$$

This completes our proof that the multi-domain wall states are the unique states with expectation values for local operators as in Eqns. 7.47 and 7.48.

7.7 Cocycle condition for complex fermions

This Appendix is dedicated to proving the cocycle condition for the case of complex fermions. That is, we want to show that

$$\frac{\nu(g,h,k)\nu(g,hk,l)\nu(h,k,l)}{\nu(gh,k,l)\nu(g,h,kl)} = (-1)^{(\rho(g,h)+\lambda(g,h))\rho(g,h)} \tag{7.55}$$

First, we start with the fact that the F-symbol must obey the standard cocycle condition from group cohomology:

$$\frac{F(\boldsymbol{a},\boldsymbol{b},\boldsymbol{c})F(\boldsymbol{a},\boldsymbol{bc},\boldsymbol{d})F(\boldsymbol{b},\boldsymbol{c},\boldsymbol{d})}{F(\boldsymbol{ab},\boldsymbol{c},\boldsymbol{d})F(\boldsymbol{a},\boldsymbol{b},\boldsymbol{cd})} = 1 \tag{7.56}$$

Setting $\boldsymbol{a} = (g,0), \boldsymbol{b} = (h,0), \boldsymbol{c} = (k,0), \boldsymbol{d} = (l,0)$, and recalling that $\nu(g,h,k) = \widetilde{F}(g,h,k)$ and $F((g,s),(h,t),(k,r) = (-1)^{(\lambda(g,h)+\rho(g,h))r}\widetilde{F}(g,h,k)$ we see that

$$\begin{aligned} 1 &= \frac{F(\boldsymbol{a},\boldsymbol{b},\boldsymbol{c})F(\boldsymbol{a},\boldsymbol{bc},\boldsymbol{d})F(\boldsymbol{b},\boldsymbol{c},\boldsymbol{d})}{F(\boldsymbol{ab},\boldsymbol{c},\boldsymbol{d})F(\boldsymbol{a},\boldsymbol{b},\boldsymbol{cd})} \\ &= \frac{F(\boldsymbol{a},\boldsymbol{b},(k,0))F(\boldsymbol{a},\boldsymbol{bc},(l,0))F(\boldsymbol{b},\boldsymbol{c},(l,0))}{F(\boldsymbol{ab},\boldsymbol{c},(l,0))F(\boldsymbol{a},\boldsymbol{b},(kl,\rho(k,l)))} \\ &= \frac{\nu(g,h,k)\nu(g,hk,l)\nu(h,k,l)}{\nu(gh,k,l)\nu(g,h,kl)}(-1)^{(\lambda(g,h)+\rho(g,h))\beta(k,l)} \end{aligned} \tag{7.57}$$

Therefore,

$$\frac{\nu(g,h,k)\nu(g,hk,l)\nu(h,k,l)}{\nu(gh,k,l)\nu(g,h,kl)} = (-1)^{(\rho(g,h)+\lambda(g,h))\rho(g,h)} \tag{7.58}$$

7.8 Kitaev chain stacking

In this Appendix, we examine how ρ and ν change when the boundary theory is stacked with a Kitaev chain.

7.8.1 Generalized Kitaev Chain

We begin by describing a model of a 1D generalized Kitaev chain. The Hilbert space on each site is the group algebra $\mathbb{C}[G]$. That is, on each site i, there is a basis element $|g\rangle_i$ for each $g \in G$. We may define an operator X_i^g which acts on site i as

$$X_i^g |h\rangle_i = |gh\rangle_i \tag{7.59}$$

and acts as the identity on all other sites. Written in the notation of ordered pairs (g, s) with $g \in G_0$, we write

$$X^{(g,0)}|(h,0)\rangle = |(gh, \lambda(g,h))\rangle \tag{7.60}$$

In particular, notice that if we define the states

$$|(g,\pm)\rangle_i = \frac{1}{2}(|(g,0)\rangle_i \pm |(g,1)\rangle_i) \tag{7.61}$$

then we have

$$X_i^{(1,1)}|(g,\pm)\rangle_i = \pm|(g,\pm)\rangle_i. \tag{7.62}$$

Although we have not yet defined fermion parity symmetry in this system, states will eventually represent fermion parity definite states. We now define the operators γ_{Li}, γ_{Ri} with the actions

$$\begin{aligned} \gamma_{Li}|(1,\pm)\rangle_i &= |(1,\mp)\rangle_i \\ \gamma_{Ri}|(1,\pm)\rangle_i &= \pm i|(1,\mp)\rangle_i \end{aligned} \tag{7.63}$$

This leads to the relation

$$-i\gamma_{Li}\gamma_{Ri}|(1,\pm)\rangle_i = \pm|(1,\pm)\rangle_i. \tag{7.64}$$

We will only need to consider the actions of these operators on the states $|(g,\pm)\rangle_i$ when $g = 1$.

Collectively, these basis states on each site describe the full Hilbert space. It is important to note that this is a fermionic system, so the construction of the full Hilbert space is not obtained through the tensor product of all sites.

We now describe the the symmetry operators. These are defined as

$$U^g = K^{\tau(g)} \prod_j X_j^{(g,0)} \tag{7.65}$$

where $g \in G_0$, K is complex conjugation using the basis states generated by $|(g,s)\rangle_i$, and $\tau(g) = 1$ if U^g is antiunitary and $\tau(g) = 0$ otherwise. We also define

$$F = \prod_j X_j^{(1,1)}. \tag{7.66}$$

Notice that all operators of the form $X_j^{(g,s)}$ are fermion parity even.

Now that we have defined the symmetry operators, we will follow our usual procedure

and break the symmetry spontaneously and completely using a Hamiltonian. We will choose a Hamiltonian corresponding to the topological superconducting phase,

$$\begin{aligned} H = &- J \sum_{g \in G_0} \sum_i U^g Z_i Z_{i+1} U^{g\dagger} \\ &- K \sum_{g \in G_0} \sum_i U^g (-i\gamma_{Ri}\gamma_{Li+1}) Z_i Z_{i+1} U^{g\dagger}. \end{aligned} \tag{7.67}$$

where $J, K > 0$ and

$$Z_i |(g,s)\rangle = \delta_{g,1} |(g,s)\rangle. \tag{7.68}$$

This Hamiltonian has a ground state $|\Omega;1\rangle$ with the properties

$$\begin{aligned} Z_i |\Omega;1\rangle &= |\Omega;1\rangle \\ -i\gamma_{Ri}\gamma_{Li+1} |\Omega;1\rangle &= |\Omega;1\rangle \end{aligned} \tag{7.69}$$

As usual, we define the other ground states by

$$|\Omega;g\rangle = U^g |\Omega;1\rangle. \tag{7.70}$$

We are now equipped to define the domain wall states. The domain wall that lives between sites $j-1$ and j will be referred to as being at the location j. Define

$$|(g,0)_x\rangle = a_x^\dagger(g) |\Omega;1\rangle \tag{7.71}$$

where

$$a_x^\dagger(g) = \prod_{j \le x \le Y} X_j^{(g,0)} \tag{7.72}$$

where Y is some point that is far to the right.

To define the decorated single domain wall states, we will use the notation for the fermion operators

$$\gamma_i = \sum g \in G_0 U^g \gamma_{Li} Z_i U^{g\dagger} \tag{7.73}$$

This defines the decorated states

$$|(g,1)_x\rangle = \gamma_x |(g,0)_x\rangle. \tag{7.74}$$

The multidomain wall states are defined using these creation operators and fermion operators. In particular,

$$|(g,0)_1,(h,0)_2\rangle = a_1^\dagger(g) a_2^\dagger(g)(-i\gamma_{RY})^{\lambda(g,h)}|\Omega;1\rangle \tag{7.75}$$

7.8.2 Calculation of data

The fusion rules for this theory are

$$(g,0)\times(h,0) = (gh,\lambda(g,h)) \tag{7.76}$$

which gives $\rho(g,h) = \lambda(g,h)$. To prove this, we will construct the splitting operators $S((g,0),(h,0))$. In particular,

$$S((g,0),(h,0)) = \sum_{k\in G_0} U^k X_2^g X_2^{h^{-1}} X_2^{g^{-1}} P_2^{gh} U^{k\dagger} \tag{7.77}$$

where P_2^{gh} projects on to the states $|(gh,0)\rangle_2, |(gh,1)\rangle_2$ at site 2. This is a symmetric operator. We now show that it has the correct action on single domain wall states.

$$
\begin{aligned}
&S((g,0),(h,0))|(gh,\lambda(g,h))_1\rangle \\
&= X_2^g X_2^{h^{-1}} X_2^{g^{-1}} \gamma_1^{\lambda(g,h)} a_1^\dagger(gh)|\Omega;1\rangle \\
&= X_2^g X_2^{h^{-1}} X_2^{g^{-1}} \gamma_1^{\lambda(g,h)} a_1^\dagger(g) a_1^\dagger(h) \left(\prod_{2\le i\le Y} (-i\gamma_{Li}\gamma_{Ri}) \right)^{\lambda(g,h)} |\Omega;1\rangle \\
&= \gamma_1^{\lambda(g,h)} a_1^\dagger(g) a_2^\dagger(h) \left(\gamma_{L2}(-i)\gamma_{RY} \prod_{i\ge 2} (-i\gamma_{Ri}\gamma_{Li+1}) \right)^{\lambda(g,h)} |\Omega;1\rangle \\
&= \gamma_1^{\lambda(g,h)} a_1^\dagger(g) a_2^\dagger(h) (\gamma_{L2}(-i)\gamma_{R2})^{\lambda(g,h)} |\Omega;1\rangle \\
&= a_1^\dagger(g) a_2^\dagger(h) (-i\gamma_{R2})^{\lambda(g,h)} |\Omega;1\rangle \\
&= |(g,0)_1,(h,0)_2\rangle
\end{aligned}
\tag{7.78}
$$

This proves that $\rho(g,h) = \lambda(g,h)$. The domain wall creation operators are all fermion parity indefinite, so one might worry that the above calculation is not well defined. However, it is possible to truncate these operators at some finite point far to the right and generate these states with fermion parity definite operators.

We now write down the movement operators for bare domain walls.

$$
\begin{aligned}
M^{(g,0)}_{(n+1)n} &= \sum_{h\in G_0} U^h (X^{g)}_{n+1})^{-1} P^g_{n+1} U^{h\dagger} \\
M^{(g,0)}_{n(n+1)} &= \sum_{h\in G_0} U^h X^{g)}_{n+1} P^g_{n+1} U^{h\dagger}
\end{aligned}
\tag{7.79}
$$

These operators are symmetric. We now show that $M^{(g,0)}_{(n+1)n}$ has the correct action on single

domain wall states

$$\begin{aligned} M^{(g,0)}_{(n+1)n}|(g,0)_n\rangle &= (X^g_{n+1})^\dagger a^\dagger_n|\Omega;1\rangle \\ &= a^\dagger_{n+1}|\Omega;1\rangle \\ &= |(g,0)_1\rangle \end{aligned} \tag{7.80}$$

Using these splitting and movement operators, we will choose

$$\begin{aligned} \widetilde{S}(g,h) &= \sum_{k\in G_0} U^k X^g_2 X^{h^{-1}}_2 X^{g^{-1}}_2 P^{gh}_2 U^{k\dagger} \gamma_1^{\lambda(g,h)} \\ \widetilde{M}^g_{(n+1)n} &= \sum_{h\in G_0} U^h (X^{g)}_{n+1})^{-1} P^g_{n+1} U^{h\dagger} \\ \widetilde{M}^g &= \sum_{h\in G_0} U^h X^{g)}_{n+1} P^g_{n+1} U^{h\dagger} \end{aligned} \tag{7.81}$$

Using Eqs. 7.75,7.78,7.81, we see that

$$\widetilde{S}(g,h)|(gh,0)_1\rangle = a^\dagger_1(g) a^\dagger_2(h) (-i\gamma_{RY})^{\lambda(g,h)}|\Omega;1\rangle \tag{7.82}$$

Using Eq. 5.51, we can now compute $\nu(g,h,k)$ by defining the states

$$\begin{aligned} |\widetilde{1}\rangle &= \widetilde{M}^h_{12}\widetilde{M}^g_{01}\widetilde{S}(g,k)\widetilde{M}^k_{32}\widetilde{S}(gh,k)|(ghk,0)_1\rangle \\ |\widetilde{2}\rangle &= \widetilde{M}^{k\,g}_{32}\widetilde{S}(h,k)\widetilde{M}^{hk}_{12}\widetilde{M}^g_{01}\widetilde{S}(g,hk)|(ghk,0)_1\rangle \end{aligned} \tag{7.83}$$

We now simplify these states.

$$
\begin{aligned}
|\widetilde{1}\rangle &= \widetilde{M}_{12}^{h}\widetilde{M}_{01}^{g}\widetilde{S}(g,h)\widetilde{M}_{32}^{k}\widetilde{S}(gh,k)|(ghk,0)_1\rangle \\
&= \widetilde{M}_{12}^{h}\widetilde{M}_{01}^{g}\widetilde{S}(g,k)\widetilde{M}_{32}^{k}a_1^{\dagger}(gh)a_2^{\dagger}(k)(-i\gamma_{RY})^{\lambda(gh,k)}|\Omega;1\rangle \\
&= \widetilde{M}_{12}^{h}\widetilde{M}_{01}^{g}\widetilde{S}(g,h)U^{gh}(X_3^k)^{-1}U^{gh\dagger}a_1^{\dagger}(gh)a_2^{\dagger}(k)(-i\gamma_{RY})^{\lambda(gh,k)}|\Omega;1\rangle \\
&= \widetilde{M}_{12}^{h}\widetilde{M}_{01}^{g}\widetilde{S}(g,h)a_1^{\dagger}(gh)a_3^{\dagger}(k)(-i\gamma_{RY})^{\lambda(gh,k)}|\Omega;1\rangle \\
&= \widetilde{M}_{12}^{h}\widetilde{M}_{01}^{g}X_2^{g}(X_2^{h})^{-1}(X_2^{g})^{-1}\gamma_1^{\lambda(g,h)}a_1^{\dagger}(gh)a_3^{\dagger}(k)(-i\gamma_{RY})^{\lambda(gh,k)}|\Omega;1\rangle \\
&= \widetilde{M}_{12}^{h}\widetilde{M}_{01}^{g}X_2^{g}(X_2^{h})^{-1}(X_2^{g})^{-1}\gamma_1^{\lambda(g,h)}a_1^{\dagger}(g)a_1^{\dagger}(h) \\
&F_1a_3^{\dagger}(k)(-i\gamma_{RY})^{\lambda(gh,k)}|\Omega;1\rangle \\
&= \widetilde{M}_{12}^{h}\widetilde{M}_{01}^{g}a_1^{\dagger}(g)a_2^{\dagger}(h)a_3^{\dagger}(k) \\
&\gamma_1^{\lambda(g,h)}F_1(-i\gamma_{RY})^{\lambda(gh,k)}|\Omega;1\rangle \\
&= \widetilde{M}_{12}^{h}a_0^{\dagger}(g)a_2^{\dagger}(h)a_3^{\dagger}(k) \\
&(-i\gamma_{RY})^{\lambda(gh,k)+\lambda(g,h)}|\Omega;1\rangle \\
&= a_0^{\dagger}(g)a_1^{\dagger}(h)a_3^{\dagger}(k) \\
&(-i\gamma_{RY})^{\lambda(gh,k)+\lambda(g,h)}|\Omega;1\rangle
\end{aligned}
\tag{7.84}
$$

We now simplify state $|\widetilde{2}\rangle$.

$$
\begin{aligned}
|\widetilde{2}\rangle &= \widetilde{M}_{32}^{k\,g}\widetilde{S}(h,k)\widetilde{M}_{12}^{hk}\widetilde{M}_{01}^{g}\widetilde{S}(g,hk)|(ghk,0)_1\rangle \\
&= \widetilde{M}_{32}^{k\,g}\widetilde{S}(h,k)\widetilde{M}_{12}^{hk}\widetilde{M}_{01}^{g}a_1^\dagger(g)a_2^\dagger(hk)(-i\gamma_{RY})^{\lambda(g,hk)}|\Omega;1\rangle \\
&= \widetilde{M}_{32}^{k}\widetilde{S}(h,k)\widetilde{M}_{12}^{hk}a_0^\dagger(g)a_2^\dagger(hk)(-i\gamma_{RY})^{\lambda(g,hk)}|\Omega;1\rangle \\
&= \widetilde{M}_{32}^{k\,g}\widetilde{S}(h,k)a_0^\dagger(g)a_1^\dagger(hk)(-i\gamma_{RY})^{\lambda(g,hk)}|\Omega;1\rangle \\
&= \widetilde{M}_{32}^{k}S((h,0),(k,0))^g\gamma_1^{\lambda(h,k)}a_0^\dagger(g)a_1^\dagger(hk)(-i\gamma_{RY})^{\lambda(g,hk)}|\Omega;1\rangle \\
&= \widetilde{M}_{32}^{k}a_0^\dagger(g)S((h,0),(k,0))\gamma_1^{\lambda(h,k)}a_1^\dagger(hk)(-i\gamma_{RY})^{\lambda(g,hk)}|\Omega;1\rangle \\
&= \widetilde{M}_{32}^{k}a_0^\dagger(g)S((h,0),(k,0))\gamma_1^{\lambda(h,k)}a_1^\dagger(h)a_1^\dagger(k)F_1(-i\gamma_{RY})^{\lambda(g,hk)}|\Omega;1\rangle \\
&= \widetilde{M}_{32}^{k}a_0^\dagger(g)X_2^g(X_2^h)^{-1}X_2^g)^{-1}a_1^\dagger(h)a_1^\dagger(k)(-i\gamma_{RY})^{\lambda(g,hk)+\lambda(h,k)}|\Omega;1\rangle \\
&= \widetilde{M}_{32}^{k}a_0^\dagger(g)a_1^\dagger(h)a_2^\dagger(k)(-i\gamma_{RY})^{\lambda(g,hk)+\lambda(h,k)}|\Omega;1\rangle \\
&= a_0^\dagger(g)a_1^\dagger(h)a_3^\dagger(k)(-i\gamma_{RY})^{\lambda(g,hk)+\lambda(h,k)}|\Omega;1\rangle \\
&= a_0^\dagger(g)a_1^\dagger(h)a_3^\dagger(k)(-i\gamma_{RY})^{\lambda(gh,k)+\lambda(g,h)}|\Omega;1\rangle \\
&= |\widetilde{1}\rangle
\end{aligned}
\tag{7.85}
$$

Therefore,

$$
\nu(g,h,k) = 1. \tag{7.86}
$$

7.8.3 Stacking rules

We will now prove the stacking rule for two fermionic SPTs in (2+1)D with no Majorana degrees of freedom. This will allow us to see how a theory transforms when stacked with the Kitaev chain. Note that in the main text when $\eta \neq 0$, we treated the case of $\lambda = 0$. In this case, the Kitaev chain is trivial.

The stacking rule for the super cohomological data is

$$\begin{aligned}\rho(g,h) =&\rho_A(g,h)+\rho_B(g,h)\\ \nu(g,h,k) =&\nu_A(g,h,k)\nu_B(g,h,k)\\ &(-1)^{\rho_A(gh,k)\rho_B(g,h)+\rho_A(g,hk)\rho_B(h,k)}\end{aligned} \tag{7.87}$$

It can be shown that these data still meet the constraints

$$\begin{aligned}d\rho &= 0\\ d\nu &= 1\end{aligned} \tag{7.88}$$

In the stacked theory, we will use the fermion operators

$$\gamma_x = \gamma_x^A \tag{7.89}$$

where γ_x^A, γ_x^B are the fermion operators in the A and B models, respectively.

The vacuum states take the form

$$|\Omega; g\rangle = |\Omega; g\rangle_A \otimes_F |\Omega; g\rangle_B \tag{7.90}$$

where $\otimes_F$ is the stacking operation for fermionic theories and $|\Omega; g\rangle_{A,B}\rangle$ are the vacuum states for A and B, respectively. The domain walls take the form

$$\begin{aligned}|(g,0)_x\rangle &= |(g,0)_x\rangle \otimes_F |(g,0)_x\rangle\\ |(g,1)_x\rangle &= \gamma_x|(g,0)_x\rangle\end{aligned} \tag{7.91}$$

We will use the movement operators

$$M^{(g,0)}_{x'x} = M^{(g,0)}_{A,x'x} M^{(g,0)}_{B,x'x} \tag{7.92}$$

This we can see that this is a valid movement operator as it is symmetric and

$$\begin{aligned} M^{(g,0)}_{x'x}|(g,0)_x\rangle &= M^{(g,0)}_{A,x'x} M^{(g,0)}_{B,x'x}|(g,0)_x\rangle \otimes_F |(g,0)_x\rangle \qquad (7.93)\\ &= M^{(g,0)}_{A,x'x}|(g,0)_x\rangle \otimes_F M^{(g,0)}_{B,x'x}|(g,0)_x\rangle \\ &\propto |(g,0)_{x'}\rangle \otimes_F |(g,0)_{x'}\rangle \\ &\propto |(g,0)_{x'}\rangle \qquad (7.94) \end{aligned}$$

If we have a valid splitting operator, then we know it must obey the following property

$$\begin{aligned} &S((g,0),(h,0))|(gh,\rho(g,h))_1\rangle \\ &\qquad \propto \widetilde{S}^A(g,h)\widetilde{S}^B(g,h)\gamma_1^{\rho(g,h)}|(gh,\rho(g,h))_1\rangle \end{aligned} \tag{7.95}$$

We will promote this proportionality to an equality by choosing the phase of the splitting operator.

$$\begin{aligned} &S((g,0),(h,0))|(gh,\rho(g,h))_1\rangle \\ &\qquad = \widetilde{S}^A(g,h)\widetilde{S}^B(g,h)\gamma_1^{\rho(g,h)}|(gh,\rho(g,h))_1\rangle \end{aligned} \tag{7.96}$$

Recalling that $\widetilde{S}(g,h) \equiv S((g,0),(h,0))\gamma_1^{\rho(g,h)}$, one can show that

$$\widetilde{S}(g,h)|(gh,0)_1\rangle \propto \widetilde{S}^A(g,h)\widetilde{S}^B(g,h)|(gh,0)_1\rangle \tag{7.97}$$

We now want to investigate the action of the operator ${}^g\widetilde{S}(h,k)$ when acting on multi-domain

wall states. We know that

$$
\begin{aligned}
&{}^{g}\widetilde{S}(h,k)|(g,0)_0,(hk,0)_1,(l,0)_3\rangle \\
&\propto {}^{g}\widetilde{S}^{A}(g,h){}^{g}\widetilde{S}^{B}(g,h)|(g,0)_0,(hk,0)_1,(l,0)_3\rangle
\end{aligned}
\tag{7.98}
$$

We will now show that this proportionality is actually an equality by taking the inner product of the left and right hand sides of the equation.

$$
\begin{aligned}
&\langle(g,0)_0,(hk,0)_1,(l,0)_3|{}^{g}\widetilde{S}^{B}(g,h)^{\dagger} \\
&{}^{g}\widetilde{S}^{A}(g,h)^{\dagger}{}^{g}\widetilde{S}(h,k)|(g,0)_0,(hk,0)_1,(l,0)_3\rangle \\
&= \langle(hk,0)_1|(U^{g})^{-1}{}^{g}\widetilde{S}^{B}(g,h)^{\dagger}{}^{g}\widetilde{S}^{A}(g,h)^{\dagger}{}^{g}\widetilde{S}(h,k)U^{g}|(hk,0)_1\rangle \\
&= \langle(hk,0)_1|\widetilde{S}^{B}(g,h)^{\dagger}\widetilde{S}^{A}(g,h)^{\dagger}\widetilde{S}(h,k)|(hk,0)_1\rangle \\
&= \langle(hk,\rho(h,k))_1|\gamma_1^{-\rho(h,k)}\widetilde{S}^{B}(g,h)^{\dagger}\widetilde{S}^{A}(g,h)^{\dagger}S(h,k)|(hk,\rho(h,k))_1\rangle \\
&= 1
\end{aligned}
\tag{7.99}
$$

Where the last line follows from Eq. 7.96. Using the states in Eq. 5.51, we may therefore write

$$
\begin{aligned}
|\widetilde{1}\rangle =&\widetilde{M}^{h}_{A,12}\widetilde{M}^{h}_{B,12}\widetilde{M}^{g}_{A,01}\widetilde{M}^{g}_{B,01}\widetilde{S}^{A}(g,h)\widetilde{S}^{B}(g,h)\widetilde{M}^{k}_{A,32}\widetilde{M}^{k}_{B,32}\\
&\cdot\widetilde{S}^{A}(gh,k)\widetilde{S}^{B}(gh,k)|(ghk)_0\rangle_A\otimes_F|(ghk)_0\rangle_B\\
=&(-1)^{\rho_A(gh,k)\rho_B(g,h)}\widetilde{M}^{h}_{A,12}\widetilde{M}^{g}_{A,01}\widetilde{S}^{A}(g,h)\widetilde{M}^{k}_{A,32}\\
&\cdot\widetilde{S}^{A}(gh,k)\widetilde{M}^{h}_{B,12}\widetilde{M}^{g}_{B,01}\widetilde{S}^{B}(g,h)\widetilde{M}^{k}_{B,32}\widetilde{S}^{B}(gh,k)|(ghk)_0\rangle_A\otimes_F|(ghk)_0\rangle_B\\
|\widetilde{2}\rangle =&\widetilde{M}^{k}_{A,32}\widetilde{M}^{k}_{B,32}{}^{g}\widetilde{S}^{A}(h,k)^{g}\widetilde{S}^{B}(h,k)\widetilde{M}^{hk}_{A,12}\widetilde{M}^{hk}_{B,12}\widetilde{M}^{g}_{A,01}\widetilde{M}^{g}_{B,01}\\
&\cdot\widetilde{S}^{A}(g,hk)\widetilde{S}^{B}(g,hk)|(ghk)_0\rangle_A\otimes_F|(ghk)_0\rangle_B\\
=&(-1)^{\rho_A(g,hk)\rho_B(h,k)}\widetilde{M}^{k}_{A,32}{}^{g}\widetilde{S}^{A}(h,k)\widetilde{M}^{hk}_{A,12}\widetilde{M}^{g}_{A,01}\widetilde{S}^{A}(g,hk)\widetilde{M}^{k}_{B,32}{}^{g}\widetilde{S}^{B}(h,k)\widetilde{M}^{hk}_{B,12}\widetilde{M}^{g}_{B,01}\\
&\cdot\widetilde{S}^{B}(g,hk)|(ghk)_0\rangle_A\otimes_F|(ghk)_0\rangle_B
\end{aligned}
\tag{7.100}
$$

Taking the inner product between these two states, we obtain

$$
\begin{aligned}
\nu(g,h,k) =&\langle\widetilde{1}|\widetilde{2}\rangle\\
=&(-1)^{\rho_A(gh,k)\rho_B(g,h)+\rho_A(g,hk)\rho_B(h,k)}\\
&\cdot\langle(ghk,0)_1|_A\otimes_F\langle(ghk,0)_1|_B\mathcal{O}^A\mathcal{O}^B|(ghk,0)_1\rangle_A\otimes_F|(ghk,0)_1\rangle_B
\end{aligned}
\tag{7.101}
$$

where

$$
\begin{aligned}
\mathcal{O}^A =&\widetilde{S}^{A}(g,hk)^{\dagger}(\widetilde{M}^{g}_{A,01})^{\dagger}(\widetilde{M}^{hk}_{A,12})^{\dagger g}\widetilde{S}^{A}(h,k)^{\dagger}(\widetilde{M}^{k}_{A,32})^{\dagger}\widetilde{M}^{h}_{A,12}\widetilde{M}^{g}_{A,01}\widetilde{S}^{A}(g,h)\widetilde{M}^{k}_{A,32}\widetilde{S}^{A}(gh,k)\\
\mathcal{O}^B =&\widetilde{S}^{B}(g,hk)^{\dagger}(\widetilde{M}^{g}_{B,01})^{\dagger}(\widetilde{M}^{hk}_{B,12})^{\dagger g}\widetilde{S}^{B}(h,k)^{\dagger}(\widetilde{M}^{k}_{B,32})^{\dagger}\widetilde{M}^{h}_{B,12}\widetilde{M}^{g}_{B,01}\widetilde{S}^{B}(g,h)\widetilde{M}^{k}_{B,32}\widetilde{S}^{B}(gh,k)
\end{aligned}
\tag{7.102}
$$

This allows us to simplify our expression for $\nu(g,h,k)$ to

$$\begin{aligned}\nu(g,h,k) =&(-1)^{\rho_A(gh,k)\rho_B(g,h)+\rho_A(g,hk)\rho_B(h,k)}\\ &\cdot \langle (ghk,0)_1|_A\mathcal{O}^A|(ghk,0)_1\rangle_A\langle (ghk,0)_1|_B\mathcal{O}^B|(ghk,0)_1\rangle_B\\ =&(-1)^{\rho_A(gh,k)\rho_B(g,h)+\rho_A(g,hk)\rho_B(h,k)}\nu_A(g,h,k)\nu_B(g,h,k)\end{aligned} \tag{7.103}$$

In particular, if we were to say that B is a Kitaev chain and A were some other system with the same symmetry, this stacking would have the effect

$$\begin{aligned}\rho_A(g,h) &\to \rho_A(g,h)+\lambda(g,h)\\ \nu_A(g,h,k) &\to (-1)^{\rho_A(gh,k)\lambda(g,h)+\rho_A(g,hk)\lambda(h,k)}\nu_A(g,h,k)\end{aligned} \tag{7.104}$$

REFERENCES

[1] David Aasen, Parsa Bonderson, and Christina Knapp. Characterization and classification of fermionic symmetry enriched topological phases, 2021. URL https://arxiv.org/abs/2109.10911.

[2] Ian Affleck, Tom Kennedy, Elliott H. Lieb, and Hal Tasaki. Rigorous results on valence-bond ground states in antiferromagnets. *Phys. Rev. Lett.*, 59:799–802, Aug 1987. doi: 10.1103/PhysRevLett.59.799. URL https://link.aps.org/doi/10.1103/PhysRevLett.59.799.

[3] Ian Affleck, Tom Kennedy, Elliott H. Lieb, and Hal Tasaki. Valence bond ground states in isotropic quantum antiferromagnets. *Communications in Mathematical Physics*, 115 (3):477–528, September 1988. ISSN 0010-3616. doi: 10.1007/BF01218021.

[4] Daniel Arovas, J. R. Schrieffer, and Frank Wilczek. Fractional statistics and the quantum hall effect. *Phys. Rev. Lett.*, 53:722–723, Aug 1984. doi: 10.1103/PhysRevLett.53.722. URL https://link.aps.org/doi/10.1103/PhysRevLett.53.722.

[5] Bojko Bakalov and A.A. Kirillov. Lectures on tensor categories and modular functors. *Amer. Math. Soc. Univ. Lect. Ser.*, 21, 01 2001.

[6] Maissam Barkeshli and Meng Cheng. Time-reversal and spatial-reflection symmetry localization anomalies in (2+1)-dimensional topological phases of matter. *Phys. Rev. B*, 98:115129, Sep 2018. doi: 10.1103/PhysRevB.98.115129. URL https://link.aps.org/doi/10.1103/PhysRevB.98.115129.

[7] Maissam Barkeshli, Parsa Bonderson, Meng Cheng, and Zhenghan Wang. Symmetry fractionalization, defects, and gauging of topological phases. *Phys. Rev. B*, 100:115147, Sep 2019. doi: 10.1103/PhysRevB.100.115147. URL https://link.aps.org/doi/10.1103/PhysRevB.100.115147.

[8] Maissam Barkeshli, Yu-An Chen, Po-Shen Hsin, and Naren Manjunath. Classification of (2+1)d invertible fermionic topological phases with symmetry, 2021. URL https://arxiv.org/abs/2109.11039.

[9] V. L. Berezinsky. Destruction of long range order in one-dimensional and two-dimensional systems having a continuous symmetry group. I. Classical systems. *Sov. Phys. JETP*, 32:493–500, 1971.

[10] V. L. Berezinsky. Destruction of Long-range Order in One-dimensional and Two-dimensional Systems Possessing a Continuous Symmetry Group. II. Quantum Systems. *Sov. Phys. JETP*, 34(3):610, 1972.

[11] Hans Bethe. Zur theorie der metalle. *Zeitschrift für Physik*, 71:205–226, Mar 1931. doi: 10.1007/BF01341708. URL https://doi.org/10.1007/BF01341708.

[12] Lakshya Bhardwaj, Davide Gaiotto, and Anton Kapustin. State sum constructions of spin-tfts and string net constructions of fermionic phases of matter. *Journal of High Energy Physics*, 2017(4):96, 2017.

[13] Zhen Bi, Alex Rasmussen, Kevin Slagle, and Cenke Xu. Classification and description of bosonic symmetry protected topological phases with semiclassical nonlinear sigma models. *Phys. Rev. B*, 91:134404, Apr 2015. doi: 10.1103/PhysRevB.91.134404. URL https://link.aps.org/doi/10.1103/PhysRevB.91.134404.

[14] P. Bonderson, C. Nayak, and X.-L. Qi. A time-reversal invariant topological phase at the surface of a 3d topological insulator. *Journal of Statistical Mechanics: Theory and Experiment*, 2013(09):P09016, 2013. URL http://stacks.iop.org/1742-5468/2013/i=09/a=P09016.

[15] S. Bravyi, M. B. Hastings, and F. Verstraete. Lieb-robinson bounds and the generation of correlations and topological quantum order. *Phys. Rev. Lett.*, 97:050401, Jul 2006. doi: 10.1103/PhysRevLett.97.050401. URL https://link.aps.org/doi/10.1103/PhysRevLett.97.050401.

[16] Jacob C. Bridgeman and Dominic J. Williamson. Anomalies and entanglement renormalization. *Phys. Rev. B*, 96:125104, Sep 2017. doi: 10.1103/PhysRevB.96.125104. URL https://link.aps.org/doi/10.1103/PhysRevB.96.125104.

[17] Nick Bultinck. Uv perspective on mixed anomalies at critical points between bosonic symmetry-protected phases. *Phys. Rev. B*, 100:165132, Oct 2019. doi: 10.1103/PhysRevB.100.165132. URL https://link.aps.org/doi/10.1103/PhysRevB.100.165132.

[18] Nick Bultinck, Robijn Vanhove, Jutho Haegeman, and Frank Verstraete. Global anomaly detection in two-dimensional symmetry-protected topological phases. *Phys. Rev. Lett.*, 120:156601, Apr 2018. doi: 10.1103/PhysRevLett.120.156601. URL https://link.aps.org/doi/10.1103/PhysRevLett.120.156601.

[19] Matthew Cha, Pieter Naaijkens, and Bruno Nachtergaele. On the stability of charges in infinite quantum spin systems. *arXiv:1804.03203*, 2018.

[20] Chi-Ming Chang, Ying-Hsuan Lin, Shu-Heng Shao, Yifan Wang, and Xi Yin. Topological defect lines and renormalization group flows in two dimensions. *Journal of High Energy Physics*, 2019(1):26, 2019.

[21] Xie Chen and Ashvin Vishwanath. Towards gauging time-reversal symmetry: A tensor network approach. *Phys. Rev. X*, 5:041034, Nov 2015. doi: 10.1103/PhysRevX.5.041034. URL https://link.aps.org/doi/10.1103/PhysRevX.5.041034.

[22] Xie Chen and Xiao-Gang Wen. Chiral symmetry on the edge of two-dimensional symmetry protected topological phases. *Phys. Rev. B*, 86:235135, Dec 2012. doi: 10.1103/PhysRevB.86.235135. URL https://link.aps.org/doi/10.1103/PhysRevB.86.235135.

[23] Xie Chen, Zheng-Cheng Gu, and Xiao-Gang Wen. Local unitary transformation, long-range quantum entanglement, wave function renormalization, and topological order. *Phys. Rev. B*, 82:155138, Oct 2010. doi: 10.1103/PhysRevB.82.155138. URL https://link.aps.org/doi/10.1103/PhysRevB.82.155138.

[24] Xie Chen, Zheng-Cheng Gu, and Xiao-Gang Wen. Classification of gapped symmetric phases in one-dimensional spin systems. *Phys. Rev. B*, 83:035107, Jan 2011. doi: 10.1103/PhysRevB.83.035107. URL https://link.aps.org/doi/10.1103/PhysRevB.83.035107.

[25] Xie Chen, Zheng-Cheng Gu, and Xiao-Gang Wen. Complete classification of one-dimensional gapped quantum phases in interacting spin systems. *Phys. Rev. B*, 84:235128, Dec 2011. doi: 10.1103/PhysRevB.84.235128. URL https://link.aps.org/doi/10.1103/PhysRevB.84.235128.

[26] Xie Chen, Zheng-Xin Liu, and Xiao-Gang Wen. Two-dimensional symmetry-protected topological orders and their protected gapless edge excitations. *Phys. Rev. B*, 84:235141, Dec 2011. doi: 10.1103/PhysRevB.84.235141. URL https://link.aps.org/doi/10.1103/PhysRevB.84.235141.

[27] Xie Chen, Zheng-Cheng Gu, Zheng-Xin Liu, and Xiao-Gang Wen. Symmetry-protected topological orders in interacting bosonic systems. *Science*, 338(6114):1604–1606, 2012. ISSN 0036-8075. doi: 10.1126/science.1227224. URL https://science.sciencemag.org/content/338/6114/1604.

[28] Xie Chen, Zheng-Cheng Gu, Zheng-Xin Liu, and Xiao-Gang Wen. Symmetry protected topological orders and the group cohomology of their symmetry group. *Phys. Rev. B*, 87:155114, Apr 2013. doi: 10.1103/PhysRevB.87.155114. URL https://link.aps.org/doi/10.1103/PhysRevB.87.155114.

[29] Xie Chen, Fa Wang, Yuan-Ming Lu, and Dung-Hai Lee. Critical theories of phase transition between symmetry protected topological states and their relation to the gapless boundary theories. *Nuclear Physics B*, 873(1):248 – 259, 2013. ISSN 0550-3213. doi: https://doi.org/10.1016/j.nuclphysb.2013.04.015. URL http://www.sciencedirect.com/science/article/pii/S055032131300223X.

[30] Xie Chen, Lukasz Fidkowski, and Ashvin Vishwanath. Symmetry enforced non-abelian topological order at the surface of a topological insulator. *Phys. Rev. B*, 89:165132, Apr 2014. doi: 10.1103/PhysRevB.89.165132. URL https://link.aps.org/doi/10.1103/PhysRevB.89.165132.

[31] Xie Chen, Yuan-Ming Lu, and Ashvin Vishwanath. Symmetry-protected topological phases from decorated domain walls. *Nature Communications*, 5, Mar 2014. doi: 10.1038/ncomms4507. URL https://doi.org/10.1038/ncomms4507.

[32] Yu-An Chen, Anton Kapustin, Alex Turzillo, and Minyoung You. Free and interacting short-range entangled phases of fermions: Beyond the tenfold way. *Phys. Rev. B*, 100:

195128, Nov 2019. doi: 10.1103/PhysRevB.100.195128. URL https://link.aps.org/doi/10.1103/PhysRevB.100.195128.

[33] Meng Cheng and Zheng-Cheng Gu. Topological response theory of abelian symmetry-protected topological phases in two dimensions. *Phys. Rev. Lett.*, 112:141602, Apr 2014. doi: 10.1103/PhysRevLett.112.141602. URL https://link.aps.org/doi/10.1103/PhysRevLett.112.141602.

[34] Meng Cheng and Dominic J. Williamson. Relative anomaly in (1 + 1)d rational conformal field theory. *Phys. Rev. Research*, 2:043044, Oct 2020. doi: 10.1103/PhysRevResearch.2.043044. URL https://link.aps.org/doi/10.1103/PhysRevResearch.2.043044.

[35] Meng Cheng, Zhen Bi, Yi-Zhuang You, and Zheng-Cheng Gu. Classification of symmetry-protected phases for interacting fermions in two dimensions. *Phys. Rev. B*, 97:205109, May 2018. doi: 10.1103/PhysRevB.97.205109. URL https://link.aps.org/doi/10.1103/PhysRevB.97.205109.

[36] Meng Cheng, Zhen Bi, Yi-Zhuang You, and Zheng-Cheng Gu. Classification of symmetry-protected phases for interacting fermions in two dimensions. *Phys. Rev. B*, 97:205109, May 2018. doi: 10.1103/PhysRevB.97.205109. URL https://link.aps.org/doi/10.1103/PhysRevB.97.205109.

[37] Clay Cordova, Kantaro Ohmori, Shu-Heng Shao, and Fei Yan. Decorated $\mathbb{Z}_2$ symmetry defects and their time-reversal anomalies, 2019.

[38] Tyler D. Ellison and Lukasz Fidkowski. Disentangling interacting symmetry-protected phases of fermions in two dimensions. *Phys. Rev. X*, 9:011016, Jan 2019. doi: 10.1103/PhysRevX.9.011016. URL https://link.aps.org/doi/10.1103/PhysRevX.9.011016.

[39] Dominic V. Else and Chetan Nayak. Classifying symmetry-protected topological phases through the anomalous action of the symmetry on the edge. *Phys. Rev. B*, 90:235137, Dec 2014. doi: 10.1103/PhysRevB.90.235137. URL https://link.aps.org/doi/10.1103/PhysRevB.90.235137.

[40] Lukasz Fidkowski and Alexei Kitaev. Topological phases of fermions in one dimension. *Phys. Rev. B*, 83:075103, Feb 2011. doi: 10.1103/PhysRevB.83.075103. URL https://link.aps.org/doi/10.1103/PhysRevB.83.075103.

[41] K. Fredenhagen, K. H. Rehren, and B. Schroer. Superselection sectors with braid group statistics and exchange algebras. *Communications in Mathematical Physics*, 125(2):201–226, Jun 1989. ISSN 1432-0916. doi: 10.1007/BF01217906. URL https://doi.org/10.1007/BF01217906.

[42] J. Frohlich and F. Gabbiani. Braid statistics in local quantum theory. *Reviews in Mathematical Physics*, 02(03):251–353, 1990. doi: 10.1142/S0129055X90000107. URL https://doi.org/10.1142/S0129055X90000107.

[43] Liang Fu, C. L. Kane, and E. J. Mele. Topological insulators in three dimensions. *Phys. Rev. Lett.*, 98:106803, Mar 2007. doi: 10.1103/PhysRevLett.98.106803. URL https://link.aps.org/doi/10.1103/PhysRevLett.98.106803.

[44] Zongping Gong, Christoph Sünderhauf, Norbert Schuch, and J. Ignacio Cirac. Classification of matrix-product unitaries with symmetries. *Phys. Rev. Lett.*, 124:100402, Mar 2020. doi: 10.1103/PhysRevLett.124.100402. URL https://link.aps.org/doi/10.1103/PhysRevLett.124.100402.

[45] Tobias Graß, Bruno Juliá-Díaz, and Maciej Lewenstein. Topological phases in small quantum hall samples. *Phys. Rev. A*, 89:013623, Jan 2014. doi: 10.1103/PhysRevA.89.013623. URL https://link.aps.org/doi/10.1103/PhysRevA.89.013623.

[46] Zheng-Cheng Gu and Xiao-Gang Wen. Tensor-entanglement-filtering renormalization approach and symmetry-protected topological order. *Phys. Rev. B*, 80:155131, Oct 2009. doi: 10.1103/PhysRevB.80.155131. URL https://link.aps.org/doi/10.1103/PhysRevB.80.155131.

[47] Zheng-Cheng Gu and Xiao-Gang Wen. Symmetry-protected topological orders for interacting fermions: Fermionic topological nonlinear σ models and a special group supercohomology theory. *Phys. Rev. B*, 90:115141, Sep 2014. doi: 10.1103/PhysRevB.90.115141. URL https://link.aps.org/doi/10.1103/PhysRevB.90.115141.

[48] Zheng-Cheng Gu, Juven C. Wang, and Xiao-Gang Wen. Multikink topological terms and charge-binding domain-wall condensation induced symmetry-protected topological states: Beyond chern-simons/bf field theories. *Phys. Rev. B*, 93:115136, Mar 2016. doi: 10.1103/PhysRevB.93.115136. URL https://link.aps.org/doi/10.1103/PhysRevB.93.115136.

[49] Jeongwan Haah. An invariant of topologically ordered states under local unitary transformations. *Communications in Mathematical Physics*, 342(3):771–801, Mar 2016. ISSN 1432-0916. doi: 10.1007/s00220-016-2594-y. URL https://doi.org/10.1007/s00220-016-2594-y.

[50] F. D. M. Haldane. Nonlinear field theory of large-spin heisenberg antiferromagnets: Semiclassically quantized solitons of the one-dimensional easy-axis néel state. *Phys. Rev. Lett.*, 50:1153–1156, Apr 1983. doi: 10.1103/PhysRevLett.50.1153. URL https://link.aps.org/doi/10.1103/PhysRevLett.50.1153.

[51] F.D.M. Haldane. Continuum dynamics of the 1-d heisenberg antiferromagnet: Identification with the o(3) nonlinear sigma model. *Physics Letters A*, 93(9):464–468, 1983. ISSN 0375-9601. doi: https://doi.org/10.1016/0375-9601(83)90631-X. URL https://www.sciencedirect.com/science/article/pii/037596018390631X.

[52] Bo Han, Apoorv Tiwari, Chang-Tse Hsieh, and Shinsei Ryu. Boundary conformal field theory and symmetry-protected topological phases in $2+1$ dimensions. *Phys. Rev. B*,

96:125105, Sep 2017. doi: 10.1103/PhysRevB.96.125105. URL https://link.aps.org/doi/10.1103/PhysRevB.96.125105.

[53] M. Z. Hasan and C. L. Kane. Colloquium: Topological insulators. *Rev. Mod. Phys.*, 82:3045–3067, Nov 2010. doi: 10.1103/RevModPhys.82.3045. URL https://link.aps.org/doi/10.1103/RevModPhys.82.3045.

[54] M. B. Hastings and Xiao-Gang Wen. Quasiadiabatic continuation of quantum states: The stability of topological ground-state degeneracy and emergent gauge invariance. *Phys. Rev. B*, 72:045141, Jul 2005. doi: 10.1103/PhysRevB.72.045141. URL https://link.aps.org/doi/10.1103/PhysRevB.72.045141.

[55] Chris Heinrich and Michael Levin. Criteria for protected edge modes with F_2 symmetry. *Phys. Rev. B*, 98:035101, Jul 2018. doi: 10.1103/PhysRevB.98.035101. URL https://link.aps.org/doi/10.1103/PhysRevB.98.035101.

[56] Chris Heinrich, Fiona Burnell, Lukasz Fidkowski, and Michael Levin. Symmetry-enriched string nets: Exactly solvable models for set phases. *Phys. Rev. B*, 94:235136, Dec 2016. doi: 10.1103/PhysRevB.94.235136. URL https://link.aps.org/doi/10.1103/PhysRevB.94.235136.

[57] Chang-Tse Hsieh, Olabode Mayodele Sule, Gil Young Cho, Shinsei Ryu, and Robert G. Leigh. Symmetry-protected topological phases, generalized laughlin argument, and orientifolds. *Phys. Rev. B*, 90:165134, Oct 2014. doi: 10.1103/PhysRevB.90.165134. URL https://link.aps.org/doi/10.1103/PhysRevB.90.165134.

[58] Yuting Hu, Yidun Wan, and Yong-Shi Wu. Twisted quantum double model of topological phases in two dimensions. *Phys. Rev. B*, 87:125114, Mar 2013. doi: 10.1103/PhysRevB.87.125114. URL https://link.aps.org/doi/10.1103/PhysRevB.87.125114.

[59] Ching-Yu Huang and Tzu-Chieh Wei. Detecting and identifying two-dimensional symmetry-protected topological, symmetry-breaking, and intrinsic topological phases with modular matrices via tensor-network methods. *Phys. Rev. B*, 93:155163, Apr 2016. doi: 10.1103/PhysRevB.93.155163. URL https://link.aps.org/doi/10.1103/PhysRevB.93.155163.

[60] Ling-Yan Hung and Xiao-Gang Wen. Universal symmetry-protected topological invariants for symmetry-protected topological states. *Phys. Rev. B*, 89:075121, Feb 2014. doi: 10.1103/PhysRevB.89.075121. URL https://link.aps.org/doi/10.1103/PhysRevB.89.075121.

[61] D. A. Ivanov. Non-abelian statistics of half-quantum vortices in p-wave superconductors. *Phys. Rev. Lett.*, 86:268–271, Jan 2001. doi: 10.1103/PhysRevLett.86.268. URL https://link.aps.org/doi/10.1103/PhysRevLett.86.268.

[62] R. Jackiw and C. Rebbi. Solitons with fermion number $\frac{1}{2}$. *Phys. Rev. D*, 13:3398–3409, Jun 1976. doi: 10.1103/PhysRevD.13.3398. URL https://link.aps.org/doi/10.1103/PhysRevD.13.3398.

[63] Shenghan Jiang and Ying Ran. Anyon condensation and a generic tensor-network construction for symmetry-protected topological phases. *Phys. Rev. B*, 95:125107, Mar 2017. doi: 10.1103/PhysRevB.95.125107. URL https://link.aps.org/doi/10.1103/PhysRevB.95.125107.

[64] Theo Johnson-Freyd. On the classification of topological orders. *Communications in Mathematical Physics*, 2022. doi: 10.1007/s00220-022-04380-3. URL https://doi.org/10.1007/s00220-022-04380-3.

[65] Robert A. Jones and Max A. Metlitski. One-dimensional lattice models for the boundary of two-dimensional majorana fermion symmetry-protected topological phases: Kramers-wannier duality as an exact Z_2 symmetry. *Phys. Rev. B*, 104:245130, Dec 2021. doi: 10.1103/PhysRevB.104.245130. URL https://link.aps.org/doi/10.1103/PhysRevB.104.245130.

[66] C. L. Kane and E. J. Mele. Z_2 topological order and the quantum spin hall effect. *Phys. Rev. Lett.*, 95:146802, Sep 2005. doi: 10.1103/PhysRevLett.95.146802. URL https://link.aps.org/doi/10.1103/PhysRevLett.95.146802.

[67] Anton Kapustin. Symmetry protected topological phases, anomalies, and cobordisms: Beyond group cohomology, 2014. URL https://arxiv.org/abs/1403.1467.

[68] Anton Kapustin, Ryan Thorngren, Alex Turzillo, and Zitao Wang. Fermionic symmetry protected topological phases and cobordisms. *Journal of High Energy Physics*, 2015, 2015. doi: 10.1007/JHEP12(2015)052. URL https://doi.org/10.1007/JHEP12(2015)052.

[69] Kyle Kawagoe and Michael Levin. Microscopic definitions of anyon data. *Phys. Rev. B*, 101:115113, Mar 2020. doi: 10.1103/PhysRevB.101.115113. URL https://link.aps.org/doi/10.1103/PhysRevB.101.115113.

[70] Kyle Kawagoe and Michael Levin. Anomalies in bosonic symmetry-protected topological edge theories: Connection to f symbols and a method of calculation. *Phys. Rev. B*, 104:115156, Sep 2021. doi: 10.1103/PhysRevB.104.115156. URL https://link.aps.org/doi/10.1103/PhysRevB.104.115156.

[71] Kyle Kawagoe and Michael Levin. In preparation. 2022.

[72] ESKO KESKI-VAKKURI and XIAO-GANG WEN. The ground state structure and modular transformations of fractional quantum hall states on a torus. *International Journal of Modern Physics B*, 07(25):4227–4259, 1993. doi: 10.1142/S0217979293003644. URL https://doi.org/10.1142/S0217979293003644.

[73] A. Yu. Kitaev. Fault-tolerant quantum computation by anyons. *Annals of Physics*, 303(1):2 – 30, 2003. ISSN 0003-4916. doi: https://doi.org/10.1016/S0003-4916(02)00018-0. URL http://www.sciencedirect.com/science/article/pii/S0003491602000180.

[74] Alexei Kitaev. Anyons in an exactly solved model and beyond. *Annals of Physics*, 321(1):2 – 111, 2006. ISSN 0003-4916. doi: https://doi.org/10.1016/j.aop.2005.10.005. URL http://www.sciencedirect.com/science/article/pii/S0003491605002381.

[75] Alexei Kitaev and John Preskill. Topological entanglement entropy. *Phys. Rev. Lett.*, 96:110404, Mar 2006. doi: 10.1103/PhysRevLett.96.110404. URL https://link.aps.org/doi/10.1103/PhysRevLett.96.110404.

[76] Liang Kong and Hao Zheng. Categories of quantum liquids i, 2020. URL https://arxiv.org/abs/2011.02859.

[77] Liang Kong, Yin Tian, and Zhi-Hao Zhang. Defects in the 3-dimensional toric code model form a braided fusion 2-category. *Journal of High Energy Physics*, 2020, 2020. doi: 10.1007/JHEP12(2020)078. URL https://doi.org/10.1007/JHEP12(2020)078.

[78] J M Kosterlitz and D J Thouless. Long range order and metastability in two dimensional solids and superfluids. (application of dislocation theory). *Journal of Physics C: Solid State Physics*, 5(11):L124–L126, jun 1972. doi: 10.1088/0022-3719/5/11/002. URL https://doi.org/10.1088/0022-3719/5/11/002.

[79] J M Kosterlitz and D J Thouless. Ordering, metastability and phase transitions in two-dimensional systems. *Journal of Physics C: Solid State Physics*, 6(7):1181–1203, apr 1973. doi: 10.1088/0022-3719/6/7/010. URL https://doi.org/10.1088/0022-3719/6/7/010.

[80] Tian Lan, Liang Kong, and Xiao-Gang Wen. Classification of (2+1)-dimensional topological order and symmetry-protected topological order for bosonic and fermionic systems with on-site symmetries. *Phys. Rev. B*, 95:235140, Jun 2017. doi: 10.1103/PhysRevB.95.235140. URL https://link.aps.org/doi/10.1103/PhysRevB.95.235140.

[81] Matthew F. Lapa and Michael Levin. Anomaly indicators for topological orders with $u(1)$ and time-reversal symmetry. *Phys. Rev. B*, 100:165129, Oct 2019. doi: 10.1103/PhysRevB.100.165129. URL https://link.aps.org/doi/10.1103/PhysRevB.100.165129.

[82] R. B. Laughlin. Anomalous quantum hall effect: An incompressible quantum fluid with fractionally charged excitations. *Phys. Rev. Lett.*, 50:1395–1398, May 1983. doi: 10.1103/PhysRevLett.50.1395. URL https://link.aps.org/doi/10.1103/PhysRevLett.50.1395.

[83] J. M. Leinaas and J. Myrheim. On the theory of identical particles. *Nuovo Cimento B Serie*, 37(1):1–23, January 1977. doi: 10.1007/BF02727953.

[84] Michael Levin and Zheng-Cheng Gu. Braiding statistics approach to symmetry-protected topological phases. *Phys. Rev. B*, 86:115109, Sep 2012. doi: 10.1103/PhysRevB.86.115109. URL https://link.aps.org/doi/10.1103/PhysRevB.86.115109.

[85] Michael Levin and Ady Stern. Classification and analysis of two-dimensional abelian fractional topological insulators. *Phys. Rev. B*, 86:115131, Sep 2012. doi: 10.1103/PhysRevB.86.115131. URL https://link.aps.org/doi/10.1103/PhysRevB.86.115131.

[86] Michael Levin and Xiao-Gang Wen. Fermions, strings, and gauge fields in lattice spin models. *Phys. Rev. B*, 67:245316, Jun 2003. doi: 10.1103/PhysRevB.67.245316. URL https://link.aps.org/doi/10.1103/PhysRevB.67.245316.

[87] Michael Levin and Xiao-Gang Wen. Detecting topological order in a ground state wave function. *Phys. Rev. Lett.*, 96:110405, Mar 2006. doi: 10.1103/PhysRevLett.96.110405. URL https://link.aps.org/doi/10.1103/PhysRevLett.96.110405.

[88] Michael A. Levin and Xiao-Gang Wen. String-net condensation: A physical mechanism for topological phases. *Phys. Rev. B*, 71:045110, Jan 2005. doi: 10.1103/PhysRevB.71.045110. URL https://link.aps.org/doi/10.1103/PhysRevB.71.045110.

[89] Joey Li, Amos Chan, and Thorsten B. Wahl. Classification of symmetry-protected topological phases in two-dimensional many-body localized systems. *Phys. Rev. B*, 102:014205, Jul 2020. doi: 10.1103/PhysRevB.102.014205. URL https://link.aps.org/doi/10.1103/PhysRevB.102.014205.

[90] Chien-Hung Lin and Michael Levin. Loop braiding statistics in exactly soluble three-dimensional lattice models. *Phys. Rev. B*, 92:035115, Jul 2015. doi: 10.1103/PhysRevB.92.035115. URL https://link.aps.org/doi/10.1103/PhysRevB.92.035115.

[91] Ying-Hsuan Lin and Shu-Heng Shao. F_N symmetries, anomalies, and the modular bootstrap. *Phys. Rev. D*, 103:125001, Jun 2021. doi: 10.1103/PhysRevD.103.125001. URL https://link.aps.org/doi/10.1103/PhysRevD.103.125001.

[92] Zheng-Xin Liu, Zheng-Cheng Gu, and Xiao-Gang Wen. Microscopic realization of two-dimensional bosonic topological insulators. *Phys. Rev. Lett.*, 113:267206, Dec 2014. doi: 10.1103/PhysRevLett.113.267206. URL https://link.aps.org/doi/10.1103/PhysRevLett.113.267206.

[93] Yuan-Ming Lu and Dung-Hai Lee. Gapped symmetric edges of symmetry-protected topological phases. *Phys. Rev. B*, 89:205117, May 2014. doi: 10.1103/PhysRevB.89.205117. URL https://link.aps.org/doi/10.1103/PhysRevB.89.205117.

[94] Yuan-Ming Lu and Ashvin Vishwanath. Theory and classification of interacting integer topological phases in two dimensions: A chern-simons approach. *Phys. Rev. B*, 86: 125119, Sep 2012. doi: 10.1103/PhysRevB.86.125119. URL https://link.aps.org/doi/10.1103/PhysRevB.86.125119.

[95] Yuan-Ming Lu and Ashvin Vishwanath. Classification and properties of symmetry-enriched topological phases: Chern-simons approach with applications to Z_2 spin liquids. *Phys. Rev. B*, 93:155121, Apr 2016. doi: 10.1103/PhysRevB.93.155121. URL https://link.aps.org/doi/10.1103/PhysRevB.93.155121.

[96] Yuan-Ming Lu and Ashvin Vishwanath. Classification and properties of symmetry-enriched topological phases: Chern-simons approach with applications to Z_2 spin liquids. *Phys. Rev. B*, 93:155121, Apr 2016. doi: 10.1103/PhysRevB.93.155121. URL https://link.aps.org/doi/10.1103/PhysRevB.93.155121.

[97] Akishi Matsugatani and Haruki Watanabe. Connecting higher-order topological insulators to lower-dimensional topological insulators. *Phys. Rev. B*, 98:205129, Nov 2018. doi: 10.1103/PhysRevB.98.205129. URL https://link.aps.org/doi/10.1103/PhysRevB.98.205129.

[98] N. D. Mermin. The topological theory of defects in ordered media. *Rev. Mod. Phys.*, 51:591–648, Jul 1979. doi: 10.1103/RevModPhys.51.591. URL https://link.aps.org/doi/10.1103/RevModPhys.51.591.

[99] Andrej Mesaros and Ying Ran. Classification of symmetry enriched topological phases with exactly solvable models. *Phys. Rev. B*, 87:155115, Apr 2013. doi: 10.1103/PhysRevB.87.155115. URL https://link.aps.org/doi/10.1103/PhysRevB.87.155115.

[100] Max A. Metlitski, C. L. Kane, and Matthew P. A. Fisher. Symmetry-respecting topologically ordered surface phase of three-dimensional electron topological insulators. *Phys. Rev. B*, 92:125111, Sep 2015. doi: 10.1103/PhysRevB.92.125111. URL https://link.aps.org/doi/10.1103/PhysRevB.92.125111.

[101] Michaël Mignard and Peter Schauenburg. Modular categories are not determined by their modular data, 2017. URL https://arxiv.org/abs/1708.02796.

[102] Gregory Moore and Nicholas Read. Nonabelions in the fractional quantum hall effect. *Nuclear Physics B*, 360(2):362 – 396, 1991. ISSN 0550-3213. doi: https://doi.org/10.1016/0550-3213(91)90407-O. URL http://www.sciencedirect.com/science/article/pii/055032139190407O.

[103] Gregory Moore and Nathan Seiberg. Polynomial equations for rational conformal field theories. *Physics Letters B*, 212(4):451–460, 1988. ISSN 0370-2693. doi: https://doi.org/10.1016/0370-2693(88)91796-0. URL https://www.sciencedirect.com/science/article/pii/0370269388917960.

[104] Gregory Moore and Nathan Seiberg. Classical and quantum conformal field theory. *Communications in Mathematical Physics*, 123(2):177 – 254, 1989. doi: cmp/1104178762. URL https://doi.org/.

[105] J. E. Moore and L. Balents. Topological invariants of time-reversal-invariant band structures. *Phys. Rev. B*, 75:121306, Mar 2007. doi: 10.1103/PhysRevB.75.121306. URL https://link.aps.org/doi/10.1103/PhysRevB.75.121306.

[106] Heidar Moradi and Xiao-Gang Wen. Universal wave-function overlap and universal topological data from generic gapped ground states. *Phys. Rev. Lett.*, 115:036802, Jul 2015. doi: 10.1103/PhysRevLett.115.036802. URL https://link.aps.org/doi/10.1103/PhysRevLett.115.036802.

[107] Pieter Naaijkens. Localized endomorphisms in kitaev's toric code on the plane. *Reviews in Mathematical Physics*, 23(04):347–373, 2011. doi: 10.1142/S0129055X1100431X. URL https://doi.org/10.1142/S0129055X1100431X.

[108] Jeremy Oon, Gil Young Cho, and Cenke Xu. Two-dimensional symmetry-protected topological phases with $\mathbf{PSU}(n)$ and time-reversal symmetry. *Phys. Rev. B*, 88:014425, Jul 2013. doi: 10.1103/PhysRevB.88.014425. URL https://link.aps.org/doi/10.1103/PhysRevB.88.014425.

[109] Frank Pollmann and Ari M. Turner. Detection of symmetry-protected topological phases in one dimension. *Phys. Rev. B*, 86:125441, Sep 2012. doi: 10.1103/PhysRevB.86.125441. URL https://link.aps.org/doi/10.1103/PhysRevB.86.125441.

[110] Frank Pollmann, Ari M. Turner, Erez Berg, and Masaki Oshikawa. Entanglement spectrum of a topological phase in one dimension. *Phys. Rev. B*, 81:064439, Feb 2010. doi: 10.1103/PhysRevB.81.064439. URL https://link.aps.org/doi/10.1103/PhysRevB.81.064439.

[111] Abhishodh Prakash, Juven Wang, and Tzu-Chieh Wei. Unwinding short-range entanglement. *Phys. Rev. B*, 98:125108, Sep 2018. doi: 10.1103/PhysRevB.98.125108. URL https://link.aps.org/doi/10.1103/PhysRevB.98.125108.

[112] John Preskill. Chapter 9. topological quantum computation. http://www.theory.caltech.edu/people/preskill/ph229/#lecture, 2004. URL http://www.theory.caltech.edu/people/preskill/ph229/#lecture.

[113] Michael Pretko, Xie Chen, and Yizhi You. Fracton phases of matter. *International Journal of Modern Physics A*, 35(06), 2020. doi: 10.1142/S0217751X20300033. URL https://www.worldscientific.com/doi/abs/10.1142/S0217751X20300033.

[114] Xiao-Liang Qi and Shou-Cheng Zhang. Topological insulators and superconductors. *Rev. Mod. Phys.*, 83:1057–1110, Oct 2011. doi: 10.1103/RevModPhys.83.1057. URL https://link.aps.org/doi/10.1103/RevModPhys.83.1057.

[115] Frank Quinn. Group categories and their field theories. 1998. doi: 10.48550/ARXIV.MATH/9811047. URL https://arxiv.org/abs/math/9811047.

[116] N. Reshetikhin and V. G. Turaev. Invariants of 3-manifolds via link polynomials and quantum groups. *Inventiones mathematicae*, 103:547 – 597, 1991. doi: 10.1007/BF01239527. URL https://doi.org/10.1007/BF01239527.

[117] Gertian Roose, Laurens Vanderstraeten, Jutho Haegeman, and Nick Bultinck. Anomalous domain wall condensation in a modified ising chain. *Phys. Rev. B*, 99:195132, May 2019. doi: 10.1103/PhysRevB.99.195132. URL https://link.aps.org/doi/10.1103/PhysRevB.99.195132.

[118] Shinsei Ryu and Shou-Cheng Zhang. Interacting topological phases and modular invariance. *Phys. Rev. B*, 85:245132, Jun 2012. doi: 10.1103/PhysRevB.85.245132. URL https://link.aps.org/doi/10.1103/PhysRevB.85.245132.

[119] Thomas Scaffidi and Zohar Ringel. Wave functions of symmetry-protected topological phases from conformal field theories. *Phys. Rev. B*, 93:115105, Mar 2016. doi: 10.1103/PhysRevB.93.115105. URL https://link.aps.org/doi/10.1103/PhysRevB.93.115105.

[120] Norbert Schuch, David Pérez-García, and Ignacio Cirac. Classifying quantum phases using matrix product states and projected entangled pair states. *Phys. Rev. B*, 84:165139, Oct 2011. doi: 10.1103/PhysRevB.84.165139. URL https://link.aps.org/doi/10.1103/PhysRevB.84.165139.

[121] Nathan Seiberg and Shu-Heng Shao. Exotic $U(1)$ Symmetries, Duality, and Fractons in 3+1-Dimensional Quantum Field Theory. *SciPost Phys.*, 9:46, 2020. doi: 10.21468/SciPostPhys.9.4.046. URL https://scipost.org/10.21468/SciPostPhys.9.4.046.

[122] Nathan Seiberg and Shu-Heng Shao. Exotic Symmetries, Duality, and Fractons in 2+1-Dimensional Quantum Field Theory. *SciPost Phys.*, 10:27, 2021. doi: 10.21468/SciPostPhys.10.2.027. URL https://scipost.org/10.21468/SciPostPhys.10.2.027.

[123] Nathan Seiberg and Shu-Heng Shao. Exotic $\mathbb{Z}_N$ Symmetries, Duality, and Fractons in 3+1-Dimensional Quantum Field Theory. *SciPost Phys.*, 10:3, 2021. doi: 10.21468/SciPostPhys.10.1.003. URL https://scipost.org/10.21468/SciPostPhys.10.1.003.

[124] T. Senthil and Michael Levin. Integer quantum hall effect for bosons. *Phys. Rev. Lett.*, 110:046801, Jan 2013. doi: 10.1103/PhysRevLett.110.046801. URL https://link.aps.org/doi/10.1103/PhysRevLett.110.046801.

[125] Bowen Shi and Yuan-Ming Lu. Characterizing topological order by the information convex. *Phys. Rev. B*, 99:035112, Jan 2019. doi: 10.1103/PhysRevB.99.035112. URL https://link.aps.org/doi/10.1103/PhysRevB.99.035112.

[126] Bowen Shi, Kohtaro Kato, and Isaac H. Kim. Fusion rules from entanglement. *Annals of Physics*, 418:168164, 2020. ISSN 0003-4916. doi: https://doi.org/10.1016/j.aop.2020.168164. URL https://www.sciencedirect.com/science/article/pii/S000349162030097X.

[127] Jun Ho Son and Jason Alicea. Commuting-projector hamiltonians for two-dimensional topological insulators: Edge physics and many-body invariants. *Phys. Rev. B*, 100: 155107, Oct 2019. doi: 10.1103/PhysRevB.100.155107. URL https://link.aps.org/doi/10.1103/PhysRevB.100.155107.

[128] Hao Song, Sheng-Jie Huang, Liang Fu, and Michael Hermele. Topological phases protected by point group symmetry. *Phys. Rev. X*, 7:011020, Feb 2017. doi: 10.1103/PhysRevX.7.011020. URL https://link.aps.org/doi/10.1103/PhysRevX.7.011020.

[129] Olabode Mayodele Sule, Xiao Chen, and Shinsei Ryu. Symmetry-protected topological phases and orbifolds: Generalized laughlin's argument. *Phys. Rev. B*, 88:075125, Aug 2013. doi: 10.1103/PhysRevB.88.075125. URL https://link.aps.org/doi/10.1103/PhysRevB.88.075125.

[130] D. Sénéchal. An introduction to bosonization, 1999. URL https://arxiv.org/abs/cond-mat/9908262.

[131] Nathanan Tantivasadakarn. Dimensional reduction and topological invariants of symmetry-protected topological phases. *Phys. Rev. B*, 96:195101, Nov 2017. doi: 10.1103/PhysRevB.96.195101. URL https://link.aps.org/doi/10.1103/PhysRevB.96.195101.

[132] Nicolas Tarantino, Netanel H Lindner, and Lukasz Fidkowski. Symmetry fractionalization and twist defects. *New Journal of Physics*, 18(3):035006, mar 2016. doi: 10.1088/1367-2630/18/3/035006. URL https://iopscience.iop.org/article/10.1088/1367-2630/18/3/035006.

[133] Jeffrey C.Y. Teo, Taylor L. Hughes, and Eduardo Fradkin. Theory of twist liquids: Gauging an anyonic symmetry. *Annals of Physics*, 360:349 – 445, 2015. ISSN 0003-4916. doi: https://doi.org/10.1016/j.aop.2015.05.012. URL http://www.sciencedirect.com/science/article/pii/S0003491615001967.

[134] Ryan Thorngren and Dominic V. Else. Gauging spatial symmetries and the classification of topological crystalline phases. *Phys. Rev. X*, 8:011040, Mar 2018. doi: 10.1103/PhysRevX.8.011040. URL https://link.aps.org/doi/10.1103/PhysRevX.8.011040.

[135] Apoorv Tiwari, Xiao Chen, Ken Shiozaki, and Shinsei Ryu. Bosonic topological phases of matter: Bulk-boundary correspondence, symmetry protected topological invariants, and gauging. *Phys. Rev. B*, 97:245133, Jun 2018. doi: 10.1103/PhysRevB.97.245133. URL https://link.aps.org/doi/10.1103/PhysRevB.97.245133.

[136] D. C. Tsui, H. L. Stormer, and A. C. Gossard. Two-dimensional magnetotransport in the extreme quantum limit. *Phys. Rev. Lett.*, 48:1559–1562, May 1982. doi: 10.1103/PhysRevLett.48.1559. URL https://link.aps.org/doi/10.1103/PhysRevLett.48.1559.

[137] Hong-Hao Tu, Yi Zhang, and Xiao-Liang Qi. Momentum polarization: An entanglement measure of topological spin and chiral central charge. *Phys. Rev. B*, 88:195412, Nov 2013. doi: 10.1103/PhysRevB.88.195412. URL https://link.aps.org/doi/10.1103/PhysRevB.88.195412.

[138] V.G. Turaev. Quantum invariants of knots and 3-manifolds (de gruyter studies in mathematics 18). *de Gruyter, Berlin*, 1994.

[139] Ashvin Vishwanath and T. Senthil. Physics of three-dimensional bosonic topological insulators: Surface-deconfined criticality and quantized magnetoelectric effect. *Phys. Rev. X*, 3:011016, Feb 2013. doi: 10.1103/PhysRevX.3.011016. URL https://link.aps.org/doi/10.1103/PhysRevX.3.011016.

[140] B. Volkov and Oleg Pankratov. Two-dimensional massless electrons in an inverted contact. *Jetp Letters - JETP LETT-ENGL TR*, 42, 01 1985.

[141] Kevin Walker. On witten's 3-manifold invariants. https://canyon23.net/math/1991TQFTNotes.pdf, 1991. URL https://canyon23.net/math/1991TQFTNotes.pdf.

[142] Chenjie Wang and Michael Levin. Weak symmetry breaking in two-dimensional topological insulators. *Phys. Rev. B*, 88:245136, Dec 2013. doi: 10.1103/PhysRevB.88.245136. URL https://link.aps.org/doi/10.1103/PhysRevB.88.245136.

[143] Chenjie Wang and Michael Levin. Topological invariants for gauge theories and symmetry-protected topological phases. *Phys. Rev. B*, 91:165119, Apr 2015. doi: 10.1103/PhysRevB.91.165119. URL https://link.aps.org/doi/10.1103/PhysRevB.91.165119.

[144] Chong Wang, Andrew C. Potter, and T. Senthil. Gapped symmetry preserving surface state for the electron topological insulator. *Phys. Rev. B*, 88:115137, Sep 2013. doi: 10.1103/PhysRevB.88.115137. URL https://link.aps.org/doi/10.1103/PhysRevB.88.115137.

[145] Juven C. Wang, Luiz H. Santos, and Xiao-Gang Wen. Bosonic anomalies, induced fractional quantum numbers, and degenerate zero modes: The anomalous edge physics of symmetry-protected topological states. *Phys. Rev. B*, 91:195134, May 2015. doi: 10.1103/PhysRevB.91.195134. URL https://link.aps.org/doi/10.1103/PhysRevB.91.195134.

[146] Qing-Rui Wang and Zheng-Cheng Gu. Towards a complete classification of symmetry-protected topological phases for interacting fermions in three dimensions and a

general group supercohomology theory. *Phys. Rev. X*, 8:011055, Mar 2018. doi: 10.1103/PhysRevX.8.011055. URL https://link.aps.org/doi/10.1103/PhysRevX.8.011055.

[147] Qing-Rui Wang and Zheng-Cheng Gu. Construction and classification of symmetry-protected topological phases in interacting fermion systems. *Phys. Rev. X*, 10:031055, Sep 2020. doi: 10.1103/PhysRevX.10.031055. URL https://link.aps.org/doi/10.1103/PhysRevX.10.031055.

[148] X. G. Wen. Topological orders in rigid states. *International Journal of Modern Physics B*, 04(02):239–271, 1990. doi: 10.1142/S0217979290000139. URL https://doi.org/10.1142/S0217979290000139.

[149] X. G. Wen. Gapless boundary excitations in the quantum hall states and in the chiral spin states. *Phys. Rev. B*, 43:11025–11036, May 1991. doi: 10.1103/PhysRevB.43.11025. URL https://link.aps.org/doi/10.1103/PhysRevB.43.11025.

[150] Xiao-Gang Wen. Topological orders and edge excitations in fractional quantum hall states. *Advances in Physics*, 44(5):405–473, 1995. doi: 10.1080/00018739500101566. URL https://doi.org/10.1080/00018739500101566.

[151] Xiao-Gang Wen. Topological orders and edge excitations in fractional quantum hall states. *Advances in Physics*, 44(5):405–473, 1995. doi: 10.1080/00018739500101566. URL https://doi.org/10.1080/00018739500101566.

[152] Xiao-Gang Wen. Classifying gauge anomalies through symmetry-protected trivial orders and classifying gravitational anomalies through topological orders. *Phys. Rev. D*, 88:045013, Aug 2013. doi: 10.1103/PhysRevD.88.045013. URL https://link.aps.org/doi/10.1103/PhysRevD.88.045013.

[153] Xiao-Gang Wen. Classifying gauge anomalies through symmetry-protected trivial orders and classifying gravitational anomalies through topological orders. *Phys. Rev. D*, 88:045013, Aug 2013. doi: 10.1103/PhysRevD.88.045013. URL https://link.aps.org/doi/10.1103/PhysRevD.88.045013.

[154] Xiao-Gang Wen. Symmetry-protected topological invariants of symmetry-protected topological phases of interacting bosons and fermions. *Phys. Rev. B*, 89:035147, Jan 2014. doi: 10.1103/PhysRevB.89.035147. URL https://link.aps.org/doi/10.1103/PhysRevB.89.035147.

[155] Xiao-Gang Wen. Construction of bosonic symmetry-protected-trivial states and their topological invariants via $g \times so(\infty)$ nonlinear σ models. *Phys. Rev. B*, 91:205101, May 2015. doi: 10.1103/PhysRevB.91.205101. URL https://link.aps.org/doi/10.1103/PhysRevB.91.205101.

[156] Xiao-Gang Wen. Exactly soluble local bosonic cocycle models, statistical transmutation, and simplest time-reversal symmetric topological orders in 3+1 dimensions. *Phys. Rev. B*, 95:205142, May 2017. doi: 10.1103/PhysRevB.95.205142. URL https://link.aps.org/doi/10.1103/PhysRevB.95.205142.

[157] Xiao-Gang Wen. Colloquium: Zoo of quantum-topological phases of matter. *Rev. Mod. Phys.*, 89:041004, Dec 2017. doi: 10.1103/RevModPhys.89.041004. URL https://link.aps.org/doi/10.1103/RevModPhys.89.041004.

[158] Frank Wilczek. Quantum mechanics of fractional-spin particles. *Phys. Rev. Lett.*, 49: 957–959, Oct 1982. doi: 10.1103/PhysRevLett.49.957. URL https://link.aps.org/doi/10.1103/PhysRevLett.49.957.

[159] Frank Wilczek. Magnetic flux, angular momentum, and statistics. *Phys. Rev. Lett.*, 48: 1144–1146, Apr 1982. doi: 10.1103/PhysRevLett.48.1144. URL https://link.aps.org/doi/10.1103/PhysRevLett.48.1144.

[160] Dominic J. Williamson, Nick Bultinck, Michael Mariën, Mehmet B. Şahinoğlu, Jutho Haegeman, and Frank Verstraete. Matrix product operators for symmetry-protected topological phases: Gauging and edge theories. *Phys. Rev. B*, 94:205150, Nov 2016. doi: 10.1103/PhysRevB.94.205150. URL https://link.aps.org/doi/10.1103/PhysRevB.94.205150.

[161] Edward Witten. Quantum field theory and the jones polynomial. *Communications in Mathematical Physics*, 121:351–399, Sep 1998. doi: 10.1007/BF01217730. URL https://doi.org/10.1007/BF01217730.

[162] Congjun Wu, B. Andrei Bernevig, and Shou-Cheng Zhang. Helical liquid and the edge of quantum spin hall systems. *Phys. Rev. Lett.*, 96:106401, Mar 2006. doi: 10.1103/PhysRevLett.96.106401. URL https://link.aps.org/doi/10.1103/PhysRevLett.96.106401.

[163] Charles Zhaoxi Xiong. Minimalist approach to the classification of symmetry protected topological phases. *Journal of Physics A: Mathematical and Theoretical*, 51 (44):445001, oct 2018. doi: 10.1088/1751-8121/aae0b1. URL https://doi.org/10.1088/1751-8121/aae0b1.

[164] Cenke Xu and J. E. Moore. Stability of the quantum spin hall effect: Effects of interactions, disorder, and F_2 topology. *Phys. Rev. B*, 73:045322, Jan 2006. doi: 10.1103/PhysRevB.73.045322. URL https://link.aps.org/doi/10.1103/PhysRevB.73.045322.

[165] Cenke Xu and T. Senthil. Wave functions of bosonic symmetry protected topological phases. *Phys. Rev. B*, 87:174412, May 2013. doi: 10.1103/PhysRevB.87.174412. URL https://link.aps.org/doi/10.1103/PhysRevB.87.174412.

[166] Michael P. Zaletel. Detecting two-dimensional symmetry-protected topological order in a ground-state wave function. *Phys. Rev. B*, 90:235113, Dec 2014. doi: 10.1103/PhysRevB.90.235113. URL https://link.aps.org/doi/10.1103/PhysRevB.90.235113.

[167] Michael P. Zaletel, Roger S. K. Mong, and Frank Pollmann. Topological characterization of fractional quantum hall ground states from microscopic hamiltonians. *Phys. Rev. Lett.*, 110:236801, Jun 2013. doi: 10.1103/PhysRevLett.110.236801. URL https://link.aps.org/doi/10.1103/PhysRevLett.110.236801.

[168] Bei Zeng, Xie Chen, Duan-Lu Zhou, and Xiao-Gang Wen. *Symmetry-Protected Topological Phases*, pages 281–332. Springer New York, New York, NY, 2019. ISBN 978-1-4939-9084-9. doi: 10.1007/978-1-4939-9084-9_10. URL https://doi.org/10.1007/978-1-4939-9084-9_10.

[169] Yi Zhang, Tarun Grover, Ari Turner, Masaki Oshikawa, and Ashvin Vishwanath. Quasiparticle statistics and braiding from ground-state entanglement. *Phys. Rev. B*, 85:235151, Jun 2012. doi: 10.1103/PhysRevB.85.235151. URL https://link.aps.org/doi/10.1103/PhysRevB.85.235151.

[170] Yi Zhang, Tarun Grover, and Ashvin Vishwanath. General procedure for determining braiding and statistics of anyons using entanglement interferometry. *Phys. Rev. B*, 91:035127, Jan 2015. doi: 10.1103/PhysRevB.91.035127. URL https://link.aps.org/doi/10.1103/PhysRevB.91.035127.